UNITED STATES DEPARTMENT OF COMMERCE
HARRY L. HOPKINS, Secretary
NATIONAL BUREAU OF STANDARDS
Lyman J. Briggs, Director

✦

Journal of Research

of the

National Bureau of Standards

✦

Volume 25, Number 1

July 1940

[Published with approval of the Director of the Budget]

UNITED STATES
GOVERNMENT PRINTING OFFICE
WASHINGTON : 1940

For sale by the Superintendent of Documents, Washington, D. C. - - - - - - Price 30 cents
$3.50 per year on subscription

The prices of the separate Research Papers appearing in this JOURNAL are given on the front cover page. If 100 or more copies of any separate are ordered, a discount of 25 percent is allowed. Those who desire copies of separate Research Papers should send their orders and remittances without delay to the Superintendent of Documents, U. S. Government Printing Office, Washington, D. C. This will aid him to determine the number of copies to be printed for sale. Research Papers are not printed from electrotypes, and usually no more reprints can be had when the first and only printing is exhausted.

U. S. DEPARTMENT OF COMMERCE NATIONAL BUREAU OF STANDARDS

RESEARCH PAPER RP1310

Part of Journal of Research of the National Bureau of Standards, Volume 25, July 1940

A DUAL BRIDGE FOR THE MEASUREMENT OF SELF INDUCTANCE IN TERMS OF RESISTANCE AND TIME

By Harvey L. Curtis and Leon W. Hartman*

ABSTRACT

A dual bridge for the measurement of self inductance in terms of resistance and time is described, its theory is developed, and experimental results are given. The dual bridge consists of a primary bridge and a detector bridge, both of which are independently balanced for continuous current. The primary bridge has the inductance to be measured in one of its resistance arms and a source of unidirectional pulsating current in its battery arm. In its galvanometer arm there is connected, through a rectifying switch, the detector bridge which has an integrating galvanometer in one of its resistance arms and a battery as a source of current. The current from the battery is adjusted until its effect on the integrating galvanometer is equal and opposite to that of the pulses of current from the primary bridge. The theory not only gives the formula for computing the inductance, but also a formula for determining the maximum number of pulses per second that may be employed with a given set of bridge constants in order to obtain a desired accuracy. The experimental results show that the method can readily be used to measure inductances as large as 1 henry, with an accuracy of 1 part in 1,000. There are indications that results of much higher accuracy can be obtained.

CONTENTS

	Page
I. Introduction	1
II. Theory of the method	2
III. Experimental test of the method	9
1. The bridge	9
2. The galvanometers	10
3. The batteries	10
4. The cam-operated switches	11
5. Control and measurement of the frequency of the pulsating current	11
6. Procedure in making observations	11
7. Results	12
IV. Summary and conclusion	13

I. INTRODUCTION

A method which employs pulsating current in a dual bridge has been developed for the measurement of self inductance in terms of resistance and time. This method, which uses two Wheatstone bridges, each of which is balanced for continuous current, has been applied to the determination of the inductance of several inductors. The distinctive feature is the use of a unidirectional pulsating current for energizing one of the bridges, and the comparison of the time integral of the current in the galvanometer arm of this bridge with the con-

*President, University of Nevada.

tinuous current in one of the arms of the other bridge. In this way a null method is employed, using a current with a known wave form.

A method for the measurement of self inductance in terms of resistance and time by means of transient currents was proposed by Maxwell.[1] The inductor is inserted in one arm of a Wheatstone bridge, the bridge is balanced with continuous current, and the ballistic deflection of the galvanometer is observed when the battery circuit is opened or closed. The inductance is computed from the deflection, sensitivity, period, and damping of the galvanometer, and from the resistances of the bridge arms. Values of inductance obtained by this method usually do not have an accuracy greater than 1 percent.

A method [2] which has frequently been employed for determining a self inductance in terms of resistance and time requires an intermediary capacitance. The inductance is measured in terms of resistance and capacitance in an alternating-current bridge, then the capacitance is measured in terms of resistance and time, using a pulsating current. If the capacitance has the same value when used in the two bridges, the inductance can be computed from the resistances in the bridges and the fundamental frequency of the pulsating current. The uncertainty in the value of an inductance obtained by this method may be only a few parts in a million.

The dual-bridge method has been devised in order to have available another method for determining the value of a self inductance in terms of resistance and time. The theory has been so developed that the inductance can be computed from the resistances of the bridges, the electromotive forces of the batteries, and the frequency of the pulsating current. All correction terms that would introduce an error of as much as 1 part in a million have been considered. Experimental determinations have been made in order to show the possibilities of the method, though the apparatus available did not permit measurements of the highest accuracy.

II. THEORY OF THE METHOD

The method may be briefly described as a primary bridge having a detector bridge connected in that arm which, in a Wheatstone bridge, contains only a galvanometer. A cam-operated switch opens and closes the current in the primary bridge at regular intervals and a second switch on the same shaft as the first opens and closes the connections from the primary bridge to the detector bridge. In this way a unidirectional pulsating current is produced in the arms of the dual bridge. The average value of the pulsating current in one of the arms of the detector bridge is made equal to a continuous current that is supplied to this arm by a separate battery. There is then no deflection of a ballistic galvanometer which is directly connected in the arm.

A schematic diagram of the dual bridge is shown in figure 1. The current for the primary bridge is supplied by a battery having an electromotive force E. The currents which originate in this battery are designated in the various arms as I with an appropriate subscript. The current for the detector bridge is supplied by a battery having an

[1] Phil. Mag. **155**, 475 (1865).
[2] For a recent description of this method, see Curtis, Moon, and Sparks, J. Research NBS **16**, 1 (1936) RP857.

electromotive force e. The currents which originate in this battery are constant and are designated as i with a suitable subscript.

In making a measurement with the dual bridge, each bridge is first balanced with continuous current by connecting it to an auxiliary galvanometer, which is not shown in the drawing. The continuous current for balancing the primary bridge is obtained from battery E by short-circuiting switch C_1, and for the detector bridge from battery e by disconnecting switch C_2. The respective bridges are balanced by adjusting the resistances in the Q and g arms. While the detector bridge is being balanced, the coil of the galvanometer in the g arm should be clamped. The resistances of the balanced bridges have the relationships $gk=fh$ and $QR=PS$. In the next step of the measure-

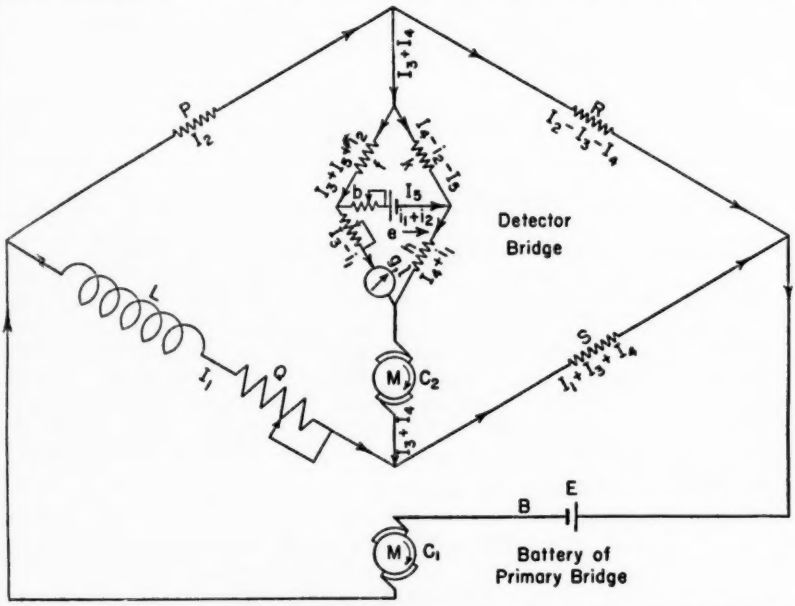

FIGURE 1.—*Diagram of the dual bridge for measuring a self inductance in terms of resistance and time.*

If $P=R=S$ and $f=h=k$, $L=T\cdot\frac{e}{E}\cdot\frac{4(B+P)(P+f)}{b+f}$.

ment, the battery and galvanometer arms of the primary bridge are connected to switches C_1 and C_2, respectively, which are attached to a single shaft that rotates with a constant speed. With the switches as shown in figure 1, switch C_1 makes and breaks the circuit of the primary bridge, and switch C_2 keeps the connection between the primary and the detector bridges closed during the time that the current is building up in the primary bridge, but opens this connection before the current starts to die down. By changing the angular position of C_2 relative to C_1, C_2 can be made to stay closed when the primary current is dying down, and to open before it starts to build up. In either case the operation of these switches produces in the detector bridge a series of pulses having a time interval, T. The magnitude of each pulse depends on the inductance L, on the electromotive force E of the battery

in the primary bridge, and on the resistances in the arms of the two bridges. The galvanometer g, in the detector bridge has a period which is at least $100T$, so that the series of pulses produces a deflection with a small periodic component. The average value of this deflection is made zero by adjusting the resistance b, which changes the constant current in the detector bridge. Since the average deflection of the ballistic galvanometer is zero, the quantity of electricity sent through it as a result of the pulsating current is the same in any complete period as the quantity resulting from the continuous current. Hence

$$\int_0^T I_3 dt = i_1 T. \tag{1}$$

since $gk=hf$, $i_1=\dfrac{ek}{b(h+k)+h(f+k)}$, so that

$$\int_0^T I_3 dt = \frac{ekT}{b(h+k)+h(f+k)}. \tag{2}$$

In order to obtain an expression for L, the value of $\int_0^T I_3 dt$ must be determined from five simultaneous equations involving I_1, I_2, I_3, I_4, and I_5. These equations also include the time derivatives of the currents in those arms which contain appreciable inductance and also the angular velocity (derivative of the displacement) of the galvanometer coil. The equations will be simplified by including only two inductances; that of the inductor in the primary bridge and that of the galvanometer in the detector bridge. The potential drops resulting from the currents i_1 and i_2 and the electromotive force e will not be included, since in every equation the sum of the terms which are thus introduced is zero.

The equations are

$$B(I_1+I_2)+PI_2+R(I_2-I_3-I_4)=E. \tag{3}$$

$$(Q+LD_t)I_1-hI_4-k(I_4-I_5)-PI_2=0. \tag{4}$$

$$S(I_1+I_3+I_4)-R(I_2-I_3-I_4)+hI_4+k(I_4-I_5)=0. \tag{5}$$

$$f(I_3+I_5)+(g+lD_t)I_3-hI_4-k(I_4-I_5)=HD_t\theta. \tag{6}$$

$$bI_5-k(I_4-I_5)+f(I_3+I_5)=0. \tag{7}$$

The meaning of all the symbols used in these equations is readily understood by reference to figure 1, except θ, which indicates the deflection of the galvanometer, and H, which signifies the electromotive force generated in the galvanometer coil when it is moving with unit angular velocity. These equations are based on the assumption that one can neglect the resistance of the commutator which is in series with the detector bridge. If an accuracy of 1 part in a million is required, and if each of the resistances of the arms of the detector bridge is 10,000 ohms or more, the resistance of the commutator and leads must be less than 0.01 ohm.

Each of the eq 3 to 7 will be multiplied by dt and integrated over one complete cycle. As the time integral of a current is a quantity of electricity, each of the integrals of current will be represented by q with the same subscript as the corresponding current. Since the detector bridge is connected to the primary bridge during a part of the cycle only, the integrals of the current in the primary bridge will be considered only during that portion of the cycle when the detector bridge is connected to it. The time that each event in the cycle occurs will be designated as follows:

t_0 = zero time = time circuit of primary bridge is closed (C_1 makes contact), the detector bridge having been previously connected to the primary bridge.

t_1 = time detector bridge is disconnected (C_2 breaks contact),

t_2 = time circuit of outer bridge is opened (C_1 breaks contact),

t_3 = time detector bridge is again connected (C_2 makes contact),

t_4 = end of cycle.

Also

$T = t_4 - t_0$ = time of a complete cycle.

The current I_3 is maintained only when the detector bridge is connected, which occurs in the intervals t_0 to t_1 and t_3 to t_4. In the interval t_3 to t_4 the circuit of the primary bridge is open, and I_3 will be zero provided the interval t_2 to t_3 has been sufficiently long to allow the currents of the primary bridge to become zero. Under this condition, the detector bridge is influenced only by the integral of I_3 during the interval t_0 to t_1. On the other hand, the current from the battery e in the detector bridge and that resulting from the motion of the galvanometer coil are effective throughout the cycle.

The time t_0 was chosen so that at $t=0$, both I_1 and I_3 would be zero. Representing the values of I_1 and I_3 at time t_1 as $I_1(t_1)$ and $I_3(t_1)$ and at other times in a corresponding manner, the assumption will now be made that $I_3(t_1)=0$, $I_1(t_1)=I_1(t_\infty)$, and $I_1(t_3)=0$. The conditions under which these assumptions are valid will be discussed later. Integrating each of the eq 3 to 7 from 0 to T, but separating each integral into parts and retaining only those parts that are integrated over the times that the integrated result affects the galvanometer of the detector bridge, the following equations result:

$$Bq_1+(B+P+R)q_2-Rq_3-Rq_4=Et_1. \tag{8}$$

$$Qq_1-PQ_2-(h+k)q_4+kq_5=-LI_1(t_1). \tag{9}$$

$$Sq_1-Rq_2+(R+S)q_3+(R+S+h+k)q_4=0. \tag{10}$$

$$(f+g)q_3-(h+k)q_4+(k+f)q_5=0. \tag{11}$$

$$fq_3-kq_4+(b+f+k)q_5=0. \tag{12}$$

These equations can be solved by determinants for q_3. In this solution, the minor by which Et_1 is multiplied vanishes, since $QR=PS$. Then, using the equality $gk=fh$,

$$q_3=\frac{RkL\ I_1(t_1)}{P(R+S)(f+k)+f(P+R)(h+k)}. \tag{13}$$

But

$$I_1(t_1)=I_1(t_\infty)=\frac{ER}{B(R+S)+S(P+R)}. \tag{14}$$

and by eq 2,

$$q_3=\frac{ekT}{b(h+k)+h(f+k)}. \tag{15}$$

Solving eq 13, 14, and 15 for L,

$$L=T\cdot\frac{e}{E}\cdot\frac{[B(R+S)+S(P+R)][P(R+S)(f+k)+f(P+R)(h+k)]}{R^2[b(h+k)+h(f+k)]} \tag{16}$$

If both bridges are "square," so that $P=R=S$ and $f=h=k$,

$$L=T\cdot\frac{e}{E}\cdot\frac{4(B+P)(P+f)}{b+f}. \tag{17}$$

Equation 17 is useful in determining the most suitable resistances to be used in a given case, but it should not be used for precise computations, since the bridges are never exactly square.

The value of the inductance L, as given by eq 16, is determined from the rate of rotation of the camshaft, the ratio of the two electromotive forces, and the resistances of the arms of the bridges. The rate of rotation can be maintained constant and can be accurately measured. The ratio of the electromotive forces can be accurately measured by means of a calibrated potentiometer. The resistances of all the arms of both bridges except the one containing the inductance in the primary bridge and the one containing the galvanometer in the detector bridge must be known. However, these excepted resistances are directly involved, since the derivation assumes that both primary and detector bridges are balanced for direct current. Hence, any change in either of these resistances between the time of balancing the two bridges with direct current, using the auxiliary galvanometer, and the time of balancing the dual bridge introduces an error in the computed value of L. With care, any error on this account can be made negligible. The precision with which the resistance B of the battery arm of the primary bridge can be measured will often determine the accuracy that can be attained by this method.

The conditions for determining that, within a specified error, $I_3(t_1)=0$, $I_1(t_1)=I_1(t_\infty)$, and $I_1(t_3)=0$ can be obtained by solving the eq 3 to 7 for the currents I_1 and I_3, and determining their values at the indicated times. The purpose is to set limits both to the values of the resistances that may be used and to the length of the period that may be employed when a given inductance is being measured. Since high accuracy is not required in setting these limits, the equations can be simplified by neglecting the very small electromotive force introduced by the motion of the galvanometer coil. Also, since the arrangement of the bridge is such that $I_3(t)$ approaches its final value more slowly than $I_1(t)$, the bridge constants that make $I_3(t_1)\cong 0$ will certainly make $I_1(t_1)\cong I_1(t_\infty)$. Also the bridge arrangement is such that I_1 dies down somewhat more rapidly than it builds up. Hence all conditions will be satisfied if $I_3(t_1)$ is sufficiently near zero.

Rearranging eq 3 to 7, solving by determinants for I_3, and noting that the application of the symbolic operator, D_t, to the electromotive force E, or to any of the resistances, gives zero, the value of I_3 can be obtained from the equation

$$\Delta I_3=0, \tag{18}$$

where Δ is the determinant formed by the coefficients of the currents in eq 3 to 7. Expanding this determinant,

$$[\alpha l L D_t^2+(\beta L+\gamma l)D_t+\delta]I_3=0, \tag{19}$$

where

$$\alpha=[(B+P)(R+S+h)+R(S+h)][b+f+k]+k(b+f)(B+P+R). \tag{20}$$

$$\beta=\frac{1}{k}\{(f+k)[B(R+S)+SR+SP+PR]+f(h+k)(B+P+R)\}$$
$$\{b(h+k)+h(f+k)\}. \tag{21}$$

$$\gamma=\frac{1}{R}\{B(R+S)+S(P+R)\}$$
$$\{[P(R+S)+h(P+R)][b+f+k]+k(P+R)(b+f)\}. \tag{22}$$

$$\delta=\frac{1}{Rk}[B(R+S)+S(P+R)][b(h+k)+h(f+k)]$$
$$[P(R+S)(f+k)+f(P+R)(h+k)]. \tag{23}$$

Solving the differential eq 19,

$$I_3=A_1\epsilon^{-(\lambda-\sigma)t}+A_2\epsilon^{-(\lambda+\sigma)t}, \tag{24}$$

where
$$\lambda=\frac{\beta L+\gamma l}{2\alpha l L},\sigma=+\frac{\sqrt{(\beta L+\gamma l)^2-4\alpha\delta l L}}{2\alpha l L} \tag{25}$$

and A_1 and A_2 are the constants of integration. Equation 25 shows that σ is always smaller than λ, but is a real number for all practical bridge arrangements.

When $t=0$, $I_3=0$, so that $A_2=-A_1$,

$$I_3=A_1[\epsilon^{-(\lambda-\sigma)t}-\epsilon^{-(\lambda+\sigma)t}]. \tag{26}$$

This equation shows that I_3 may be considered as the difference of two currents, each of which has the value A_1 when $t=0$, and both of which decrease to zero at infinite time. However, the current for which the exponent of ϵ is the smaller decreases less rapidly than the other current, so that the difference goes through a maximum and decreases towards zero. The relationship of these two currents to each other and to their difference is shown in figure 2. In this figure the value of A_1 is taken as unity, and the value of $\lambda+\sigma$ only twice that of $\lambda-\sigma$, which is a much smaller difference than would be found in an actual bridge. The values of y correspond to the current and its components. However, even in this case, the difference curve rapidly approaches the value of the curve with the smaller exponent.

The total quantity of electricity which passes through the ballistic galvanometer, and which produces the torque on its coil, is the integral of I_3, as given in eq 25. When the time is indefinitely long,

$$\int_0^\infty I_3 dt=A_1\int_0^\infty \epsilon^{-(\lambda-\sigma)t}dt-A_1\int_0^\infty \epsilon^{-(\lambda+\sigma)t}dt=A_1\left[\frac{2\sigma}{\lambda^2-\sigma^2}\right]. \tag{27}$$

The quantity which actually passes through the galvanometer when the circuit is opened at time t_1 is less than the above amount by the integral

$$\int_{t_1}^{\infty} I_3 dt = A_1 \left[\frac{\epsilon^{-(\lambda-\sigma)t_1}}{\lambda-\sigma} - \frac{\epsilon^{-(\lambda+\sigma)t_1}}{\lambda+\sigma} \right]. \tag{28}$$

Hence the ratio, ζ, of the deficiency in quantity at time t_1 to the quantity at infinite time is

$$\zeta = \frac{\lambda+\sigma}{2\sigma} \epsilon^{-(\lambda-\sigma)t_1} - \frac{\lambda-\sigma}{2\sigma} \epsilon^{-(\lambda+\sigma)t_1}. \tag{29}$$

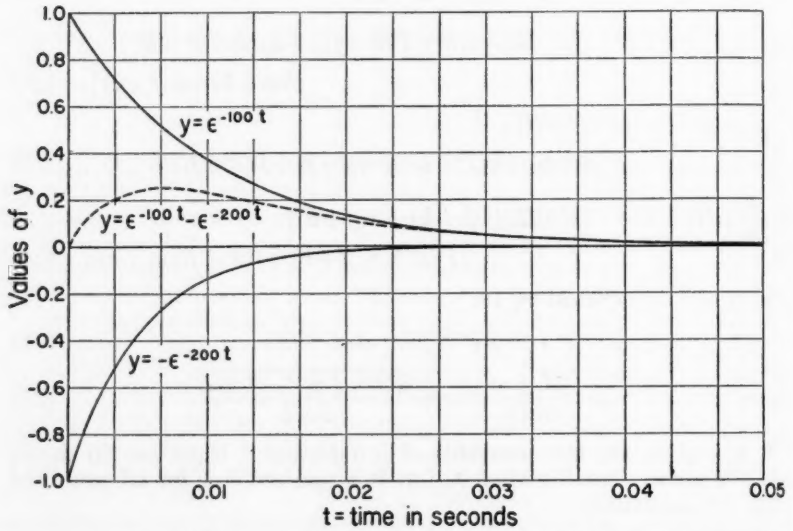

FIGURE 2.—*Curves of exponential functions to show the difference of two functions with negative exponents when one exponent has twice the value of the other.*

This equation can be used to compute, for any given bridge arrangement, the error that will be introduced by allowing only the time t_1 for the currents to reach a steady state. The reverse process of determining the maximum value of t_1 when the error is to be no greater than ζ, is not readily carried out. However, the second term of eq 29 decreases so much more rapidly than the first term that at time t_1 only the first term needs to be considered. This decrease makes the second term negligibly small in a shorter interval than is shown by the curve of $\epsilon^{-(\lambda+\sigma)t}$ in figure 2, since the coefficient of the second term of eq 29 is smaller than the coefficient of the first term, whereas in the plotted curves, both terms have the same coefficient. Hence the shortest time, t_1, during which both switches C_1 and C_2 must be closed when an accuracy of ζ is required, can be determined from the equation

$$\zeta = \frac{\lambda+\sigma}{2\sigma} \epsilon^{-(\lambda-\sigma)t_1}. \tag{30}$$

This equation is used only to set a lower limit for t_1, and any approximation that makes this limit lower than that given by eq 30 will not

affect the accuracy of a determination of the inductance L, although it may increase the difficulty of choosing suitable constants for the dual bridge. Hence $(\lambda+\sigma)/2\sigma$ may be taken as unity, since it is always larger than that, and such an error would make t_1 too small. Using this approximation, and taking the natural logarithm of both sides of eq 30,

$$(\lambda-\sigma)t_1=-ln\,\zeta=-2.3\,\log\,\zeta. \tag{31}$$

The following example indicates a suitable procedure for computing the limiting value for the period, T, of the pulsating current when the bridge constants have been selected. Assume that both the primary and detector bridges are square, that the resistances of the detector bridge are at least 10 times greater than those of the primary bridge, and that the inductances are of the same order of magnitude. Then $P=Q=R=S$; $f=g=h=k=aP$; and $l=cL$, where a is greater than 10 and c is less than one-tenth of a. Assume also that $B=0$, that b is very large relative to any other resistance in the bridges, that $T=2t_1$, and that the required accuracy is 1 part in a million ($\zeta=10^{-6}$). Substituting these values in eq 20 to 25 to obtain values of λ and σ, using these values in eq 31, and neglecting some terms that introduce an error of less than 10 percent in the value of T,

$$T\geqslant\frac{14L}{P}. \tag{32}$$

If $L=0.1$ henry and $P=100$ ohms, no error will be introduced in the value of L because of the shortness of the cycle if T is greater than 0.014 sec (the frequency of the pulsating current less than 70 c/sec).

III. EXPERIMENTAL TEST OF THE METHOD[3]

The experimental test of the method was undertaken before the complete theory had been developed in order to determine whether there were serious defects in it that could only be discovered by such a test. The work showed that the method had possibilities for use in precision measurements. The complete theory given in the preceding pages was then developed. However, the formula for computing the inductance was not changed by the more complete analysis.

1. THE BRIDGE

The resistance of each of the arms (P, Q, R, S) of the primary bridge was 300 ohms, and that of each of the arms (f, g, h, k) of the detector bridge was 10,000 ohms. The resistor b was a dial box which could be varied from 1 ohm to 10,000 ohms. All of these resistors were guaranteed by the makers to be accurate to 1/20 percent, but they were not calibrated during the experimental work. Variable resistors in the Q and g arms permitted the primary and detector bridges to be balanced to closer than 1 part in 10,000 when the auxiliary galvanometer was employed.

[3] The junior author started the experimental work at the National Bureau of Standards in the summer of 1930. He made an entirely new setup in the Physics Department at the University of Nevada, where the work was carried to completion. The role of second observer to control the speed of the motor generator set was taken by one or another of the children of the junior author.

2. THE GALVANOMETERS

The galvanometer used in the detector bridge had a period of 15 sec. This instrument was adjusted until it integrated correctly the current passing through it.[4] In order to test the effect of the inductance of the galvanometer, additional inductances varying from 50 to 550 mh were inserted in series with the galvanometer, but no change in the balance of the bridge could be observed. The auxiliary galvanometer, which was provided with a suitable Ayrton shunt, had a sensitivity of 4.5×10^{-9} amp/mm at a distance of 1 m.

3. THE BATTERIES

Battery e in the detector bridge was a dry cell, and battery E in the primary bridge was a storage battery. The electromotive forces

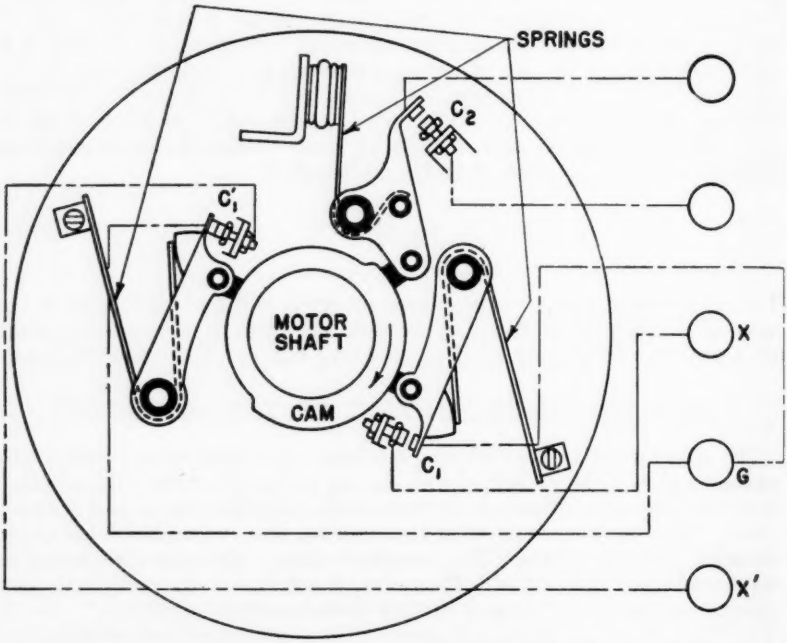

FIGURE 3.—*Diagram of motor-operated switches for the dual bridge.*

Either switch C_1 or C'_1 may be used for making and breaking the current in the primary bridge; the switch C_2 opens and closes the connection between the primary and detector bridges. If C_1 is used in the primary bridge, the unbalance of the primary bridge on closing the circuit is measured by the detector bridge; if C'_1 is used, the balance on opening is measured.

of e and E were compared by means of a potentiometer. The resistance of the storage battery was determined by measuring, with a potentiometer, the electromotive force on open circuit and then the fall of potential through a known resistance connected directly across its terminals. The difference between these two values gave the drop in potential through the battery when a known current was passing through it, from which the internal resistance of the primary battery was computed.

[4] See p. 507 of paper by Curtis and Moon, BS Sci. Pap. 22 (1927) S564.

4. THE CAM-OPERATED SWITCHES

The device finally adopted for opening and closing the circuits (see fig. 3) consisted essentially of the contact maker of a Liberty airplane motor. This device was mounted upon the free end of the shaft of a motor generator set and was adjusted so that it was free from "chattering" when the motor was driven at relatively low speed. Oscilloscope tests showed that the rise and fall of current due to the induced electromotive force in Q gave a smooth and apparently complete logarithmic curve. The circuit through switch C_2, which joined the secondary bridge to the primary, was closed about one-fifth of a revolution of the motor before the closing of the circuit through switch C_1, which joined battery B to the primary bridge. The circuits through the two switches then remained closed for slightly less than one-quarter of a revolution of the motor, at which time the circuit to the detector bridge was opened while the circuit of the primary bridge remained closed for slightly more than one-sixth of a revolution of the motor. During the remainder of the revolution of the cam, both bridge circuits were open. Thus the inductance of the coil was measured by the effect produced when the current through the inductor was rising from zero to its maximum value. By changing one lead to the primary bridge from X to X' and reversing the leads connecting the secondary bridge to C_2, the inductance of the coil could be measured by the effect produced when the current through the inductor was falling from its maximum value to zero.

5. CONTROL AND MEASUREMENT OF THE FREQUENCY OF THE PULSATING CURRENT

The frequency of the pulsating current was determined by the speed of a motor generator on the shaft of which was mounted the cam for opening and closing the circuits. The speed was maintained constant by an observer who so varied the pressure of his finger on the rim of a flywheel attached to the shaft that a pointer rotating with the shaft appeared to remain stationary when illuminated by a neon lamp that was flashed by contacts on a tuning fork. The speed was measured by a chronograph[5] which was geared to the shaft. The time intervals for this chronograph depended on a standard clock that was frequently calibrated by means of radio signals. The average speed for any one observation was not in error by as much as 1 part in 10,000.

6. PROCEDURE IN MAKING OBSERVATIONS

In making a set of observations, one observer controlled the speed of the motor generator set and obtained a record of it on the chronograph while a second observer made the necessary bridge adjustments. During the 2 or 3 minutes which were required to make a record on the chronograph that was sufficiently long to permit an accurate measurement of the speed, the second observer would make several cycles of adjustments of the bridges. In each cycle the primary bridge was first connected directly to the battery and balanced by using the auxiliary galvanometer and varying Q, then the secondary bridge was connected to its battery and balanced by using the same galvanometer and varying g, and finally the dual bridge was connected to the two

[5] Phil. Mag. 155, 518 (1865).

batteries through the cam-operated switches and balanced by varying b until the ballistic galvanometer in the detector bridge showed no deflection. When a cycle was reached in which no change from the preceding cycle was required in any of the resistances Q, g, or b, the dual bridge was considered balanced. The electromotive forces of the cells were then immediately compared by a potentiometer.

7. RESULTS

The results given in table 1 were obtained on two fixed standards of self inductance having nominal values of 1 henry and 0.1 henry, on the 1-henry inductor and an 0.01-henry inductor connected in series, and on a group of the three inductors mentioned above connected in series. In the series connections, the coils were so arranged that there was no mutual inductance between them. The measurements with the dual bridge were made at the University of Nevada. The alternating-current values were obtained at the National Bureau of Standards, by measuring each inductor separately, using a frequency of 60 c/sec. The values obtained for a given inductor with the dual bridge differ among themselves by as much as 3 parts in 1,000, which is the result of experimental error. The average values for the inductances having a value of about 1 henry, for which the setup was particularly adapted, differ from the alternating-current value by only 2 or 3 parts in 10,000. This difference might be the result of instability in the inductors themselves. Hence there is no indication that a systematic error occurred in the measurements with the dual bridge.

TABLE 1.—*Results obtained with the dual bridge, on four different inductances, compared with their alternating-current values*

Measurements with dual bridge				Alternating current inductance
Number of makes and breaks per second	Measured inductance	Number of makes and breaks per second	Measured inductance	
100-mh INDUCTOR				
	mh		*mh*	*mh*
9.0883	99.89	10.0006	100.13	----------
9.0897	99.80	9.9974	100.11	----------
		Mean	99.98	100.08
1-h INDUCTOR				
	mh		*mh*	*mh*
14.2980	994.8	10.0196	996.0	----------
14.2977	994.7	10.0169	995.2	----------
14.2856	994.6	10.0238	994.1	----------
11.1118	994.0	10.0253	994.0	----------
9.0967	995.0	10.0242	994.0	----------
9.0941	994.4	10.0228	994.8	----------
11.1403	994.5	10.0216	995.4	----------
9.9976	995.2	10.0262	995.6	----------
10.0165	995.8	10.0242	996.0	----------
8.3248	995.0	8.3467	994.7	----------
12.4970	994.2	8.3472	994.2	----------
9.1020	994.9	8.3424	994.1	----------
14.2980	994.8	8.8908	994.1	----------
10.0223	996.1	4.1753	995.1	----------
10.0204	995.6	4.5551	995.9	----------
		Mean	994.9	994.7

TABLE 1.—*Results obtained with the dual bridge, on four different inductances, compared with their alternating-current values*—Continued

Measurements with dual bridge				Alternating current inductance
Number of makes and breaks per second	Measured inductance	Number of makes and breaks per second	Measured inductance	
1-h INDUCTOR IN SERIES WITH A 10-mh INDUCTOR				
	mh		*mh*	*mh*
14.3017	1004.3	9.9950	1004.9	----------
14.3002	1004.0	8.3330	1005.1	----------
14.3002	1004.0	8.3341	1005.1	----------
14.2906	1004.8	9.1128	1005.4	----------
16.6485	1004.6	11.1373	1005.6	----------
11.0970	1005.3	9.9972	1005.0	----------
9.9889	1005.2	----------	----------	----------
		Mean.....	1004.9	1004.7
1-h INDUCTOR, 100-mh INDUCTOR, AND 10-mh INDUCTOR, ALL IN SERIES				
	mh		*mh*	*mh*
10.0006	1106.4	11.1041	1105.0	----------
10.0006	1106.4	11.1041	1105.3	----------
9.9927	1106.6	11.1073	1104.8	----------
10.0035	1103.6	11.1073	1104.5	----------
11.1075	1104.6	11.1136	1103.9	----------
		Mean.....	1105.1	1104.8

IV. SUMMARY AND CONCLUSION

A new method for the absolute measurement of inductance, which employs a dual bridge, has been described. The theory of the bridge has been developed showing that the inductance can be determined in terms of certain constants of the bridge, which can be accurately measured. In developing the theory, factors which might introduce an error of 1 part in a million in measuring an inductance of 0.1 henry or larger have been considered.

The inductances of several coils have been measured by this method, giving results, within experimental error, which agree with those obtained by an alternating-current method. The experimental determinations were undertaken to determine if there were any unsurmountable difficulties in applying the method and were not carried out in a manner to obtain high precision. Both the theory and the results of the measurements indicate that the method is capable of giving precise results.

WASHINGTON, April 18, 1940.

U. S. DEPARTMENT OF COMMERCE NATIONAL BUREAU OF STANDARDS

RESEARCH PAPER RP1311

Part of Journal of Research of the National Bureau of Standards, Volume 25, July 1940

LENGTH CHANGES OF WHITEWARE CLAYS AND BODIES DURING INITIAL HEATING, WITH SUPPLEMENTARY DATA ON MICA

By R. F. Geller and E. N. Bunting

ABSTRACT

Changes in length during initial heating from room temperature to a maximum of 1,250° C were observed on nine kaolins, four ball clays, and three whiteware bodies. The effects of various forming methods, admixtures, and heating rates were observed also. Supplementary data were obtained in the form of differential heating curves for two clays, and of specific gravity and weight-loss determinations for muscovite mica. Mica exerts the greatest influence of any one factor below 1,000° C, and particle size is the predominating factor above this temperature.

CONTENTS

	Page
I. Introduction	15
II. Materials	16
III. Methods	17
IV. Results	21
1. Clays	21
2. Bodies	29
V. Discussion	33
1. Clays	33
(a) Beginning of contraction	33
(b) Length changes between 500° and 900° C	34
(c) Length changes between 900° and 1,000° C	35
(d) Final contraction	36
2. Bodies	37
(a) Length changes below 1,000° C	37
(b) Length changes above 1,000° C	38
(c) Total shrinkage	38
VI. Summary and conclusions	39

I. INTRODUCTION

The work of Steger [1] and others [2] on the length changes occurring in whiteware clays and in body mixtures during initial heating indicates that interesting information could be obtained by similar studies on the American clays and on body mixtures containing them.

It was thought possible that some explanation might be forthcoming also for certain effects of various heating rates on absorption and shrinkage. In 1936, Watts [3] published values for five whiteware bodies heated to "cone 10 nearly down" in 76 hr and in 108 hr. He found that the shorter schedule produced from 0.20 to 0.42 percent greater shrinkage, from 0.70 to 1.07 percent lower absorption, and from 300 to 600 lb/in.^{2} higher transverse strength. Rittgen [4] supports

[1] W. Steger, Ber. deut. keram. Ges. **19**, 2 (1938).
[2] R. Schwarz and Wm. Klös, Z. anorg. allgem. Chem. **169**, 213 (1931). L. Tscheischwili, W. Bussem and W. Weyl, Ber. deut. keram. Ges. **20**, 249 (1939).
[3] Arthur S. Watts, J. Am. Ceram. Soc. **19**, 175 (1936).
[4] A. Rittgen, Ber. deut. keram. Ges. **19**, 113 (1938).

this finding in an article on the development of electric tunnel kilns. He found that the average porosity for the bodies he investigated was about 9 percent after a 130-hr cycle to a maximum temperature of 1,280° C in a periodic kiln, and 8 percent after a 108-hr cycle to 1,270° C and 6 percent after a 54-hr cycle to 1,280° C in tunnel kilns. Shrinkage was reported as about the same during each cycle.

II. MATERIALS

The three body mixtures tested included two talcose bodies prepared in the laboratory and one commercial "semiporcelain" body. The compositions of the laboratory bodies are given in table 1. Available chemical compositions of the clays are given in table 2.

TABLE 1.—*Batch composition of laboratory-prepared bodies*

Body number	Talc, *L*	Fla. Kaolin, *U*	N. C. kaolin, *K*	Tenn. ball clay, *CC*	Tenn. ball clay, 5	Ky. ball clay, 4	Potash feldspar, *D*	Flint, *P*
	%	%	%	%	%	%	%	%
27	25	5	20	------	7.5	7.5	15	20
35	20	26.7	------	21.3	------	------	10.7	21.3

TABLE 2.—*Chemical composition and major mineral constituents of clays investigated* [a]

[tr=trace, nd=no determination]

Material	Laboratory designation	K_2O	Na_2O	CaO	MgO	Fe_2O_3	TiO_2	SiO_2	Al_2O_3	Ignition loss	Drying loss	Feldspar and mica	Kaolinite	Free silica
		%	%	%	%	%	%	%	%	%	%	%	%	%
German kaolin (Zettlitz) [b]	*Z*	0.84	0.44	0.29	0.27	0.65	0.18	46.9	37.4	12.9	-----	11.9	84.8	1.0
English china clay [c]	*P*	1.6	.2	.2	.2	.9	.2	47.0	37.7	12.4	-----	16.2	80.4	1.7
Vermont kaolin:														
Coarse fraction [d]	*Vc*	3.60	----	----	----	.98	1.33	63.92	22.78	6.54	0.53	30.5	27.9	37.1
Fine fraction [d]	*Vf*	1.62	----	----	----	.49	1.01	47.4	36.5	12.35	.58	13.7	79.0	4.5
North Carolina kaolin [e]	*K*	0.58	.10	.37	.42	.57	0.04	46.18	38.38	13.28	-----	7.6	90.1	0.3
Georgia "soft" kaolin [f]	*S*	.15	.10	nd	nd	.27	1.54	45.3	39.1	13.7	-----	2.1	97.2	-----
Georgia hard kaolin:														
Coarse fraction [g]	*Gc*	-----	.21	----	----	.19	1.31	45.37	38.59	13.09	1.12	1.8	96	-----
Fine fraction [g]	*Gf*	-----	.18	----	----	.21	1.76	45.06	37.84	12.75	2.09	1.5	97	-----
Florida kaolin [h]	*E*	.2	0.0	.5	tr	.8	0.5	46.3	37.7	13.7	-----	4.5	91.2	2.0
Do.[h]	*U*	.2	0.0	tr	0.0	.4	.2	46.9	38.5	13.8	-----	1.5	95.8	1.7
Alabama kaolin [i]	*T*	-----	----	(j)	.2	.49	1.44	43.5	41.2	13.7	1.26	1	93	(s)
Tennessee ball clay [k]	5	2.0	.3	.2	.3	.6	1.3	50.3	31.5	13.6	-----	20.5	61.0	11.7
Do.[l]	*J*	1.84	.22	.22	.61	1.07	1.21	53.57	29.18	11.55	-----	17.8	57.7	17.7
Do.[l]	*CC*	0.21	.08	.25	.39	0.98	1.75	57.07	27.86	11.32	-----	2.9	68.4	22.6
Kentucky ball clay [k]	4	1.2	.2	.2	.3	.6	1.5	49.9	31.4	14.7	-----	12.9	67.7	11.9
Talc [m]	*L*	nd	nd	6.9	30.5	nd	nd	55.9	1.3	5.4	-----	-----	-----	-----
Feldspar	*D*	13.4	2.0	nd	nd	nd	nd	65.6	18.4	-----	-----	-----	-----	-----

[a] Mineral compositions calculated by the method of H. S. Washington, J. Am. Ceram. Soc. **1**, 405 (1918) and assuming K_2O present as muscovite mica.
[b] For complete analysis see BS Tech. News Bul. **138**, p. 146 (1928).
[c] From J. Research NBS **19**, 65 (1937) RP1011.
[d] Composition supplied by S. C. Lyons. Alkalies reported as K_2O.
[e] Composition supplied by Kaolin Incorporated. Analysis includes also 0.08 percent of ZrO_2.
[f] From BS J. Research **11**, 327 (1933) RP594.
[g] Composition supplied by S. C. Lyons. Alkalies reported as Na_2O.
[h] From J. Am. Ceram. Soc. **18**, 163 (1935). Value for TiO_2 includes ZrO_2.
[i] Composition of clay from same deposit as sample tested, supplied by Bureau of Mines.
[j] Spectographic determinations indicated 0.17% of ZrO_2, 0.15% of CaO.
[k] From J. Am. Ceram. Soc. **21**, 371 (1938).
[l] Composition supplied by the H. C. Spinks Clay Co. Table does not include values determined for FeS_2, CO_2, P_2O_5, SO_3, and MnO.
[m] From J. Am. Ceram. Soc. **18**, 259 (1935).
[n] Excess Al_2O_3 may be present as bauxite.

The study was amplified to include several clays in addition to those used in bodies 27 and 35, as follows:

Georgia "soft" kaolin used in a previous study.[5]

Two fractions (*Gf* and *Gc*) of a Georgia "hard" kaolin supplied by S. C. Lyons.[6] Approximately 97 percent of fraction *Gf* consisted of particles 2 microns and smaller in diameter, whereas about 50 percent of fraction *Gc* was coarser than 7 microns. Diffraction patterns of each fraction showed identifiable lines of kaolinite only.

Two fractions of a Vermont kaolin were supplied by S. C. Lyons, who reports the following particle-size analyses:

Finer than	Coarse fraction (*Vc*)	Fine fraction (*Vf*)
Microns	%	%
10	28	100
4	8	98
1	6	60

X-ray diffraction patterns showed unmistakable lines for mica, quartz, and kaolinite in the coarse fraction. Mica lines were not discernible in the pattern for the fine fraction. (The patterns were made and interpreted by H. F. McMurdie.)

Florida kaolin designated *E* in table 2.[7]

Zettlitz kaolin, a portion of the international standard material described in the National Bureau of Standards Technical News Bulletin 138 (1928) and for which a heating curve has been published.[8]

English china clay, additional values for which have been published.[9]

Tennessee ball clay (designated *J* in table 2) supplied by Hewitt Wilson.

Alabama kaolin (designated *T* in table 2) supplied by Hewitt Wilson.

The bentonite used as an admixture was estimated, by petrographic examination, to be approximately 80 percent montmorillonite. (Examination by H. Insley.)

The mica used as an admixture was muscovite and had been passed dry through a No. 325 U. S. Standard Sieve.

The feldspar used as an admixture had been reground, and at least 95 percent of the particles were under 10 microns in diameter.

III. METHODS

Specimens for length-change determinations were equilateral triangular prisms, approximately 0.5 cm^2 in cross-sectional area and 5 cm long. They were obtained by grinding pieces which had been formed from plastic masses or by pressing. The pressed specimens

[5] R. F. Geller, D. N. Evans, and A. S. Creamer, BS J. Research **11**, 327 (1933) RP594.
[6] S. C. Lyons, Bul. Am. Ceram. Soc. **18**, 321 (1939). The fine and coarse fractions are identified by the letters *D* and *E*, respectively, in his publication.
[7] This clay is designated by the letter X in the report by T. A. Klinefelter and W. W. Meyer, J. Am. Ceram. Soc. **18**, 163 (1935).
[8] Herbert Insley and Raymond H. Ewell, J. Research NBS **14**, 615 (1935) RP792.
[9] William W. Meyer and Theron A. Klinefelter, J. Research NBS **19**, 65 (1937) RP1011.

were usually made up with 15 percent of water, and the pressure was approximately 2,400 lb/in.^{2}, or 170 kg/cm.^{2} The length of each specimen was determined directly, before and after the tests, by measurements at each of the three long edges with a vernier caliper reading to 0.02 mm. By this means any appreciable deformation of a specimen could be detected.

The apparatus for measuring the length changes was adapted for use in an electrically heated furnace in which the heating chamber is a porcelain tube 63 cm long and 2 cm inside diameter. The platinum resistance winding extends over about 16 cm of the central portion of the tube. The device (fig. 1) is, in principle, the same as the fused-quartz dilatometer described by Hidnert and Sweeney,[10] the fused quartz being replaced by porcelain. A tripod of porcelain rods supports a gage reading to 0.01 mm, and a fourth porcelain rod extends from the top of the specimen to the stem of the gage. Principally because of the spring pressure in this gage, the specimens were under a total load varying from approximately 150 g at the beginning to 100 g at the end of the test. The arrangement, which will be referred to as the porcelain dilatometer, was calibrated by using specimens of fused MgO. This MgO was taken from the same shipment of material used by Heindl [11] in his study of thermal expansions to 1,800° C. For the calibration tests, appropriate specimens for the porcelain dilatometer, and also for the interferometer, were formed by using finely ground material (through a 400-mesh sieve) and a solution of gum tragacanth. The dried specimens were calcined and then heated to 1,750° C in an Arsem furnace. The rates of heating and cooling used in the calibration tests, and in the later tests of clays and bodies, are shown in figure 2.

In addition to calibrating the dilatometer, the net shrinkage indicated by the gage readings could be checked by comparison with the shrinkage obtained directly from measurements of the prisms before and after the test. It was found that the total length change of clay specimens as shown by the gage was consistently about 0.3 percent greater than that calculated from the direct measurements. This discrepancy was independent of the amount of shrinkage and is believed to have been caused by "adjustments" of the contacts at the ends of the specimen, probably during the latter portion of the test. By adjustments is meant the probable conforming of the ends of the specimens, which were comparatively uneven because of the friable nature of dry clay, to the contour of the top and bottom dilatometer contacts.

Tests with the MgO indicated that the corrections to be applied to the gage readings are the same as the thermal-expansion values for the porcelain rods, as they should be theoretically. For readings obtained at temperatures above the upper limit of the interferometer, it was necessary to extrapolate the curve for the porcelain rods. Since Heindl's values above the range of the interferometer also are based on an extrapolated correction curve, one cannot say with certainty which set of results more nearly represents the true expansion of MgO. Naturally, all of the data presented here for length changes obtained with the porcelain dilatometer involve the same extrapolated correction values.

[10] Peter Hidnert and W. T. Sweeney, BS J. Research **1**, 771 (1928) RP29.
[11] R. A. Heindl, BS J. Research **10**, 715 (1933) RP562.

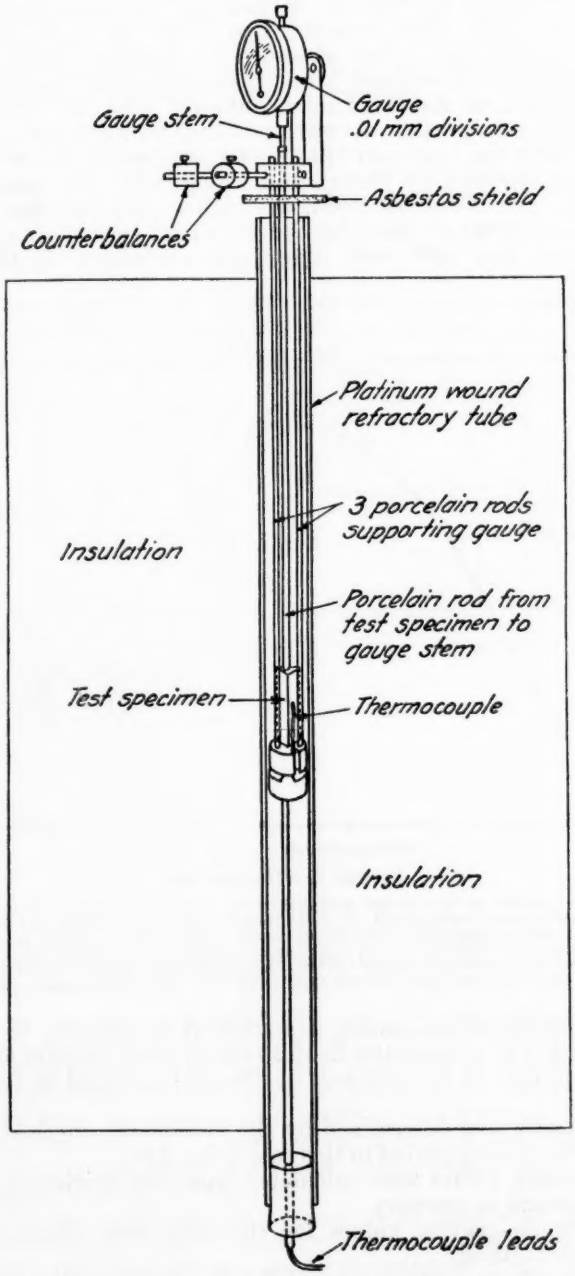

FIGURE 1.—*Porcelain dilatometer.*

Apparatus designed for measuring length changes of clay and body specimens during initial heating.

Values obtained for MgO by Heindl and by the authors are given in table 3. This table contains also values for a fine fraction of Georgia kaolin, and values obtained for Zettlitz kaolin by Steger (footnote 1), by Heindl and Mong,[12] and in the present study. The length changes for Zettlitz kaolin, obtained with the interferometer, are significantly greater at corresponding temperatures than those obtained with the porcelain dilatometer, and are in better agreement with those reported by Heindl and Mong, who also used the interferometer. On the other hand, the values with the dilatometer are greater than those obtained by Steger, whose specimens were 10 mm in diameter and 100 mm long. The inference is that length

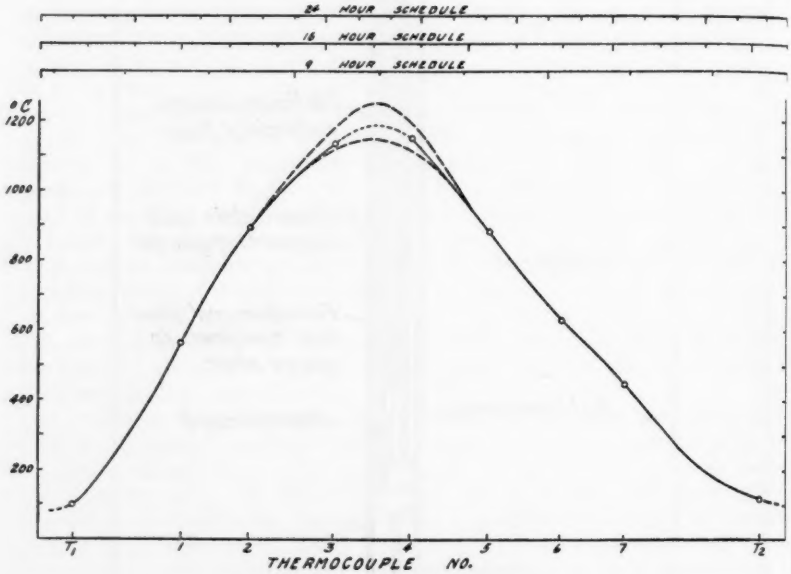

FIGURE 2.—*Heating rates.*

These curves are based on temperatures indicated by seven thermocouples and two thermometers (T_1 and T_2) in the electrically heated tunnel kiln at the National Bureau of Standards and show the heating rates followed in length-change tests both in the dilatometer and for specimens under no load.

The time-temperature relations between approximately 900° C and the end temperatures are the same regardless of the maximum temperature of the test. Above 900° C the curves diverge as indicated by the broken lines. The 9-, 16-, and 24-hr schedules apply to each one of the various heating curves.

changes during initial heating are affected by the size of the specimen. As will be shown later in this report, these changes are affected also by the rate of heating and by the method used in forming the specimens.

Absorptivity was determined by the well-known method of boiling in water, the boiling period in this case being 2 hr.

Bulk-density values were calculated from the weights of the specimens in air and in mercury.

True specific-gravity values for the mica were obtained by the pycnometer method.

Thermal effects were measured by the Le Chatelier differential-thermocouple method, using a Chromel-Alumel thermocouple and a

[12] Raymond A. Heindl and Lewis E. Mong, J. Research NBS 23, 427 (1939) RP1243.

type K potentiometer, artificial alpha-alumina as the reference material and a heating rate of 2°C/min.

TABLE 3.—*Length-change values obtained with the interferometer and with the porcelain dilatometer in this investigation, compared with results obtained by other investigators*

[Values preceded by (−) indicate contraction]

From room temperature to—	Porcelain [a]	Electrically fused MgO						Kaolin Z (Zettlitz)						Kaolin Gf (fine fraction)	
		[b]	Schedule 9 hr [a] (1)	Schedule 9 hr [a] (2)	Schedule 24 hr [a] (1)	Schedule 24 hr [a] (2)	Heindl [d]	Schedule 16 hr [b] (1)	Schedule 16 hr [b] (2)	Heindl and Mong [b, e]	Steger [f]	[c]		[b]	[c]
°C	%	%	%	%	%	%	%	%	%	%	%	%		%	%
100	0.020	0.070	0.08	0.06	0.07	----	0.08	0.03	−0.10	----	----	0.02		−0.05	0.03
200	.055	.190	.19	.17	.19	0.19	.19	.07	−.02	0.0	0.1	.08		−.10	.04
300	.095	.317	.32	.31	.32	----	.31	.18	.07	.05	----	.15		.00	.10
400	.140	.446	.45	.45	.45	.45	.45	.27	.15	.14	.2	.20		.07	.17
500	.190	.582	.59	.58	.57	----	.59	[h]	[i]	[j]	[k]	[l]		[m]	[n]
600	.245	.721	.72	.72	.72	.72	.73	−.82	−1.00	−.78	.1	−.20		−1.30	.55
700	.300	.866	.89	.86	.86	----	.87	−1.22	−1.40	−1.10	−.4	−.67		−1.98	−1.20
800	.355	1.012	1.02	1.00	1.01	1.14	1.00	−1.52	−1.70	−1.43	−.7	−.93		−2.50	−1.58
900	.410	1.162	1.17	1.13	1.14	----	1.15	−1.85	−2.10	−1.74	−.8	−1.10		−2.85	−1.87
1,000	(.470)	----	1.31	1.27	1.27	1.27	1.30	----	−3.65	−3.22	−1.8	−2.63		−4.40	−3.16
1,100	(.530)	----	1.47	1.41	1.41	1.41	1.47	----	----	----	−2.4	−3.50		----	−3.54
1,200	(.590)	----	1.62	1.59	1.53	1.54	1.62	----	----	----	−6.5	−8.66		----	−7.63
1,250	(.620)	----	----	1.62	----	1.59	1.70								
R. T. [g]	----	----	.03	.02	.04	.06	----	----	----	----	----	----		----	----

[a] Values obtained with the interferometer and used to correct the gage readings. Values given parenthetically are extrapolated.
[b] Values obtained with the interferometer. Columns (1) and (2) indicate duplicate tests.
[c] Values obtained with the porcelain dilatometer.
[d] BS J. Research **10**, 715 (1933) RP562.
[e] J. Research NBS **23**, 427 (1939) RP1243.
[f] Ber. deut. keram. Ges. 19, 2 (1938).
[g] Reading upon return to room temperature.
[h] Maximum expansion 0.39% at 498°.
[i] Maximum expansion 0.26% at 496°.
[j] Maximum expansion 0.33% at 545°
[k] Maximum expansion 0.3% at 560°.
[l] Maximum expansion 0.30% at 520°.
[m] Maximum expansion 0.14% at 508°.
[n] Maximum expansion 0.25% at 505°.

IV. RESULTS

1. CLAYS

The curves in figure 3 show the characteristic differences in length changes between three typical primary kaolins (*Z*, *P*, and *K*) and four secondary kaolins (*S*, *E*, *U*, and *T*). In figure 4, which shows the length changes for three ball clays, the curves for kaolins *P* and *E* are repeated to emphasize the similarity of the ball clays to the primary kaolins in the range from room temperature to 1,000° C.

The curves in figure 5, drawn on an enlarged vertical scale, show more clearly how the behavior of kaolin *K* differs from the others shown in figures 3 and 4. These curves show also the effect of predrying at 110° versus air-drying (room temperature), and of plastic forming versus "dry-press" forming.

In figure 6, the curves shown as continuous lines were taken from reports by Steger (footnote 1) and by Rieke and Wen.[13] Curves for kaolin *K* and ball clay *CC* are given to facilitate comparison. By calculation, kaolin *K* contains 7.6 percent of feldspar and mica (table 2), of which 4.9 percent is assigned to mica. The informa-

[13] R. Rieke and Pu-Yi Wen, Ber. deut. keram. Ges. **20**, 43 (1939).

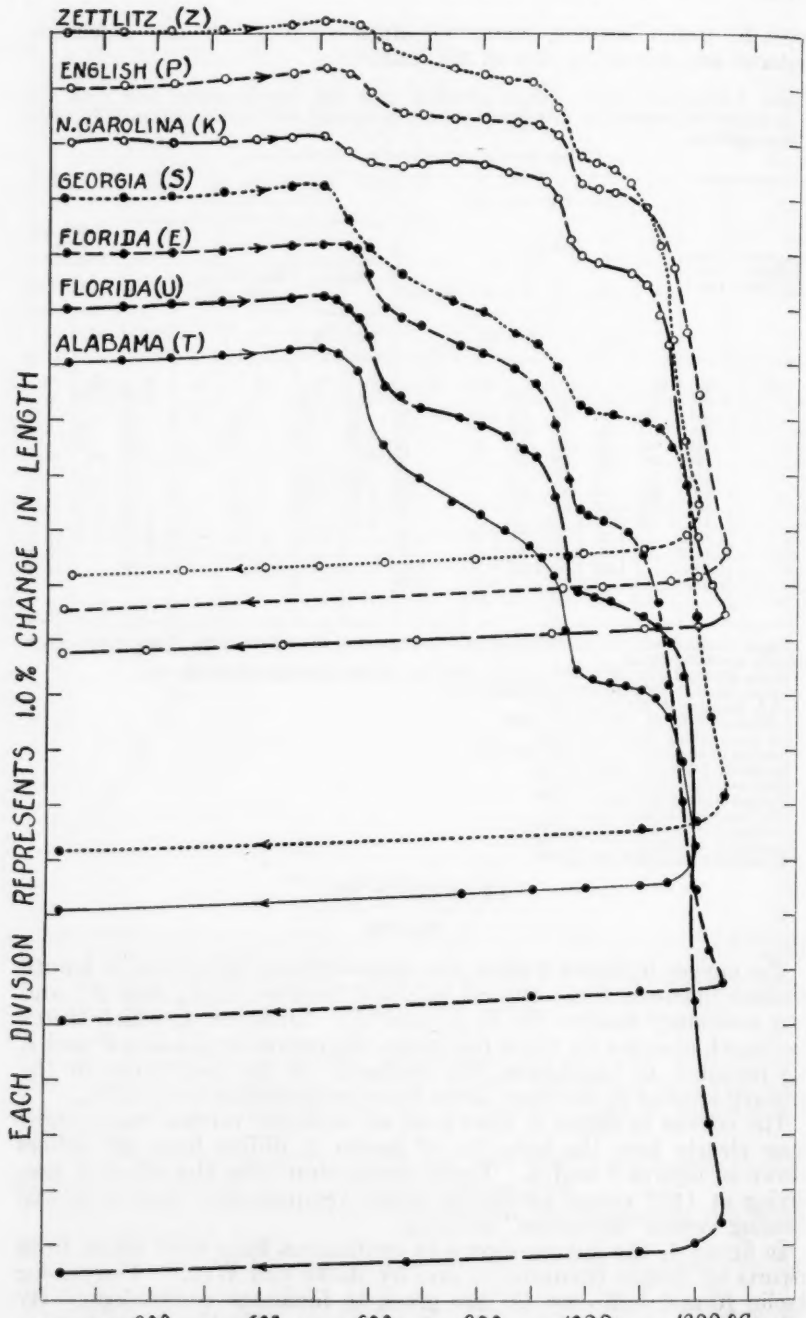

FIGURE 3.—*Length changes of three primary kaolins (Z, P, and K) and four secondary kaolins during initial heating and cooling.*

All specimens were pressed, dried at 110° C before testing, and heated on the 16-hr schedule.

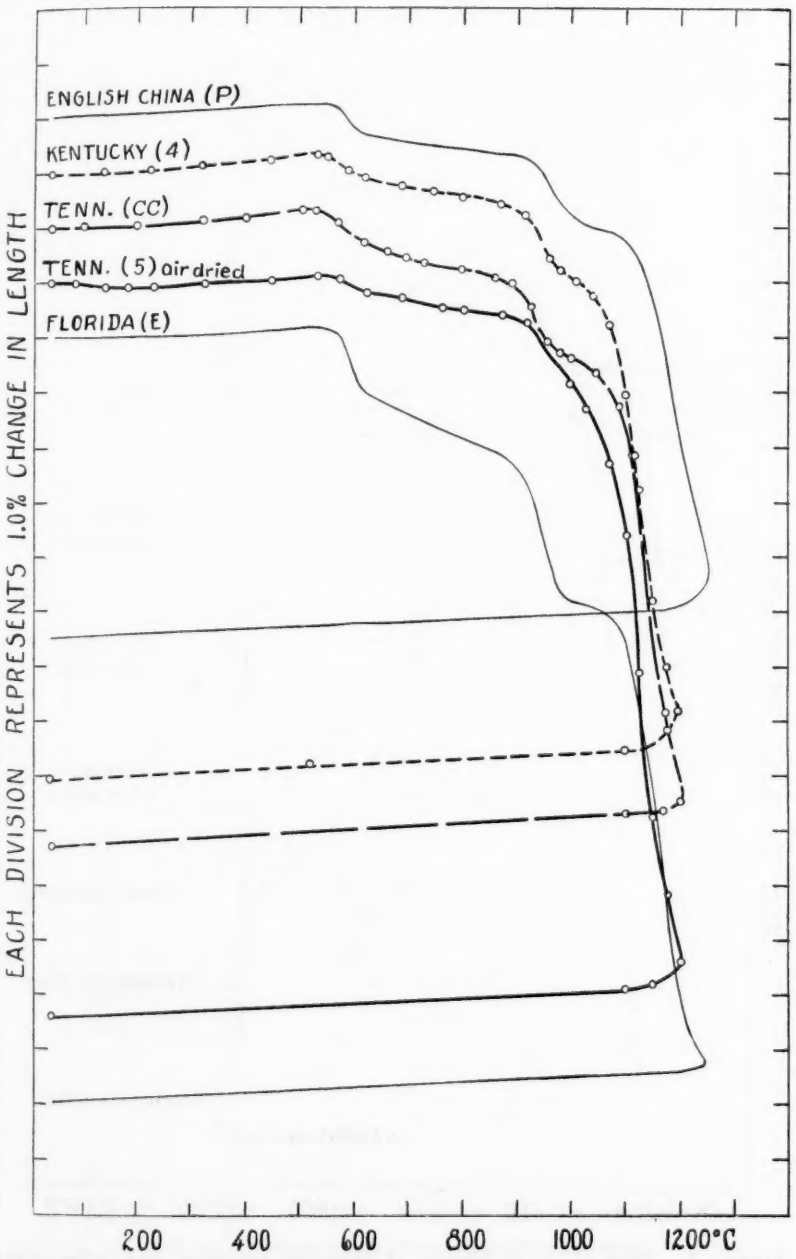

FIGURE 4.—*Length changes of three ball clays during initial heating and cooling.*

Curves for kaolins *P* and *E* are repeated from figure 3 to facilitate comparison. All specimens were pressed and, excepting clay 5, dried at 110° C before testing. Clays 4 and 5 were heated on the 16-hr schedule and clay *CC* on the 24-hr schedule.

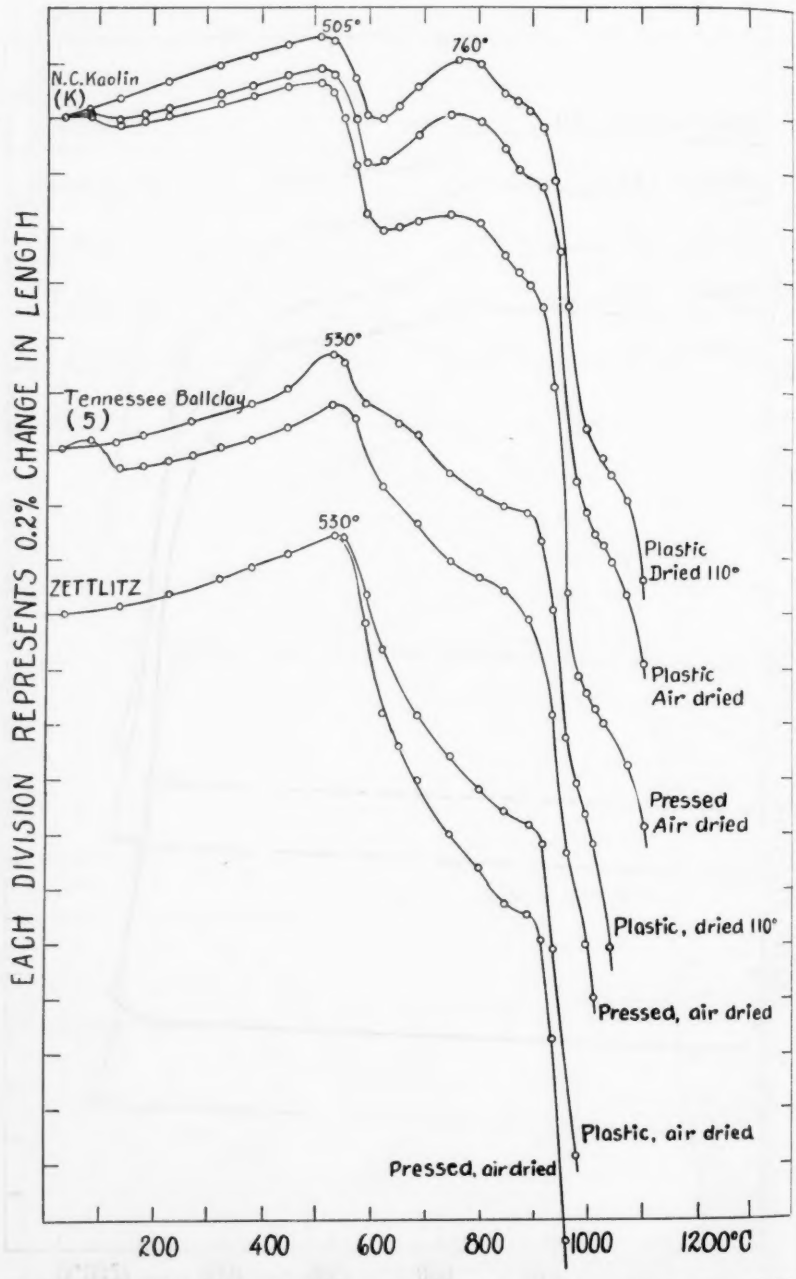

FIGURE 5.—*Effect on length changes of preparing specimens from either plastic (hand-wedged) bodies or by dry-pressing; also, effect of drying in air (room temperature) and at 110° C.*

The clays were heated on the 16-hr schedule. Note the expansion of kaolin *K* between 600° and 760° C;

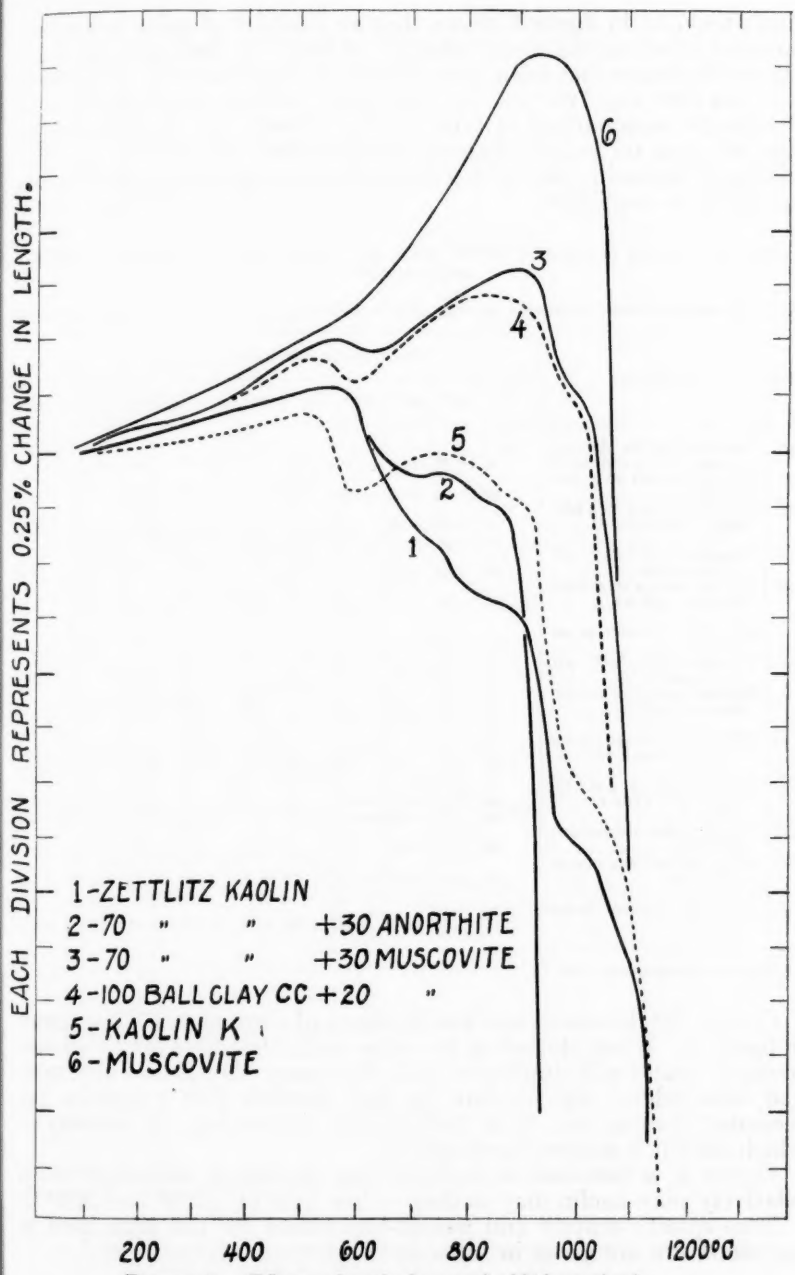

FIGURE 6.—*Effect on length change of additions of mica.*

A curve for kaolin *K* is repeated to facilitate comparison. Curves 1, 2, and 3 are taken from a report by W. Steger (Ber. deut. keram. Ges. **19**, 2, 1938) and curve 6 from a report by R. Rieke and Pu-Yi Wen (Ber. deut. keram. Ges. **20**, 43, 1939).

tion presented in figure 6 shows that an addition of mica has a pronounced effect on the length changes of kaolin *Z* during initial heating and indicates that mica may account for the expansion of kaolin *K* between 600° and 760° C. Several other variables were studied and the results, summarized in table 4, show clearly the dominant influence of mica on length changes between 500° and 1,000° C. The effects of bentonite, and of the state of flocculation or deflocculation, appear to be negligible.

TABLE 4.—*Length changes of several clays as received and after various additions and treatments*

[All specimens were formed by pressing and were dried in air (room temperature) unless otherwise stated.]

Clay	Treatment	Schedule	Length change from room temperature to (°C)								
			135°	500°	600°	700°	800°	900°	1,000°	1,100°	1,200°
S	Secondary kaolin. Pressed as received. Dried 110° C.	*hr.* 16	% +0.03	% +0.21	% −1.00	% −1.65	% −2.10	% −2.62	% −4.85	% −5.05	% −7.65
S	80 g kaolin and 20 g bentonite	16	+.03	+.21	−0.90	−1.50	−2.00	−2.60	−4.80	−5.04	−9.16
S	100 g kaolin and 10 g feldspar. Dried 110° C	9	+.03	+.26	−.10	−1.15	−1.54	−1.86	−3.65	−3.95	−9.41
	Do	24	+.04	+.26	−.75	−1.88	−1.72	−2.05	−3.75	−4.30	.....
S	Flocculated with HCl. pH of suspension 4.2	16	+.03	+.22	−.85	−1.53	−1.98	−2.50	−4.67	−4.87	−7.64
S	Deflocculated with sodium tannate. pH 6.9	16	−.02	+.22	−.87	−1.55	−2.01	−2.55	−4.71	−4.91	−8.10
5	Ball clay. Pressed as received	16	−.07	+.11	−.07	−0.31	−0.47	−0.66	−1.86	−4.58	−12.34
5	Flocculated with HCl. pH of suspension 3.9	16	+.02	+.24	+.03	−.25	−.39	−.53	−1.76	−4.67	−12.22
5	Deflocculated with sodium tannate. pH 5.7	16	.00	+.21	.00	−.22	−.36	−.50	−1.83	−5.59	−12.64
CC	Ball clay. Pressed as received. Predried 110° C	9	+.03	+.22	−.01	−.56	−.82	−1.05	−2.37	−3.30	−9.00
	Do	24	+.05	+.31	−.17	−.55	−.76	−1.07	−2.37	−3.50	−10.41
CC	100 g clay and 20 g of feldspar. Dried 110° C	9	+.06	+.31	+.11	−.29	−.50	−0.67	−1.93	−5.25	[a]−12.00
	Do	24	+.04	+.30	−.14	−.40	−.59	−.80	−2.06	−6.93	[a]−12.74
CC	100 g clay, 20 g feldspar and 20 g flint	16	+.04	+.37	+.13	−.06	−.16	−.27	−1.16	−3.96	−9.85
CC	100 g clay and 20 g muscovite mica	16	+.07	+.40	+.31	+.52	+.69	+.66	+0.25	−3.45	[a]−7.49
J	Ball clay. Pressed as received	16	+.05	+.43	+.40	+.38	+.31	+.23	−.41	−2.44	−8.35

[a] Maximum temperature 1,180° C.

Curves for the coarse and fine fractions of clays *G* and *V* are shown in figure 7. When plotted on the same scale, the curve for *Vc* (coarse fraction) practically duplicates that of primary clay *Z* to which mica had been added (fig. 6), but the fine fraction (Vf) resembles the secondary kaolins (fig. 3) in its behavior, rather than the primary to which class it is assigned geologically.

Figure 8 is included to indicate the continued shrinkage which relatively pure kaolin may undergo when held at 1,200° to 1,250° C.

True specific-gravity and weight-loss values for the mica used as an admixture are given in table 5.

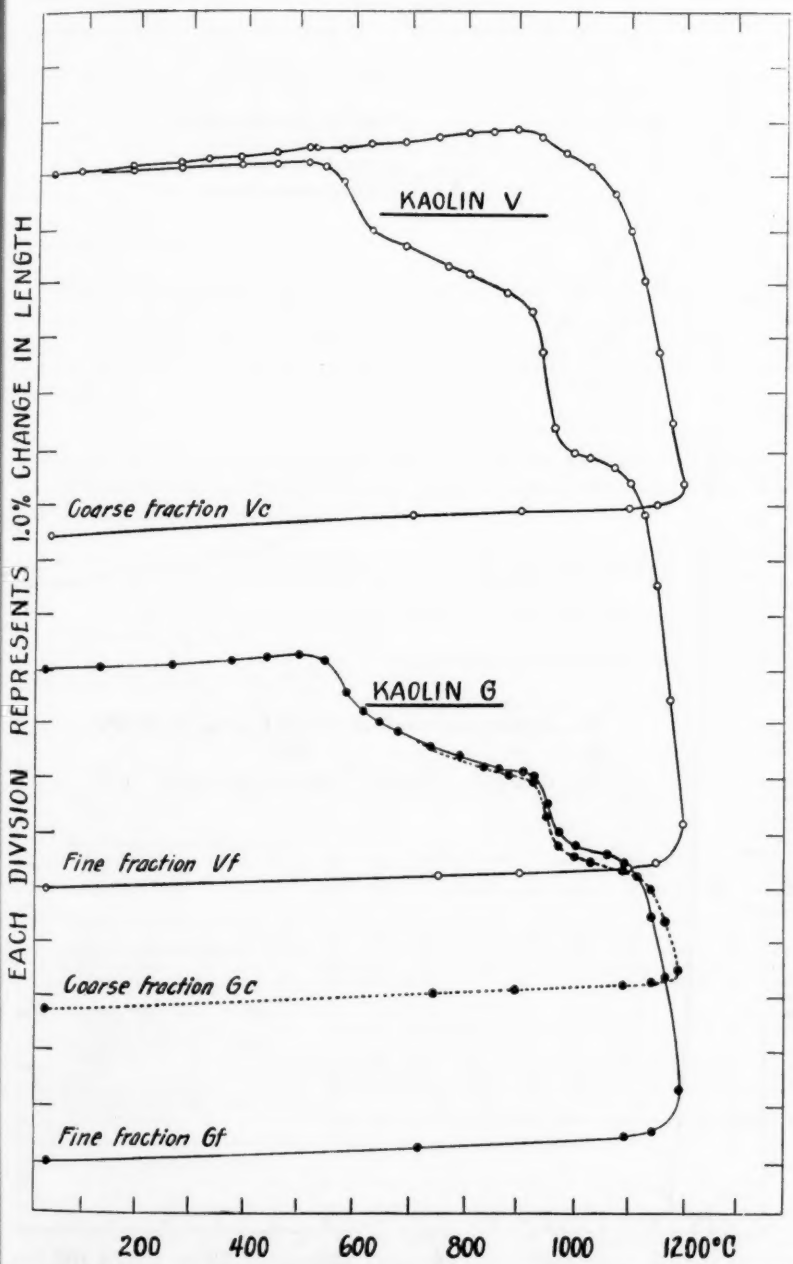

FIGURE 7.—*Length changes of coarse and fine fractions of primary Vermont kaolin V and secondary Georgia kaolin G.*

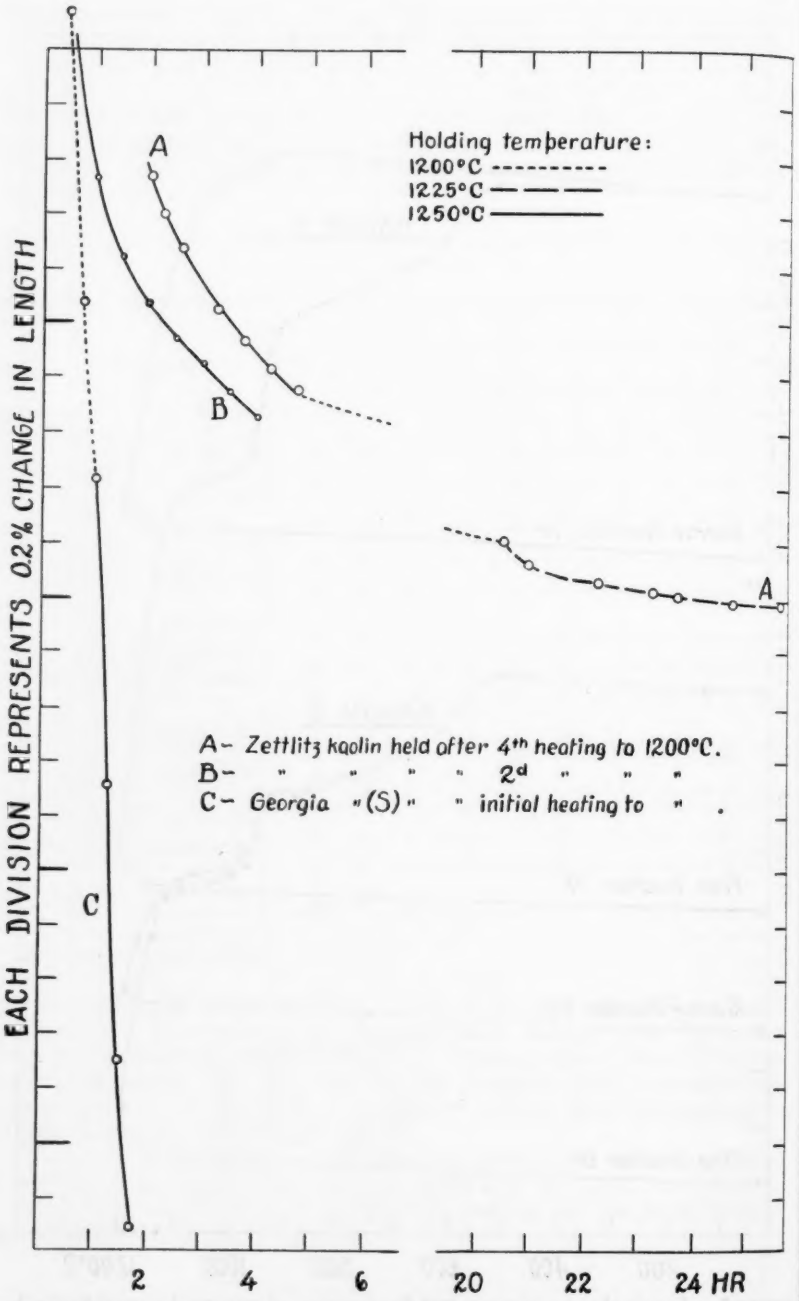

FIGURE 8.—*The continued shrinkage of two kaolins when held at 1,200°, 1,225° or 1,250° C.*

TABLE 5.—*True specific gravity of mica (25°/25°) and weight loss after various heat treatments*

Holding temperature	Specific gravity		Weight loss
° C			%
Raw	2.848	2.849	[a] 0.12
600	2.823	2.822	1.57
900	2.664	2.663	4.70
1,000	2.651	2.650	4.71
1,200	2.660	2.660	4.74

[a] Loss after holding at 110° C.

Differential heating curves, showing thermal effects, were obtained for kaolins *E* and *Z*. The endothermic effect was maximum at 578° and 574° C, respectively, and the exothermic effect was maximum at 964° and 961° C, respectively. There was no evidence of other heat effects.

2. BODIES

Results of the length-change observations on commercial body *H*, and laboratory-prepared bodies 27 and 35, are summarized in table 6 and in figures 9 and 10.

TABLE 6.—*Effects of various methods of forming, and two heating rates, on the length changes of three bodies*

[All specimens dried in air (room temperature) unless otherwise noted.]

Body	Treatment	Schedule	Length change from room temperature to—(° C)								
			200°	500°	600°	700°	800°	900°	1,000°	1,100°	1,190°
		hr	%	%	%	%	%	%	%	%	%
H	Deaired and extruded	9	+0.11	+0.57	+0.79	+0.77	+0.74	+0.71	+0.43	0.00	−2.74
H	do	24	+.09	+.56	+.77	+.76	+.72	+.70	+.42	−.38	−4.23
H	Deaired and extruded. Dried at 100° C	24	+.09	+.56	+.77	+.75	+.72	+.70	+.43	−.21	−3.81
27	Hand-wedged and dried at 110° C	9	+.12	+.42	+.48	+.51	+.54	+.49	+.07	−4.50	[a] −8.29
27	do	24	+.07	+.37	+.40	+.45	+.48	+.41	−.02	−5.27	[a] −9.02
27	do	24	+.09	+.37	+.41	+.45	+.46	+.39	−.08	−5.42	[a] −8.99
35	Hand-wedged and dried at 110° C	9	+.10	+.45	+.52	+.46	+.42	+.41	+.06	−.28	−8.80
35	Deaired and extruded	9	+.11	+.46	+.46	+.44	+.40	+.35	+.06	−2.30	−10.60
35	Hand-wedged	24	+.09	+.45	+.46	+.44	+.42	+.38	+.10	−1.85	−8.86
35	Deaired and extruded	24	+.12	+.46	+.43	+.40	+.38	+.33	.00	−3.15	−9.93
35	Pressed with 15% water. Dried 110° C	9	+.13	+.48	+.49	+.39	+.34	+.24	−.07	−2.75	−12.35
35	Pressed with 8% water. Dried 110° C	9	+.13	+.49	+.49	+.37	+.30	+.22	−.20	−2.86	−12.00
35	do	24	+.12	+.46	+.39	+.30	+.27	+.18	−.31	−5.76	−13.33
35	Pressed with 3% water	9	+.07	+.40	+.33	+.20	+.13	−.03	−.50	−3.20	−13.61
35	Pressed with 3% water. Dried 110° C	9	+.11	+.44	+.37	+.26	+.18	+.08	−.40	−3.33	−11.95

[a] Maximum temperature 1,160° C.

Body *H*, typical of the fine earthenware (or semiporcelain) type, shows the same general trend in behavior as the talcose bodies 27 and 35 which were heated to practical vitrification. There is less than 1-percent change in length until the almost abrupt shrinkage beginning above 1,100° C in body *H*, and above 1,050° C in the other two bodies.

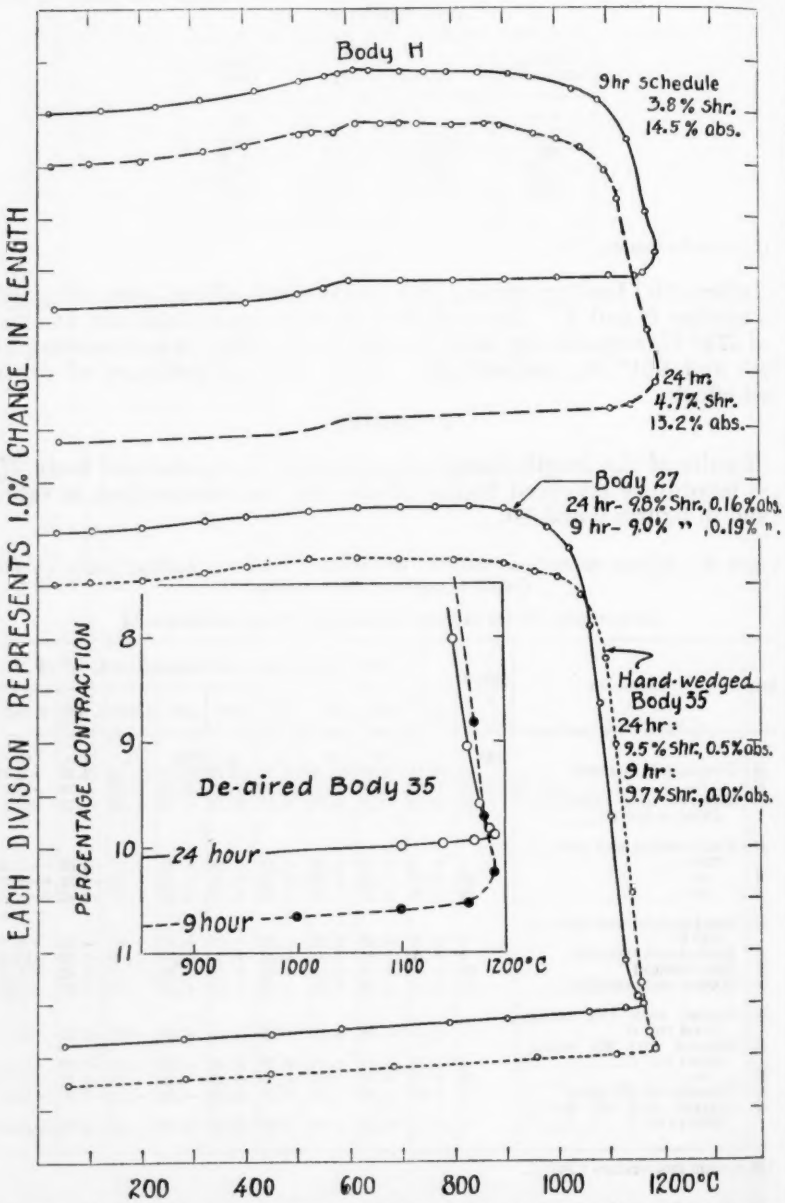

FIGURE 9.—*Length-change curves, shrinkage (shr.), and absorption (abs.) for commercial earthenware body H (deaired and extruded) and laboratory talcose bodies 27 and 35.*

Shrinkage values show total net length change during heating and cooling as indicated by the gage. The curves for hand-wedged bodies 27 and 35 were obtained on the 24-hr schedule. The curves for deaired body 35 (insert) show how the shrinkage during the 9-hr schedule exceeded that during the 24-hr schedule.

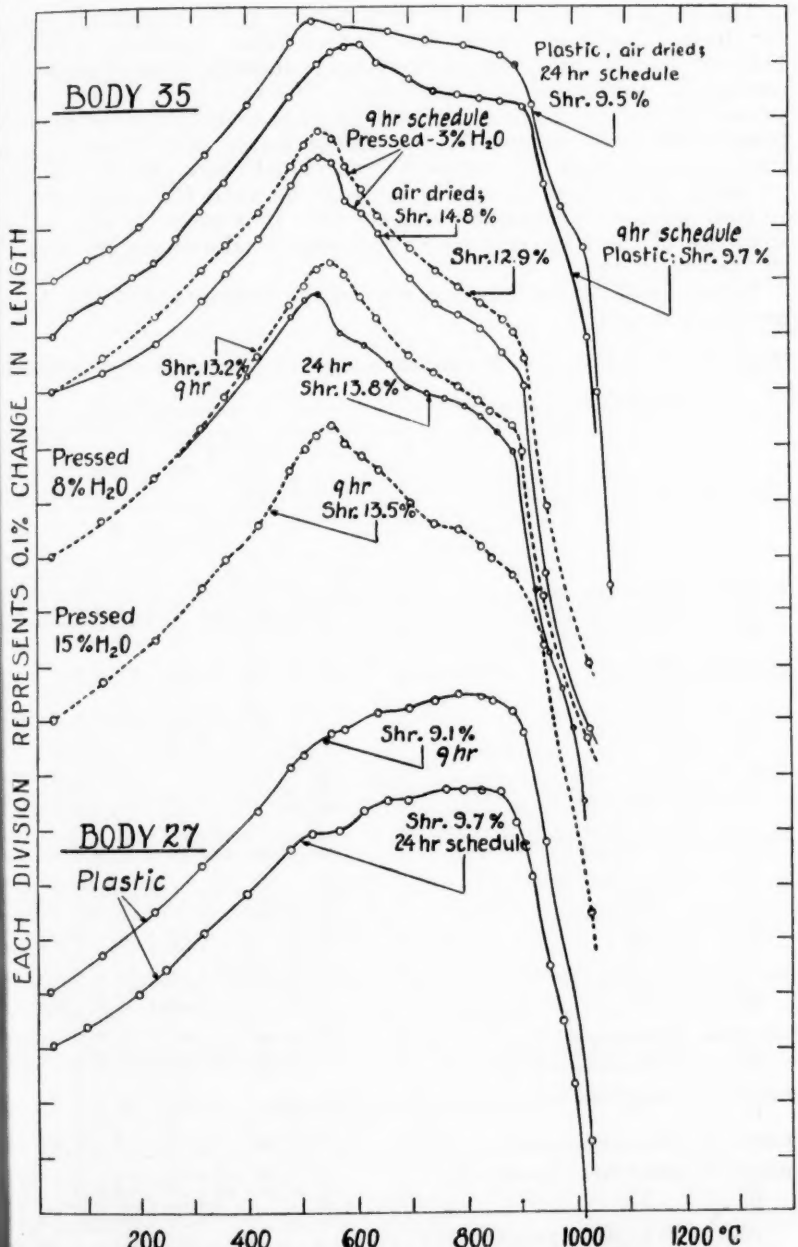

FIGURE 10.—*Length changes of bodies 27 and 35 showing effect of method of forming.*

Unless otherwise noted, the specimens were dried at 110° C. Shrinkage (shr.) values are for specimens after cooling to room temperature.

The insert in figure 9 shows that portion of the shrinkage curves for deaired body 35 during the 9- and 24-hr schedules, which is believed to illustrate why a body may undergo greater shrinkage during the shorter of two schedules. The curves in figure 10 are presented to show the greater shrinkage of pressed specimens, as compared with those formed from a plastic mass. The same relation may be noted from the curves for individual clays (fig. 5). Figure 10 shows also the shrinkage of body 35 between 600° and 900° C, in contrast to the expansion of body 27. It is probably due to the influence of the relatively high percentage of the secondary clay *U* in the former body.

Values for several other properties of the bodies (and of the clays) are given in table 7.

TABLE 7.—*Some properties, in addition to length changes, of the clays and bodies tested*

[Specimens made by pressing with 15 percent of water unless otherwise stated.]

Material	Treatment and method of forming	Method of test[a]	Maximum temperature of heating	Schedule	Maximum expansion at		Bulk density			Absorption	Total shrinkage[a]
							Before	After	Δ		
			°C	hr	°C	%			%	%	%
Kaolin *S*	Pressed as received	*L*	1,250	16	445	0.22				13.0	11.6
Do	80 g of kaolin, 20 g of bentonite	*L*	1,200	16	505	.21	1.532	1.954	21.6	13.8	10.3
Do	Flocculated with HCl	*L*	1,200	16	475	.23	1.623	1.823	11.0	17.3	8.8
Do	Deflocculated with Na-tannate	*L*	1,200	16	505	.23	1.712	1.906	10.2	15.0	9.1
Kaolin *Gf*	Fine fraction	*L*	1,200	16	505	.27	1.635	1.899	13.9	15.7	8.9
Kaolin *Gc*	Coarse fraction	*L*	1,200	16	505	.26	1.776	1.850	4.0	16.8	5.8
Kaolin *Vf*	Fine fraction	*L*	1,200	16	505	.19	1.477	1.978	25.3	13.9	12.0
Do	do	*NL*	1,180	9			1.495	1.822	18.0	18.1	10.2
Do	do	*NL*	1,180	24			1.501	1.941	22.7	14.8	11.8
Kaolin *Vc*	Coarse fraction	*L*	1,200	16	890	.75	1.701	1.927	11.7	14.0	6.7
Do	do	*NL*	1,180	9			1.692	1.801	6.0	17.8	3.8
Do	do	*NL*	1,180	24			1.715	1.878	8.7	15.5	4.5
Kaolin *K*	Clay as received. Hand-wedged	*L*	1,250	16	505	.17	1.505	1.761	17.0	19.1	7.9
Do	Clay as received. Pressed	*L*	1,250	16	505	.12	1.596	1.848	15.8	17.4	8.9
Kaolin *U*	Pressed as received	*L*	1,250	9	505	.15	avg. 1.530	2.334	34.4	5.5	17.4
Do	do	*L*	1,250	16	505	.22		2.379	35.7	4.3	17.6
Do	do	*L*	1,250	24	460	.13		2.424	36.9	3.4	18.1
Do	do	*NL*	1,180	9			1.508	1.758	14.2	20.2	9.5
Do	do	*NL*	1,180	24			1.526	1.933	21.0	14.8	11.8
Kaolin *Z*	Pressed as received	*L*	1,200	16	520	.30	1.607	1.928	16.6	14.7	9.8
Do	do	*NL*	1,180	9			1.607	1.803	10.9	18.3	7.7
Do	do	*NL*	1,180	24			1.606	1.890	15.0	16.2	8.9
Ball clay 5	Pressed as received	*L*	1,200	16	530	.16	1.677	2.283	26.5	4.4	13.2
Do	Flocculated with HCl	*L*	1,200	16	535	.26	1.667	2.226	25.1	5.2	13.2
Do	Deflocculated with Na-tannate	*L*	1,200	16	535	.23	1.700	2.270	25.1	3.9	13.2
Ball clay 4	Pressed as received	*NL*	1,180	9			1.752	2.103	16.7	9.6	9.3
Do	do	*NL*	1,180	24			1.750	2.137	18.1	8.7	9.9
Ball clay *J*	Pressed as received	*L*	1,200	16	550	.47	1.778	2.140	16.9	8.6	9.2
Ball clay *CC*	100 g of clay and 20 g of feldspar	*L*	1,180	9	555	.34	1.755	2.352	25.4	2.1	12.6
Do	do	*L*	1,180	24	505	.30	1.755	2.384	26.4	1.0	13.0
Do	do	*NL*	1,180	9			1.758	2.340	24.9	2.5	11.9
Do	do	*NL*	1,180	24			1.752	2.395	26.8	0.9	12.3
Do	100 g of clay, 20 g of feldspar, 20 g of flint	*NL*	1,180	9			1.798	2.244	19.9	4.2	9.8
Do	do	*NL*	1,180	24			1.796	2.270	20.8	4.1	10.2
Do	do	*L*	1,200	16	520	.38	1.798	2.285	21.3	3.5	10.6
Body *H*	Deaired and extruded	*L*	1,190	9	610	.80	avg. 1.810	1.907	5.1	14.5	3.7
Do	do	*L*	1,190	24	615	.78		1.946	7.0	13.2	4.5
Do	do	*NL*	1,190	9				1.913	5.7	14.2	3.8
Do	do	*NL*	1,190	24				1.913	5.7	14.1	3.9

See footnotes at end of table.

TABLE 7.—*Some properties, in addition to length changes, of the clays and bodies tested*—Continued

[Specimens made by pressing with 15 percent of water unless otherwise stated.]

Material	Treatment and method of forming	Method of test[a]	Maximum temperature of heating	Schedule	Maximum expansion at		Bulk density			Absorption	Total shrinkage[b]
							Before	After	Δ		
			°C	hr	°C	%			%	%	%
Body 27	Hand-wedged	L	1,160	9	790	.54		2.390	27.6	0.2	8.7
Do	do	L	1,160	24	765	.46	avg.	2.400	27.9	.2	9.5
Do	do	NL	1,190	9			1.730	2.362	26.7	.2	8.0
Do	do	NL	1,190	24				2.355	26.5	.3	8.5
Body 35	Pressed with 15 percent of H_2O	L	1,190	9	555	.53		2.447	32.5	.6	13.3
Do	do	NL	1,190	9			avg.	2.424	31.3	1.6	11.1
Do	do	NL	1,190	24			1.846	2.397	29.8	2.3	10.9
Body 35	Pressed with 8 percent of H_2O	L	1,190	9	555	.54	1.884	2.471	31.1	.4	12.8
Do	do	L	1,190	24	530	.47	1.884	2.331	23.7	.8	13.2
Do	Pressed with 3 percent of H_2O	L	1,190	9	530	.47	1.824	2.467	35.5	.6	12.5
Do	Dealred and extruded	L	1,190	9	610	.51	1.782	2.470	38.6	.4	11.3
Do	do	L	1,190	24	505	.47	1.783	2.448	37.3	.8	10.6
Do	Hand-wedged	L	1,190	9	610	.52		2.458	36.3	.0	9.4
Do	do	L	1,190	24	520	.47	avg.	.....	.....	.5	9.2
Do	do	NL	1,190	9			1.803	2.451	35.9	1.1	8.5
Do	do	NL	1,190	24				2.436	35.1	1.0	8.3

[a] *L* signifies that the specimen was tested under load in the porcelain dilatometer.
NL signifies that the specimen was under no superimposed load.
[b] Values are based on direct measurements before and after the test.

V. DISCUSSION

1. CLAYS

A reversal from expansion to contraction between 500° and 600° C, an appreciable increase in the contraction per unit temperature rise between 900° and 1,000° C and a comparatively abrupt contraction beginning at 1,050° to 1,100° C characterize the length changes for all the clays tested.[14] The reversal between 500° and 600° C, and the comparatively rapid contraction between 900° and 1,000° C, are in all probability associated with the loss of chemically combined water and with the formation of gamma-Al_2O_3. The final contraction accompanies a process known among ceramists as "vitrification," the exact physical chemistry of which is still obscure but involves increase in true density[15] and bulk density, and the formation of glass and of new or altered crystalline phases which may be submicroscopic in particle size.

a. BEGINNING OF CONTRACTION

The temperature at which a reversal from expansion to contraction takes place is affected by the rate of heating and by the nature of the clay, as the data in table 7 show, but not by the method of forming the specimens (fig. 5). It is, in general, higher for ball clays than for kaolins and higher for the more rapid heating rates.

[14] This generalization does not include the coarse fraction of Vermont kaolin, which fraction contains, by calculation, less than 30 percent of kaolinite.
[15] T. Nakai and Y. Fukami, J. Soc. Chem. Ind. (Japan), **37**, 430 (1934). Abs. in J. Amer. Ceram. Soc. **18**, 22 (1935).

b. LENGTH CHANGES BETWEEN 500° AND 900° C

If one assumes that the length changes of the secondary kaolins approximate those of pure kaolinite, then the normal behavior of kaolinite in the range 500° to 900° C is to contract about 3 percent. This shrinkage is slightly greater for dry-pressed specimens than for those formed from plastic masses, as shown in figure 5.

Feldspar and quartz counteract the contraction, but to a much smaller degree than does mica in equivalent amounts. That mica may alter the length-change behavior considerably has been shown by Steger and by Rieke and Wen (fig. 6). For clay *CC*, an addition of 20 g of mica to 100 g of the clay completely nullified the contraction, and the net change was an expansion of 0.26 percent (table 4). This effect of mica probably involves a reaction between it and the clay, because the changes caused by it cannot be wholly accounted for by calculations based on its expansion or altered specific gravity.

The data as arranged in table 8 indicate that the characteristic group differences in length change between 500° and 900° C for the secondary kaolins, as compared with ball clay and primary kaolins, are due to the mica content rather than to their geologic history. It is suggested that the lack of a close relation between mica content and contraction, for individual clays, may be caused by the state of subdivision of the mica. For example, the length changes for ball clays *J* and 5, and the fine fraction of clay *V*, are 0.2, 0.8, and 2.6 percent, respectively. The calculated mica contents are 16, 17, and 14 percent, respectively. Petrographic examinations (by H. Insley) showed the mica particles to be coarsest in clay *J* and finest in the clay *V* fraction. The particle size of the mica may affect not only the rate and temperature range at which it decomposes, but also the extent to which the decomposition products affect other constituents in a clay-mica mixture. Zwetsch [16] found, by X-ray examinations, that mica remains unaltered below 900° C,[17] and that a break-down to alpha-alumina, gamma-alumina, and leucite begins at about 950° C.

Several investigators [18] have proposed the formation of an anhydrous alumino-silicate, or "meta-kaolin", following the expulsion of combined water from the clay molecule (about 450° to 550° C). The results of de Keyser's [19] dielectric constant determinations are interpreted by him as supporting the meta-kaolin theory. This meta-kaolin presumably breaks down between 700° and 900° C. The curves obtained in this study, for both heat effects and length changes, do not indicate a phase change in this temperature range and, to that extent, support the claim (footnotes 8 and 15) that an anhydrous alumino-silicate is not formed.

---

[16] A. Zwetsch, Ber. deut. keram. Ges. **15**, 2 (1934).

[17] That diffraction patterns do not indicate an alteration in mica below 900° C, even though water of crystallization is given off at lower temperatures, may be explained by the finding of F. Rinne (Ber. Verhandl. sachs. Akad. Wiss. Leipzig, **76**, 261, 1924) that the crystal structure of muscovite was not destroyed by dehydration.

[18] R. Schwarz and G. Trageser, Chem. Erde **7**, 566 (1932). R. Schwarz and K. Nüchter, Ber. deut. keram. Ges. **15**, 514 (1934).
See also footnote 2.

[19] W. de Keyser, Ber. d. deut. keram. Ges. **21**, 29 (1940).

TABLE 8.—*Relation of mineral composition and length changes (average values)*

Material	Length change in the interval—(° C)				Mineral composition		
	500° to 900°	900° to 1,000°	1,000° to 1,100°	1,100° to 1,200°	Mica	Quartz	Kaolinite
	%	%	%	%	%	%	%
Ball clay *J*	0.2	0.6	2.1	5.9	16	18	58
Ball clay 5	.8	1.2	2.7	7.8	17	12	61
Ball clay 4	.9	1.5	1.9	6.0	10	12	68
Ball clay *CC*	1.3	1.3	.9	6.6	2	24	68
Average	0.8	1.1	1.9	6.6	11	16	64
Primary kaolin *K*	0.8	1.2	0.7	4.5	5	<1	90
Primary kaolin *P*	1.0	1.2	.3	3.4	13	2	80
Primary kaolin *Z*	1.4	1.4	1.0	5.1	7	1	85
Average	1.0	1.3	0.7	4.4	8	1	85
Secondary kaolin *E*	2.5	2.4	0.7	6.1	4	2	91
Secondary kaolin *U*	2.8	2.6	.4	6.9	1	2	96
Secondary kaolin *S*	2.8	2.1	.3	2.6	1	<1	97
Secondary kaolin *T*	3.6	2.3	.2	2.8	<1	<1	93
Average	2.7	2.3	0.4	4.6	2	1	94
Fine fraction, clay *V*	2.6	2.5	0.6	6.2	14	4	79

c. LENGTH CHANGES BETWEEN 900° AND 1,000° C

There seems to be complete unanimity of opinion in the literature that the accelerated shrinkage between 900° and 1,000° C accompanies the crystallization of amorphous alumina, derived from the kaolinite molecule, to form gamma-alumina. This has been discussed at length by Insley and Ewell (footnote 8), Heindl and Mong (footnote 12), and others (footnotes 1 and 2).

TABLE 9.—*Relation of alumina content of clays and the length change between 900° and 1,000° C*

Clay	Type	Length change	Al_2O_3 from kaolinite	Al_2O_3 from mica
		%	%	%
Vf	Primary	2.5	31	3.5
S	Secondary	2.1	38	0.3
E	do	2.4	36	1.2
U	do	2.6	38	0.4
T	do	2.3	37	.0
Average		2.4	36	1.1
Z	Primary	1.4	33	1.7
P	do	1.2	32	3.5
K	do	1.2	36	1.3
4	Ball clay	1.5	27	2.6
5	do	1.2	24	4.4
CC	do	1.3	27	0.4
Average		1.3	30	2.3
Vc	(a)	0.6	11	7.8
J	Ball clay	.6	23	4.0
Average		0.6	17	5.9

[a] Coarse fraction of primary kaolin *V*.

The data as arranged in table 9 show a fairly good direct relation for the three groups between the alumina derived from kaolinite and the contraction, if one excepts the fine fraction of Vermont kaolin (*Vf*). In this case the alumina from mica may be a contributing factor, since this alumina also crystallizes in the 900° to 1,000° C temperature range according to Zwetsch (footnote 16). In fact, to avoid placing too much emphasis on the direct relation of length change and alumina from the kaolinite, it should be noted that an equally good indirect relation is shown between the length changes and alumina from the mica.

It is interesting that a primary kaolin and four secondary kaolins constitute the group of greatest contraction, and three primary kaolins and three ball clays the intermediate group. The indication is that the particle-size distribution, which is well known [20] to be materially different in these three types of clay, does not significantly affect the length changes in this temperature range.

d. FINAL CONTRACTION

The ball clays begin their final contraction in a comparatively gradual manner at about 1,000° C, whereas the kaolins begin sharply at about 1,100° C (figs. 3 and 4). There is, however, no clearly defined difference in behavior between the ball clays and the kaolins, as shown for example by ball clay *CC* and kaolin *Z* (table 8), but the group averages show a definite trend. They indicate that chemical composition (within the limits of composition studied) is a factor, but that particle size exerts the greater influence on the final contraction. The fineness of Florida clays (*E* and *U*) was commented on by Klinefelter and Meyer (footnote 7), who refer to them as "ball kaolins." Another evidence of the influence of grain size is the greater contraction of clay *Gf* (fine fraction) compared to the coarse fraction *Gc* (fig. 7), although the chemical compositions are nearly identical.

Once under way, the final shrinkage proceeds almost abruptly but reaches a maximum in the temperature range 1,100° to 1,150° C for the ball clays (excepting clay *CC*) and in the range 1,150° to 1,200° C for the kaolins (table 10). Results are presented in this table as "contraction per 1° C temperature rise" in order to emphasize the differences in shrinkage which may exist in industrial practice within a piece of ware, or from piece to piece, because of temperature differentials. Tables 10 and 4 show also that addition of feldspar accelerated the final contraction because, at these temperatures, it acts as a flux. Below 1,000° C it had retarded contraction, probably because it acts as an inert aggregate.

It should be observed that in no case (table 7) did an individual clay, or a clay-flint-feldspar mixture, show greater shrinkage or lower absorption after heating to the same temperature on the 9-hr schedule than after the 24-hr schedule. This was noted also by Shelton and Meyer.[21]

[20] R. H. Bray, J. Am. Ceram. Soc. **20**, 257 (1937).
[21] Geo. R. Shelton and Wm. W. Meyer, J. Am. Ceram. Soc., **21**, 371 (1938).

TABLE 10.—*Contraction of clays and bodies above 1,000° C (average values)*

Material	Schedule	Contraction per 1 degree C. rise in temperature in the range—				
		1,000° to 1,050°	1,050° to 1,100°	1,100° to 1,150°	1,150° to 1,200°	1,200° to 1,250°
	hr	%	%	%	%	%
Ball clay *J*	16	0.009	0.03	0.07	0.05	
Ball clay 4	16	.009	.03	.07	.04	
Ball clay 5	16	.015	.04	.10	.05	
Ball clay *CC*	9	.006	.01	.05	.08	
Do	24	.006	.01	.06	.07	
Ball clay *CC* plus feldspar [a]	9	.010	.05	.11	[b].03	
Do.[a]	24	.024	.07	.10	[b].03	
Kaolin *S*	16	.001	.003	.01	.05	0.06
Do. plus feldspar [a]	9	.002	.004	.02	.09	
Do.[a]	24	.002	.009	.03	.10	
Kaolin *E*	16	.004	.010	.05	.07	.03
Kaolin *U*	16	.003	.005	.01	.13	.08
Kaolin *T*	16	.002	.002	.01	.05	
Kaolin *K*	16	.004	.006	.03	.06	.03
Kaolin *P*	16	.003	.005	.02	.05	.06
Kaolin *Z*	16	.004	.013	.05	.05	
Body *H*, deaired, extruded	9	.002	.01	.01	[c].05	
Do	24	.002	.01	.03	[c].05	
Body 35, deaired, extruded	9	.005	.04	.08	[c].10	
Do	24	.008	.06	.10	[c].05	
Body 35, pressed	9	.006	.05	.09	[c].12	
Do	24	.014	.09	.13	[c].03	
Body 27, hand-wedged	9	.015	.07	.06	[d].01	
Do	24	.023	.08	.06	[d].01	

[a] These specimens were prepared as described in table 4.
[b] Maximum temperature 1,180° C.
[c] Maximum temperature 1,190° C.
[d] Maximum temperature 1,160° C.

2. BODIES

The effect of varying the amount of free, or mechanical, water in pressed specimens was studied briefly in connection with body 35 (tables 6 and 7). The highest density in the dry state (table 7) was obtained with 8 percent of water, which agrees with the findings of Dodd, whose work was done on much coarser-grained mixtures.[22] He obtained maximum density when using 8 to 10 percent of water and the range covered was 5 to 12 percent.

a. LENGTH CHANGES BELOW 1,000° C.

The length changes of the three bodies during the heating to 1,000° C are comparatively small (fig. 9). The presence of free silica in body *H* was shown by a small but clearly defined acceleration in the length change between 550° and 600° C during both heating and cooling. In bodies 27 and 35, the effect of the quartz inversion was overshadowed by the other body constituents (fig. 10).

It might appear that bodies such as these could be heated rapidly to 1,000° C with little danger of rupture from shrinkage differentials alone, and that the limiting factors are the internal pressures built up by volatilization of water and the combustion of organic matter. At this stage, however, bodies are very weak mechanically, and the possibility remains that microscopic lines of structural weakness could be caused by the widely divergent length changes of (for example)

[22] E. M. Dodd, J. Am. Ceram. Soc. **17**, 465 (1938).

mica, quartz, and the secondary clays. That such internal weaknesses can develop in coarser structures, such as clay refractories, has been considered probable.[23] It seems hardly likely, however, that cracks or lines of weakness too large to be "healed" by the glass formed above 1,000° C could develop in an intimately blended mixture of particles of which practically none exceed 80 microns in diameter and of which over 90 percent (by count) are under 4 microns in diameter.

b. LENGTH CHANGES ABOVE 1,000° C.

The importance of a carefully controlled heating schedule, and uniformity in temperature distribution, during the very rapid shrinkage accompanying vitrification (fig. 9) is evident. The values in table 10 show that shrinkages of as much as 0.13 percent per 1° C rise in temperature may be expected. This rate is equivalent to a difference in shrinkage of about ⅛ in. across a 10-in. specimen for a temperature differential of only 10° C.

Figure 9 and table 10 show how the shrinkage of body 27 is retarded as it approaches vitrification during the last 60 degrees of temperature rise, and how the contraction becomes almost purely thermal as soon as the maximum temperature is passed and cooling begins. In contrast, body *H*, which is still highly absorbent after the test, shows little retardation and also continues to undergo permanent contraction as the temperature drops to 1,100° C. A similar difference may mark the shrinkage of a body heated on a long schedule as compared with the shrinkage of the same body heated on a short schedule (deaired body 35, see insert, fig. 9).

On the faster (9-hr) schedule, the deaired and extruded body 35 shows a greater contraction per degree centigrade temperature rise between 1,150° and 1,190° C (table 10) than it does between 1,100° and 1,150° C, whereas on the slower (24-hr) schedule the contraction in the higher temperature range is only half that in the lower range. Similar, but more pronounced, differences are shown by the dry-pressed specimens tested on the 9-hr and 24-hr schedules. As a result, the shrinkage on the faster schedule (which had been less than that on the slower schedule until about 1,150° C was reached) now becomes greater than that on the slower schedule. In contrast, body 27 (table 10) shows the same decrease in shrinkage as the maximum temperature is approached, regardless of heating rate, and consequently the greater shrinkage attained during the earlier stages of heating on the slower schedule is maintained to the end of the test.

The results for body 35 support Watts' findings (footnote 3). Watts suggests that bodies heated on long schedules show the lesser shrinkage because the feldspar glass has had more time to dissolve clay and silica, thereby increasing its viscosity.

According to the data obtained in this study, the greater shrinkage and lower absorption after the shorter of two heating schedules is not a fundamental and common characteristic of all ceramic bodies. It is rather the result of certain combinations of body ingredients and heating schedules favoring such a result.

c. TOTAL SHRINKAGE

Table 7 shows the effect, on total shrinkage, of the load to which specimens were subjected during test in the porcelain dilatometer.

[23] R. F. Geller, Am. Refractories Inst., Tech. Paper No. 4 (1927).

Comparable values for specimens heated under no superimposed load were obtained for the mixture of clay *CC* and feldspar, and for bodies *H* and 35. The load apparently had no effect on body *H* during the short schedule. It increased the shrinkage 0.4 percent for body *H* during the 24-hr schedule, and the maximum increase was 2.2 percent for body 35 pressed with 15 percent of water.

Another point of interest is the effect of deairing (body 35, table 7). If the limited data are significant, they mean that deaired plastic bodies will shrink more than nondeaired ones. In any case, there is sufficient evidence to indicate that both the deaired and nondeaired plastic-formed bodies shrink appreciably less during heating than the same bodies when pressed. As pointed out previously in this paper, the greater shrinkage of pressed specimens applies also to individual clays (fig. 5).

VI. SUMMARY AND CONCLUSIONS

Length changes of 9 kaolins, 4 ball clays, and 3 whiteware bodies were observed during their initial heating to a maximum temperature of 1,250° C. The apparatus used was an especially designed porcelain dilatometer. Differential heating curves for two clays and the specific gravity and weight losses of mica after holding at several temperatures were obtained as supplementary data.

Primary kaolins and ball clays show less contraction between 500° and 900° C than do the secondary kaolins. The contraction (about 3 percent in a relatively pure clay) and the mica content show a sufficiently close relation to indicate strongly that the mica content, rather than geological history or particle-size distribution, is the predominating factor determining length change in this temperature range.

The contraction between 900° and 1,000° C is believed to be caused by the crystallization of amorphous alumina, resulting from the breakdown of the kaolinite molecule, to gamma-alumina. The data show a direct relation between the amount of this contraction and the calculated amount of alumina contributed by kaolinite.

The very rapid contraction accompanying vitrification, beginning at about 1,050° C in ball clays and 1,100° C in kaolins, varied from about 6 percent of the original length for primary kaolins to 12 percent for a secondary "ball kaolin." Particle size appears to be the principal factor determining this contraction.

Changes in length of the bodies, in the range from room temperature to 1,000° C, were gradual, and the maximum change (expansion) was 0.8 percent of the original length. Above 1,000° C the rate of change (contraction) increased rapidly. The maximum rate noted was 0.3 percent per minute for a talcose body on a "9-hr schedule" in the temperature range 1,135° to 1,170° C. Based on unit temperature rise, the maximum length change noted was 0.13 percent per 1° C for the same body during a "24-hr schedule" in the temperature range 1,100° to 1,150° C.

In every test of a body (or of an individual clay) the shrinkage per unit temperature rise during the first stages of the final rapid contraction was greater on the 24-hr schedule than on the 9-hr schedule.

In some cases, the shrinkage rate decreased more on the long schedule, during the last 25 to 50 degrees of temperature rise and the first 50

to 100 degrees of cooling, than on the shorter schedule. As a result, the shrinkage during the shorter schedule forged ahead with the effect that the total shrinkage during the shorter schedule was greater than during the longer schedule.

The authors express their thanks to S. C. Lyons and the Georgia Kaolin Company, to Hewitt Wilson and the Bureau of Mines, to the Sprinks Clay Company, to Kaolin Incorporated, and to A. V. Bleininger, for materials and information furnished.

WASHINGTON, May 3, 1940.

U. S. Department of Commerce National Bureau of Standards

RESEARCH PAPER RP1312

Part of Journal of Research of the National Bureau of Standards, Volume 25, July 1940

A VACUUM-TUBE ALTERNATING-VOLTAGE COMPENSATOR

By Irvin L. Cooter, Frank Wenner, and Chester Peterson

ABSTRACT

A vacuum-tube amplifier of the type described is a simple and inexpensive means for compensating small alternating voltages. Two such amplifiers and an iron-cored inductor with air gaps are used as a choke in a circuit having a resistance of approximately 20 ohms and in which there is a direct current of approximately 1 ampere. The effectiveness of the arrangement is such that rapid variations of the potential drop amounting to 0.1 volt in a part of the circuit result in variations in the current of less than 1 microampere.

One of the methods now being used in this Bureau in an absolute measurement of electrical resistance requires that the test current through a standard resistor be kept very nearly constant over successive time intervals of a few hundredths of a second. This requirement must be met even though, in the same circuit, there are rapid variations of resistances and voltages of sufficient magnitude to disturb the constancy of the current unless their effects are nullified. The purpose of this paper is to describe briefly the means employed to hold the current constant.

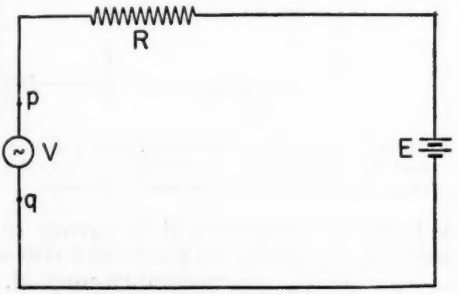

FIGURE 1. *Simplified circuit containing a resistor, R, in which it is necessary to maintain a direct current which, over short intervals of time, is constant to one part in a million while there is a pulsating potential difference between p and, q.*

The problem may be visualized by referring to figure 1. In this figure, E represents a battery supplying direct current of approximately 1 ampere through the 1-ohm resistor, R. For the purpose of measurement, it is necessary that the fluctuations of current in R should be less than 1 microampere from its average value over successive time intervals of a few hundredths of a second. However, the operation of a rotating commutator and other parts connected to p and q, but not shown in figure 1, constitutes in effect a source of alternating voltage, V, between the points p and q. Although this alternating voltage has a fundamental frequency of approximately 45 cycles per second,

the wave shape is nonsine and not strictly the same in successive cycles. The mechanisms connected to p and q are so constructed and adjusted that peak values of this fluctuating voltage do not exceed 0.1 volt.

In a problem such as is stated above, an iron-cored inductor with suitable air gaps in the magnetic circuit constitutes one of the simplest and most effective known means for reducing the amplitude of pulsations in the current. An inductor of this type could readily be made to reduce the amplitude of the current pulsations to one part in ten thousand, but not to one part in a million of the average current. Consequently it was necessary to devise means for supplementing the inductor.

The solution to our problem, found after considerable experimentation, is shown in figure 2. In figure 2, L is an iron-cored inductor having a resistance of approximately 6 ohms. With a direct current of 1 ampere in the windings, the reactance of the inductor L to 0.1

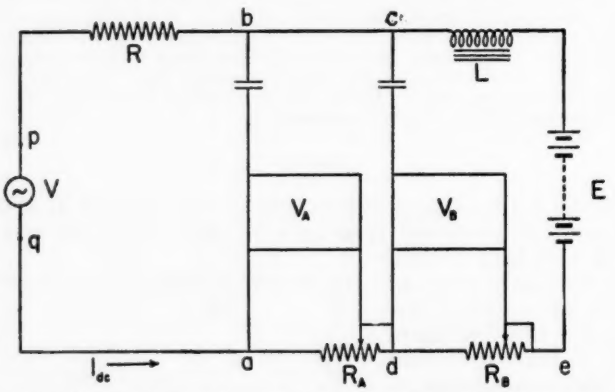

FIGURE 2. *Simplified circuit of figure 1 shown with the additions of the inductor, L, and the vacuum-tube amplifiers, V_A and V_B, which taken as a whole serve as a choke to the pulsating potential difference.*

volt at the fundamental frequency of approximately 45 cycles per second is somewhat in excess of 1,000 ohms.

V_A and V_B are resistance-coupled, phase-inverter, vacuum-tube amplifiers adjusted very nearly to a 1 to 1 voltage amplification. Consequently, sudden and cyclic changes in their input voltage cause very nearly equal and opposite changes in the potential drops in their load resistors, R_A and R_B.

Referring to figure 2, since the reactance of L is much larger than the a-c resistance of R, R_A, and R_B, the small fluctuating voltage, V, between p and q is impressed on amplifier V_A between a and b. A fluctuating potential difference of approximately the same magnitude but opposite in phase appears across output resistor R_A of amplifier V_A. This output potential drop between a and d will largely compensate the input voltage across a and b; and the uncompensated voltage, which was found to be approximately equal to $v/20$, will appear across c and d. This uncompensated voltage serves as the input voltage for amplifier V_B and is largely compensated by the output potential drop across d and e. The resultant uncompensated voltage between c and e

is approximately equal to $v/(20\times20)$, or $v/400$. The large reactance of the inductor, L, prevents this small voltage from changing the test current by as much as 1 microampere.

Details of one of the vacuum-tube amplifiers used as an alternating-voltage compensator are shown in figure 3. The values for the resistors, capacitors, and biasing voltages were selected experimentally. With an input voltage of 0.1 volt between a and b, output resistor R_A is adjusted until a minimum voltage between c and d is indicated by a vacuum-tube voltmeter. This indicated minimum will not be zero, since there is some distortion in the voltage compensator. Furthermore, this distortion depends to some extent on the characteristics of the tubes, since the indicated minimum was found to be

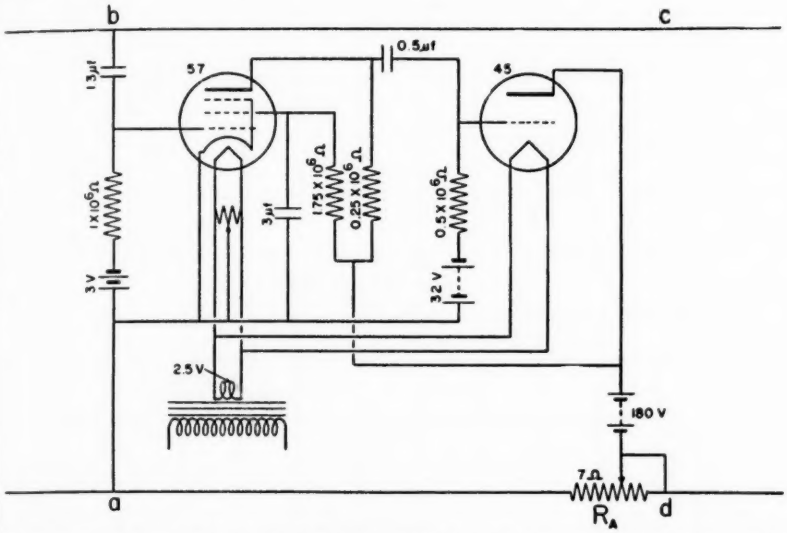

FIGURE 3. *Details of a vacuum-tube amplifier used for compensating pulsating potential differences.*

different on changing a tube for another of the same type number and then making the best obtainable adjustment.

The performance characteristics of the alternating-voltage compensators for voltages of different frequencies are shown in figures 4 and 5. These data were obtained with a direct current, I_{dc}, of 0.7 ampere in resistor R. However, the performance of the amplifiers will not be appreciably affected if the magnitude of I_{dc} is changed to a different value, provided that the final adjustments of the output resistors R_A and R_B are made when the direct current in R has the desired magnitude.

The data shown in figure 4 were obtained using only the amplifier V_A for compensation. It will be seen from figures 2 and 4 that when the input alternating voltage between a and b is 0.1 volt, the uncompensated voltage between b and d is approximately 0.005 volt. In this case, using only one amplifier, the input voltage has been compensated within approximately 5 percent.

The data shown in figure 5 were obtained using both amplifiers for compensation. It will be seen from figures 2 and 5 that when the alternating input voltage between a and b is less than 0.1 volt the uncompensated voltage between c and e is less than 0.0002 volt for frequencies between 25 and 180 cycles per second.

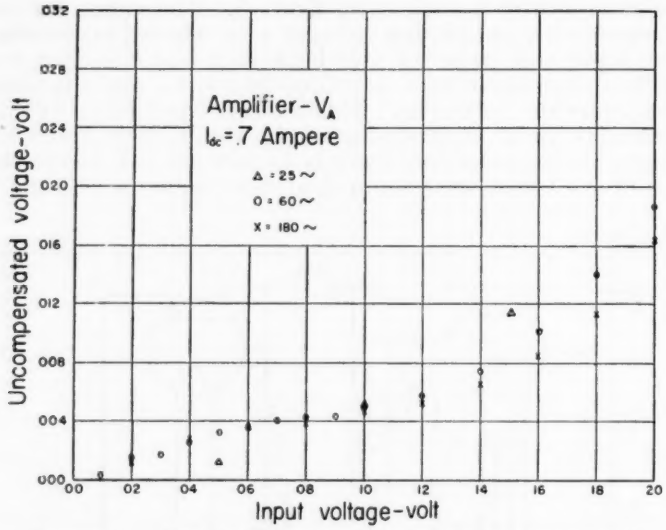

FIGURE 4.—*Data obtained using one amplifier for compensation.*

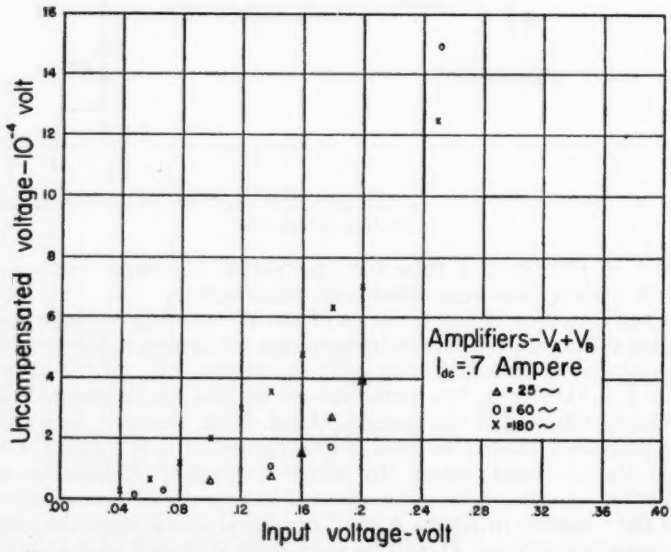

FIGURE 5.—*Data obtained using two amplifiers for compensation.*

As the initial impedance of the inductor at the fundamental frequency of 45 cycles per second is approximately 1,000 ohms, the

fluctuating voltage of 0.0002 volt between c and e of figure 2 causes fluctuations in the test current through the battery of approximately 2×10^{-7} ampere. However, the alternating component of the current in R is larger by approximately 1×10^{-7} ampere as a result of the alternating component of the current in the grid resistor of the 57 tube.

By the use of the two alternating-voltage compensators and the iron-cored inductor, it has been possible to limit the alternating component of the current in R to less than one part in a million of the direct current.

WASHINGTON, April 18, 1940.

U. S. DEPARTMENT OF COMMERCE NATIONAL BUREAU OF STANDARDS

RESEARCH PAPER RP1313

Part of Journal of Research of the National Bureau of Standards, Volume 25, July 1940

RELATION OF CATION EXCHANGE TO THE ACIDIC PROPERTIES OF COTTON

By Arnold M. Sookne and Milton Harris [1]

ABSTRACT

The acid-binding capacity of cotton is quantitatively determined by its content of cationic ash (the total content of the cations of inorganic bases), most of which is associated with the pectic substance. This conclusion emerges from a study of the hydrochloric-acid titration curves of dewaxed, water-washed cotton and of depectinized cotton, and from a comparison of the maxima of these curves with direct determinations, by an electrodialysis method, of the hydrogen-ion equivalence of the cationic ashes of both of these samples. The difference between the two maxima, each of which corresponds to the cationic ash, is equivalent to the carboxyl content of the pectic substance, as determined by uronic-acid analyses.

At low values of pH, the results for the acid-binding capacities were corrected for the selective sorption of water by the cotton. The nature and magnitude of this correction, and the method in which it was applied, are discussed in detail.

Measurements of the capacity of the fiber to bind hydrochloric acid were made in the absence of added salt, and in potassium-chloride solutions of 0.1 and 1.0 *M* ionic strength. The titration curves obtained in the presence of 0.1 *M* salt were slightly shifted from those obtained in the absence of salt, but no further shift was obtained by further increase in ionic strength. Subtraction at corresponding values of pH of the acid-binding capacities obtained in salt solutions with depectinized cotton from the acid-binding capacities for the dewaxed cotton yielded the titration curve for the pectic substance in the presence of salt. The curve conforms closely to the mass-action law for an acid of pK 3.3. This value is close to pK values for other polyhydroxy carboxylic acids. A titration curve for pectic substance in the absence of added salt was obtained by a similar process of subtraction. The shift in this curve from the curve for pectic substance in the presence of salt is shown to be qualitatively consistent with the predictions of the Donnan equilibrium.

The maximum acid bound by the dewaxed cotton used in this work was 0.066 M-eq/g (milliequivalent per gram). The content of pectic substance, determined directly as well as by the difference in the maxima of the titration curves, accounts for 0.056 M-eq/g. The difference between these two values, 0.010 M-eq/g, is contributed by acidic groups in the depectinized cotton. The possible source and significance of these acidic groups are discussed. It is tentatively assumed that these acidic groups are an integral part of the cellulose molecule, such as an end group. On the basis of this assumption, the cellulose has an equivalent weight of about 100,000, which corresponds to a minimum chain length of about 600 glucose residues.

CONTENTS

	Page
I. Introduction	48
II. Experimental procedure	48
1. Materials	48
2. Methods	49

[1] Research Associates at the National Bureau of Standards, representing the Textile Foundation.

235535—40——4

Page
III. Results and discussion 50
1. Selective sorption of water by cotton 50
2. Combination of dewaxed and of lime-washed, depectinized cotton with hydrochloric acid 52
3. Hydrogen-ion equivalence of the cationic ashes of dewaxed and of lime-washed depectinized cottons 54
4. Temperature coefficient of the titration curve of dewaxed cotton 55
5. Significance of the acidic groups in depectinized cotton 56
6. Application of the Donnan theory to the titration curves of the pectic substance 57
IV. References 60

I. INTRODUCTION

Cotton and other naturally occurring cellulosic materials yield, on ignition, an ash which is alkaline in reaction. This results from the fact that the fiber normally exists as a salt, many of the anions being provided by the cellulose of the fiber and by associated materials, such as pectic substance [1, 2, 3].[2] The cations in water-washed cotton have been shown by Walker and Quell to consist principally of Ca^{++}, Mg^{++}, Fe^{+++}, and Al^{+++} [2]. In addition, raw cotton also contains a quantity of neutral salt, most of which is removed during washing of the fiber with water.

The manner in which cotton binds acid may be considered as an exchange process between the hydrogen ions of the acid and the cations associated with the fiber. The extent of the exchange is a function of the number and nature of the cations, the concentration of the acid, and the tendency of the hydrogen of the acidic groups in the cotton to ionize. This concept of cation exchange has been employed from time to time by earlier investigators to explain the reaction of cellulosic materials with acids and salts [1, 2, 3, 4]. The importance and wide applicability of these exchange reactions have been recognized and discussed by McLean and Wooten [3], who demonstrated that the amount of acid bound by different cellulosic materials at an arbitrary pH is proportional to their ash contents. They also suggested that the major portion of the ash is contributed by noncellulosic materials associated with the cellulose.

In the present investigation, which involved a detailed study of the acid-binding capacity of cotton fibers over a wide range of pH values, it is shown that the acid-binding capacity of cotton at any pH is determined by its cationic ash. From the complete titration curves, and the hydrogen-ion equivalence of the ash, the maximum acid bound by different samples of cotton was ascertained, which in turn permitted the quantitative allocation of the acid bound to the principal constituents of the fiber.

II. EXPERIMENTAL PROCEDURE

1. MATERIALS

Raw cotton was extracted with hot alcohol for 24 hours, and then washed thoroughly with distilled water at room temperature for several hours. Such samples will henceforth be described as *dewaxed cotton.*

A portion of the dewaxed material was further purified by extraction for 4 or 8 hours with a boiling 1-percent solution of sodium hy-

[2] Figures in brackets indicate the literature references at the end of this paper.

droxide, according to the method recommended for the preparation of standard cellulose. The procedure was essentially the same as that described by Corey and Gray [5], except that the apparatus of Worner and Mease [6] was used. Fibers treated in this way were shown by the method of Whistler, Martin, and Harris [7] to be free of pectic substance. In one step of this purification, the fibers were washed with a dilute solution of acetic acid. This undoubtedly removed some of the cations from the fiber and since cotton binds acid by a cation-exchange process which involves the back titration of the acid groups of the fiber by an added acid, it was necessary to make certain that all of the acidic groups were in the salt form. This was accomplished by soaking the purified samples for about 3 hours in a solution of calcium hydroxide at room temperature. They were then washed in running distilled water for about 24 hours. Cotton from which both wax and pectic substance were removed is designated *depectinized cotton*. Depectinized cotton which has been washed with a solution of calcium hydroxide is designated *lime-washed depectinized cotton*.

All samples were conditioned at 21° C and 65-percent relative humidity before weighing. The moisture contents of the fibers were determined by drying representative samples at 105° C for 2 hours in a vacuum oven.

2. METHODS

Determination of the acid-binding capacity.—Samples of cotton weighing about 5 g and containing a known amount of moisture were immersed in 100-ml portions of the acid solutions at the temperature of the experiment (0° or 25° C). Large test tubes (1½ by 8 in.) were found to be convenient for this purpose, since the samples could be easily pressed into the bottom of the tube to insure uniform wetting of the fibers or to permit squeezing the liquor from the fibers after equilibrium was reached. The amount of acid absorbed was determined by titration with sodium hydroxide of 50-ml aliquots of the original solution and of the solution in equilibrium with the sample, using bromcresol purple as the indicator. From the difference between these titers, the weight of the sample, and its content of moisture, the amount of acid taken up per gram of dry cotton was calculated. In a number of measurements, the concentrations of strongly acid solutions (in the region of pH 1) were determined by adding a weighed quantity of strong alkali to the solution, after which the titration was completed with weak acid or alkali.

Preliminary measurements at several acidities indicated that a close approximation to a final equilibrium is attained in a few hours. In most of the experiments, however, the samples were allowed to remain in contact with the solutions overnight.

Determination of pH.—Measurements of pH were made with a McInnes and Belcher-type glass electrode and a vacuum-tube potentiometer, using a cathode-ray "eye" as null indicator. The pH values were referred to potassium acid phthalate, 0.05 *M*, to which was assigned a pH value of 4.01 [8].

Temperature.—With the exception of one experiment at 25° ± .02° C, all of the acid solutions in contact with the cotton were kept at 0° ± .01° C to inhibit decomposition of the fibers.

Determination of cationic ash.—The hydrogen-ion equivalence of the cationic ash was determined by an electrodialysis method described elsewhere [9].

III. RESULTS AND DISCUSSION

1. SELECTIVE SORPTION OF WATER BY COTTON

The determination of the maximum acid-binding capacity of cellulose is complicated by the fact that the fibers may selectively sorb water from a solution of acid, and thus affect its titer. Since the acid-binding capacity is calculated from titer differences, a correction must be applied to compensate for this effect. At pH values below 1.5, the magnitude of the correction is appreciable compared with the acid-binding capacity of cotton, but it becomes negligible at pH values above 2.5.

If B is the amount of water selectively sorbed per gram of dry cotton, then the amount sorbed per gram from the solution by a sample which originally contains W g of water per gram is $(B-W)$. Water taken up in this manner is no longer available for dilution of the acid, and would thus tend to cause an increase in concentration of the acid solution in contact with the fiber. At the same time, however, a quantity of acid, A (M- eq/g), will be bound by the sample, and produce a decrease in concentration of the acid solution. Obviously, if any of the acid solution as such is dissolved in the sample, the titer of the solution will not be affected. From the above, it follows that if S g of dry cotton is immersed in G ml of acid solution of concentration C_0, and the concentration of the solution after equilibrium is attained is C, the corrected acid-binding capacity of the cotton is given by the equation,

$$A=\frac{G(C_0-C)}{S}+C(B-W), \tag{1}$$

where A is the corrected acid-binding capacity, $G(C_0-C)/S$ is the apparent acid-binding capacity, and $C(B-W)$ is the correction for the selective sorption of water.

The actual measurement of the quality B presents considerable experimental difficulty. In the region of the maximum acid-binding capacity, measurement of titer differences in solutions of different initial acid concentrations, or in solutions of the same initial acid concentration which have been allowed to come to equilibrium with samples of different moisture contents, gives equations of the form of eq1. The solution of any two of such equations should give values for A and B, but such a procedure demands the assumption that both A and B are constant for the conditions employed. Measurements made in 0.1 and 0.2 M solutions of hydrochloric acid indicated that this assumption is not valid. The results were such as to indicate that more acid or less water was sorbed in the more concentrated of these solutions. If calculations are made from measurements of solutions for which the above assumption should be more nearly valid (0.10 and 0.11 M solutions of hydrochloric acid), the values for A and B are too sensitive to experimental error to be useful.

It was found that the following method for evaluating A and B leads to less equivocal results. A substance which is assumed not to be sorbed by the fiber was added to the solution of acid as a reference substance. The change in concentration of this substance gives a

direct measure of the amount of water ($B-W$) sorbed by the fiber. Two reference substances, sodium chloride and trehalose, were used in this work. The change in concentration of the former was determined by evaporating an aliquot of the solution and determining the dry weight of salt. In the case of the disaccharide, trehalose, the change in concentration was measured polarimetrically. The actual determinations were made as follows: Samples of cotton of known weights and moisture contents were immersed in solutions that were 0.1 M with respect to hydrochloric acid, and 3.43 M with respect to sodium chloride, and the changes in concentration of both acid and salt were determined. The acid-binding capacity, A, was then calculated, due account being taken of the water sorbed as determined by the change in salt concentration. The mean of four values, so determined, was 0.067 M-eq/g.

The value for B in solutions in the region of pH 1 was then calculated by substituting the value 0.067 for A in eq 1. The value (C_0-C) is small, and therefore the determination of B by this procedure is subject to the uncertainty of this quantity. In order to improve the reliability of B, a series of 20 samples of dewaxed cotton of known weights and moisture contents was immersed in solutions of hydrochloric acid of known concentrations, the acidities of which were in the region of pH 1. The 20 equations of the form of eq 1, obtained from these measurements, were summed up and gave the equation,

$$28.63A-3.87B=1.489. \qquad (2)$$

Substitution of the value 0.067 for A in eq 2 gave a value for B (in HCl solution) of 0.11 g of water per gram of dry cotton.

The values of A and B were also determined by a second method, in which trehalose was used as the reference substance. Samples of cotton of known weights and moisture contents were immersed in trehalose solutions that were 0.04 M with respect to hydrochloric acid. The concentration of trehalose before and after the introduction of the samples was measured polarimetrically. By this procedure, a value for B of 0.13 g of water per gram of dry cotton was obtained.

TABLE 1.—*Application of the correction for the selective sorption of water to the acid-binding capacity of dewaxed cotton in 0.1 M hydrochloric acid*

Initial water content	Apparent acid-binding capacity, $G(C_0-C)/S$	Correction, $C(B-W)$	Corrected acid-binding capacity, A
g/g of cotton	*M-eq/g*	*M-eq/g*	*M-eq/g*
0.000	0.054	+0.012	0.066
.100	.063	+.002	.065
.190	.075	−.007	.068
.308	.085	−.019	.066
.720	.124	−.059	.065
1.135	.164	−.097	.067
		Mean.....	0.066

The validity of this method of correction for the selective sorption of water is shown in table 1, which presents data on dewaxed fibers of widely different initial moisture contents. The measurements were

made in 0.1 *M* solutions of hydrochloric acid, and the results are corrected, using the mean value 0.12 for *B*. Each figure represents the mean of at least two determinations. In the cases of the samples of high moisture contents, some of the water was added directly to the solution with the sample. The discordant values for the apparent acid-binding capacity, $G(C_0-C)/S$ for all of these samples are brought into close agreement by application of the correction $C(B-W)$, to give the corrected acid-binding capacity, *A*.

It is of interest to note that the values for *B*, 0.11 and 0.13 g of water per gram of dry cotton, are considerably lower than the known moisture content of cotton at relative humidities between 99 and 100 percent (about 0.3 g of water per gram of cotton) [10], which corresponds approximately to the humidity of air in equilibrium with 0.1 *M* hydrochloric acid. The result suggests that the average partition coefficient of the hydrochloric acid between the water in the external solution and the water held by the fiber is greater than unity. The average value of *B* of 0.12 g of water per gram of cotton represents the portion of the total sorbed water which is unavailable for dilution of the acid.

2. COMBINATION OF DEWAXED AND OF LIME-WASHED, DEPECTINIZED COTTON WITH HYDROCHLORIC ACID

Measurements of the combination of dewaxed and of lime-washed depectinized cotton with hydrochloric acid are given in table 2 and shown graphically in figure 1. The data were obtained in the absence

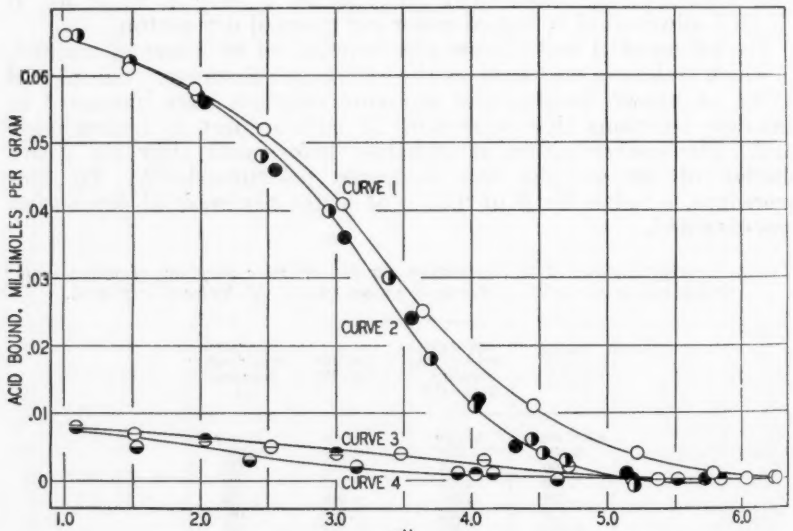

FIGURE 1.—*Combination of dewaxed and of lime-washed depectinized cotton with hydrochloric acid at 0°C.*

Curve 1, dewaxed cotton in the absence of added salt, ○. Curve 2, dewaxed cotton in hydrochloric acid-potassium chloride solutions of 0.1 *M* ionic strength, ◑; and in solutions of 1.0 *M* ionic strength, ●. Curve 3, depectinized cotton in the absence of added salt, ⊖. Curve 4, depectinized cotton in solutions of 0.1 *M* ionic strength, ◒; and in solutions of 1.0 *M* ionic strength, ◓.

of added salt, and in solutions made up to 0.1 and 1.0 *M* ionic strengths with potassium chloride. The increase of ionic strength from 0.1 to 1.0 *M* produced no measurable effect on the titration curve of either sample, and accordingly only one curve is drawn for each sample at the two ionic strengths. The curves for dewaxed and for lime-washed depectinized cotton tended to approach maxima, at about pH 1, of 0.066 and 0.008 M-eq/g, respectively. The failure to arrive at unambiguous maxima may be due to the uncertainty in the correction for the selective sorption of water or to other secondary effects which may occur in solutions of high acid concentrations.

TABLE 2.—*Combination of dewaxed and of lime-washed depectinized cotton with hydrochloric acid at 0°C, in the presence of varying amounts of potassium chloride*

DEWAXED COTTON					
No added salt		0.1 *M* ionic strength		1.0 *M* ionic strength	
pH	Acid bound	pH	Acid bound	pH	Acid bound
	M-eq/g		*M-eq/g*		*M-eq/g*
1.08	0.066	1.08	0.066	2.03	0.056
1.47	.061	1.48	.062	2.55	.046
1.96	.058	1.98	.057	3.06	.036
2.47	.052	2.45	.048	3.56	.024
3.05	.041	2.94	.040	4.05	.012
3.64	.025	3.39	.030	4.62	.005
4.45	.011	3.70	.018	5.24	.001
5.22	.004	4.02	.011	5.72	.000
5.78	.001	4.44	.006	--------	--------
6.04	.000	4.52	.004	--------	--------
6.30	.000	4.69	.003	--------	--------
		5.20	−.001	--------	--------
LIME-WASHED DEPECTINIZED (4 HR), COTTON					
1.08	0.008	1.08	0.008	2.04	0.006
1.51	.007	1.53	.005	3.00	.004
2.04	.006	2.36	.003	4.03	.001
2.52	.005	3.15	.002	5.18	.000
3.00	.004	3.90	.001	5.84	.000
3.48	.004	4.16	.001	--------	--------
4.09	.003	4.63	.000	--------	--------
4.71	.002	5.52	.000	--------	--------
5.67	.000	--------	--------	--------	--------
6.27	.000	--------	--------	--------	--------
6.38	.000	--------	--------	--------	--------

None of the pectic substance appeared to dissolve during the titration with acid. This was indicated by sharp indicator end points, lack of frothing, exact correspondence between acid-binding capacity calculated from pH differences and from titer differences, and the pH of 0.1 *M* potassium chloride solution in contact with the sample (about 5.3). If any soluble potassium pectate had been formed, the pH value of the solution would necessarily have been appreciably higher. The pectic substance may be insoluble because it exists as an insoluble salt of polyvalent cations or as the free acid, which is insoluble in acid solutions.

The difference between the maxima of the curves indicates that about 85 percent of the acid groups of dewaxed cotton is furnished by the pectic substance. This conclusion is confirmed by direct chemical analyses presented elsewhere. The remaining acid groups appear to be associated with the depectinized cotton. Further consideration of these groups and their probable significance is given later.

The titration curves for dewaxed cotton (curves 1 and 2, fig. 1) must be considered as composites of the curves for depectinized cotton and the pectic substance. Accordingly, subtraction, at corresponding values of pH, of the ordinates of curve 3 from those of curve 1 should give a titration curve for the pectic substance in the absence of added salt. Similarly, subtraction of the ordinates of curve 4 from those of curve 3 gives the curve for pectic substance in the presence of added salt (0.1 or 1.0 *M* potassium chloride). The data thus obtained interpolated at intervals of 0.5 pH unit, are shown by the points in figure 2. The smooth curves in this figure are not drawn to fit these points, but are explained in section III–6. It should be noted that the data obtained by the subtraction process described above are not subject to errors inherent in the method of correction for the selective sorption of water by the samples, since the subtraction would presumably

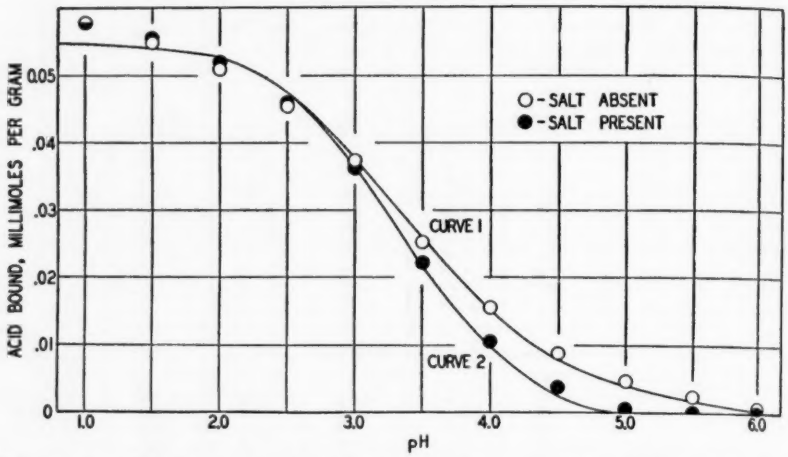

FIGURE 2.—*Calculated data for the combination of pectic substance with hydrochloric acid at 0° C.*

Curve 1, pectic substance in the absence of added salt, ○. Curve 2, pectic substance in solutions of 0.1 *M* or 1.0 *M* ionic strength, ●. The smooth curves are not drawn to fit the data, but are explained in the text (section III–6).

cancel any such errors. Furthermore, these results should not be susceptible to secondary effects (section III–2) for the same reason. As a result, it is not surprising that a somewhat more definite maximum is obtained. The curve approaches a maximum value of 0.058 M-eq/g.

3. HYDROGEN-ION EQUIVALENCE OF THE CATIONIC ASHES OF DEWAXED AND OF LIME-WASHED DEPECTINIZED COTTONS

The hydrogen-ion equivalence of the cationic ashes of several different samples of cotton are given in table 3. A comparison of the data for the ash determinations on dewaxed cotton with those on dewaxed cotton which had been washed with lime water and then with distilled water indicate that all of the acidic groups in the former existed in the form of salts. The data also show that if the extraction is extended from 4 to 8 hours, the cationic ashes of the lime-washed samples remain unaltered. The difference between the mean values

of the cationic ashes of dewaxed and of lime-washed depectinized cottons is 0.054 M-eq/g. This represents the cationic ash bound by the pectic substance.

TABLE 3.—*Hydrogen-ion equivalence of the ashes of various cotton samples*

Sample	Cationic ash
	M-eq/g
Dewaxed cotton	0.063
Lime-washed dewaxed cotton	.064
Lime-washed depectinized (4 hr) cotton	.010
Lime-washed depectinized (8 hr) cotton	.010

A comparison is given in table 4 of the maximum acid-binding capacities of dewaxed cotton, lime-washed depectinized cotton, and the pectic substance with their respective cationic ashes. The correspondence is very close for each sample. In addition to the excellent agreement obtained by the two methods, these values also agree well with independent determinations.[3] Calculation of the data of Walker and Quell [2] for the total cationic ash as obtained by direct methods, in samples of water-washed cotton, gave a value of about 0.064 M-eq/g. Similarly, direct determinations of the uronic acid–carboxyl content, by the method of Whistler, Martin, and Harris [7] of the cotton used in this work gave a value of 0.055 M-eq/g. Since the entire uronic acid–carboxyl content of the cotton can be accounted for by titratable groups, the results suggest that the pectic substance exists on the fiber as the salts of pectic acid.

TABLE 4.—*Comparison of the maximum acid-binding capacities of various samples with their contents of cationic ash*

Sample	Maximum acid-binding capacity	Cationic ash
	M-eq/g	*M-eq/g*
Dewaxed cotton	0.066	0.063
Lime-washed depectinized cotton	.008	.010
Pectic substance (calculated)	.058	.054

4. TEMPERATURE COEFFICIENT OF THE TITRATION CURVE OF DEWAXED COTTON

Table 5 gives the data for the titration curve at 25°C of dewaxed cotton in the absence of added salt. These data are compared with the corresponding data for dewaxed cotton at 0° C in figure 3. The results indicate that there is no measurable temperature coefficient of the equilibrium values in this range of temperature, a result in keeping with the identification of the acidic groups of the fiber as carboxyl groups [11].

[3] Further investigations now in progress in this laboratory indicate that these values are also approximately verified by direct titration, with alkali, of samples of cotton freed of cationic ash by electrodialysis.

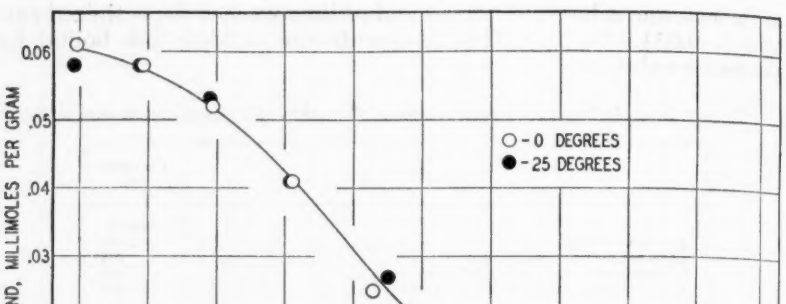

FIGURE 3.—*Titration curves of dewaxed cotton at 0° and 25° C.*

TABLE 5.—*Combination of dewaxed cotton with hydrochloric acid at 25° C in the absence of added salt*

pH	Acid bound	pH	Acid bound
	M-eq/g		*M-eq/g*
1.45	0.058	4.49	0.012
1.93	.058	5.32	.004
2.45	.053	6.38	.001
3.04	.041	6.54	.000
3.75	.027	--------	---------

5. SIGNIFICANCE OF THE ACIDIC GROUPS IN DEPECTINIZED COTTON

The results in the foregoing sections show that about 85 percent of the acidic groups in dewaxed cotton can be allocated to the pectic substance. The question arises, however, as to the source of the acidic groups in the depectinized cotton. The following explanations for their presence might be offered:

1. Removal of the pectic substance by the alkali may be incomplete.

2. The protein fraction of the cotton may have an appreciable acid-binding capacity.

3. The acidic groups may be present in low molecular weight degradation products of cellulose.

4. The acidic groups may be an integral part of the cellulose itself.

A comparison of the acid bound by samples of cotton which had been extracted with sodium hydroxide for 4 and 8 hours showed that both bound essentially the same maximum amount of acid. Since it has been shown by direct analyses for uronic acids that both samples were free of detectable amounts of pectic substance [12], the first of the three possibilities is immediately ruled out. Furthermore, since increasing the duration of the alkali-treatment lowered

the nitrogen content from 0.06 to <0.015 percent, and the maximum acid-binding capacities of the two samples are the same, it is difficult to see how the protein fraction could account for any substantial portion of the acid bound. The third possibility also appears unlikely because it would be expected that acidic compounds of low molecular weight would be readily removed during the treatment with alkali.

It therefore appears that the residual acidic groups in depectinized cotton may well be an integral part of the cellulose molecule, as for example, an end-group. Further work, which is necessary for establishing the validity of such a conclusion, is now in progress in this laboratory. By making the tentative assumption that these acidic groups are contained in the cellulose molecule and are present to the extent of about 0.010 M-eq/g, as determined experimentally, it is found that the cellulose has an equivalent weight of about 100,000, which corresponds to a minimum chain length of about 600 glucose residues.

6. APPLICATION OF THE DONNAN THEORY TO THE TITRATION CURVES OF THE PECTIC SUBSTANCE

As shown in figures 1 and 2, addition of salt produced shifts in the positions of the titration curves to lower pH values. The direction of this shift and the fact that it is not measurably augmented by an increase of ionic strength to 1.0 M suggest that the results may be explained by the Donnan equilibrium. Calculation shows that any alternative mechanism involving the competition of cations for the carboxyl groups requires a still further shift with increased concentration of these ions.[4]

The derivations of the Donnan equations for the titration curves in the absence of salt and in solutions of hydrochloric acid and potassium chloride of 0.1 M ionic strength are given below. Bracketed quantities are molar concentrations. The density of the phase which consists of the pectic substance is taken as unity. The subscripts "o" and "i" refer to quantities in the outside (solution) and inside (pectic substance) phases, respectively. R is the ratio of the activity coefficient of an ion in the inside phase to its activity coefficient in the outside phase, referred to the same standard state, and is assumed to be the same for all the ions involved. This is a reasonable assumption only when all the ions bear similar charges. K is the ionization constant of the acid, α is the fraction of the total acid $[A^-]+[HA]$ in the ionized form $[A^-]$, V represents volume, and ρ equals $[H^+]_i/[H^+]_o$. The acid groups were assumed to be present as salts of the divalent metal, M, [2]. The positions and shapes of the curves are not affected much by the valence of M, in any case. The equations follow:

[4] The titration curves for wool have been shown to be consistent with an ion-association mechanism which involves the combination of cations other than hydrogen ions with basic groups, and anions other than hydroxyl ions with acidic groups on the wool [13]. Since, according to this view, ions of unlike sign are bound by the fiber, the differences in ion concentrations inside and outside the wool phase which would be predicted by the simple application of the Donnan equations (taking into account the binding of hydrogen ions alone) would tend to be minimized, and may apparently be neglected. With cellulose, which is not amphoteric, there is no clear evidence for the existence of association of cations with carboxyl groups, and a Donnan effect is therefore to be expected.

In the absence of added salt,

$$\frac{[H^+]_i R\alpha}{1-\alpha}=K. \tag{3}$$

$$[H^+]_o[Cl^-]_o=[H^+]_i[Cl^-]_i R^2. \tag{4}$$

$$[M^{++}]_o[Cl^-]_o^2=[M^{++}]_i[Cl^-]_i^2 R^3 \tag{5}$$

$$2[M^{++}]_o+[H^+]_o=[Cl^-]_o \tag{6}$$

$$[A^-]+[Cl^-]_i=[H^+]_i+2[M^{++}]_i \tag{7}$$

$$2\frac{V_o}{V_i}[M^{++}]_o+2[M^{++}]_i=[A^-]+[HA]=0.055 \tag{8}$$

These reduce to

$$\{[A^-]+[HA]\}\rho R^2\alpha^2-\frac{\{[A^-]+[HA]\}(\rho^3R^3-1)}{\rho^2R+\frac{V_o}{V_i}}\alpha+\frac{(\rho^2R^2-1)K}{\rho R}(\alpha-1)=0. \tag{9}$$

$$\mathrm{pH}=pK+\log\frac{\rho R\alpha}{1-\alpha} \tag{10}$$

In hydrochloric acid-potassium chloride solutions of 0.1 M ionic strength

$$\frac{[H^+]_i R\alpha}{(1-\alpha)}=K. \tag{11}$$

$$[H^+]_o[Cl^-]_o=[H^+]_i[Cl^-]_i R^2. \tag{12}$$

$$[M^{++}]_o[Cl^-]_o^2=[M^{++}]_i[Cl^-]_i^2 R^3. \tag{13}$$

$$[K^+]_o[Cl^-]_o=[K^+]_i[Cl^-]_i R^2. \tag{14}$$

$$[K^+]_o+2[M^{++}]_o+[H^+]_o=[Cl^-]_o=0.1. \tag{15}$$

$$[A^-]+[Cl^-]_i=[H^+]_i+[K^+]_i+2[M^{++}]_i. \tag{16}$$

$$2\frac{V_o}{V_i}[M^{++}]_o+2[M^{++}]_i=[A^-]+[HA]=0.055. \tag{17}$$

These reduce to the following equations, neglecting 2 $[M^{++}]_0$ in eq 15:

$$\alpha=\frac{0.1(\rho^2R^2-1)}{\{[A^-]+[HA]\}\rho R^2}+\frac{\rho^2R}{\rho^2R+\frac{V_o}{V_i}}. \tag{18}$$

$$\mathrm{pH}=pK+\log\frac{\rho R\alpha}{1-\alpha}. \tag{19}$$

Figure 4 shows the calculated acid titration curves for the salt of a carboxylic acid of pK 3.3 present to the extent of 0.055 M-eq/ml.[5] These curves were calculated by varying the parameter, ρ, and taking R as unity. Curve 1 was calculated from eq 9 and 10 and curve 2 from eq 18 and 19. The latter curve is only very slightly altered by increasing the ionic strength from 0.1 to 1.0 M. From the shape of the curves and the direction of the pH shift (fig. 4), it is seen that the titration data for the pectic substance (fig. 2) are qualitatively consistent with the Donnan equilibrium, but the shift produced by the addition of salt is considerably smaller in the experimental curves than in the theoretical. It is interesting to note that the experimental data (circles) of figure 2 can be fitted very closely with calculated curves (solid lines) obtained by taking R equal to 0.05. It should be noted that R is present in each term of eq 9, 10, 18, and

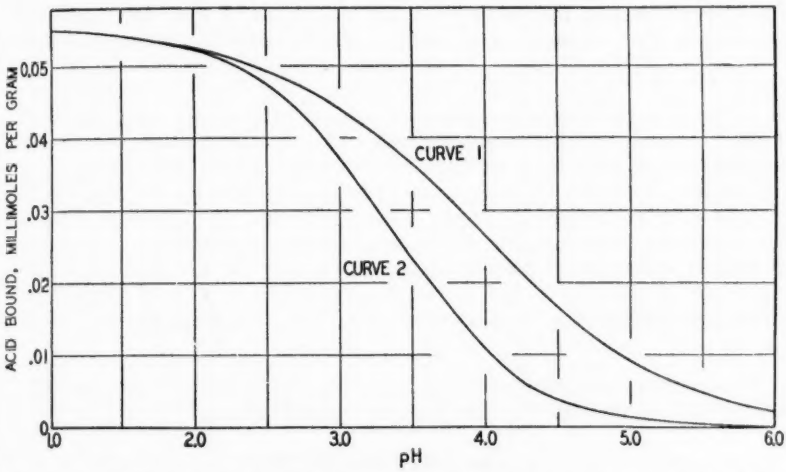

FIGURE 4.—*Theoretical Donnan titration curves for an insoluble acid of pK 3.3.*

Curve 1, in the absence of added salt. Curve 2, in solutions of 0.1 M ionic strength. The assumptions and conditions used are described in the text (section III–6).

19 in the relationship R/V_1. Therefore, the adjustment of either R or V_1 can eliminate the discrepancy between the theoretical curves of figure 4 and the experimental data of figure 2. However, V_1 has been fixed at the highest reasonable value by taking a value of unity for the specific volume, and the rather improbable value of R equals 0.05 is therefore required to make the calculated curves conform with the data.

Aside from the a priori unlikelihood of this value of R, the agreement of the calculated curves with the data is subject to question on the following grounds: The solid lines of figures 2 and 4 represent the calculated amounts of acid fixed by the fiber by exchange with cations held by carboxyl groups. Experimentally determined acid-binding capacities are a measure of the *total* amount of acid adsorbed by the solid phase. If the value for R were 0.05, it would have as a consequence the presence within the solid phase of large quantities of dis-

[5] The value 0.055 M-eq/g is the mean of the values for the maximum acid-binding capacity, cationic ash, and uronic acid-carboxyl content of the pectic substance (section III–3).

solved acid at low values of pH, with resulting large discrepancies between the calculated and experimental values for the total amount of acid adsorbed. If the pectic substance is thought of as being dispersed throughout the fiber, which is rather unlikely [14], the circles of figure 2 would represent only the acid fixed by the carboxyl groups, since they were calculated by a subtraction process that should cancel the effect of any acid dissolved in the fiber. For such a case, however, calculations show that there would be a sharp rise, not found by experiment, in the total amount of acid adsorbed by both the dewaxed and depectinized cotton at low values of pH (fig. 1). If, on the other hand, the pectic substance is thought of as existing in a shell around the fiber, the subtraction process should not cancel the effect of the acid dissolved in the shell, and the circles of figure 2 should show a sharp rise at low values of pH, which was also not found experimentally. The quantitative agreement of the data of figure 2 with the curves cannot therefore be accepted as being too significant, but it is clearly shown that they are consistent with the Donnan equilibrium.

Because of the form of the function, the equation for the titration curve in the presence of salt (curve 2, fig. 2) is virtually identical with the equation for the mass-action law for a monobasic acid of pK 3.3. This is merely an algebraic statement of the fact that the Donnan treatment predicts that as the concentration of salt is increased, the differences between the ion concentrations of the inside and outside phases disappear, and a simple mass-action law is approximated. It is reasonable that the data for pectic substance in the presence of salt should be thus fitted by the mass-action law for an acid of pK 3.3, since pK values for other polyhydroxy acids are near this figure. Thus, glyceric and gluconic acids, e. g., have pK values near 3.5 [15].

The authors are indebted to John Beek, Jr., for assistance in formulating the equations for the Donnan equilibrium.

IV. REFERENCES

[1] I. M. Kolthoff, Pharm. Weekblad **58,** 233 (1921).
[2] A. C. Walker and M. H. Quell, J. Textile Inst. **24,** T123, 131 (1933).
[3] D. A. McLean and L. A. Wooten, Ind. Eng. Chem. **31,** 1138 (1939).
[4] H. Rath and H. Dolmetsch, Klepzig's Textil-Z. **41,** 475 (1938).
[5] A. B. Corey and H. LeB. Gray, Ind. Eng. Chem. **16,** 853, 1130 (1924).
[6] R. K. Worner and R. T. Mease, J. Research NBS **21,** 609 (1938) RP1146.
[7] R. L. Whistler, A. R. Martin, and M. Harris, J. Research NBS **24,** 13 (1940) RP1268; Textile Research **10,** 109 (1940); Am. Dyestuff Reptr. **29,** 1 (1940).
[8] D. I. Hitchcock and A. C. Taylor, J. Am. Chem. Soc. **60,** 2710 (1938).
[9] A. M. Sookne, C. H. Fugitt, and J. Steinhardt, J. Research NBS 25, 61 (1940) RP1314.
[10] A. C. Walker, J. Textile Inst. **24,** T145 (1933).
[11] H. S. Harned and N. D. Embree, J. Am. Chem. Soc. **56,** 1050 (1934).
[12] R. L. Whistler, A. R. Martin, and M. Harris, J. Research NBS **24,** 555 (1940) RP1299.
[13] J. Steinhardt and M. Harris, J. Research NBS **24,** 335 (1940) RP1286; Textile Research **10,** 181 (1940); Am. Dyestuff Reptr. **29,** 103, 131 (1940).
[14] C. W. Hock and M. Harris [In preparation].
[15] R. K. Cannan and A. Kibrick, J. Am. Chem. Soc. **60,** 2314 (1938).

WASHINGTON, April 4, 1940

U. S. Department of Commerce National Bureau of Standards

RESEARCH PAPER RP1314

Part of Journal of Research of the National Bureau of Standards, Volume 25, July 1940

ELECTRODIALYTIC ESTIMATION OF ASH AND OF ACIDIC AND BASIC GROUPS IN TEXTILE FIBERS

By Arnold M. Sookne, Charles H. Fugitt, and Jacinto Steinhardt [1]

ABSTRACT

The method of combustion, usually employed in the determination of the ash of textile fibers, yields results which acquire significance in terms of equivalents only when an estimate of the composition of the ash can be made. It is shown in the present paper that the hydrogen-ion equivalence of the cationic ash of fibers may be obtained directly, without ignition, by slight modifications of simple electrodialytic procedures hitherto applied to solutions. The content of any given diffusible anion in the fiber may be similarly determined. A simple extension of the method which permits the quantitative determination of the acidic and basic groups of fibers (and of other nondiffusible substances) consists in engaging these groups with suitable cations or anions, which are then estimated by electrodialysis.

Examples are given of the application of the method to samples of dewaxed and depectinized cotton. In both cases the results are shown to correspond with the capacity of the fibers to combine with acid. Examples are also given of electrodialytic determinations of the cations of wool fibers, and in samples of wool cloth at several stages in processing subsequent to the carbonizing process. A comparison of these results with the ash obtained gravimetrically after combustion permits the calculation of the average equivalent weight of the constituents of the ash, and indicates that most of the ignited residue of wool consists of sulfates. Since sulfates are known not to be present to any appreciable extent in washed defatted root wool fibers which have not undergone carbonizing, the presence of this anion in the ash of these fibers must be attributed to the oxidation of part of the sulfur of the wool during combustion.

CONTENTS

	Page
I. Introduction	61
II. Method	62
III. Results and discussion	63
1. Cotton	63
2. Wool	64
3. Electrodialytic determination of acidic and basic groups of fibers and other nondiffusible materials	67
IV. References	69

I. INTRODUCTION

Considerable practical and theoretical interest attaches to the estimation of the ash of textile fibers. The method of combustion usually employed is time-consuming and yields values which acquire significance in terms of equivalents only when an estimate can be made of the composition of the igneous residue. In addition, this method may sometimes give values which do not accurately represent the

[1] Research Associates at the National Bureau of Standards, representing the Textile Foundation.

inorganic constituents in the unburned fiber. Thus the ignition of wool results in the formation of sulfate from the oxidation of part of the organic sulfur of the amino acid, cystine, which constitutes an appreciable part of this protein. Consequently, the ash of wool is heavier than it would be if all of the inorganic bases combined with it were found as carbonates or oxides.

The method of electrodialysis used by Joseph and Stadie [1] [2] for the determination of total cations and chloride in blood has been found to be of value for the estimation of the equivalence of the cationic ash of textile fibers (the term "cationic ash" in this paper signifies the total content of the cations of bases, whether free, or combined as salts of acids or of the acid groups of the fibers).[3] This method permits the direct estimation of the hydrogen-ion equivalence of the cationic ash; in addition, it may be extended to include the estimation of specific anions, such as sulfate, which are important in the control of textile finishing processes. Unlike the combustion method, electrodialysis has preparative as well as analytical value, since the samples used in analysis may be recovered, freed of most of their ash, at the end of the determination.

Besides describing the procedure which may be employed with a number of textile fibers and demonstrating the accuracy of the results obtained, the present paper also suggests simple extensions of the procedure which render it applicable to the direct determination of the acidic and basic groups of a wide variety of materials, including fibers.

II. METHOD

In the present investigation, the method of Joseph and Stadie was followed with two modifications: a) The addition of dilute acid to the sample to be dialyzed aided in the liberation of cations combined with the fibers, and greatly shortened the time required for their recovery at the cathode. b) The formation of a reliable seal between the Cellophane membranes and the sides of the dialysis tubes was considerably expedited by the substitution of a commercial cellulose nitrate cement,[4] for the collodion employed by Joseph and Stadie. A diagram of the apparatus employed, copied from the original article, is given in figure 1. The application of a potential difference across the electrodes brings about the migration of cations to the mercury cathode, where they are discharged and form amalgams. Subsequent mixing of the amalgam with the standard solution of hydrochloric acid above the mercury causes a reduction in its titer which corresponds to the hydrogen-ion equivalence of the cationic ash. The titers of the original and final solutions were measured with a 0.02 *M* solution of sodium hydroxide, using bromcresol purple as the indicator. When chloride is among the anions present, it is discharged at the anode unless, as in Joseph and Stadie's method, a suitable reducing agent is added to the anode chamber in order to prevent this. When sulfate is present, oxygen is evolved and sulfate accumulates in the anode chamber.

[1] Figures in brackets indicate the literature references at the end of this paper.
[2] The term is equivalent to the conventional expression "total base" used by Joseph and Stadie in the paper cited, and by biochemists generally.
[3] Duco cement, made by E. I. DuPont de Nemours & Co., was employed.

The quantity of sulfate in the sample may then be determined gravimetrically by precipitation as barium sulfate.

In the method actually employed, a sample of purified cotton, wool, or silk weighing between 0.5 and 1 g was placed in the sample chamber, and soaked in a dilute solution of hydrochloric acid for an hour, after which the sample was electrodialyzed for 2 hours. A resistance of 1,000 ohms in series with the electrodes gave an initial passage of current of about 100 milliamperes, which diminished rapidly as the removal of ions progressively raised the resistance of the dialysis chamber. The accumulation of bubbles of gas on the membranes is avoided by occasionally tapping the outer glass tube. With cotton, identical results for the cationic ash were obtained when 0.02 *M* or 0.15 *M* solutions of hydrochloric acid were used for the soaking treatment. Longer periods of electrodialysis did not appear to increase the effectiveness of recovery of the cationic ash of cotton. With wool, however, slightly more consistent results were obtained with longer initial periods of exposure to acid, and with the higher concentration of acid. Samples of cotton freed of inorganic ions by this treatment yielded no measurable residue when ignited.

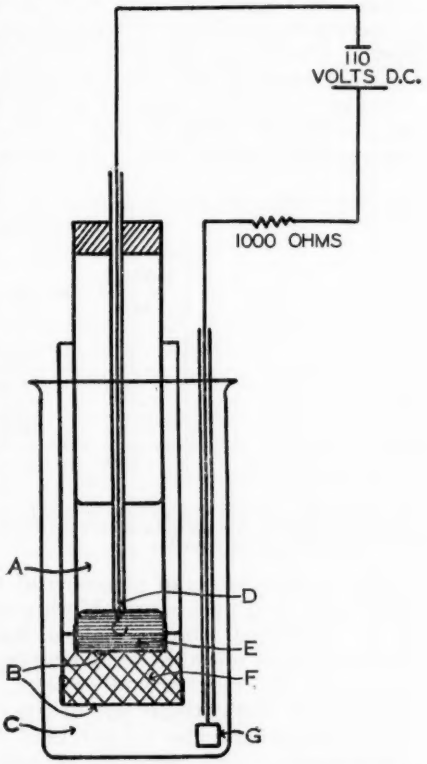

FIGURE 1.—*Diagram of electrodialysis apparatus.*

A, cathode vessel; *B*, Cellophane membranes; *C*, anode vessel; *D*, cathode; *E*, mercury; *F*, sample; *G*, anode

III. RESULTS AND DISCUSSION

1. COTTON

The cationic ash is a factor of primary importance in the behavior of naturally occurring cellulosic materials toward acids. Following the demonstration by McLean and Wooten that a linear relationship obtains between the contents of cationic ash and the acid-binding capacities of various cellulosic materials at an arbitrary pH [2], Sookne and Harris have shown that the limiting amount of acid with which cotton can be made to combine at low values of pH corresponds to the hydrogen-ion equivalence of its cationic ash [3]. The results of electrodialytic analysis of cotton may therefore be compared directly with the results obtained by an independent method. Table

1 lists determinations of the cationic ash of a sample of dewaxed cotton, the preparation of which has been described elsewhere [3]. The values given have been corrected by subtracting a blank of 0.0040 M-eq (milli-equivalent) of acid, a value determined empirically by numerous control runs on the dilute acid solutions in the absence of fibers. Experience has shown that the major source of uncertainty in the final result is the extent to which the blank is reproducible. The mean of the values given is 0.0627 M-eq/g of cotton, in good agreement with the value for the maximum acid-binding capacity of the same sample, 0.066 M-eq/g [3] determined by direct titration.

TABLE 1.—*Hydrogen-ion equivalence of the cationic ash of samples of dewaxed cotton*

Weight of fibers, dry basis	Cationic ash	Cationic ash
g	*M-eq*	*M-eq/g*
0.5065	0.0324	[a] 0.0640
.5159	.0340	.0659
.5092	.0305	.0599
.5176	.0334	.0645
.5095	.0302	.0593
Mean		0.0627

[a] Since the titer differences from which the data of these tables were computed had a precision of 1 part in 150, the data could be represented by either 2 or 3 significant figures. They are given to 3 figures to permit a better estimate of their reliability.

The completeness of recovery of the cations was tested by adding 0.0200 M-eq of potassium chloride to weighed samples, identical with those described above, before making the determinations. The results of these measurements are given in table 2. The second column represents the recovery of cations, combined plus added; the third column lists the cationic ash of the cotton calculated from the weight of the sample and the value 0.0627 M-eq/g obtained in the preceding experiments. The recovery of *added* potassium, shown in column 4, is obtained by subtracting the figures of the third column from the corresponding figures of column 2. The resulting figures indicate very complete recovery of added potassium, and furnish strong evidence for the accuracy of the figures for the naturally occurring cations.

TABLE 2.—*Recovery by electrodialysis of potassium ion added to samples of cotton*

Weight of fibers, dry basis	Total cationic ash	Cationic ash of cotton	K+, recovered	K+, added
g	*M-eq*	*M-eq*	*M-eq*	*M-eq*
0.5106	0.0519	0.0320	0.0199	0.0200
.5115	.0523	.0321	.0202	.0200
.5129	.0525	.0322	.0203	.0200

2. WOOL

The ash content of samples of wool from different sources may vary over wide limits. A large part of the cation content of wool is combined with the acidic groups of the protein (as $RCOO^-M^+$). Consequently, close agreement between measurements of the amounts

of acid bound by wool protein in different lots of wool at any given pH may only be achieved by subtracting the hydrogen-ion equivalent of the combined cations in each lot of wool from all directly determined values of the acid bound under any given conditions [4]. Thus a method is required for determining the equivalence of the ash rather than its weight percent, unless its composition is accurately known. Such a method, described in this paper, is also useful in wool processing, as for example in the control of neutralization and rinsing after the carbonization of wool.

Representative determinations of the ash of fibers, from two different sources, which had been extracted with alcohol and ether and washed with water are given in table 3. It will be noted that longer intervals of time were employed than in the work with cotton. When appreciably shorter periods were allowed for soaking in acid, or for electrodialyzing, the resulting figures were lower and lacking in reproducibility. It has been shown that when wool is immersed in dilute solutions of acid the attainment of equilibrium requires much longer periods than when cotton fibers are similarly treated [3, 4]. The shorter times sufficing for cotton are probably due to the fact that the greater part of the combined cations of dewaxed cotton are associated with an outer shell of pectic substance, which is more readily dissolved in dilute aqueous solutions than is the cellulosic part of the fiber, [3, 5, 6]. The longer interval required for complete ionic recoveries in the electrodialysis of wool is probably a consequence of the same factors which delay its attainment of equilibrium with solutions of acid.

TABLE 3.—*Equivalence of the cationic ash in wool fibers*

[3 ml of 0.15 *M* HCl were added to approximately 0.5 g of wool]

Time of preliminary soaking in acid	Time of passage of current	Cationic ash	Ash by combustion at 700° C	Empirical equivalent weight of ash
hr	*hr*	*M-eq/g*	*mg/g*	*g*
2.0	2.0	0.035	2.60	74.2
2.0	2.0	.029	2.60	89.5
2.0	3.5	.037	2.60	70.3
1.5	4.3	.036	2.60	72.2
3.0	3.0	.036	2.75	76.3
3.0	3.0	.151	11.4	75.5

• In the course of this measurement, it was observed that the passage of current was impeded by the accumulation of gas bubbles. It seems likely that this observation explains the apparently incomplete recovery of combined cations in this single determination.

The empirical combining weights of the ash (milligrams of ash on ignition divided by milliequivalents of cations recovered on electrodialysis), are given in the last column of table 3. These have been calculated in order to provide a partial test of the reasonableness of the values obtained by electrodialysis and incidentally to determine approximate empirical factors for interconverting the quantities determined by electrodialysis and by combustion. The combining weights shown are somewhat higher than can be accounted for, if the ash is largely composed of the oxides of potassium, calcium, magnesium, iron, or aluminum, the combining weights of which are 47, 28, 20, 26, and 17, respectively. Since spectroscopic examination of the ignited residue indicated the presence of relatively large amounts of calcium,

aluminum, and silicon, the average combining weight may be accounted for in part by the presence of silicates or of silicon dioxide, neither of which would affect the equilibria with dilute acids. In addition, part of the sulfur of the protein is oxidized to sulfate on ignition, and the weight of the ignited residue, and thus the empirical combining weight, is increased. The combining weights in the table are very close to those which would characterize the sulfates of the cations known to be present.[5] A comparison of the combining weights in the table with the combining weights calculated from the results of direct titration of the ignited residue with acid showed that less than half of the residue obtained after combustion was capable of combining with acid. This is consistent with the fact that a very large part of the ash is in the form of sulfate. The results tabulated also furnish a strong indication that the average combining weights of the ash from lots of wool characterized by widely different ash contents are sufficiently alike for these combining weights to be used as factors for interconverting the results which would be obtained by electrodialysis and by combustion.

An example of the manner in which the electrodialysis may be applied to routine mill analyses is given below. Both ash and cation determinations were made on pieces of undyed worsted and woolen cloths at different stages of the neutralization and rinsing processes directly following the carbonizing process.[6] The results of these measurements are summarized in table 4.

TABLE 4.—*Ash content of undyed pieces of wool cloth at various stages in processing*

[Averages of three determinations on samples of 0.8 g soaked for 2 hours in 3 ml of 0.15 *M* hydrochloric acid and electrodialyzed for 2 hours]

Nature of cloth	Stage in process	Cationic ash	Ash by combustion at 700° C.	Empirical equivalent weight of ash
		M-eq/g	*mg/g*	*g*
Lightly woven worsted	Water-rinsed [1]	0.025	0.65	26.0
Do.	Soda-washed	.439	23.6	53.8
Do.	Partially neutralized	.071	5.0	70.8
Open weave, woolen and worsted combination.	Water rinsed [1]	.020	.90	45.5
Do.	Soda-washed	.143	8.15	57.0
Do.	"Completely neutralized"	.015	1.35	89.5

[1] These samples contained over 2 percent of sulfuric acid.

All the samples, including those which had been carbonized with sulfuric acid and then merely rinsed with water, contained a nonvolatile mineral residue. In those samples which were merely rinsed, this residue was so small as to render the calculated combining weights uncertain. However, the combining weights of the much larger amounts of ash obtained from the two samples treated with sodium carbonate are closely similar and are not far different from the combining weight of sodium carbonate, which is 53. Owing to the large excess of ash in these samples over the amount of ash originally in

[5] Gravimetric analysis of some of the ashes reported in table 3 showed that 42 percent of their weight was SO_4.

[6] The authors are indebted to Werner von Bergen, Director of the Research and Control Laboratories, Forstmann Woolen Co., Passaic, N. J., for furnishing the samples used. A description of the stages in the neutralizing and rinsing process to which the table and text refer will be found in the American Wool Handbook, 1st edition, page 503.

untreated wool, the effects of the original ash on the average combining weight of these samples is practically negligible. Nevertheless, the close agreement between the experimental and theoretical combining weights of the ash of these samples may be in part coincidence. A considerable part of the carbonate originally present must, however, have been transformed into sodium sulfate by neutralization of sulfuric acid remaining on the cloth; if all of it were so transformed, the combining weight would have been 71. It therefore appears likely that sulfates and oxides (formed by decomposition of carbonates, and from sodium ions combined with the wool itself) were present in addition to carbonate, with a resulting average equivalent weight close to the theoretical value for sodium carbonate. This suggestion receives some measure of support from the fact that a large part of the soda *in the unburned sample* had reacted with sulfuric acid and was present as sulfate. Thus only 0.24 millimole of acid per gram was required to neutralize the free base in a sample of the soda-treated cloth, although the total cation equivalence, as determined by electrodialysis, was 0.44 millimole, or almost twice as great.

As shown in table 4, the combining weights tend to rise after even partial neutralization and washing out of the soda-ash. On "complete neutralization" they rise still more. Since the "neutralized" material was low in ash before the soda treatment, the ash remaining after neutralization must have resulted largely from this treatment. The rise in the combining weight indicates that most of the carbonate, which would yield an ash of low combining weight, has been removed by washing, leaving sulfates of sodium and, to a much less extent, of other heavier ions initially in the fiber.

The feasibility of determining electrodialytically the sulfuric acid in the carbonized fibers, as distinguished from the sum of this quantity plus the sulfate formed in combustion, has been demonstrated in work with wool yarn previously treated with sulfuric acid. Samples of wool in the central chamber of the apparatus were immersed in 0.15 *M* sodium hydroxide and exposed to the passage of current for 4 hours. At the end of this period the contents of the anode chamber were analyzed gravimetrically for sulfate. The results agreed closely with similar sulfate analyses made on the total hydrolytic products of other samples of sulfuric-acid-treated wool which had been decomposed by hot concentrated hydrochloric acid.

By simultaneously measuring the hydrogen-ion equivalence of the cations and of sulfate and determining the difference between them, a figure of interest in mill technology, the content of excess acid or base may be obtained.

3. ELECTRODIALYTIC DETERMINATION OF ACIDIC AND BASIC GROUPS OF FIBERS AND OTHER NONDIFFUSIBLE MATERIALS

Application of the methods already described permits the estimation of the acidic or basic groups of substances which possess the following properties:

1. Nondiffusibility through Cellophane or collodion.
2. The capacity to form tightly bound complexes with at least one species of cation (for the estimation of acidic groups), or with at least one species of anion (for the estimation of basic groups). The complexes must not readily dissociate or hydrolyze on dialysis or washing

sufficiently prolonged to remove the unbound excess of these ions. Such complexes are formed by calcium in the case of dewaxed cotton, and by various acid dyes in the case of protein substances [7].

3. A large difference between the strength of the acidic or basic groups to be estimated and the strengths of the other acidic or basic groups present. Thus, in cellulose, the estimation of the total number of carboxyl groups with calcium is possible only because these groups are very much more acidic than the hydroxyl groups; the latter do not combine with base under the conditions used.

The acidic (or basic) groups of substances which fulfill these three requirements may be determined by engaging the groups with a suitable cation (or anion) by treatment with a suitable base (or acid), removing the excess reagent by washing (if the product is insoluble) or dialyzing (if the product is soluble), and electrodialyzing to determine the amount of cation (or anion) remaining combined.

In order to illustrate the application of the above general procedure, the determination of the acidic groups of cotton is described below.

Table 5 gives data for the cationic ashes of samples of dewaxed cotton which had been soaked in limewater for 3 hours, and washed with running distilled water for 24 hours. Comparison of these results with those of table 1 shows that the limewater treatment does not increase the cationic ash of dewaxed cotton appreciably. It has been stated in section III–1 that the hydrogen-ion equivalence of the cationic ash of dewaxed cotton corresponds closely with the number of carboxyl groups as determined by an independent method, the direct titration of these groups with acid. It therefore follows that the cationic ash of lime-washed dewaxed cotton is a measure of the total number of carboxyl groups of the fiber and, further, that the carboxyl groups of unprocessed cotton are almost entirely present as the carboxylates of various tightly bound ions [3].

TABLE 5.—*Hydrogen-ion equivalence of the cationic ash of lime-washed, dewaxed cotton*

Weight of fibers, dry basis	Cationic ash	
g	*M-eq*	*M-eq/g*
0.749	0.0474	0.0633
.776	.0500	.0644
.780	.0506	.0649
Mean		0.0642

The method has also been applied to the measurement of the acidic groups of depectinized cotton. The material was prepared by the modification of the American Chemical Society procedure for the purification of cotton described by Worner and Mease [8]. This procedure involves the extraction of the fibers with a boiling 1-percent solution of sodium hydroxide. At a later stage in the process the fibers are thoroughly washed with a 1-percent solution of acetic acid, a treatment which undoubtedly removes some of the cations initially combined with the fiber or taken up from the basic solution. In order to replace cations on the carboxyl groups, the samples were soaked in a saturated solution of calcium hydroxide for 3 hours and

washed with running distilled water for 24 hours. The results of determinations of the cationic ashes of these samples are given in table 6. Samples 1 to 4 were extracted with alkali for 4 hours, and had a maximum acid-binding capacity of 0.008 M-eq/g. Samples 5 and 6 were extracted with alkali for 8 hours, and had a maximum acid-binding capacity of 0.009 M-eq/g [3]. The data show the close correspondence between the carboxylate content and the hydrogen-ion equivalence of the cationic ash.

TABLE 6.—*Hydrogen-ion equivalence of the cationic ash of lime-washed depectinized cotton*

Sample number	Weight of fibers, dry basis	Cationic ash	
	g	*M-eq*	*M-eq/g*
1	0.5168	0.0054	•0.0104
2	.7063	.0067	.0095
3	.8775	.0079	.0090
4	.754	.0069	.0092
Mean			0.0095
5	.746	.0080	0.0107
6	.731	.0067	.0090
Mean			0.0099

• Since the titer differences from which the data of these tables were computed had a precision of 1 part in 25, the data could be represented either as shown, or by one less significant figure. They are given as shown to permit a better estimate of their reliability.

IV. REFERENCES

[1] N. R. Joseph and W. C. Stadie, J. Biol. Chem. **125,** 795 (1938).
[2] D. A. McLean and L. A. Wooten, Ind. Eng. Chem. **31,** 1138 (1939).
[3] A. M. Sookne and M. Harris. J. Research NBS **25,** 47 (1940) RP1313.
[4] J. Steinhardt and M. Harris, J. Research NBS **24,** 335 (1940) RP1286; Am. Dyestuff Reptr. **29,** 103, 131 (1940); Textile Research **10,** 181 (1940).
[5] R. L. Whistler, A. R. Martin, and M. Harris. [In preparation.]
[6] C. W. Hock and M. Harris. [In preparation.]
[7] J. Steinhardt and M. Harris. J. Biol. Chem. **133,** 97 (1940).
[8] R. K. Worner and R. T. Mease, J. Research NBS **21,** 609 (1938) RP1146.

WASHINGTON, April 4, 1940.

U. S. Department of Commerce National Bureau of Standards

RESEARCH PAPER RP1315

Part of Journal of Research of the National Bureau of Standards, Volume 25, July 1940

DETERMINATION OF THICKNESS OF ACID-RESISTANT PORTION OF VITREOUS ENAMEL COATINGS

By William N. Harrison and Leo Shartsis

ABSTRACT

A method is described whereby an oblique section of the enamel approximately 1 cm wide is exposed by grinding. The boundaries of this section are permanently marked, and the oblique section is given a fire polish by refiring. The surface is then exposed to acid, after which it is coated with colored wax. Upon rubbing the surface, this wax is removed from the acid-resisting enamel, which retains its gloss in the acid, but is retained by the etched portion of the oblique section. The fraction of the oblique section which is occupied by the acid-resisting enamel is then determined, and this fraction is multiplied by the total thickness of enamel as measured by a magnetic gage. The product gives the thickness of the layer of acid-resisting enamel.

CONTENTS

	Page
I. Introduction	71
II. Method of test	71
III. Accuracy of method	73
IV. Conclusion	74

I. INTRODUCTION

In the course of revision of the Federal specification for plumbing fixtures, including the incorporation of specifications for formed-metal sanitary ware, the Enameled Metals Section of the National Bureau of Standards was asked to make recommendations. Because the practice in enameling sheet iron by the wet process is to apply first a non-acid-resistant coating over the ground coat and to follow this by an acid-resistant coating (when required), it is not possible by a mere determination of the total thickness of enamel to discover how heavy a coating of acid-resistant enamel has been applied. Since it is desirable to specify a minimum thickness for the acid-resistant layer of enamel, it was necessary to devise a test method for determining this thickness. The present paper describes a method which was found satisfactory.

II. METHOD OF TEST

The method of test is based on a principle illustrated by figure 1, which shows in diagrammatic form an oblique section through an enamel coating on iron. The device of cutting an oblique section at a small angle to the enamel surface permits measurements of distances much larger than the comparatively small thickness of acid-resistant enamel which may be present.

By geometry, it can be shown that in a specimen as represented in figure 1 the thickness, ab', of the acid-resistant enamel may be computed from measurements of other distances, as follows:

$$\frac{ab'}{ad'}=\frac{ab}{ad}, \text{ or } ab'=ad'\times\frac{ab}{ad}$$

Stated verbally, the thickness of the acid-resistant coating equals the total enamel thickness multiplied by the ratio of the width of the acid-resistant section to the total width of the oblique section of enamel.

Using this principle, the following procedure was adopted for testing commercial articles:

Remove a flat or nearly flat section of the article to be tested, not less than 5 by 5 cm in size.[1] (The article may be cut with the flame

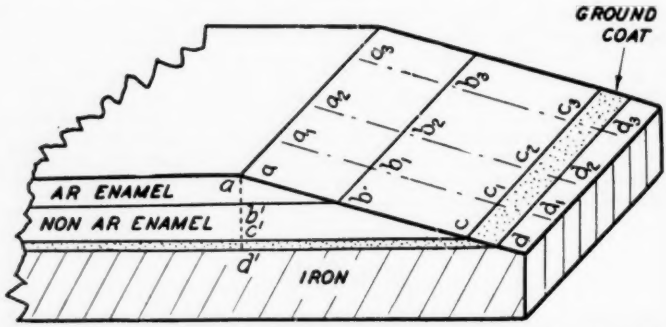

FIGURE 1.—*Sketch of specimen showing cross section and oblique section of enamel applied in three coats over iron.*

AR means acid-resisting. Lines a_1d_1, a_3d_3, etc., are explained in the text.

of a suitable torch, or with a hacksaw.) Along one edge of the specimen, other than an edge of the original article, grind off the enamel in a plane at an angle of approximately 5° to the surface of the enamel, exposing an oblique section of the enamel coating and part of the underlying metal at least 5 cm in length (see line dd_3, fig. 1). The width of the exposed oblique section of the enamel, measured along its surface (distances a_1d_1 and a_3d_3), shall be 1.0 ± 0.25 cm for sheet-metal articles, or 2.0 ± 0.5 cm for dry-process cast-iron articles. The abrasive[2] used in grinding shall pass a No. 150 sieve and shall be moistened during grinding. The grinding may be done on a brass or glass flat, using a shim under one side of the specimen to obtain the desired 5° angle. After grinding, mark the boundary between the original glossy surface and the treated surface of the enamel by a very narrow line, made with a ceramic underglaze pencil,[3] and rub with a dry cloth until any marking on the glossy surface is removed. There will remain the line aa_3, figure 1.

With the same marking agent, make three straight lines (a_1d_1, a_2d_2, and a_3d_3) as narrow as can be plainly seen, at intervals of 1 cm or more, across the oblique section of enamel, perpendicular to the

[1] Obviously, small laboratory specimens may be tested by this method without reducing their size.
[2] Silicon carbide was found to be satisfactory for this purpose.
[3] For this particular method of marking the boundary the authors are indebted to M. G. Ammon, of the Ferro Enamel Corporation.

boundary, dd_3, between the enamel and the exposed iron base. None of these lines shall be closer than 1.5 cm to an edge of the specimen which was an edge of the original article. Along each of these lines, measure the width of the oblique section of enamel between the exposed iron base and the original enamel surface. (The width of the line, aa_3, made with the ceramic underglaze pencil, must be included in the measured distances.)

Refire the specimen just sufficiently to obtain a fire polish on the oblique section of enamel. After cooling, immerse the treated portion of the specimen in 10-percent citric acid for 15 minutes, at room temperature ($80° \pm 10°$ F). After rinsing and drying the specimen, rub the entire oblique section of enamel with a colored-wax pencil, then rub the deposit of colored wax with a dry cloth. The acid-resistant portion of the enamel coating (between lines aa_3 and bb_3) will have retained its fire polish in the acid solution, and the colored deposit of wax will be readily removed from it but will remain on the etched portion of the cross-section (between lines bb_3 and dd_3, fig. 1). The acid-resistant band of enamel in the oblique section will then be bounded on one side by the colored-wax deposit and on the other by the edge of the ceramic-pencil mark, aa_1, which is adjacent to the original glossy surface of the enamel.

Measure the width of this acid-resistant band at the three pencil marks along which the width of the total oblique section has previously been measured (a_1d_1, a_2d_2, and a_3d_3), and compute the average width ratio of the acid-resistant portion to the total oblique section of enamel (the average of a_1b_1/a_1d_1, a_2b_2/a_2d_2, and a_3b_3/a_3d_3). All measurements on the oblique section shall be made with an accuracy of ± 0.1 mm (0.004 inch), using preferably a transparent millimeter scale. Measure the total enamel thickness adjacent to the location of the measurements described above, using a magnetic thickness gage or other suitable means having an error less than 0.001 in. (0.025 mm). Multiply the average value for total thickness by the average ratio of acid-resisting enamel to total enamel, determined as described above. The product equals the thickness of the acid-resisting portion of the enamel coating.

When this test is used for control purposes by a manufacturer, it may frequently be possible to shorten the procedure considerably, because the line of demarcation, bb_3, between the acid-resistant and the non-acid-resistant enamel is frequently visible immediately after the grinding of the oblique section. Since all necessary boundaries in such a case are already visible, no marking of boundaries with ceramic underglaze pencil, nor refiring, nor acid treatment, is necessary.

III. ACCURACY OF METHOD

A number of determinations were made to check the experimentally determined thicknesses of the acid-resistant portions of enamel coatings against known amounts of the enamel applied to laboratory specimens. Known weights per unit area of acid-resistant enamel were applied over nonresistant enamels, and the thicknesses of the final coatings were determined by the method described in section II. They were also computed from the specific gravity of the enamel.

The coatings of acid-resistant enamel were applied over fired coats, and also over coats which had been sprayed on and dried, but not

fired. In either case the acid-resisting coating was, of course, fired. Table 1 shows some typical results, which indicate that the estimated and determined thicknesses usually agree within about one-half to three-fourths of a mil. Such discrepancies as occur are doubtless due, in considerable part, to the variation in thickness from spot to spot on the specimen, for which no allowance was made in estimating the thickness from the applied weight of enamel. For specimens having the acid-resistant coating sprayed on before the under coat was fired, the line of demarcation between the two was more irregular, as might have been expected. Also, with this type of application, the tendency was for the determined thickness to be slightly greater than the estimated thickness, but the limits of error were no larger than indicated by table 1.

TABLE 1.—*Comparison of estimated and determined thickness of enamel on 6 specimens*

Specimen	Prefired under coat	Thickness of *A R* coating		Difference (*E*−*D*)
		Estimated (*E*)	Determined (*D*)	
		Mils	*Mils*	*Mils*
1	Yes	7.6	6.8	+0.8
2	Yes	5.5	5.3	+.2
3	Yes	4.6	4.9	−.3
4	Yes	4.8	4.3	+.5
5	Yes	2.9	2.9	0
6	No	2.6	3.2	−.6

IV. CONCLUSION

The method described appears to be suitable for use in specifications. It should also prove useful to manufacturers in studying the distribution of the acid-resistant layer of enamel over their products. The data gained in this way could profitably replace the assumption that the average weight per unit area applied to a commercial shape is indicative of the thickness of acid-resistant enamel on each part of the fixture, whether vertical or horizontal. The method is equally applicable to wet-process and dry-process enamels.

WASHINGTON, May 7, 1940.

U. S. DEPARTMENT OF COMMERCE NATIONAL BUREAU OF STANDARDS

RESEARCH PAPER RP1316

Part of Journal of Research of the National Bureau of Standards, Volume 25, July 1940

CORROSION OF METALS USED IN AIRCRAFT

By Willard Mutchler

ABSTRACT

Investigations of the corrosion of metals used in aircraft have been in progress continuously at the National Bureau of Standards since 1925. The projects have been sponsored by the National Advisory Committee for Aeronautics, the Army Air Corps, and the Bureau of Aeronautics of the Navy Department. The present paper reviews the work that has been done, summarizes the more important results, and lists the publications in which fuller details appear.

CONTENTS

	Page
I. Introduction	75
II. Procedure	77
III. Methods of exposure	78
IV. Summary of tests and results	78
1. Corrosion of aluminum alloys	78
2. Protective coatings on aluminum alloys	79
3. Corrosion of magnesium alloys	80
4. Protective coatings on magnesium alloys	80
5. Corrosion of stainless steels	80
6. Corrosion of rivets and welds	81
7. Corrosion of dissimilar metals in contact	81
V. References	81

I. INTRODUCTION

When aluminum-rich alloys of the duralumin type were first used in aircraft construction, there occurred numerous instances of extremely rapid corrosion, accompanied by embrittlement. An investigation was begun at this Bureau (1) to develop methods for producing and determining the causes of this corrosion-embrittlement, and (2) to evolve methods for its elimination or prevention. Early studies of such variables as chemical composition, heat treatment, and aging of the alloys were successful in these two respects. The efficiencies of various oxide coatings, particularly in combination with organic or paint coatings, were next studied. Currently, the corrosion of aluminum alloys when in contact with each other, or with dissimilar metals, or when joined by rivets and welds, is being investigated.

Studies of the corrosion of magnesium-rich alloys, with and without protective coatings, were begun in 1929 with the object of developing more corrosion-resistant alloys and better surface coatings. An investigation of the corrosion of stainless steels was started in 1938 to determine the effect of the addition of such elements as columbium, titanium, and molybdenum to steels of the 18-chromium 8-nickel type and to determine the behavior of shot welds on such steels.

Approximately 25,000 specimens of 60 alloys have been tested. The alloys, their nominal chemical compositions, and condition of fabrication are listed in tables 1 to 3, inclusive. The greatest number of specimens were in sheet form, usually from 0.040 to 0.064 inch thick.

TABLE 1.—*Summary of data on the aluminum alloys included in the investigation*

Alloy designation	Fabrication [c]	Exposure [d]	Nominal chemical composition						Relative corrosion resistance [e]	Literature reference [f]
			Mg	Cu	Mn	Fe	Si	Other elements		
			%	%	%	%	%			
14S	*fp*	*W, T*	0.4	4.4	0.8	0.5	0.8		*E*	[18]
25S	*s*	*I, S, W*	.0	4.5	.8	.4	.8		*E*	[5 II, 5 III, 5 V, 10, 17]
24S [a]	*s, ep*	*I, S, W, T*	1.5	4.4	.5	.2	.1		*D, A* [e]	[17, 18]
I-2 [b]	*s*	*I, W*	0.5	4.0	.5	.07	.08		*D*	[5 II, 5 V, 10]
I-1 [b]	*s*	*I, W*	.5	4.0	.5	.2	.2		*D*	[5 II, 5 V, 10]
17S [a]	*s, r*	*I, S, W, T*	.5	4.0	.5	.3	.3		*D, A* [e]	[1 to 11, 15 to 18]
Baush dural	*s*	*I, S, W*	.5	4.0	.5	.3	.3	Cr. 0.15	*D*	[5, 10]
Carbium	*s*	*I*	.5	4.0	.5	.3	.3	C 0.01	*D*	
63A [b]	*s*	*I, W*	.6	3.8	.5	1.1	.2		*D*	[5 II, 5 V, 10]
B17S	*s*	*I, W*	.5	3.7	.02	0.3	.3		*D*	[5 II, 5 V, 10]
58B [b]	*s*	*I, W*	.6	3.1	.5	.5	.2		*D*	[5 II, 5 V, 10]
A17S	*s, r*	*I, W, T*	.3	2.5	.02	.3	.3		*D*	[5 II, 5 V, 10]
Nicralumin (Hybium).	*s*	*I, S, W*	.5	0.4	.2	.5	.3	Ni 1.0, Mo 0.1, Zn 0.2, W 0.1, Cr 0.2.	*C*	[17]
Major Metal	*s, b*	*I, W, T*	.3	1.4	.1	.5	.3	Ni 0.9, Ag 0.5, Zn 0.2, Pb 0.1, Cr <0.05	*D*	
Hiduminium *RR50*	*fb, cb*	*S*	.5	2.0	.02	1.2	1.0	Ni 1.2, Ti <0.2	*D*	
Hiduminium *RR58*	*fb, cb*	*S*	1.6	2.2	.01	1.6	1.3	Ni 1.1, Ti <0.2	*D*	
Aeral	*s*	*I, S, W*	0.8	4.0	.3	0.3	0.4	Cd 2.0	*D*	[17]
Y alloy	*s*	*I*	1.6	4.0	<.01	.3	.2	Ni 2.0	*D*	[5 II]
51S	*s*	*I, S, W*	0.6	0.05	.01	.3	1.0		*C*	[5 II, 5 III, 5 V, 10, 17]
XA51S	*s*	*S, W*	.6	.05	.01	.3	1.0	Cr 0.25	*C*	[17]
4S	*s*	*S, W*	1.0	.1	1.1	.4	0.2		*B*	[17]
53S	*s, r, ep*	*S, W, T*	1.2	.02	0.0	.2	.7	Cr 0.25	*B*	[18]
X52S	*s*	*S, W*	1.25	.02	.0	.4	.2	Cr 0.2	*A*	[17]
52S	*s*	*S, W, T*	2.5	.02	.0	.1	.1	Cr 0.25	*A*	[17, 18]
XB52S	*s, r*	*S, W*	3.5	.02	.0	.2	.1	Cr 0.25	*A*	[17]
AM55S	*r*	*W, T*	4.5	.01	.0	.1	.07		*B*	[18]
56S	*s, r*	*S, W*	6.0	.02	.0	.1	.06		*B*	[17]
Inalium	*s*	*I, S, W*	0.8	.0	.0	.2	.4	Cd 2.0	*B*	[17]
Al-Be No. 1 [b]	*s*	*I*	1.2	.05	.0	.1	.1	Be 0.8	*C*	[5 II]
Al-Be No. 2 [b]	*s*	*I*	0.0	.05	.0	.1	.8	Be 0.4	*C*	[5 II]

[a] Alloys also exposed with high-purity aluminum (Alclad) surface coatings, which afforded excellent protection against corrosion.

[b] Alloys prepared especially for this investigation. The duralumins were *I-1*, controlled impurities; *I-2*, high-purity ingredients; *58B*, low copper; *63A* high iron.

[c] *s*, sheet; *p*, plate; *r*, rivet; *b*, bar; *c*, cast; *e*, extruded; *f*, forged.

[d] *I*, intermittent immersion; *S*, salt spray; *W*, weather; *T*, tidewater.

[e] The ratings are approximations only, based on the assumption that the alloy was exposed in its most resistant form to severely corrosive saline conditions. They are applicable to the aluminum alloys only. *A* is the highest rating.

[f] Further details are reported in cited references at end of this paper.

TABLE 2.—*Summary of data on the magnesium alloys included in the investigation*

Alloy designation	Fabrication [1]	Exposure [2]	Nominal chemical composition			Relative corrosion resistance [3]	Literature reference [4]
			Al	Mn	Other elements		
			%	%	%		
AM3S, Dowmetal *M*, Elektron *AM503*.	*s, p*	*W, T, S*		1.5		*A*	[17, 18]
M	*s*	*W*	0.4	0.01		*C*	[11]
MM (*AM55S*), Dowmetal *F*	*s, cp, eb*	*W, S*	4.0	.3		*C*	[11, 17]
MA	*s*	*W*	3.9	.01		*C*	[11]
Dowmetal *E*	*s*	*W*	6.0	.3		*D*	[17]
AM241 (*AM7.4*), Dowmetal *A*	*cp, eb*	*W*	7.4	.3		*D*	[17]
AM240	*cp*	*W, S*	9.0	.1		*D*	[17]
AZM (*AM57S*), Dowmetal *J*	*eb, hp*	*W, S*	6.5	.2	Zn 0.75	*B*	[17]
Dowmetal *H*, Elektron *AZG*	*eb, ep*	*W, T, S, I*	6.5	.2	Zn 3.0	*B*	[17, 18]
AM764	*cp*	*W*		.3	Zn 3.4, Sn 4.6	*B*	[17]
Dowmetal "*S*"	*s*	*W, S*			Zn 1.0, Cd 3.0	*E*	[17]
AM61S	*fp, p*	*W*		1.0	Sn 6.5	*A*	[17]
AM65S	*fp*	*W, S*	4.0	1.0	Sn 5.0	*A*	[17]
Dowmetal *T*	*cp*	*W*	2.0	0.1	Cu 4.0, Cd 1.7	*E*	[11]

[1] *s*, sheet; *p*, plate; *b*, bar; *c*, cast; *e*, extruded; *f*, forged; *h*, hot-pressed; products rolled, if not otherwise indicated.
[2] *I*, intermittent immersion; *S*, salt spray; *W*, weather; *T*, tidewater.
[3] The ratings are approximations, with *A* the highest rating. They are applicable to the magnesium alloys only, and are based on behavior under saline conditions of exposure.
[4] Further details are reported in the literature references at end of this paper.

TABLE 3.—*Summary of data on the stainless steels and nickel alloys included in the investigation*

Alloy designation [1]	Nominal chemical composition								Relative corrosion resistance [2]
	Cr	Ni	C	Mn	S	P	Si	Other elements	
Stainless steels:	%	%	%	%	%	%	%		
Type 302	17.6	7.5	0.10	0.5	0.01	0.01	0.4		*B*
Type 304	18.4	8.3	.08	.4	.01	.01	.4		*B*
Type 306	19.5	9.5	.09	.4	.01	.02	.3		*B*
Type 316	17.8	10.7	.05	1.3	.01	.01	.3	Mo 2.7	*A*
Type 317	17.9	12.4	.07	1.5	.01	.01	.3	Mo 3.7	*A*
Type 347	18.3	9.9	.08	0.4	.01	.01	.2	Cb 0.5	*B*
Do	18.4	8.6	.08	.4	.02	.01	.4	Cb 0.8	*B*
Type 321	17.6	9.1	.07	.4	.01	.01	.5	Ti 0.5	*B*
16-1	17.7	1.6	.08	.7	.02	.01	.5		*C*
Nickel alloys:									
Nickel		99.4	.1	.2	.005		.05	Cu 0.1, Fe 0.15	*B*
Monel		67.0	.3	.9			1.25	Cu 29.0, Fe 1.5	*A*
Inconel	13.5	78.5	.25	.9			0.6	Cu 0.25, Fe 6.0	*A*

[1] The alloys were in sheet form and were exposed to weather and tidewater at Hampton Roads, Va. Literature reference [18] contains results of the tests.
[2] The highest rating is *A*, and ratings are applicable only to alloys given in this table.

II. PROCEDURE

Tensile bars, strips, or large panels were exposed to accelerated tests in the laboratory, to the weather, or to tidewater corrosive conditions, and corroded specimens from each set were removed at progressive intervals for test. Diagrams of typical specimens are shown in figure 1. Each corroded specimen was photographed and then broken in a tensile test. Differences in the tensile properties from those of uncorroded specimens (stored in a dry atmosphere in sealed containers in

the laboratory) served as an indirect measure of the corrosion. Microscopic examinations were made subsequently of metallographic sections of the tested specimens to determine the nature of the corrosive attack, and measurements were made of the depth and extent of its penetration. Permanent records of the corrosive attack were made by a special method developed for the purpose [15][1], at 50 to 250 magnifications on photostat paper negatives, at a rate of approximately 650 per day.

III. METHODS OF EXPOSURE

The majority of the accelerated laboratory corrosion tests were conducted by either the intermittent-immersion or the salt-spray methods (fig. 2). In the intermittent-immersion tests, specimens were immersed in the corroding medium for approximately 1 minute and suspended in air for 14 minutes, the cycle being repeated continuously. The corroding medium usually consisted of a mixture of 9 parts of a normal sodium chloride solution and 1 part of commercial hydrogen peroxide, although other reagents were used. An apparatus was designed to permit flexural stressing of the sheet specimens in order to study the effect of the combined action of stress and corrosion. The majority of the salt-spray tests were conducted in a finely atomized spray or mist of a 20-percent sodium-chloride solution.

The weather-exposure localities (fig. 3) were Washington, D. C., Hampton Roads, Va., and Coco Solo, C. Z. The first two localities were selected as representative of temperate climate, with and without a saline atmosphere, whereas the third combined a tropical climate with marine conditions. At Hampton Roads, in 1938, tidewater exposure racks were installed to permit immersion of the panels in salt water twice each day.

IV. SUMMARY OF TESTS AND RESULTS

1. CORROSION OF ALUMINUM ALLOYS

Early in the investigation, corrosion in alloys of the duralumin type was found to be of two distinct types (fig. 4): (a) the "pitting" type, in which surface pits are formed that bear no evident relation to the microstructure of the metal, analogous to the rusting of ferrous metals, and (b) the intercrystalline type, of which only slight evidence may be seen on the surface, but which penetrates into the interior, largely between the grain boundaries.

Intercrystalline attack was shown to be responsible for the serious embrittlement of duralumin. It was found to be associated with certain microstructural conditions that resulted from incorrect heat treatment, namely, those in which particles of the constituent $CuAl_2$ were precipitated along the grain boundaries and quite abundantly within the grains. The rate of cooling during the quenching that followed the preliminary "solution" heat treatment was found to be a determining factor. After a solution heat treatment at 500° C, it had been the practice to quench duralumin in warm water to minimize distortion. It was shown (fig. 4, f) that quenching in cold water, preferably below 25° C, resulted in retention of the $CuAl_2$ particles

[1] Figures in brackets indicate the literature references at the end of this paper.

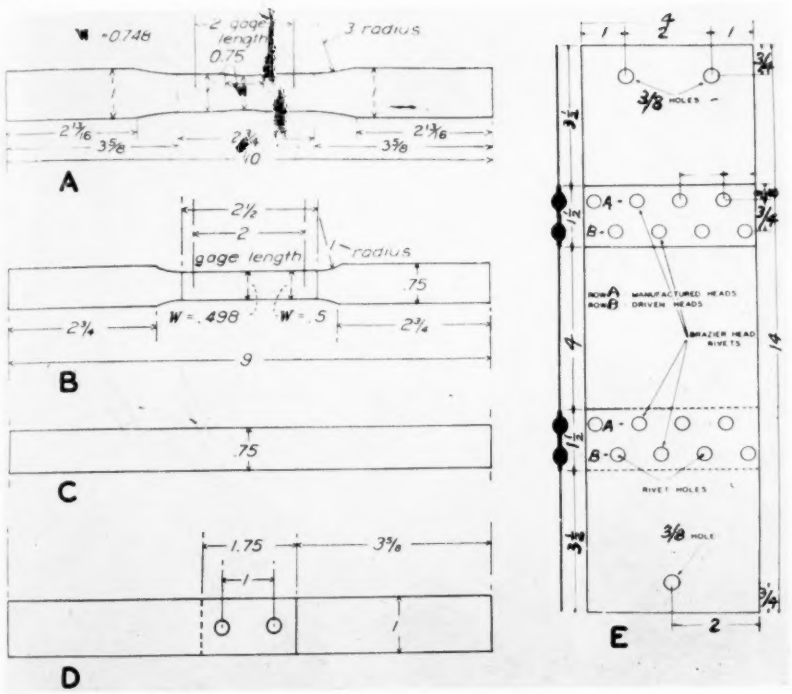

FIGURE 1.—*Types and dimensions of specimens.*

A and *B*, tensile bars; *C* and *D*, strips; *E*, panel used in the current exposure program, superseding previous types. Circles on specimen *D* indicate spot welds or rivets.

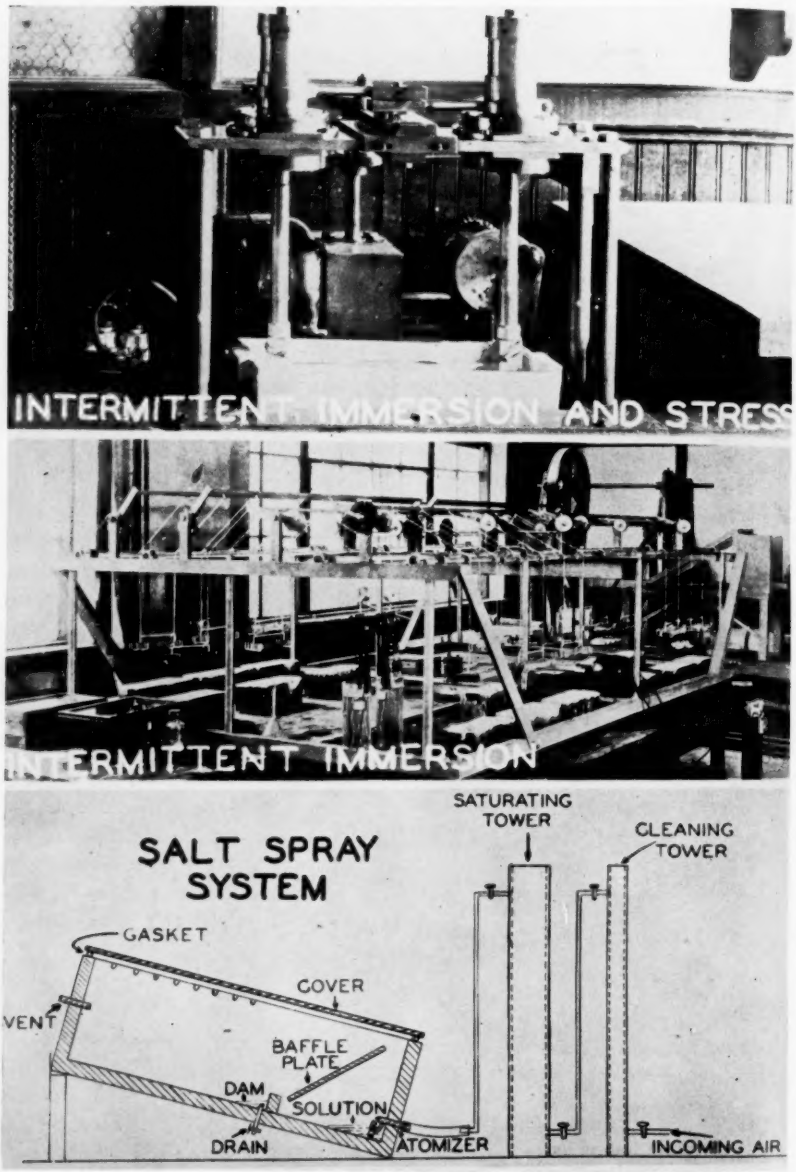

FIGURE 2.—*Apparatus used in the laboratory corrosion tests.*

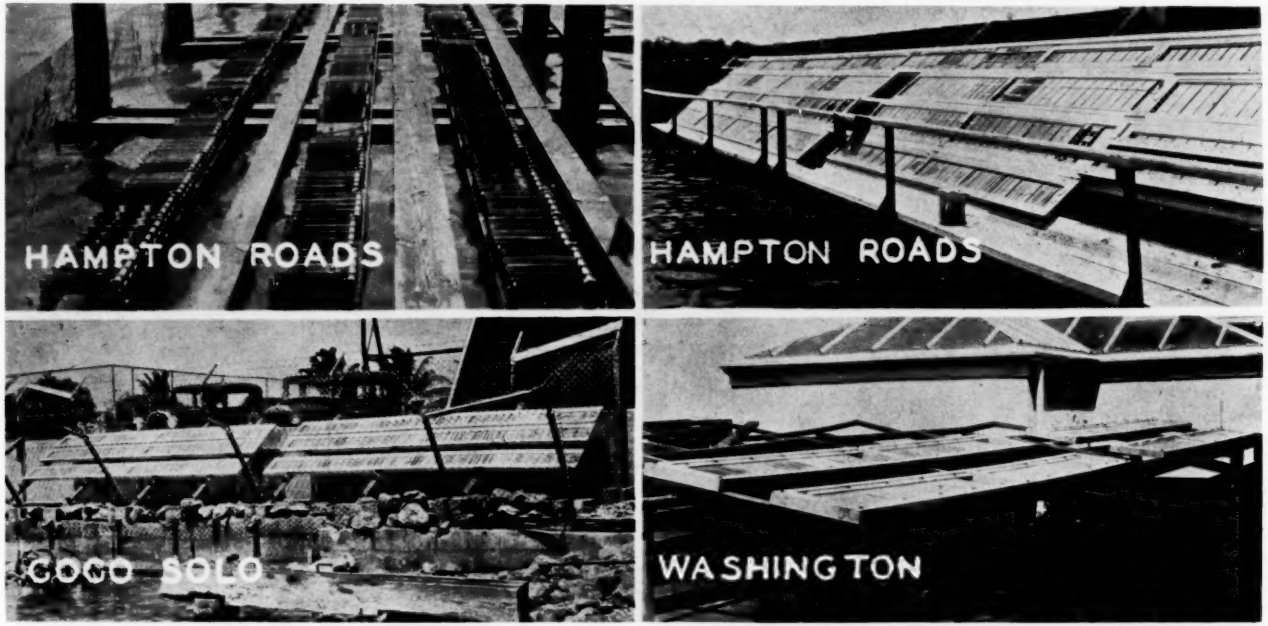

FIGURE 3.—*Weather-exposure, and tidewater (upper left) installations.*

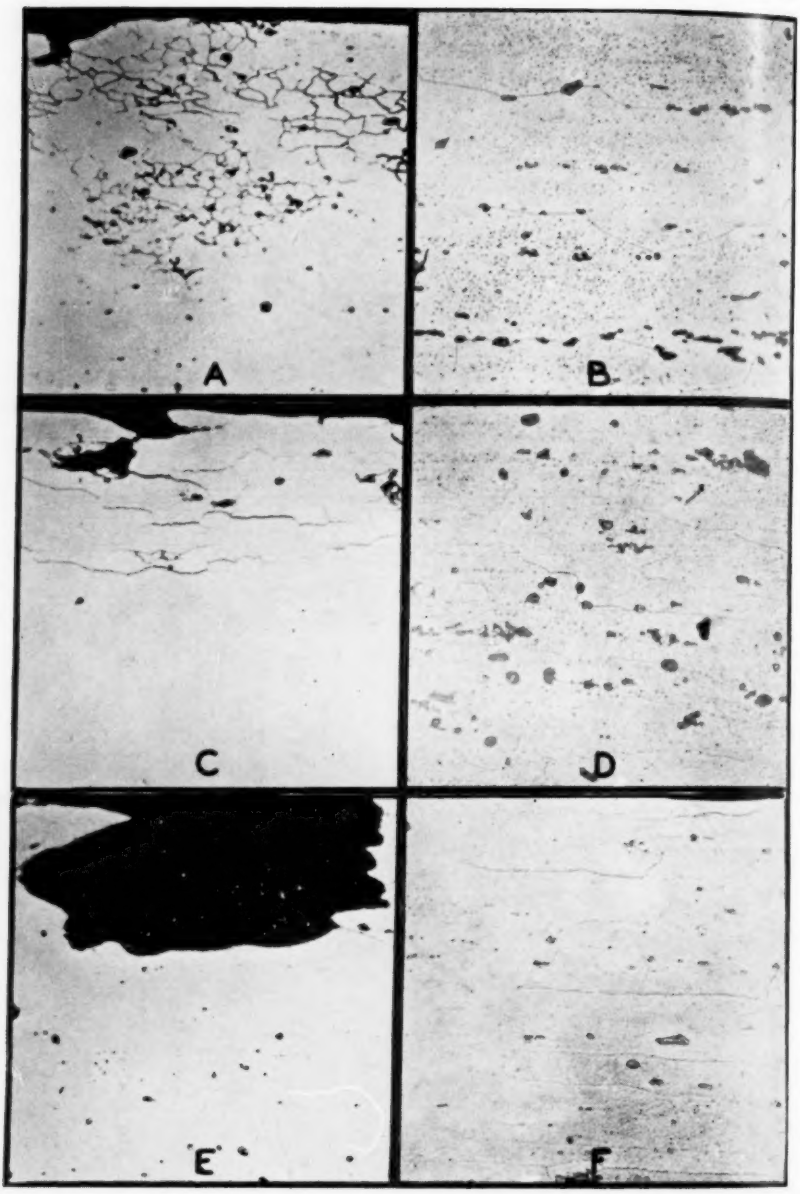

FIGURE 4.—*Cross sections of characteristic types of corrosive attack found in duralumin, and the microstructures associated with each.*

A, Intercrystalline attack; *C*, intercrystalline "pock-form" corrosion; *E*, pitting attack. Etching reveals much precipitation of $CuAl_2$ particles within the grains and along the boundaries in specimens, *B* and *D*, that are susceptible to intercrystalline attack. These particles are retained in solid solution in *F*. ×500.

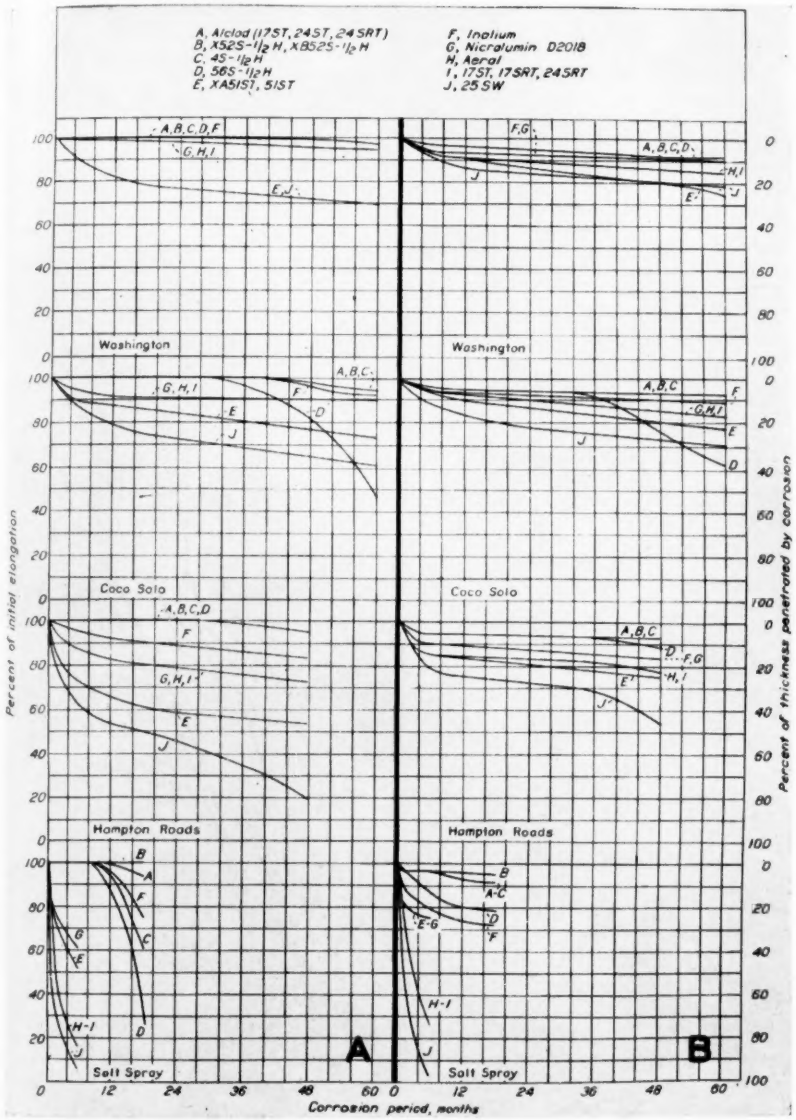

FIGURE 5.—*Rates of loss in ductility, A, and of penetration of corrosive attack, B, for the various aluminum alloys at each exposure locality.*

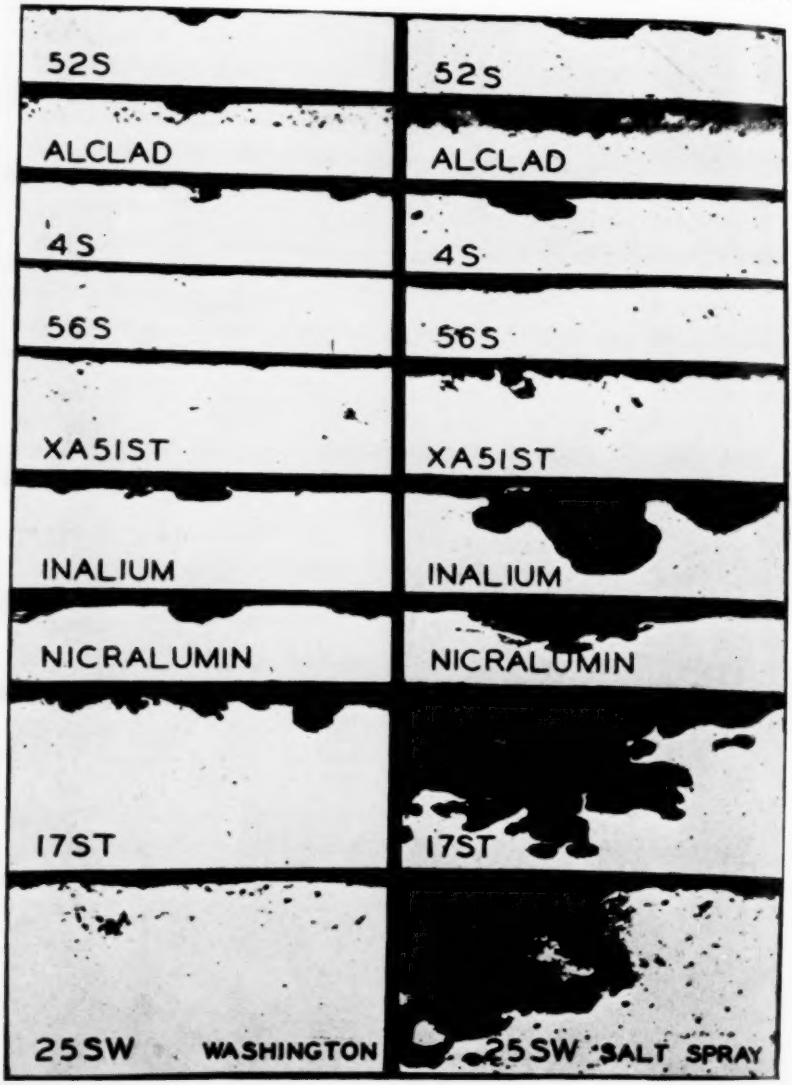

FIGURE 6.—*Representative cross sections of the maximum penetration of corrosive attack on sheets exposed 5 years at Washington (left column) and in the laboratory salt-spray tests (right column).*

The Nicralumin, *XA51ST*, *17ST*, and *25SW* specimens were exposed 6 months to the spray. The others were exposed 18 months. Note the intercrystalline attack on alloys *56S*, *XA51ST*, and *25SW*. ×33.

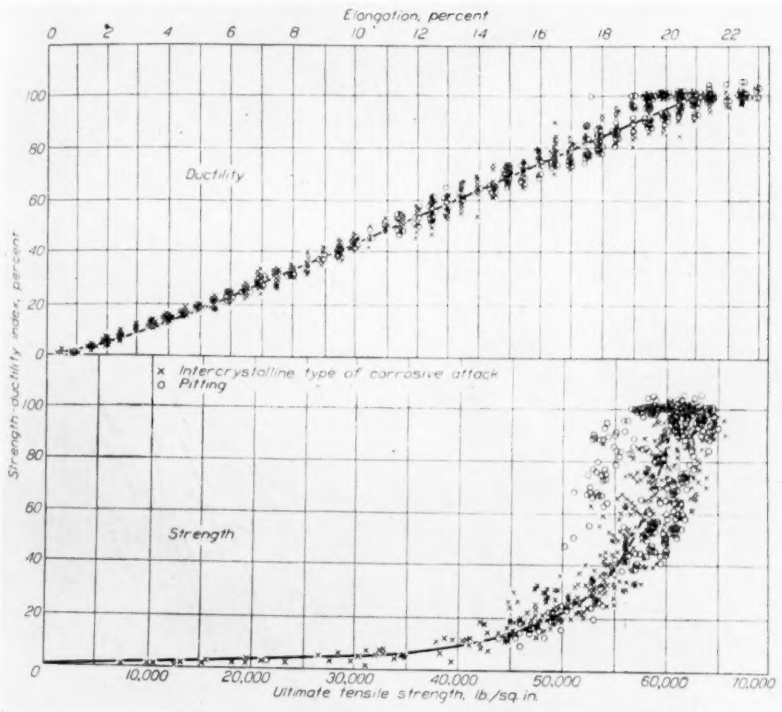

FIGURE 7.—*Relation of physical properties of heat-treated duralumin specimens exposed to the weather.*

The strength-ductility index represents the ratio, on a percentage basis, of the product of the tensile strength and elongation of the corroded specimen to the corresponding average product for the uncorroded specimens. The changes in strength relative to ductility show that the latter is a better measure of corrosion on this alloy, although neither is accurate during the initial stages of attack.

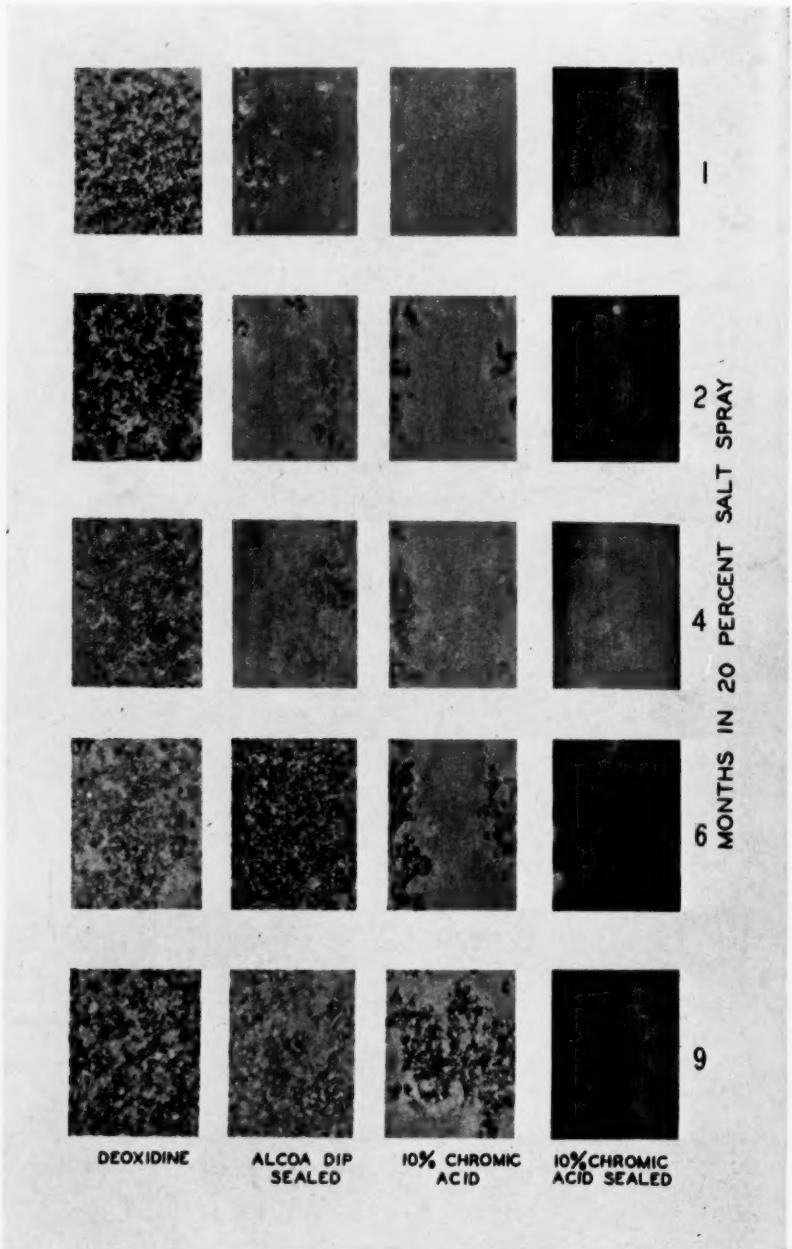

FIGURE 8.—*Surface appearance, showing relative efficiencies of some oxide coatings applied to 17S specimens that were exposed to the laboratory salt-spray test for the periods indicated.*

Note the marked superiority of the anodic coating, especially when given a sealing treatment. ×1.

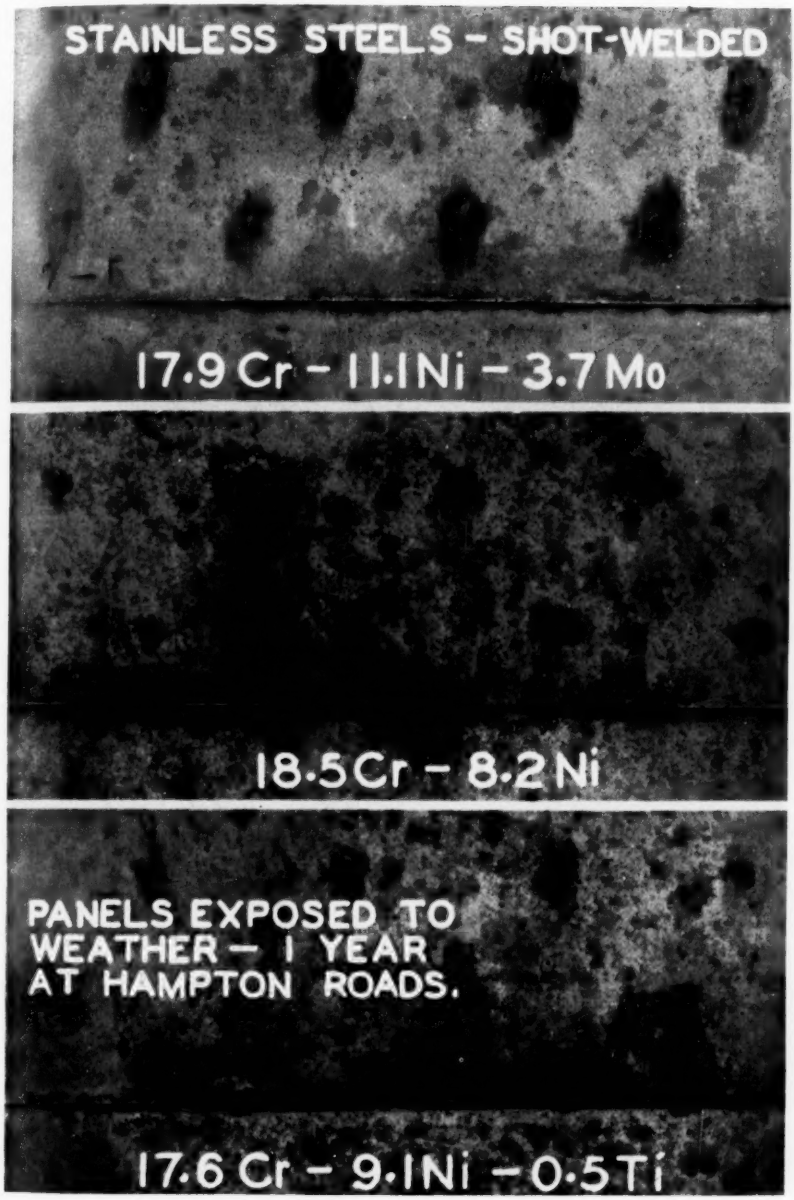
STAINLESS STEELS - SHOT-WELDED
17.9 Cr - 11.1 Ni - 3.7 Mo
18.5 Cr - 8.2 Ni
PANELS EXPOSED TO WEATHER — 1 YEAR AT HAMPTON ROADS.
17.6 Cr - 9.1 Ni - 0.5 Ti

FIGURE 9.—*Stainless steel panels exposed to the weather.*

Steels containing molybdenum rusted much less readily than the others tested. ×1.

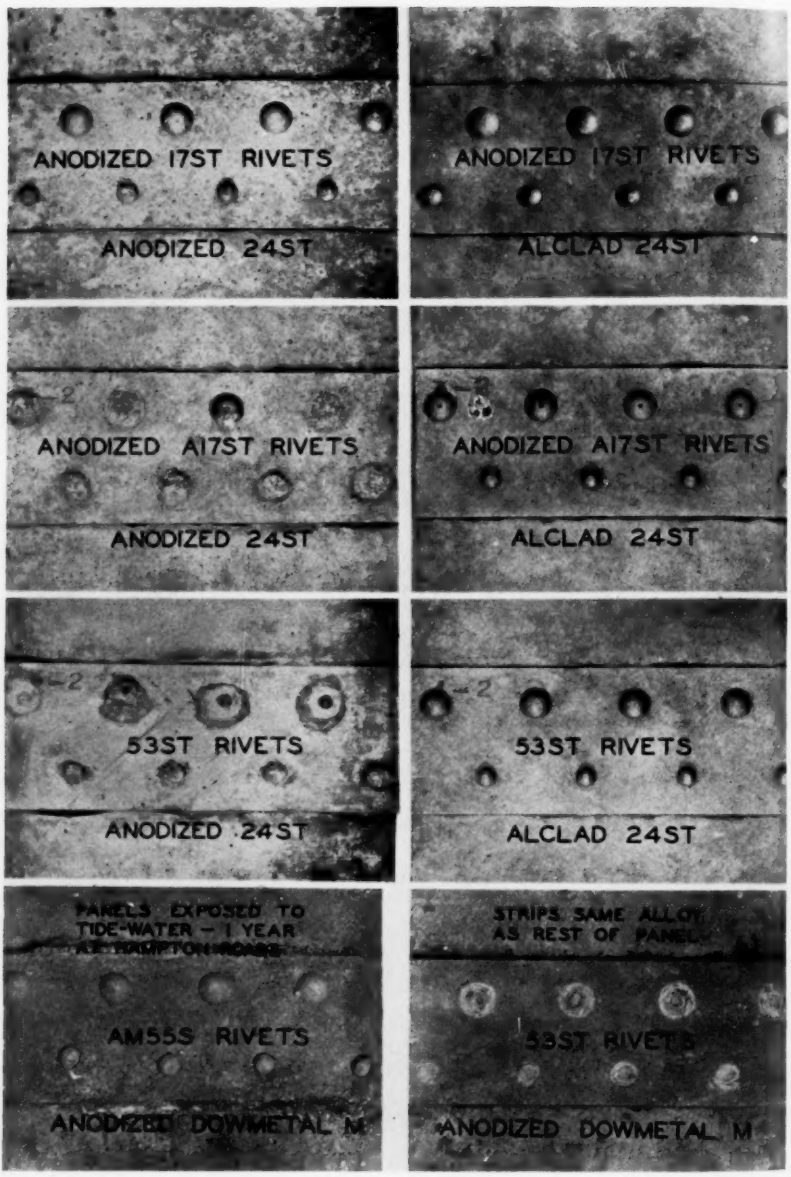

FIGURE 10.—*Corrosion on rivets used for joining on panel sections of aluminum- and magnesium-rich alloys exposed to tidewater.* ×½.

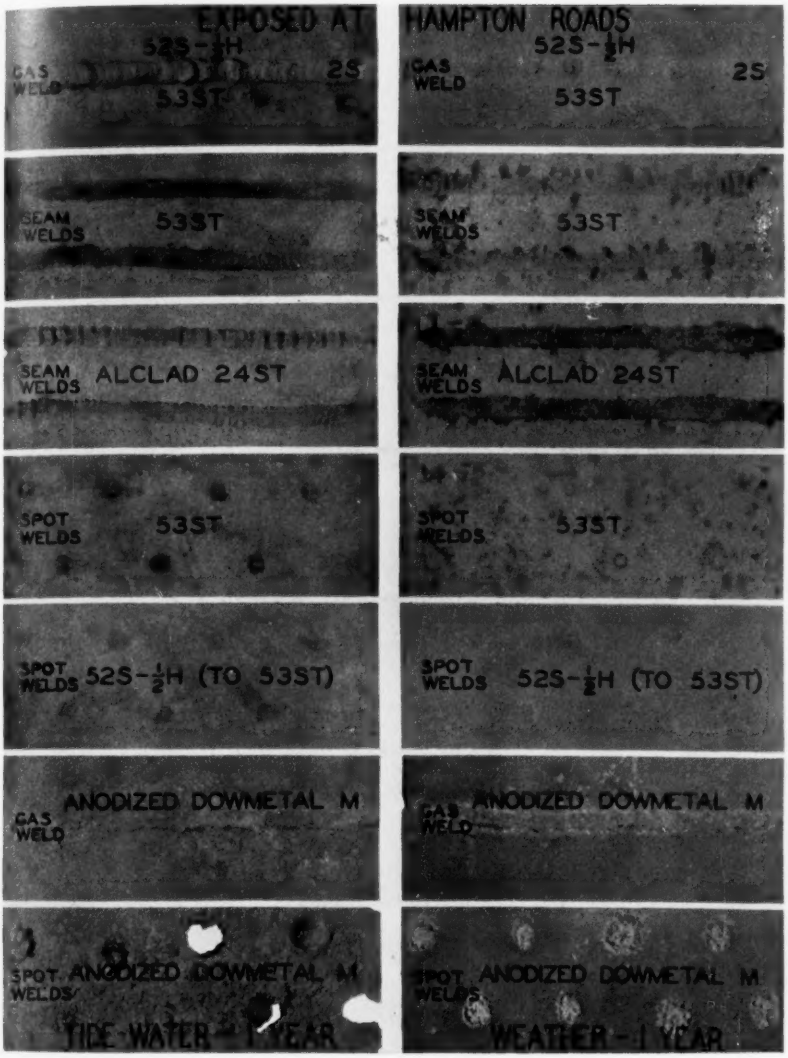

FIGURE 11.—*Corrosion on welds used for joining aluminum- and magnesium-rich alloys exposed to tidewater.* ×½.

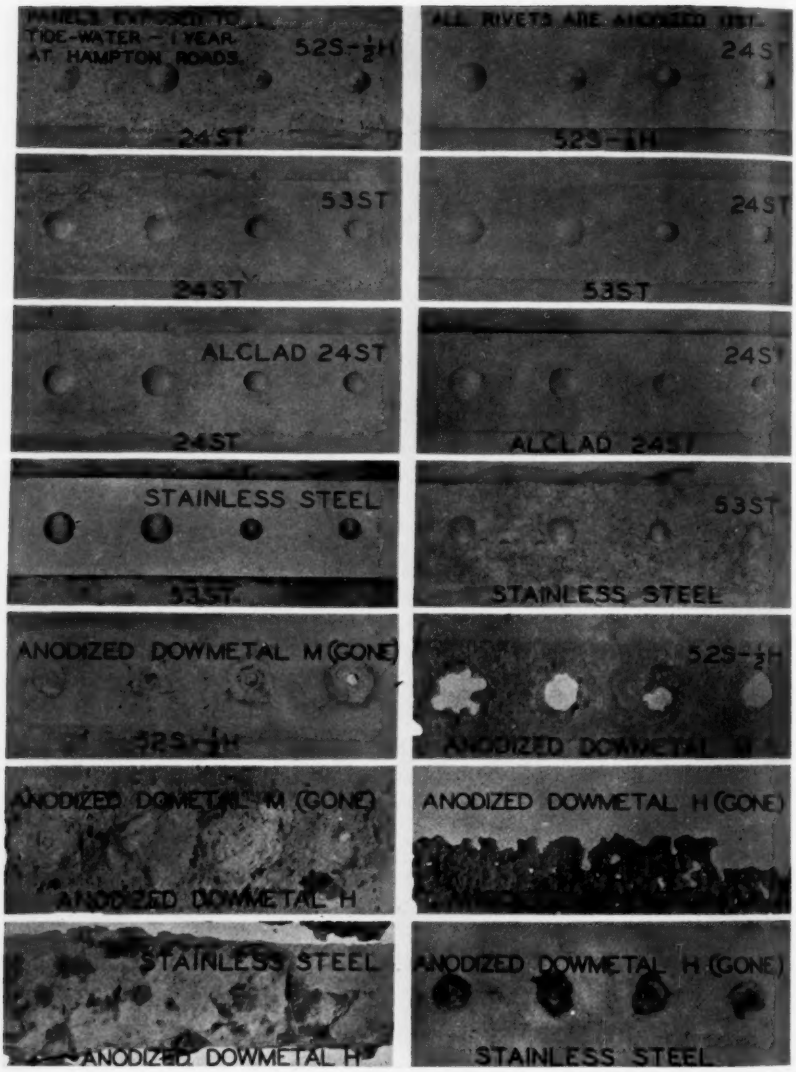

FIGURE 12.—*Corrosion on panels having dissimilar metals in contact and exposed to tidewater.* ×½.

in solid solution. This eliminated intercrystalline corrosive attack. Reheating above 100° C of properly quenched-and-aged material also caused precipitation of the $CuAl_2$ compound and so promoted intercrystalline corrosion. Specifications now require proper heat treatments, which eliminate the intercrystalline attack.

An effort was next made to minimize the pitting type of attack. The results indicated that this could be accomplished by preparing alloys from high-purity components and, where possible, by using alloys of slightly lower strength, in which the iron and copper contents are low. Private industry, in line with these findings, developed a series of aluminum-rich alloys that contain from 1 to 6 percent of magnesium and no copper, and that proved to be extremely resistant to corrosion. Certain of these alloys have exhibited only a slight loss in tensile properties after 1 year in the salt-spray test or after 5 years' exposure to the weather at the marine localities. The rates of corrosion of a number of aluminum alloys are shown in figure 5, and figure 6 reveals the typical appearance of cross sections of corroded samples under the microscope.

Owing to the large number of specimens tested, it was possible to obtain fundamental data upon changes in physical properties that resulted from corrosion, irrespective of both time and conditions of exposure. These relations and the amount of "scatter" in results are shown in figure 7 for a duralumin alloy, *17ST*.

2. PROTECTIVE COATINGS ON ALUMINUM ALLOYS

The advisability of applying protective coatings to duralumin to be used under marine conditions was early demonstrated. Metal-sprayed coatings of high-purity aluminum were found to be very efficient in protecting the duralumin basis metal. Private industry subsequently developed materials, known as "Alclad", which consist of a duralumin basis, to which a coating of aluminum is integrally bonded through interalloying. The tests (figs. 5 and 6) have demonstrated the superior corrosion resistance of these materials, which have proved of immense value to the aircraft industry.

Oxide films, applied to aluminum alloys by means of chemical or electrochemical (anodic) treatments, are of particular value, because they greatly improve the adherence of paints and varnishes applied on such surfaces. Many methods of surface protection were systematically investigated. Specimens bearing various oxide films were used in weather-exposure tests with and without an aluminum-pigmented varnish of known quality. This and various other paint and varnish coatings were applied to specimens that had received no surface treatment and to duplicates oxidized by an anodic treatment. The tests disclosed that, in general, anodic coatings were more efficient than those applied by simple immersion methods. Anodic films "sealed" by heating in dichromate solutions or by permitting chromic acid to dry on their surfaces were found to be very corrosion-resistant (fig. 8). Such coatings, used in conjunction with good grades of aluminum-pigmented varnishes, proved satisfactory for use under relatively severe corrosive conditions for periods in excess of 3 years.

An excellent method of anodic treatment for aluminum alloys, developed at this Bureau, consists in anodizing at 40 volts in a 10-percent

chromic-acid bath at 35° C for ½ to 1 hour. This method, and another one developed at the Bureau for anodically treating magnesium-rich alloys, have been included in Government specifications.

3. CORROSION OF MAGNESIUM ALLOYS

Since intercrystalline corrosion does not occur in magnesium-rich alloys, the main objective has been to determine which compositions (table 2) are most resistant to corrosive attack and to discover adequate means for surface protection. Alloys of essentially the binary type, containing from 4 to 10 percent of aluminum, were shown to be increasingly susceptible to corrosive attack as their contents of aluminum were increased. The addition of zinc to magnesium-aluminum alloys somewhat improved their corrosion resistance, and additions of from 4 to 6 percent of tin proved very beneficial. The latter and a binary magnesium-manganese alloy were the most corrosion-resistant magnesium alloys tested. Because of improvements in the purity of the constituent metals, the corrosion resistance of all the magnesium alloys has been improved markedly within the past decade.

4. PROTECTIVE COATINGS ON MAGNESIUM ALLOYS

The surface coatings for magnesium alloys so far developed are not so protective as are the anodic coatings on aluminum alloys, but they serve a useful purpose by improving the adherence of paints. In this respect some coatings obtained by simple immersion methods have proved as efficient as anodic coatings. If dimensional changes must be avoided, however, the latter treatment is recommended. The anodic treatment developed at the National Bureau of Standards for magnesium alloys uses an aqueous solution containing 10 percent by weight of sodium dichromate and 2 percent of monobasic sodium phosphate. The bath should be operated at a pH of 4.5 ± 0.2. Articles are treated for 45 minutes at 50° C and at a current density of from 2 to 10 amperes per square foot, depending upon the alloy. Good grades of aluminum-pigmented paint, used in conjunction with satisfactory surface treatments, have adequately protected the more corrosion-resistant magnesium alloys during 5 years of exposure to the weather at the marine localities, and for 1 year in the tidewater racks.

5. CORROSION OF STAINLESS STEELS

All the stainless steels investigated (table 3) were in the form of polished cold-rolled sheets, 0.018 inch thick, with surfaces passivated by immersion for approximately 1 hour in 20-percent nitric acid at 60° C. Panels exposed to the weather became covered more or less uniformly with thin, but adherent, rust films (fig. 9). The rust formed during the first month, and accumulations of dust and soot may have been partly responsible. However, corrosive attack on the panels exposed to tidewater was slight and was confined to a few small localized areas. Alloys that contained molybdenum proved more resistant to attack than did those with additions of titanium or columbium, or than those without any added alloying elements. An alloy containing 16 percent of chromium and 1 percent of nickel was much more susceptible to corrosion than the others.

6. CORROSION OF RIVETS AND WELDS

In the current program, which has been in progress approximately 2 years, panels are being exposed to the weather and to tidewater at Hampton Roads only. The tidewater tests have proved especially valuable for rapidly determining the behavior of different alloys in contact with each other and the best methods for joining them. For example, anodized *17ST* rivets (fig. 10) proved best for joining anodized *24ST* sheets, but other rivets were equally satisfactory for joining other alloys. *AM55S* rivets, which contain approximately 95.4 percent of aluminum and 4.5 percent of magnesium, were far superior to other rivets for joining magnesium alloys. On both the aluminum-rich and magnesium-rich alloys, gas welds were very resistant to corrosion (fig. 11). Spot welds were somewhat more susceptible to attack, while seam welds were noticeably so. Shot welds on stainless steel (fig. 9) tended to acquire greater deposits of rust than did the remainder of the panel. Although no visible evidence was obtained of the presence of deep pits on the welds, it is planned to verify this condition by means of flexural fatigue tests. Preliminary tests of this type on unwelded portions of the panels have indicated that shallow pits are present. Somewhat lower fatigue limits were obtained on panels exposed to the weather than on those exposed to tidewater for equal periods.

7. CORROSION OF DISSIMILAR METALS IN CONTACT

The frequent necessity, in aircraft construction, of making contacts between dissimilar metals shows the importance of the electrolytic effects involved. In order to obtain basic information, no insulating materials were used at the faying surfaces, and the panels were not painted. The ratio of the areas of the dissimilar metals very often proved a determining factor in the resulting corrosion. For example, a strip of *52S–1/2H* aluminum alloy, 1 inch wide, joined to a main panel of *24ST* alloy was severely pitted (fig. 12); whereas with the relative areas reversed, the corrosion was much less severe. Aluminum and aluminum-magnesium alloys were anodic to alloys of the duralumin type and were attacked when in contact with them. The corrosion resulting from a few other contacts of dissimilar metals is shown in figure 12. More detailed information on these and on most of the features discussed in the present paper is available in the literature references which follow.

It may be possible to minimize, or eliminate, the corrosion of dissimilar metals in contact by inserting appropriate insulators between their faying surfaces. Some preliminary studies have been included in the current exposure program, and more detailed research upon insulators for this purpose is planned.

V. REFERENCES

[1] H. S. Rawdon, A. I. Krynitsky, and J. F. T. Berliner, *Brittleness developed in aluminum and duralumin by stress and corrosion*, Chem. Met. Eng. **26,** 154 (1922).

[2] H. S. Rawdon, *The intercrystalline corrosion of metals*, Ind. Eng. Chem. **19,** 613 (1927); Met. Ind. (London) **30,** 647 (1927).

[3] H. S. Rawdon, *Protection of duralumin against corrosion*, Brass World **24,** 147 (1928).

[4] H. S. Rawdon, *Duralumin for airplane use*, Mining and Met. **9,** 234 (1928).
[5] H. S. Rawdon, Corrosion Embrittlement of Duralumin, I. Practical Aspects of the Problem, NACA Tech. Note 282 (1928). II. Accelerated Corrosion Tests and the Behavior of High-Strength Aluminum Alloys of Different Compositions, NACA Tech. Note 283 (1928). III. Effect of the Previous Treatment of Sheet Material on the Susceptibility to This Type of Corrosion, NACA Tech. Note 284 (1928). IV. The Use of Protective Coatings, NACA Tech. Note 285 (1928). V. Results of Weather-Exposure Tests, NACA Tech. Note 304 (1929). VI. The Effect of Corrosion, Accompanied by Stress, on the Tensile Properties of Sheet Duralumin, NACA Tech. Note 305 (1929); Proc. Am. Soc. Testing Materials **29,** pt. 2, 314 (1929).
[6] H. S. Rawdon, *Correlation of laboratory corrosion tests with service: Weather-exposure tests of sheet duralumin*, Trans. Am. Inst. Mining Met. Engrs., Inst. Metals Div., p. 220 (1929).
[7] H. S. Rawdon, *Corrosion prevention methods as applied in aircraft construction*, Proc. Am. Soc. Testing Materials **30,** pt. 2, 61 (1930); Aviation Eng. **3,** 23 (1930).
[8] R. W. Buzzard and W. H. Mutchler, Advantages of Oxide Films as Bases for Aluminum Pigmented Surface Coatings for Aluminum Alloys, NACA Tech. Note 400 (1931).
[9] W. H. Mutchler, *Surface coatings for aluminum alloys*, Metals & Alloys, **2,** 324 (1931).
[10] W. H. Mutchler, The Weathering of Aluminum Alloy Sheet Materials Used in Aircraft, NACA Tech. Report 490 (1934).
[11] W. H. Mutchler, Weather-Exposure Tests on Magnesium Alloys, Confidential report to NACA (available only to Federal Departments) (Aug. 20, 1935).
[12] R. W. Buzzard and J. H. Wilson, *Deterioration of chromic acid baths used for anodic oxidation*, J. Research NBS **18,** 53 (1937) RP961.
[13] R. W. Buzzard and J. H. Wilson, *Anodic coating of magnesium alloys*, J. Research NBS **18,** 83 (1937) RP964.
[14] R. W. Buzzard, *Anodizing of aluminum alloys in chromic acid solutions of different concentrations*, J. Research NBS **18,** 251 (1937) RP975.
[15] W. H. Mutchler and H. O. Willier, *A note on rapid photomicrography*, Trans. Am. Soc. Metals **26,** pt. 1, 279 (1938).
[16] W. H. Mutchler, R. W. Buzzard, and P. W. C. Strausser, Salt Spray Test, Letter Cir. NBS 530 (1938).
[17] W. H. Mutchler, The Effect of Continuous Weathering on Light Metals Used in Aircraft, NACA Tech. Report 663 (1939).
[18] W. H. Mutchler and W. G. Galvin, Tidewater and Weather-Exposure Tests on Metals Used in Aircraft, NACA Tech. Note 736 (1939).

WASHINGTON, April 23, 1940.

U. S. Department of Commerce National Bureau of Standards

RESEARCH PAPER RP1317

Part of Journal of Research of the National Bureau of Standards, Volume 25
July 1940

DESCRIPTION AND ANALYSIS OF THE SECOND SPECTRUM OF VANADIUM (V II)

By William F. Meggers and Charlotte E. Moore [1]

ABSTRACT

Wavelength measurements and intensity estimates are presented for 1,700 V II lines with wavelengths ranging from 7015.49 A in the red to 1313.82 A in the extreme ultraviolet. The main criterion for selecting these lines was enhancement in the spark as compared with the arc. Supplementary data on furnace-temperature classes and Zeeman patterns for many of these lines support their characterization of singly ionized vanadium atoms.

Analysis of all the available data resulted in the identification of 89 spectral terms, combinations of which account for 1,456, or 86 percent, of the observed lines. The identified terms include 31 singlets, 41 triplets, and 17 quintets. This is the first spectrum in which all theoretical terms arising from electron configurations d^3s and d^4 have been established (except the highest singlet in each set).

The lowest energy state of V^+ ions is represented by $(3d^4)a\,{}^5D_0$, but the strongest emission lines involve $(3d^3\,4s)a\,{}^5F$, a metastable term. Without doubt, the most intense line of the V II spectrum is $(3d^3\,4s)a\,{}^5F_5-(3d^3\,4p)z\,{}^5G^o_6$, with wavelength of 3093.108 A, arising from a simple $s-p$ transition.

A great majority of the observed lines are explained as combinations of low (even) terms with middle (odd) terms resulting from the configurations $3d^3\,4p$ and $3d^3\,4s4p$. The first high (even) terms probably originate with $3d^3\,4d$ and $3d^3\,5s$, but only fragments of the former and none of the latter could be found.

Line intensities in multiplets, level separations in complex terms, and magnetic splitting factors (g-values) indicate that LS coupling predominates among the four electrons involved in the production of the V II spectrum. With few exceptions, the polyfold terms are regular, and many obey the Landé interval rule rather well. Zeeman-effect observations for 380 lines disclose the g-values for 143 atomic-energy levels. A comparison of observed and Landé g-sums for levels given by the $d^3\,4s$ configuration shows satisfactory compliance with the g-sum rule if the scale of the observations is increased 2 to 3 percent.

Guided by theoretical expectations and analogies with similar spectra, the electronic configurations responsible for the observed terms have been identified in nearly all cases.

Inability to establish any levels belonging to the $d^3\,5s$ configuration, in series with $d^3\,4s$, postpones a spectroscopic determination of the ionization potential of V^+ ions until this spectrum has been studied under conditions which favor the emission of spectral series. For the present, the only value of this constant is an estimate of 14.1 volts by Russell.

CONTENTS

	Page
I. Introduction	84
II. Observational data	84
1. Wavelength measurements	85
2. Intensities	86
3. Temperature classes	87
4. Zeeman effect	87
5. Absorption and self-reversal	88

[1] Princeton University Observatory.

Page
III. Term analysis of V II 88
1. Lines of the V II spectrum 88
2. Terms of the V II spectrum 120
3. Electron configurations and spectral terms 127
IV. References 132

I. INTRODUCTION

The structure of vanadium spectra was first adopted as a research problem by one of the present authors in 1923, and during that year the first regularities in the arc spectrum of vanadium were announced [1].[2] The first regularities among spark lines of vanadium were presented [2] in 1924. These were extended [3] in 1925 and 1926, until approximately 300 lines characteristic of singly ionized vanadium atoms were accounted for as combinations of identified spectral terms.

In those pioneer days of the quantum theory of atomic spectra, regularities in various complex spectra were eargerly sought, primarily for the purpose of testing the proposed alternation and displacement laws of spectral structure [4]. Thus the quartet and sextet multiplets that were found in the V I spectrum were the first regularities among fifth-group elements, and they verified the predictions of the alternation law. Similarly, discovery in the V II spectrum of triplet and quintet multiplets resembling those of the Ti I spectrum confirmed the displacement law.

Within a few years the quantum theory of atomic spectra became highly developed (as regards multiplet structure, interpretation of Zeeman patterns [5], correlation of terms with electron configurations [6]), and thus presented analytical spectroscopists with tools and a challenge to classify completely the most complex spectra. But any attempt to interpret a complex spectrum invariably entails much time and labor to observe, compile, and analyze the basic data. Details of exhaustive studies of the first spectrum of vanadium [7] were recently published.

Following 1926, the analysis of the second spectrum of vanadium rested a decade, until it was resumed and advanced to its present state by cooperation of the present authors. From the beginning the term analysis of the vanadium spark spectrum was handicapped by incompleteness and poor quality of wavelength and intensity values, so from time to time efforts were made to improve the fundamental data. Most of the new observing was done at the National Bureau of Standards, and the analysis was extended mainly at Princeton. Preliminary reports of these investigations were presented [8] at scientific meetings in 1938 and 1939; and since a stage has now been reached where further observational and analytical activities appear to be unprofitable, we are persuaded to publish our final results.

II. OBSERVATIONAL DATA

The analysis of the V II spectrum is based on observed facts consisting of wavelength measurements, intensity estimates, temperature classification, Zeeman effect, absorption and reversal data, all of which are presented in table 1.

[2] Figures in brackets indicate the literature references at the end of this paper.

1. WAVELENGTH MEASUREMENTS

Spectroscopic observations of vanadium began in 1866, when Thalén [9] studied the spark spectrum and published the first measurements of the stronger lines. The first attempt to distinguish between arc and spark lines of vanadium was made in 1899 by Lockyer [10], who published a brief list of lines enhanced in the spark as compared with their intensities in the arc. The most extensive table of vanadium spark lines is that of Exner and Haschek [11] published in 1912. It lists 2,837 lines (2131.95 to 6753.3 A, Rowland's scale), but considerably less than half of them appear to be enhanced, and the errors in wavelength values are too large to permit safe use of the combination principle in seeking regularities. Inadequacy of existing data for the purpose of analyzing vanadium spark spectra was recognized in 1924, when a new list of 1,200 enhanced lines (2050 to 6500 A) was prepared from observations of juxtaposed arc and spark spectra [3]. These observations were made with vanadium chloride on graphite electrodes, and with spectrographs of moderate dispersion. These results were later displaced by improved ones obtained with pure metal electrodes and more powerful spectrographs. In 1932 Jerome K. Strauss of the Vanadium Corporation of America kindly presented the National Bureau of Standards with massive electrodes of pure vanadium metal for use in spectroscopic investigations. With these electrodes it became possible for the first time to obtain fully exposed spectrograms of vanadium free from impurity lines and undesired lines from graphite, copper, or other electrodes. The spark spectrum of vanadium was accordingly reobserved (2000 to 8500 A) with these pure-metal electrodes and the following spectrographs. The ultraviolet range 2000 to 2210 A was recorded on Schumann plates with a Littrow quartz spectrograph giving an average dispersion of about 1 A/mm in this range. An ultraviolet interval 2100 to 2800 A was photographed with a large quartz spectrograph of 3-m focus with 60-cm prism base which produced dispersions of 0.4 to 1.0 A/mm. The range 2500 to 5000 A was recorded in the second-order spectrum of a Rowland grating with 20,000 lines per inch, the average scale being 1.7 A/mm. The longer wave region (5000 to 8500 A) was investigated in the first-order spectrum of this grating. The spark for these observations (completed in 1936) was excited by a condensed discharge from an X-ray coil with a high-voltage rating of 50,000. In 1937 an aluminized Pyrex grating with 30,000 lines per inch was obtained from R. W. Wood, and with it the vanadium spark spectrum from 2500 to 8500 A was again observed with 50 percent greater dispersion and complete freedom from ghosts. For this last series of spectrograms the spark was operated by means of a 30,000-volt 60-cycle transformer, but the spectra were indistinguishable from those produced by the X-ray coil.

The schedule of exposures was invariably as follows: (1) Vanaduim conventional arc spectrum, 220 volts, 5-ampere d-c arc, 2 seconds to 1 minute; (2) iron arc spectrum, 1 second to 1 minute; (3) vanadium spark spectrum, primary current 110 volts, 5 to 8 amperes a-c, 0.006-μf capacity in parallel with the spark, 2 to 60 minutes. Relative exposure times were chosen so that fully exposed vanadium arc and spark spectrograms resulted in each spectral region with comparable intensities of high-level V I lines. Under such conditions the lines

enhanced in the spark spectrogram, or appearing only there, positively belong to ionized vanadium atoms. No special effort was made to distinguish between V II and V III lines, but relatively few, if any, of the latter occur above 2600 A. Below 2600 A the lines appearing only in sparks, and greatly enhanced at the electrodes, are generally found to represent V III and V IV spectra. These have been removed from our V II list.

All wavelength measurements were made relative to international secondary standards of iron in the same spectral order. As usual, the prism spectrograms were reduced with the Hartmann dispersion formula, and the grating spectrograms on the assumption of linear dispersion, small final corrections required by each spectrogram being determined from standards.

A variety of line types occur in the conventional spark spectrum, and obviously not all are measurable with equal precision. Especially difficult are the high-level lines, which in condensed sparks operated at atmospheric pressure always appear hazy and unsymmetrically shaded. Also many V II lines are widened by hyperfine structure which is noticeable with powerful spectrographs.

The visible and infrared spectra of atomic vanadium in atmospheric sources always appear on a background of molecular spectra arising from metallic oxides. Although the molecular spectra are relatively weaker in a disruptive spark than in a continuous arc discharge, they are nevertheless prominent enough in fully exposed spark spectrograms to obscure or falsify faint lines. It is likely that V II lines in general would be sharper, and fainter lines could be observed, in discharges in a partial atmosphere of inert gas; but the present description is confined to the conventional spark in air or in pure nitrogen.

A. G. Shenstone kindly made for the authors a spark spectrogram extending from 2172 to 1308 A in the extreme ultraviolet. The spark was operated in pure nitrogen, and the spectrum was recorded on a Schumann plate with a normal-incidence vacuum spectrograph having a 2-m glass grating ruled 30,000 lines per inch. The dispersion is 4.2 A/mm. This spectrogram was measured and reduced relative to Cu II and Fe III lines identified on the plate. Criteria for the separation of successive spectra of vanadium are lacking, except enhancements at the electrodes, which are assumed to characterize V III and V IV lines. Shorter than 2600 A, only lines believed to belong to the V II spectrum are retained in table 1, and even these are omitted when unclassified and fainter than 20 below 2000 A, or unclassified below 1550 A.

2. INTENSITIES

In this revised description of the V II spectrum an effort was made, for the first time, to assign relative intensities which bear some semblance to reality. The strongest V II line, 3093.11 A, is certainly thousands of times more intense than the faintest observed lines. For such an intensity range the scale of 10 to 1 allows only 10 classes of lines and permits no fine distinctions. Even the scale of 100 to 1 is inadequate, so in the present case we have adopted a scale of 2,500 to 1. Of course, the intensity values are only visual estimates of line strength based on image width and blackness; but since they are

usually averages from several fully exposed spectrograms, they are probably comparable over considerable intervals. No quantitative measurements of relative intensities in vanadium spark spectra have ever been made.

When relative intensities are carefully estimated on an open scale, different lines are found to show varying degrees of enhancement from arc to spark exposures. Low-level spark lines usually appear with considerable intensity in ordinary arcs, but high-level spark lines are either weak or nonexistent in light from the central part of an arc. In the spark, low-level lines often show self-reversal, whereas high-level lines are generally characterized by haziness and dissymmetry. Because degrees of enhancement (as well as other features of the lines) are significant in the analysis of spectral structure, both arc and spark intensities are presented in table 1.

3. TEMPERATURE CLASSES

As stated above, many lines of low or medium intensity in the arc are enhanced in a spark, and such intensity comparisons yield a trustworthy separation of lines due to neutral and to ionized atoms. An independent method of recognizing these enhanced lines is found in a comparison of the arc and high-temperature furnace spectra as studied by King. The enhanced lines are either absent or relatively weak in furnace spectra. In other words the furnace, the arc, and the spark are characterized mainly by differences in ionizing power; and lines belonging to ionized atoms in the arc can be identified either by enhancement in the spark or by diminishment in the furnace. Comparison of the spectra of vanadium excited in a vacuum furnace at various temperatures enabled King [12] to assign, to 1,600 lines (2340 to 6842 A) appearing in the arc spectrum, temperature-class numbers that correspond to successive stages of excitation. This classification was an important aid in the analysis of the V I spectrum [7]. Similar data pertinent to the V II spectrum are quoted in table 1. The assignment of lines to V II, based on arc and furnace comparisons, is confirmed in every case by our independent arc and spark comparisons.

4. ZEEMAN EFFECT

The Zeeman effect for several hundred vanadium lines (3665 to 6625 A) was published by Babcock [13] in 1911. These observations were improved and extended (to 2314 A), and in manuscript form were kindly lent to those actively engaged in multiplet analysis. With the consent of Babcock, the data for V I lines were recently published, together with their interpretation, in a term analysis of the first spectrum of vanadium [7]. The revised data for V II lines have not been published, but with Babcock's permission they are fully presented in table 1, together with their interpretation. Needless to say, these Zeeman patterns were most helpful in this term analysis of the V II spectrum, and they constitute overwhelming confirmation of the quantum numbers assigned to the terms. The observations quoted in table 1 are given in the usual form, that is, the component distances from the undisplaced line are in terms of a normal triplet separation, the *p*-components are in parentheses and are followed by the *n*-components, the strongest components being distinguished by boldface type. The same is true for calculated patterns, except that in

some cases these are simplified to aid their comparison with the observations.

The calculated patterns are derived from the observed g values (table 5) resulting from Babcock's material quoted in table 1. When the observed components are wholly or partially resolved, the complete computed pattern is given; but when only blends of the components of a given polarization are measured, the calculated position of the blend is given. For the stronger lines this is assumed to coincide with the center of gravity of the theoretical group, as described in the formulas of Shenstone and Blair, and of Russell [14]. These cases are marked *b* in table 1. For weak lines it is probable that the measurement applies more nearly to the strongest component of the group, and such cases are marked *s*.

5. ABSORPTION AND SELF-REVERSAL

The absorption spectrum of vanadium vapor at 2,000° C was investigated by Gieseler and Grotrian [15] to determine the normal state of the atoms. They observed 52 absorption lines (2915 to 6252 A), all of which originated either from a low quartet F or a slightly higher sextet D term, and concluded that the normal state of neutral vanadium atoms is described by $(d^3s^2)\ {}^4F_{1\frac{1}{2}}$. The only laboratory absorption data extant for V II lines are those by King [16], who observed 10 enhanced lines (2672 to 2691 A) faintly absorbed in vanadium vapor near 2,600° C. All of these involve the lowest quintet D term, which is the ground state of the ion. No further laboratory observations of V II lines in absorption have been made, but additional information about the normal state of V^+ atoms is found in the phenomenon of self-reversal in the spark. Without exception, the lines which are observed to be more or less self-reversed involve either the low quintet D term or a slightly higher quintet F term, and there can be no doubt that the normal state of singly ionized vanadium atoms (V^+) is $(d^4)\ {}^5D_0$.

V II absorption lines are observed in the solar spectrum [17]. The strongest of those observed originate with $(d^3s)\ {}^5F$, because the strongest combinations with $(d^4)\ {}^5D$ are shorter than 2900 A and therefore are not transmitted by the terrestrial atmosphere.

III. TERM ANALYSIS OF V II

Since the terms of the V II spectrum are deduced directly from observed properties of the lines, we present in the following order (1) a complete list of observational data, with the addition of term combinations for all classified lines, and calculated Zeeman patterns to compare with observed; (2) facts concerning the established spectral terms; (3) correlation of electron configurations and terms.

1. LINES OF THE V II SPECTRUM

Successive columns of table 1 contain the following data: (1) measured wavelength, (2) arc and spark intensity, (3) temperature class, (4) vacuum wave number, (5) term combination, and (6) observed and computed Zeeman patterns.

All wavelengths listed here are on the International Scale; those exceeding 2000 A are observed in a standard atmosphere, but shorter

than 2000 A they are vacuum values. The vacuum wave numbers of the former are derived from Kayser's Table [18].

The letters *a*, *b*, *c*, etc., appearing with wavelengths in column 1 have the following meaning:

a=Blend with V 1.
b=Zeeman pattern diffuse.
c=Short-wave member of observed Zeeman pattern double line.
d=Observed Zeeman pattern possible blend with V 1.
e=Observed Zeeman pattern affected by superposed line.
f=Long-wave member of observed Zeeman pattern double line.
g=Observed Zeeman pattern affected by reversal.
h=Observed Zeeman pattern unsymmetrical; doubtful.
i=Observed Zeeman pattern blended.
j=Intensities in observed Zeeman pattern unsymmetrical.
k=Multiplet designation discordant with observed Zeeman pattern.
l=Short-wave *n*-component of observed Zeeman pattern blended.
m=Long-wave *n*-component of observed Zeeman pattern blended.
n=Long-wave *n*-component of observed Zeeman pattern weaker.
o=*n*-component of observed Zeeman pattern blended.
*=Line probably a blend.

Symbols accompanying some of the intensity estimates in column 2 have the following significance, as officially adopted by the International Astronomical Union [20]:

h=Hazy.
H=Very hazy.
I=V 1.
p=Part of band structure.
l=Shaded to longer waves.
s=Shaded to shorter waves.
d=Double.
e=Enhanced at electrode.
r=Narrow self-reversal.
R=Wide self-reversal.
Bl=Blend.

In column 3, Roman numerals represent King's temperature class. The accompanying symbols are to be interpreted as follows:

a=Observed in absorption.
E=Enhanced line.
r=Self-reversal.

The term combinations in column 5 show the quantum theoretical interpretation of the observed lines, the notation being that which is in general use [19] and officially adopted by the International Astronomical Union [20].

Symbols accompanying the observed Zeeman patterns in column 6 have the following meanings: *w1*=slightly widened; *w2*=moderately widened; *w3*=greatly widened; while the apparent intensity distribution in such unresolved patterns is qualitatively represented by letters as follows:

For unresolved *p*-components *B*= ; *D*=⊓; *E*=∧.
For unresolved *n*-components *A*=; *B*=; *C*=⊓⊓.

As explained above, the letters *b* and *s*, appearing with calculated patterns in column 6, indicate blended- and strongest-component values, respectively. Comparison with values computed from Landé *g*-values may be made by referring to the tables of theoretical Zeeman effects published by Kiess and Meggers [21]. Some remarks on *g*-values and *g*-sums are reserved for presentation in connection with a discussion of V II terms (see next section).

TABLE 1.—*Second spectrum of Vanadium*

a=absorbed line.
h=Hazy.
I=V I.
p=Band line.
E=Enhanced line.
H=Very hazy.
l=Shaded to longer waves.
R=Wide self-reversal.
r=Narrow self-reversal.
s=Shaded to shorter waves.
e=Enhanced at electrode.
d=Double.
II=V II.
Bl=Blend.

1	2		3	4	5	6	
λ_{air} A	Intensity		Temp. class	Wave No. vac cm^{-1}	Term combination	Zeeman effect	
	Arc	Spark				Observed	Computed
7015.49		4*h*		14250.25			
6987.12		5*h*		14308.11			
6891.30		4*h*		14507.05			
6801.16		5		14699.33	$d\,^3P_2-z\,^3P_2^\circ$		
6748.10		2*h*		14814.90			
6672.84		3*h*		14982.00	$b\,^1F_3-y\,^3F_3^\circ$		
6517.27		15*h*		15339.62	$b\,^1F_3-z\,^1F_3^\circ$		
6380.11		40*h*		15669.39	$b\,^1F_3-z\,^1D_2^\circ$		
6226.29		10*h*		16056.50	$b\,^3D_2-z\,^3F_2^\circ$		
6120.98		5		16332.74	$c\,^3P_0-z\,^3F_1^\circ$		
6095.93		3		16399.86	$c\,^3P_1-z\,^3F_1^\circ$		
6086.93		15*h*		16424.11	$b\,^3D_2-z\,^3D_2^\circ$		
6083.82		10*h*		16432.50	$b\,^3D_1-z\,^3D_1^\circ$		
6080.11		6		16442.53	$d\,^3F_4-z\,^3H_4^\circ$		
6031.07		40		16576.23	$c\,^3P_2-z\,^3F_3^\circ$		
6028.98		20		16581.94	$b\,^3D_3-z\,^3D_3^\circ$		
6028.26		40		16583.95	$c\,^3P_1-z\,^3F_2^\circ$		
6027.23		8		16586.79	$a\,^1S_0-z\,^1F_1^\circ$		
6026.81		6		16587.94	$b\,^3D_2-z\,^3D_2^\circ$		
5967.77		6		16752.05	$b\,^3D_2-z\,^3D_3^\circ$		
5951.45		4		16797.99	$c\,^3P_0-z\,^3D_1^\circ$		
5928.86		100		16861.99	$c\,^3P_2-z\,^3D_3^\circ$	(0) 1.31	(0) 1.28*b*
5916.364		15		16897.60	$b\,^3D_3-z\,^3D_3^\circ$		
5914.28		5		16903.56	$b\,^3D_3-z\,^3D_2^\circ$		
5897.54		50		16951.54	$c\,^3P_1-z\,^3D_2^\circ$	(0) 0.96	(0) 0.94*b*
5862.80	*p*	15+*p*?		17051.98	$a\,^1S_0-z\,^3D_1^\circ$		
5819.93		80		17177.59	$c\,^3P_2-z\,^1D_2^\circ$	(0) 1.50	(0) 1.58*b*
5791.47		15		17262.00			
5642.01		60*h*		17719.27	$c\,^1G_4-y\,^1G_4^\circ$	(0) 0.97	(0.13) 0.98*b*
5562.02	*p*	4*hp*?		17974.10	$c\,^3D_3-w\,^3F_3^\circ$		
5530.10		4		18077.85	$c\,^3D_3-w\,^3F_4^\circ$		
5487.00		8		18219.85	$a\,^3D_1-z\,^3F_2^\circ$		
5457.10		4		18319.67	$a\,^3D_3-z\,^3F_3^\circ$		
5439.30		15		18379.62	$a\,^3D_2-z\,^3F_2^\circ$		
5432.09		2		18404.02	$a\,^3D_1-z\,^3F_2^\circ$		
5384.89		8		18565.33	$a\,^3D_3-z\,^3F_4^\circ$	(0?) 1.29 pw_1; nw_1 B?	(0.15) 1.27*b*
5357.35		2		18660.77	$a\,^3D_3-z\,^3D_3^\circ$		
5350.37		5		18685.11	$a\,^3D_1-z\,^3D_2^\circ$	(0.30) 0.37	(0.25) 0.36*b*
5349.75		3		18687.28	$a\,^3D_3-z\,^3D_2^\circ$		
5341.22		2		18717.12	$c\,^1G_4-y\,^1F_3^\circ$		
5332.65		9		18747.20	$a\,^3D_3-z\,^3D_2^\circ$	(0) 1.15	(0.09) 1.10*b*
5322.81		5		18781.86	$c\,^1G_4-z\,^3G_4^\circ$	(?) 1.49 pw_2 D; nw_2 O	(0) 1.53*b*
5303.26		40		18851.09	$a\,^3D_2-z\,^3D_2^\circ$	(0) 1.37	(0.05) 1.31*b*
5290.74	*p*	6+I		18895.70	$d\,^3F_2-z\,^1F_3^\circ$	(0) 1.20	(0) 1.27*b*
5288.31		5		18904.39	$c\,^3F_4-y\,^3F_3^\circ$		

See footnotes at end of table.

TABLE 1.—*Second spectrum of Vanadium*—Continued

1	2		3	4	5	6	
λ_{air}A	Intensity		Temp. class	Wave No. vac	Term combination	Zeeman effect	
	Arc	Spark				Observed	Computed
5280.00		3?		18934.14	$c\ ^3F_3 - y\ ^3F_3^\circ$		
5275.65[a]	?	10+I		18949.75	$c\ ^3F_4 - y\ ^3F_4^\circ$	(0.61) 1.27	(0.23) 1.22
5263.99		15		18991.72	$b\ ^3H_4 - z\ ^3G_4^\circ$	(0) 0.88	(0) 0.79*b*
5249.22		1?		19045.16	$d\ ^3P_2 - y\ ^3D_2^\circ$		
5241.19		100*h*		19074.34	$c\ ^1G_4 - y\ ^1H_4^\circ$	(0) 1.16	(0) 1.17*b*
5232.82		2		19104.85			
5227.70		20		19123.56	$b\ ^3H_5 - z\ ^3G_4^\circ$		
5215.928		25		19166.72	$a\ ^3D_3 - z\ ^3D_3^\circ$	(?) 1.42pw_2 D	(0.44) 1.33*b*
5214.98	*p*	2		19170.21			
5202.94		2		19214.57	$a\ ^1D_2 - z\ ^3F_3^\circ$		
5199.68	*p*	4		19226.61	$a\ ^3D_2 - z\ ^3D_2^\circ$		
5191.59		2		19256.58	$d\ ^3F_3 - z\ ^1D_2^\circ$		
5157.28		2?		19384.69	$b\ ^3D_3 - z\ ^3F_3^\circ$		
5151.87		2		19405.03	$c\ ^3F_4 - z\ ^1G_4^\circ$		
5143.89		3		19435.14			
5132.19		2		19479.45	$b\ ^3D_1 - z\ ^3F_2^\circ$		
5106.233		5		19578.47	$b\ ^3D_2 - z\ ^3F_2^\circ$	(0) 0.83	(0) 0.79*b*
5060.67	?	15		19754.74		(0?) 1.16pw_2 D; nw_1 A?	
5048.91		15		19800.75	$d\ ^3F_3 - y\ ^3D_3^\circ$	(0) 0.73	(0) 0.76*b*
5047.308		10+I		19807.04	$b\ ^3D_3 - z\ ^3F_4^\circ$	(0) 1.05	(0) 1.10*s*
5019.855		100*h*		19915.36	$b\ ^1F_3 - y\ ^1G_4^\circ$	(0?) 1.02pw_1D	(0) 1.00*b*
5016.60		4		19928.28	$c\ ^1D_2 - x\ ^1D_2^\circ$		
4973.16		2		20102.34	$d\ ^3F_3 - y\ ^3D_3^\circ$		
4968.50		1		20121.20	$b\ ^1G_4 - z\ ^3G_4^\circ$		
4965.40		40		20133.76	$d\ ^3F_4 - y\ ^3D_3^\circ$	(0) 1.03	(0) 0.99*b*
4963.75		2		20140.46	$d\ ^3P_2 - z\ ^3S_1^\circ$	(?) 1.16pw_1 D; nw_1 A	(0) 1.14*b*
4947.58		40		20206.28	$c\ ^3F_2 - y\ ^3D_1^\circ$	(0?) 0.75 pw_2 D	(0) 0.76*b*
4912.38		2		20351.07	$d\ ^3P_2 - x\ ^3F_2^\circ$		
4884.06		50		20469.07	$c\ ^3F_3 - y\ ^3D_2^\circ$	(0?) 1.02pw_1 D	(0) 1.01*b*
4883.415		100		20471.77	$d\ ^3F_4 - y\ ^3D_3^\circ$	(?) 1.14pw_2 D	(0) 1.17*b*
4874.805		4		20507.93	$c\ ^3F_3 - y\ ^3D_3^\circ$		
4842.50		2*h*		20644.74	$c\ ^3D_3 - v\ ^3D_3^\circ$		
4839.08		3		20659.33	$d\ ^3P_2 - x\ ^3D_2^\circ$	(?) 1.15pw_1 D; nw_1 B?	(0.50) 1.24*b*
4823.396	3?	6		20726.50	$d\ ^3P_2 - x\ ^3D_3^\circ$	(?) 1.15pw_1 D	(0) 1.14*b*
4813.952[b]		50		20767.17	$c\ ^3F_4 - y\ ^3D_3^\circ$	(0) 1.15	(0) 1.19*s*
4813.00		1?		20771.27	$c\ ^3D_3 - v\ ^3D_3^\circ$		
4811.14		6		20779.30	$c\ ^3F_3 - y\ ^3D_2^\circ$	(0.64) 1.24nw_2	(0.21, 0.42, **0.63**), 0.64, 0.85, **1.06**, **1.27**, 1.48, 1.69
4810.17		1?		20783.49	$b\ ^3G_4 - z\ ^3D_3^\circ$		
4737.59		1		21101.89	$b\ ^3F_3 - z\ ^3G_4^\circ$		
4634.21		3*h*		21572.63	$d\ ^3F_3 - x\ ^3F_3^\circ$		
4627.48		1		21604.00	$d^3\ F_3 - x\ ^3F_2^\circ$		
4618.52		3		21645.91	$c\ ^1D_2 - x\ ^1F_3^\circ$		
4605.352		15		21707.80	$a\ ^3D_3 - z\ ^3F_3^\circ$		
4600.19		150		21732.16	$a\ ^3D_1 - z\ ^3F_2^\circ$	(0)0.77	(0)0.73*b*
4596.37		5*h*		21750.22	$d\ ^3F_3 - x\ ^3F_3^\circ$		
4590.505		7*h*		21778.01	$d\ ^3F_4 - x\ ^3F_3^\circ$	(?)1.44	(0)1.47*b*
4564.592	4	200		21901.64	$a\ ^3D_2 - z\ ^3F_2^\circ$	(0)0.97pw_1 D; nw_1A	(0)0.91*b*
4558.46		20		21931.10	$d\ ^3F_3 - x\ ^3D_2^\circ$		
4556.765		4		21939.26	$c\ ^3F_3 - x\ ^3F_3^\circ$		
4538.64		2		22026.87	$d\ ^3F_3 - x\ ^3D_3^\circ$		
4535.215		3*h*		22043.51	$d\ ^3F_4 - x\ ^3F_4^\circ$		
4532.188		40*h*		22058.23	$d\ ^3F_3 - x\ ^3D_3^\circ$	(0)1.02	(0)1.00*b*
4529.08		5?		22073.37	$c\ ^3F_4 - x\ ^3F_3^\circ$		
4528.51	3	300		22076.15	$a\ ^3D_3 - z\ ^3F_4^\circ$	(0?)1.13	(0)1.10*b*
4520.55		5	V *E*	22115.02			
4518.38		2*h*		22125.64	$d\ ^3F_3 - x\ ^3D_2^\circ$		
4517.35		3*h*		22130.69	$d\ ^3F_2 - z\ ^1P_1^\circ$		
4512.72		60*h*		22153.39	$d\ ^3F_4 - x\ ^3D_3^\circ$	(0)1.20	(0)1.18*b*
4483.50		2*h*		22297.77	$d\ ^3P_0 - x\ ^3P_1^\circ$		
4475.70		20*h*		22336.63	$c\ ^3F_2 - x\ ^3D_1^\circ$	(0)0.66	(0)0.69*b*

See footnotes at end of table.

TABLE 1.—*Second spectrum of Vanadium*—Continued

1	2		3	4	5	6	
λ_{air} A	Intensity		Temp. class	Wave No. vac	Term combination	Zeeman effect	
	Arc	Spark				Observed	Computed
4475.24		1		22338.92	$c\ ^3F_4-x\ ^3F_4^\circ$		
4464.32		40h		22393.56	$c\ ^3F_3-x\ ^3D_2^\circ$	(0)1.04	(0)1.02b
4456.53		3h		22432.71	$c\ ^3F_3-x\ ^3D_3^\circ$		
4453.35		30h		22448.72	$c\ ^3F_4-x\ ^3D_3^\circ$	(0)1.19	(0)1.22s
4440.41		5h		22514.14	$d\ ^3P_1-x\ ^3P_0^\circ$		
4439.42		1		22519.16	$a\ ^1G_4-z\ ^3F_4^\circ$		
4408.92		40*H*?		22674.94	$d\ ^3P_2-x\ ^3P_2^\circ$		
4404.68		2		22696.77	$a\ ^3G_5-z\ ^3F_5^\circ$		
4398.52		4h		22728.56	$a\ ^1F_3-z\ ^1F_3^\circ$		
4370.27		3		22875.47	$a\ ^3G_5-z\ ^3D_4^\circ$		
4366.91		5h		22893.08	$b\ ^3G_3-z\ ^3G_3^\circ$		
4349.97		6h		22982.23	$b\ ^3G_4-z\ ^3G_4^\circ$	(0)1.05	(0.00)1.03b
4346.89		3		22998.51	$b\ ^3F_3-z\ ^3F_3^\circ$		
4331.79		2		23078.68	$a\ ^5P_3-z\ ^5F_3^\circ$		
4331.55		6h		23079.96	$b\ ^5G_5-z\ ^5G_4^\circ$	(0)1.18	(0.12)1.18b
4325.22		9h		23113.73	$b\ ^1F_3-y\ ^1D_2^\circ$	(0)1.02	(0)1.02b
4322.02		4		23130.85	$b\ ^5F_3-z\ ^5F_3^\circ$	(0)1.03	(0)1.04b
4316.258		2		23161.73	$a\ ^5P_1-z\ ^5F_1^\circ$		
4313.30		2		23177.61	$a\ ^5P_3-z\ ^5F_3^\circ$		
4304.15		2		23226.88	$d\ ^5F_3-w\ ^5D_3^\circ$		
4301.130		40h		23243.19	$d\ ^3P_0-y\ ^3S_1^\circ$	(0)1.94	(0)1.92
4288.78	2	5?		23310.12	$b\ ^5F_4-z\ ^5F_5^\circ$		
4286.13	2?	3		23324.53	$a\ ^5P_2-z\ ^5F_2^\circ$		
4278.893		60h		23363.98	$d\ ^3P_1-y\ ^3S_1^\circ$	(0.45)1.44, 1.96	(0.44)1.48, 1.92
4270.64		2		23409.13	$a\ ^5P_3-z\ ^5F_4^\circ$		
4264.50		1		23442.83	$a\ ^5P_1-z\ ^5D_1^\circ$		
4263.836		4h		23446.48	$a\ ^5P_2-z\ ^5D_2^\circ$	(0.41, **1.21**) 0.36, 1.11, 1.82, 2.48	(0.70, **1.40**)0.38, **1.08, 1.78,** 2.48
4260.75		9h		23463.47	$a\ ^5P_3-z\ ^5D_3^\circ$ $b\ ^5F_2-z\ ^5D_1^\circ$		
4257.02		15h		23484.02	$c\ ^5F_3-w\ ^5D_1^\circ$	(0)0.76	(0)0.76b
4254.41	4?	15h		23498.43	$b\ ^5F_3-z\ ^5D_2^\circ$	(?)1.07pw_3 D; nw_3 A Cr?	(0)1.04b
4248.820		4		23529.35	$a\ ^5P_1-z\ ^5D_0^\circ$		
4242.894		30h		23562.21	$c\ ^5F_3-w\ ^5D_2^\circ$	(0)0.98	(0)1.02b
4236.82		4		23595.99	$b\ ^5F_4-z\ ^5D_4^\circ$	(0)1.02	(0)0.98b
4234.55		40h+I		23608.63	$c\ ^5F_4-w\ ^5D_3^\circ$		
4234.251		7		23610.30	$a\ ^5P_2-z\ ^5D_3^\circ$		
4232.065		80h		23622.50	$d\ ^3P_2-y\ ^3S_1^\circ$	(**0,** 0.49) **1.01,** 1.40, 1.91	(**0,** 0.54)**0.84,** 1.38, 1.92
4231.165		4		23627.52	$a\ ^5P_3-z\ ^5D_2^\circ$	(0)1.93	(0)1.85b
4225.228	1	120		23660.72	$b\ ^3G_3-z\ ^3F_2^\circ$	(0)0.81	(0)0.87b
4224.51	4?	10		23664.74	$a\ ^5P_2-z\ ^5D_1^\circ$	(**0,** 0.38)?nw_3 A	(**0,** 0.39)1.39, 1.78, **2.17**
4220.047		10		23689.77	$a\ ^5P_1-z\ ^5D_2^\circ$	(0)2.47	(0)2.39
4209.74*		10		23747.77	$a\ ^5P_1-z\ ^5D_1^\circ$	(?) 1.43, 2.47pw_3 B; nw_3 C	(1.00) 1.39, 2.39
4205.080	2	250		23774.09	$b\ ^3G_4-z\ ^3F_3^\circ$	(0) 1.00	(0) 1.04b
4202.20		20		23779.06	$a\ ^5P_3-z\ ^5D_3^\circ$	(?) 1.58, 2pw_1; nw_3 C	(0.38) 1.54b
4202.350	2	150		23780.53	$a\ ^5P_3-z\ ^5D_2^\circ$	(?) 1.19pw_3 D; nw_3 A	(0) 1.17b
4195.83		1		23826.50	$b\ ^3F_3-z\ ^5D_3^\circ$		
4190.89		10		23854.58	$b\ ^3G_3-z\ ^3F_3^\circ$		
4190.40		15		23857.37	$a\ ^5P_1-z\ ^5D_0^\circ$	(0) **0.41,** 1.42	(**0,** 1.00) **0.39,** 1.39, 2.39
4183.435	2	250		23897.09	$b\ ^3G_4-z\ ^3F_4^\circ$	(0) 1.09	(0) 1.04b
4180.86	3	6?		23911.81	$b\ ^5F_4-z\ ^5D_4^\circ$		
4179.062		3		23922.09	$b\ ^5F_4-z\ ^5D_3^\circ$		
4178.390	1	60		23925.94	$a\ ^5P_2-z\ ^5D_2^\circ$	(**0,** 0.41, 0.82) **0.61,** 1.00, 1.45, 1.86	(**0,** 0.31, 0.62) **0.85,** 1.16, 1.47, 1.78, 2.09
4175.87		3		23940.38		(0) 1.06	
4164.015		15		24008.54	$b\ ^3G_4-z\ ^3F_4^\circ$	(0.72) 1.16pw_3 D; nw_3 A?	(0.63) 1.12b
4163.655		2		24010.62	$b\ ^1D_2-y\ ^3F_3^\circ$		
4162.072		2		24019.75	$b\ ^1D_2-y\ ^3F_2^\circ$		

See footnotes at end of table.

TABLE 1.—*Second spectrum of Vanadium*—Continued

1	2		3	4	5	6	
λ_{air}A	Intensity		Temp. class	Wave No. vac	Term combination	Zeeman effect	
	Arc	Spark				Observed	Computed
4142.90	5?	6+I		24130.90	$d\ ^3P_3-y\ ^1P_1^\circ$		
4140.08		2		24147.34		(0?) 0.59pw_2 D; nw_2 B	
4101.00	4?	8+I		24377.44	$b\ ^1D_2-z\ ^1F_3^\circ$	(0) 0.94	(0) 0.95
4085.67[b]		10h		24468.91	$d\ ^3F_2-y\ ^1F_3^\circ$	(?) 1.24pw_2 D; nw_2	(0) 1.21
4080.44		2		24500.27	$d\ ^3F_3-y\ ^1F_3^\circ$		
4075.66		3		24529.00	$a\ ^3H_5-z\ ^3F_4^\circ$		
4067.03		5		24581.05	$a\ ^3P_2-z\ ^3F_1^\circ$	**(0,** 1.16) 0.39, 1.50, **2.62**	**(0,** 1.14) 0.35, 1.40, **2.63**
4065.070[b]		100		24592.90	$d\ ^3F_4-x\ ^3G_5^\circ$	(0) 0.92	(0) 0.99
4056.270		7		24646.26	$a\ ^3H_6-z\ ^3F_5^\circ$	(?)0.98pw_2 D	(0) 0.94
4053.59		60		24662.55	$d\ ^3F_3-x\ ^3G_4^\circ$	(0) 0.97	(0) 0.98
4051.34	50	100+I		24676.24	$d\ ^3F_3-x\ ^3G_3^\circ$		
4051.06[d]		20+I		24677.95	$a\ ^3G_4-z\ ^3G_5^\circ$	(0) 1.15	(0) 1.24
4049.03		3		24690.32	$d\ ^3F_4-x\ ^3G_4^\circ$		
4046.269		50		24707.17	$b\ ^1D^2-z\ ^1D_2^\circ$	(0) 0.95	(0.11) 0.96
4039.574	1	20		24748.12	$a\ ^3G_3-z\ ^3G_4^\circ$	(0?) 1.78pw_2 D; nw_2 A	(0) 1.73
4038.545		2		24754.43	$a\ ^1P_1-y\ ^1D_2^\circ$	(0) 0.99	(0) 0.97
4036.779	3	60	V *E*	24765.25	$a\ ^3P_2-z\ ^3F_2^\circ$	(0. 38, **0.80**) 0.66, **1.08, 1.49,** 1.88	(0. 41, **0.82**) 0. 67, **1.08, 1.49,** 1.90
4035.631	10	400	V *E*	24772.30	$a\ ^3G_3-z\ ^3G_3^\circ$	(0) 0. 75	(0. 26) 0. 79
4027.30		1		24823.54	$c\ ^3F_4-y\ ^1F_3^\circ$		
4023.388	12	600	V *E*	24847.68	$a\ ^3G_4-z\ ^3G_4^\circ$	{(0) 0. 85} {(0) 1. 02}	(0. 10) 1. 02
4019.05		7h		24874.50	$c\ ^3F_2-y\ ^1F_3^\circ$		
4017.29		15h		24885.39	$d\ ^3F_4-y\ ^1H_5^\circ$		
4016.82		20h		24888.31	$c\ ^3F_4-x\ ^3G_5^\circ$	(0?) 0.92pw_2 D; nw_2 A	(0) 0. 95
4008.17	1	20		24942.02	$a\ ^3G_3-z\ ^3G_3^\circ$	(?) 1.91pw_2 D; nw_2 B	(0) 1. 90
4005.712	15	800	V	24957.32	$a\ ^3G_3-z\ ^3G_3^\circ$	(0) 1. 17	(0. 08) 1. 18
4002.940	4	80	V *E*	24974.60	$a\ ^3P_1-z\ ^3F_1^\circ$	(1. 18) 0. 29, **1.47**	(1.13) **0.35, 1.48**
4001.17		2		24985.65	$c\ ^3F_4-x\ ^3G_4^\circ$		
3999.195		30h		24997.99	$c\ ^3F_3-x\ ^3G_3^\circ$	(0) 0. 95	(0) 0. 96
3997.126	5	200	V *E*	25010.93	$a\ ^3P_2-z\ ^3F_2^\circ$	(?) 1.00pw_2 D; nw_2 A	(0) 0. 99
3991.965		2		25043.26	{$c\ ^3F_3-x\ ^3G_4^\circ$ $d\ ^3P_1-y\ ^1D_2^\circ$}		
3991.47		3		25046.37	$a\ ^3P_2-z\ ^3D_1^\circ$		
3989.803	1	15		25056.83	$a\ ^3G_4-z\ ^3G_5^\circ$	(0) 1. 64	(0) 1. 57
3985.783		30		25082.10	$c\ ^3F_3-x\ ^3G_3^\circ$	(?) 1. 02pw_2 D; nw_2 B	(0) 0. 97
3977.732	2	60		25132.87	$a\ ^3P_2-z\ ^3D_2^\circ$	(0. 36, **0.77**) 0. 68, **1.10, 1.49,** 1.87	(0.41, **0.82**) 0. 67, **1.08, 1.49,** 1.90
3973.642	8	300		25158.74	$a\ ^3P_1-z\ ^3F_2^\circ$	**(0,** 0.47) **0.62,** 1.10, 1.51	**(0,** 0.40) **0.68,** 1.08, 1.48
3970.15		5		25180.87	$c\ ^3F_4-y\ ^1H_5^\circ$		
3968.11	5	150	V *E*	25193.81	$a\ ^3P_0-z\ ^3F_1^\circ$	(0) 0.34	(0) 0.35
3960.37		1		25243.05	$a\ ^1F_3-y\ ^3H_4^\circ$		
3951.968	10	500	V *E*	25296.72	$a\ ^3P_2-z\ ^3D_3^\circ$	(0) 1. 17	(0) 1. 15
3948.00		1		25322.14			
3929.734	2	50		25439.84	$a\ ^3P_1-z\ ^3D_1^\circ$	(1.21) 0.30, 1.45	(1.24) 0.24, 1.48
3926.497	1	10		25460.81	$a\ ^3P_2-z\ ^3D_2^\circ$	(0) 1.44	(0.18) 1.44
3926.32		5		25461.96	$a\ ^1H_5-y\ ^3G_4^\circ$		
3916.418	5	200	V *E*	25526.33	$a\ ^3P_1-z\ ^3D_2^\circ$	**(0,** 0.43) **0.64,** 1.02, 1.49	**(0,** 0.40) **0.68,** 1.08, 1.48
3914.333	15	250		25539.93	$a\ ^3G_3-z\ ^3F_3^\circ$	(0) 0.84	(0) 0.83
3907.52		3		25584.46	$b\ ^1D_2-y\ ^3D_2^\circ$		
3903.27	10	250	V *E*	25612.32	$a\ ^3P_2-z\ ^3D_3^\circ$	(0) 1.35	(0) 1.45
3899.140	8	200	V *E*	25639.44	$a\ ^3G_4-z\ ^3F_3^\circ$	(0) 1.01	(0) 0.97
3896.155[c]	20?	60+I		25659.09	$a\ ^3P_0-z\ ^3D_1^\circ$	(0) 0.27	(0) 0.24
3891.25		4		25691.43	$b\ ^3F_3-z\ ^3G_3^\circ$		

See footnotes at end of table.

TABLE 1.—*Second spectrum of Vanadium*—Continued

1	2		3	4	5	6	
λ_{air} A	Intensity		Temp. class	Wave No. vac	Term combination	Zeeman effect	
	Arc	Spark				Observed	Computed
3884.847	2	50	V *E*	25733.77	*a* $^5G_3 - z\ ^5F_4^1$	(0.98) 0.94nw_3 D	(0.72) 0.88*b*
3883.43		2		25743.16	*b* $^5F_2 - z\ ^5G_3^1$		
3883.208		5		25744.64	*a* $^5P_1 - z\ ^5D_1^1$		
3881.04		2		25759.01	*a* $^1D_2 - z\ ^5P_2^1$		
3878.715	10	300		25774.46	*a* $^5G_3 - z\ ^5F_3^1$	(0) 1.08	(0) 1.07*b*
3875.67		5		25794.71	*b* $^5F_4 - z\ ^5G_5^1$		
3866.744	3	60		25854.25	*a* $^5P_1 - z\ ^5D_2^1$	(0) 1.40	(0) 1.34*b*
3865.72		5		25861.10	*b* $^5F_3 - z\ ^5G_4^1$		
3863.81	?	60+I?		25873.88	*a* $^5G_4 - z\ ^5F_4^1$		
3852.10		4		25952.53	*a* $^5F_3 - z\ ^5G_3^1$		
3850.409		7		25963.93	*a* $^5P_0 - z\ ^5D_1^1$	(0) 1.39	(0) 1.39
3849.758[k]		3		25968.32	*a* $^5G_3 - z\ ^5F_2^1$	Unaffected	(0) 1.94*b*
3847.323	50?	100+I		25984.76	*a* $^1P_1 - z\ ^1S_0^1$		
3831.017		6		26095.35	*a* $^5F_4 - z\ ^5G_4^1$	(0) 1.07	(0) 1.04*b*
3829.655		5		26104.63	*a* $^5F_3 - z\ ^5G_3^1$		
3829.53[l]		4		26105.49	*a* $^5F_2 - z\ ^5G_2^1$	(0) 0?, 1.21	(0) 1.21*b*
3826.968		30		26122.96	*b* $^5D_3 - z\ ^5P_2^1$	(0.48) 1.40nw_3 C	(0.41) 1.36*b*
3815.38	2	200		26202.30	*a* $^1H_5 - z\ ^1H_5^1$	(0) 0.98	(0.37) 1.00*b*
3813.12		3		26217.83	*b* $^5D_1 - z\ ^5P_2^1$		
3806.22		2		26265.36			
3804.38		2		26278.06			
3796.48	?	10+I?		26332.74	*a* $^1H_5 - z\ ^1G_4^1$		
3794.366	1	50		26347.40	*c* $^5P_2 - z\ ^5P_1^1$	(0) 1.24	(0) 1.28*s*
3787.235	3	150		26397.02	*c* $^5P_3 - z\ ^5P_2^1$	(0. 27) 1.47	(0.22) 1.42*b*
3778.357	2	100	V *E*	26459.04	*b* $^5F_4 - z\ ^5F_5^1$	(0, 0.41, 0.84)—, 0.62, 1.06, 1.46, **1.90**	(**0**, 0.41, 0.82) 0.24, 0.65, 1.06, 1.47, **1.88**
3774.678		15		26484.83	*b* $^5D_2 - y\ ^5D_3^1$	(0.48) ? nw_1 C?	(0.40) 1.36*b*
3773.80		5		26490.99	*b* $^5D_3 - y\ ^5D_4^1$		
3772.962	1	80		26496.87	*c* $^5P_1 - z\ ^5P_0^1$	(0) 1.33	(0) 1.35
3770.974	10	400	V *E*	26510.83	*b* $^5F_2 - z\ ^5F_3^1$	(0) 0.62	(0.11) 0.62*b*
3767.720		40		26533.74	*c* $^5P_0 - z\ ^5P_1^1$	(0) 1.47	(0) 1.44*b*
3761.20		1		26579.73	*b* $^5D_1 - y\ ^5D_2^1$		
3760.24[b]	3	140		26586.52	*b* $^5F_4 - z\ ^5F_4^1$	(0) 1.53	(0) 1.44*b*
3758.22	?	40+I		26600.81	*c* $^5P_1 - z\ ^5P_1^1$	(?) 1.41 pw_1	(0.09) 1.40*b*
3751.222	2	150		26650.43	*c* $^5P_1 - z\ ^5P_2^1$	(0) 1.49	(0) 1.54*b*
3750.88	8	600	V *E*	26652.86	*b* $^5F_3 - z\ ^5F_3^1$	(0) 1.03	(0.10) 1.04*b*
3745.806	10	800	V *E*	26688.96	*a* $^5H_4 - z\ ^5G_4^1$	(0) 0.84	(0) 0.82*b*
3743.610	2	40		26704.62	*b* $^5F_2 - z\ ^5F_1^1$	(**0**, 0.39, 0.81) 0.20, 0.62, 1.01, 1.40, **1.80**	(**0**, 0.43, 0.86) 0.16, 0.59, 1.02, 1.45, **1.94**
3736.017	1	70		26758.89	*c* $^5P_2 - y\ ^5D_2^1$	(0.26) 1.32	(0.11, **0.22**) 1.25, **1.36, 1.47**, 1.58
3735.158	1	30		26765.05	*c* $^5P_3 - y\ ^5D_4^1$	(0) 1.30	(0) 1.29*s*
3733.607		4		26776.16	*b* $^5H_5 - z\ ^5H_4^1$		
3732.760	10	800 *l*	V *E*	26782.23	*a* $^5H_4 - z\ ^5G_3^1$	(0) 0.95	(0) 0.98*s*
3731.983		20		26787.82	*a* $^1S_0 - z\ ^5P_1^1$		
3731.64		1		26790.28	*c* $^5P_1 - z\ ^5P_2^1$		
3728.335	4	200	V *E*	26814.03	*b* $^5H_4 - z\ ^5H_5^1$	(0) 0.77	(0.13) 0.80*b*
3727.351	15	1000 *l*	V *E*	26821.10	*b* $^5F_4 - z\ ^5F_4^1$	(0) 1.18	(0.10) 1.20*b*
3724.984		2		26838.15	*c* $^5P_2 - y\ ^5D_3^1$		
3722.16	?	10+I		26858.51	*a* $^5H_4 - z\ ^5G_5^1$		
3718.159	2	60	V *E*	26887.41	*b* $^5F_5 - z\ ^5F_5^1$	(0)1.53pw_1D;nw_1B	(0) 1.46*b*
3715.476	20	1200 *l*	V *E*	26906.83	*a* $^5H_5 - z\ ^5G_6^1$	(0) 1.03	(0) 1.47*b*
3712.533		8		26928.16	*a* $^1P_1 - y\ ^5F_2^1$;	(0?) 0.44pw_1D	(0) 0.46*b*
3711.751		10		26933.83	*b* $^5H_6 - z\ ^5H_5^1$	(0?) 1.51pw_1D; nw_1 B	(0) 1.46*b*
3711.118	1	50		26938.42	*c* $^5P_1 - y\ ^5D_1^1$	(0)1.34	(0)1.35
3709.335		40		26951.37	*c* $^5P_0 - y\ ^5D_1^1$	(0)1.39	(0)1.43
3705.41		5?		26979.92			
3703.832		7		26991.41	*a* $^5H_5 - z\ ^5G_4^1$		
3700.96		30		27012.36	*c* $^5P_1 - y\ ^5D_2^1$	(0)1.54	(0)1.53*b*
3700.337	2	200	V *E*	27016.90	*b* $^5H_5 - z\ ^5H_6^1$	(0?)1.02	(0.00)1.01*b*
3700.126		40		27018.45	*c* $^5P_1 - y\ ^5D_1^1$	(0)1.36	(0.08)1.39*b*
3697.72		1		27036.03	*c* $^5P_2 - y\ ^1D_2^1$		
3695.158		8		27054.77	*b* $^5H_4 - z\ ^5H_5^1$ *b* $^1D_2 - z\ ^5F_3^1$		

See footnotes at end of table.

TABLE 1.—*Second spectrum of Vanadium*—Continued

1	2		3	4	5	6	
λ_{air}A	Intensity		Temp. class	Wave No. vac	Term combination	Zeeman effect	
	Arc	Spark				Observed	Computed
3690.70		1		27087.45	$a\ ^1F_3 - w\ ^3D_3^4$		
3674.691		30		27205.45	$a\ ^1S_0 - y\ ^3D_1^2$	(0)1.43	(0)1.43
3669.410b	3	300	V *E*	27244.61	$b\ ^3H_6 - z\ ^3H_6^5$	(0)1.11	(0.05)1.14b
3661.383b	2	200		27304.33	$a\ ^1F_3 - y\ ^1G_4^4$	(0)0.96	(0)1.04b
3658.266		10		27327.60	$b\ ^3H_5^5 - z\ ^3H_6^6$	(0?)1.51 pw$_3$ D; *nw*$_3$ A	(0)1.43b
3646.848		7		27413.16	$b\ ^1D_2 - x\ ^3D_1^2$	(0)1.21 *pw*$_1$; *nw*$_1$ B?	(0)1.17b
3645.905		30		27420.25	$b\ ^3P_1 - z\ ^3P_0^1$	(0)1.39	(0)1.40
3634.13		1		27509.09	$b\ ^1D_2 - x\ ^3D_2^3$		
3632.126		15		27524.27	$b\ ^3P_1 - z\ ^3P_1^1$	(0)1.41	(0.04)1.42b
3631.482		10		27529.15	$b\ ^3P_0 - z\ ^3P_1^1$	(0)1.38 *pw*$_3$ D; *nw*$_3$ A	(0)1.44
3627.713	1	60		27557.75	$b\ ^3P_2 - z\ ^3P_1^1$	(0)1.37	(0)1.35b
3626.64		1		27565.90			
3625.608	1	50		27573.75	$b\ ^3P_1 - z\ ^3P_2^2$	(0)1.45	(0)1.52b
3623.03		1		27593.37	$b\ ^3P_0 - z\ ^3P_1^1$		
3622.289		10		27599.01	$a\ ^1D_2 - y\ ^3G_3^4$		
3621.203	2	150	V *E*	27607.29	$b\ ^3P_2 - z\ ^3P_2^2$	(0)1.41	(0.18)1.43b
3620.496		20		27612.68	$b\ ^1D_2 - z\ ^1P_1^1$	(0)1.01	(0)1.02b
3618.924b	2	200		27624.68	$a\ ^1P_1 - z\ ^1D_2^2$	(0)0.92	(0)0.91b
3611.58		10h		27680.85		(0)1.31	
3608.32		1		27705.85	$c\ ^1G_4 - w\ ^3G_4^4$		
3607.30		1		27713.69	$b\ ^3P_1 - z\ ^3P_2^3$		
3604.375		4		27736.18	$b\ ^3D_1 - z\ ^1S_0^0$	(0)0.59	(0)0.58
3602.94		3h		27747.22		(?) 1.22nw$_1$ A	
3598.72		3		27779.76			
3597.41		3		27789.88			
3593.323b	15	600	V *E*	27821.48	$a\ ^3F_4 - z\ ^3F_3^3$	(0?) 1.14	(0) 1.16s
3592.012b	20	800	V *E*	27831.64	$a\ ^3F_3 - z\ ^3F_2^2$	(0) 1.01	(0) 1.00b
3589.745b	25	1000	V *E*	27849.21	$a\ ^3F_2 - z\ ^3F_1^1$	(0?) 0.79	(0) 0.80b
3588.13		15		27861.75	$b\ ^3P_1 - y\ ^3D_0^1$	(0) 1.40	(0) 1.40
3578.636		15		27935.66	$b\ ^3P_1 - y\ ^3D_1^2$		
3577.857d	7	20+I?		27941.74	$b\ ^3P_1 - y\ ^3D_1^1$	(?) 1.28pw$_1$ D	(0.03) 1.42b
3577.644		3		27943.41	$b\ ^1G_4 - z\ ^3H_4^4$		
3577.220		10		27946.72	$b\ ^3P^0 - y\ ^3D_1^1$	(0) 1.45	(0) 1.43
3574.340	1	60		27969.24	$b\ ^3P_2 - y\ ^3D_2^3$	(0) 1.41	(0.16) 1.42b
3573.557		50		27975.36	$b\ ^3P_2 - y\ ^3D_1^1$	(0) 1.34	(0) 1.33s
3566.177	10	200		28033.26	$a\ ^3F_2 - z\ ^3F_2^3$	(0.38, 0.87) 0.26, 0.61, 1.04, 1.49	(0.43, **0.86**) 0.22, **0.65, 1.08,** 1.51
3563.71		3h		28052.66	$a\ ^3F_4 - z\ ^3F_3^4$		
3560.594	4	90		28077.21	$a\ ^3F_3 - z\ ^3F_2^3$	(0.50) 1.08nw$_2$ C	(0.20, 0.40, **0.60**) 0.64, 0.84, **1.04, 1.24,** 1.44, 1.64
3556.800	40	1500	V *E*	28107.16	$c\ ^3F_4 - z\ ^3D_3^3$	(0) 1.09	(0) 1.07b
3550.51		3		28156.95			
3549.030c		3		28168.70	$c\ ^3P_1 - z\ ^1S_0^0$	(0) 0.95?	(0) 1.35
3547.07		5		28184.26	$b\ ^1G_4 - z\ ^3H_5^5$		
3545.190x	30	1000	V *E*	28199.20	$a\ ^3F_3 - z\ ^3D_2^2$	(0) 0.97	(0) 0.96s
3542.480		4		28220.78	$a\ ^1D_2 - y\ ^3F_3^4$		
3541.341		50		28229.85	$a\ ^1D_2 - y\ ^3F_2^3$	(0)0.98	(0)0.96b
3538.238	3	50		28254.61	$a\ ^3F_4 - z\ ^3F_3^4$	(?)1.75pw$_1$ D; nw$_1$ C	(0) 1.76b
3534.14		2		28287.37	$a\ ^3P_2 - z\ ^3F_2^3$		
3532.285		20		28302.23	$a\ ^1F_3 - y\ ^1F_3^3$	(0.20)0.92	(0.08) 0.96b
3531.48		10		28308.68	$a\ ^3F_3 - z\ ^3F_3^4$		
3530.765	20	500	V *E*	28314.41	$a\ ^3F_2 - z\ ^3D_1^1$	(0, 0.47) 0.21, 0.62, **1.11**	(0, 0.41) 0.24, 0.65, **1.06**

See footnotes at end of table.

TABLE 1.—*Second spectrum of Vanadium*—Continued

1	2		3	4	5	6	
λ_{air}A	Intensity		Temp. class	Wave No. vac	Term combination	Zeeman effect	
	Arc	Spark				Observed	Computed
3530.45		10		28316.94	$a\ ^3D_1 - z\ ^3P^0_0$	(0)0.52	(0) 0.49
3527.867		10		28337.67	$b\ ^3H_4 - y\ ^3G^0_3$		
3524.713	10	200	VE	28363.02	$a\ ^3F_3 - z\ ^3D^0_3$	2p; nw 3	
3521.836	2	90	VE	28386.19	$a\ ^3D_3 - z\ ^3P^0_2$	(0)1.04pw$_1$ D; nw$_1$ A	(0) 1.12*b*
3520.547	1	15		28396.58	$a\ ^3D_3 - z\ ^3P^0_1$	(?)0.74pw$_2$ D; nw$_2$ A	(0) 0.82*s*
3520.022	5	120	VE	28400.98	$a\ ^3F_2 - z\ ^3D^0_2$	(0.27, **0.90**) 0.19, 0.60, 1.06, **1.52** pw$_2$ D?; nw$_2$ A?	(0.43, **0.86**) 0.22, **0.65, 1.08**, 1.51
3517.298	40	800	VE	28422.82	$a\ ^3F_4 - z\ ^3D^0_3$		
3516.00		5		28433.31	$a\ ^3F_4 - z\ ^3D^0_4$		
3514.422		20		28446.08	$a\ ^3D_2 - z\ ^3P^0_2$	(0.66) 1.43 nw$_2$ C	(0.63) 1.30*b*
3513.877		15		28450.49	$b\ ^3H_5 - y\ ^3G^0_4$	(0) 0.93	(0) 0.97*s*
3512.13		3		28464.64	$a\ ^1F_3 - x\ ^3G^0_4$	(0) 1.09	(0) 1.10*b*
3511.42		3		28470.39	$a\ ^3D_1 - z\ ^3P^0_2$		
3509.684		2		28484.48			
3509.024	1	40		28489.83	$b\ ^3H_4 - y\ ^3G^0_3$	(0) 1.06	(0) 0.94*b*
3507.534	1	20		28501.94	$a\ ^1P_1 - y\ ^3D^0_2$	(0) 1.17	(0) 1.18*b*
3506.57		7		28509.77	$a\ ^1F_3 - x\ ^3G^0_3$	(0.47)? nw$_2$ D	(0.39) 0.90*b*
3504.432	20	400		28527.16	$a\ ^3F_3 - z\ ^3D^0_2$	(?) **0.29**, 0.67, 1.02, 1.36, 1.72 pw$_2$	(**0**, 0.35, 0.70) **0.34**, 0.69, 1.04, 1.39, 1.74
3499.823	2	20		28564.73	$a\ ^3F_2 - z\ ^3D^0_2$	(**0**, 0.66, 1.31) 0, 0.65, 1.30, 1.95, **2.63**	(**0**, 0.67, 1.34)−0.02, 0.65, 1.32, 1.99, **2.66**
3497.39		4		28584.60	$b\ ^3D_3 - y\ ^3F^0_3$		
3497.031	2	200		28587.54	$a\ ^1D_2 - z\ ^1F^0_3$	(0) 0.96	(0) 0.92*b*
3493.163	8	150		28619.19	$a\ ^3F_2 - z\ ^3D^0_1$	(0, 0.75) **0**, 0.68, 1.38	(**0**, 0.74)−**0.09**, 0.65, 1.39
3489.947	1	20		28645.56	$b\ ^3D_3 - y\ ^3F^0_4$	(0) 0.88pw$_1$ D; nw$_1$ C	(0) 0.94*s*
3485.916	10	250		28678.69	$a\ ^3F_2 - z\ ^3D^0_3$	(1.07) 1.31pw$_2$ B; nw$_2$ B	(1.11) 1.26*b*
3484.65		3		28689.11	$a\ ^3F_2 - z\ ^3D^0_2$		
3484.32		2		28691.82	$a\ ^1H_5 - y\ ^3H^0_4$		
3479.837	5	80		28728.78	$a\ ^3F_3 - z\ ^3D^0_3$	(0.72, **1.50**) 0, 0.65, **1.37**, 2.11	(0.74, **1.48**)−0.09, **0.65, 1.39**, 2.13
3478.961		6		28736.02	$b\ ^1D_2 - w\ ^3D^0_3$	(0) 1.75pw$_2$ D; nw$_2$ B	(0) 1.75*b*
3477.514	2	40		28747.97	$a\ ^3D_3 - y\ ^3D^0_3$	(0) 1.08	(0) 1.13*b*
3476.252	1	20		28758.41	$a\ ^3D_1 - y\ ^3D^0_2$	(0) 0.49	(0) 0.49
3470.263	1	20		28808.04	$a\ ^3D_2 - y\ ^3D^0_3$	(0.64) 1.30 nw$_2$ C	(0.61) 1.30b
3469.528	2	50		28814.14	$a\ ^3D_3 - y\ ^3D^0_4$	(?) 0.95nw$_2$ A	(0) 0.98b
3467.33		2		28832.41	$a\ ^3D_1 - y\ ^3D^0_2$		
3466.59	1	20		28838.56	$a\ ^3D_1 - y\ ^3D^0_1$	(0.96) 0.47, **1.45**	(0.94) **0.49**, 1.43
3465.25	1	4		28849.72	$a\ ^1P_1 - y\ ^3P^0_2$		
3464.17		6		28858.71	$c\ ^3P_2 - y\ ^3F^0_3$	(1.35) ?nw$_2$ D	(1.31) 1.00b
3463.831		4		28861.53	$a\ ^1H_5 - y\ ^3H^0_5$		
3463.079		4		28867.80	$c\ ^3P_2 - y\ ^3F^0_2$		
3461.580		5		28880.30	$a\ ^3F_3 - z\ ^3D^0_2$		
3457.153	3	300		28917.28	$a\ ^1D_2 - z\ ^1D^0_2$	(0) 0.96 (0) 1.05	(0.16) 0.98*b*
3453.78		1		28945.52	$b\ ^3D_3 - z\ ^1F^0_3$		
3453.087	1	90		28951.33	$b\ ^3D_3 - z\ ^1F^0_3$	(0?) 0.71pw$_2$ D; nw$_2$ A	(0) 0.69*b*
3451.046		12		28968.45	$b\ ^3H_4 - y\ ^3F^0_3$		
3448.69		1		28988.24	$b\ ^3H_5 - y\ ^3F^0_4$		
3438.232		2		29076.40			
3436.393		2		29091.97	$b\ ^3P_1 - z\ ^1S^0_0$	(0) 1.41	(0) 1.40
3435.38		7		29100.55	$b\ ^3D_3 - z\ ^1G^0_4$		
3424.46		1		29108.34	$b\ ^3D_3 - z\ ^1S^0_0$		
3434.024 [h]		4		29112.04	$c\ ^3P_1 - y\ ^3F^0_2$	(0.12) —?	(0) 0.27*b*
3433.767		3		29114.22	$b\ ^3D_3 - z\ ^1S^0_0$		
3422.259		3h		29212.12		(0) 1.48	

See footnotes at end of table.

TABLE 1.—*Second spectrum of Vanadium*—Continued

1	2		3	4	5	6	
λ_{air}A	Intensity		Temp. class	Wave No. vac	Term combination	Zeeman effect	
	Arc	Spark				Observed	Computed
3420.709		5		29225.35	$c\,^3P_2 - z\,^1F_3^\circ$		
3420.15		2		29230.13	$b\,^3H_6 - z\,^1H_5^\circ$		
3415.91		2		29266.41	$a\,^1H_5 - x\,^3F_4^\circ$		
3414.879		3		29275.25	$b\,^3D_3 - z\,^1D_2^\circ$		
3414.192	6	10+I		29281.14	$b\,^3D_2 - z\,^1D_2^\circ$		
3410.46		1		29313.18	$b\,^3H_5 - z\,^1H_5^\circ$		
3408.955		15		29326.12	$b\,^3H_4 - z\,^1F_3^\circ$		
3406.06		7		29351.04	$b\,^3H_4 - z\,^1H_5^\circ$	(0) 1.07	(0) 1.21*b*
3404.43		8*l*		29365.10	$c\,^1G_4 - x\,^1G_4^\circ$	(0) 0.96	(0.07) 0.95*b*
3403.159		3		29376.06	$b\,^3D_1 - z\,^1D_2^\circ$		
3401.997		2		29386.10	$a\,^1G_4 - z\,^3H_4^\circ$	(0) 1.02	(0) 1.13*b*
3401.740		1		29388.32	$c\,^3P_2 - z\,^5S_2^\circ$		
3394.92		1		29447.35	$b\,^3P_2 - y\,^3G_3^\circ$		
3392.659	1	50		29466.97	$b\,^1G_4 - y\,^3G_4^\circ$	(?) 1.41pw_3 B; nw_3 B	(0) 1.44*b*
3391.01		1		29481.31	$b\,^3H_4 - z\,^1G_4^\circ$		
3385.790		3		29526.76	$b\,^1D_2 - x\,^3P_1^\circ$		
3382.529	1	30		29555.22	$c\,^3P_2 - z\,^1D_2^\circ$	(0.78) 1.13nw_3 C	(0.77) 1.15*b*
3372.666		3		29641.65	$c\,^3P_1 - z\,^5S_2^\circ$		
3370.40		2		29661.58	$a\,^1I_6 - y\,^3G_5^\circ$		
3367.666		3		29685.66	$a\,^1H_5 - z\,^3I_5^\circ$		
3364.692		1		29711.90			
3361.506	2	60		29740.06	$b\,^1G_4 - y\,^3G_5^\circ$	(?) 1.83pw_2 D; nw_3 B	(0) 1.70*b*
3359.50		2		29757.81	$a\,^1D_2 - y\,^3P_1^\circ$		
3355.366	1	20		29794.47	$a\,^1D_2 - y\,^3D_2^\circ$	(0.25) 1.07nw_1 ?	(0.16) 1.06*b*
3353.776	2	30		29808.60	$c\,^3P_1 - z\,^1D_2^\circ$	(**0**, 0.37)nw_3 A	(**0**, 0.42) **0.51**, 0.93, 1.35
3351.53		1		29828.58	$b\,^1F_3 - w\,^3G_4^\circ$		
3348.372		4		29856.71	$b\,^3D_3 - y\,^3D_3^\circ$	(0, 0.85)	(**0**, 0.76) 0.49, 1.25, **2.01**
3345.899		70		29878.77	$c\,^1G_4 - x\,^1F_3^\circ$	(0) 0.96	(0) 0.98*b*
3343.312		2		29901.79	$b\,^1F_3 - w\,^3G_4^\circ$	(0) 1.11	(0) 1.08*s*
3337.845[b]	2	200		29950.87	$b\,^1D_2 - y\,^1F_3^\circ$	(0) 0.86	(0) 0.84*s*
3335.482		10		29972.08	$a\,^1P_1 - x\,^3F_2^\circ$	(?) 0.49pw_3; nw_3	(0) 0.54*b*
3333.608		2		29988.93	$a\,^3D_1 - z\,^5S_2^\circ$		
3323.731		3		30078.05	$b\,^3P_2 - y\,^3F_3^\circ$		
3321.539	3	150		30097.90	$b\,^1G_4 - y\,^3F_4^\circ$	(0) 1.02	(0) 0.96*b*
3320.780		4		30104.78	$a\,^1D_2 - y\,^3D_3^\circ$	(?) 1.75pw_3 D; nw_3 B	(0) 1.77*s*
3318.907		20		30121.76	$b\,^3D_2 - y\,^3P_1^\circ$	(0) 1.08	(0) 1.11*s*
3317.912	1	20		30130.80	$c\,^3P_2 - y\,^3D_1^\circ$	(**0**, 0.83) 0.49, 1.35, **2.18**	(**0**, 0.87) 0.49, 1.36, **2.23**
3317.295		2		30136.40	$a\,^3F_4 - z\,^3G_3^\circ$		
3316.873		20		30140.24	$b\,^3D_1 - y\,^3P_0^\circ$	(0) 0.59	(0) 0.58
3315.53[1]		5		30152.44	$b\,^3D_3 - y\,^3D_2^\circ$	(0) 0.68	(0) 1.41*b*
3315.176[1]	2	50		30155.66	$b\,^1G_4 - y\,^3F_3^\circ$	(0.67) 1.07nw_3	(0.67) 1.08*b*
3314.862[1]	1	50		30158.52	$b\,^3D_2 - y\,^3D_2^\circ$	(?) 0.77pw_3; nw_3	(0.25) 1.18*b*
3308.480	1	20		30216.69	$b\,^3D_1 - y\,^3P_1^\circ$	(0.86) 0.56, 1.43	(0.81) **0.58, 1.39**
3307.445		2		30226.15	$a\,^3D_3 - y\,^3G_3^\circ$		
3304.474	1	40		30253.32	$b\,^3D_1 - y\,^3D_2^\circ$	(**0**, 0.56) 0.56, 1.10, **1.68**	(**0**, 0.53) 0.58, 1.11, **1.64**
3301.66		10		30279.11		(0) 0.96	
3300.905		6		30286.03	$a\,^3D_3 - y\,^3G_4^\circ$		
3298.738	5	130		30305.93	$a\,^3F_4 - z\,^3G_4^\circ$	(0.66) 1.12	(0.63) 1.12*b*
3297.528		20		30317.05	$c\,^3P_0 - y\,^3D_1^\circ$	(0) 0.46pw_1 D	(0) 0.49
3296.052		8		30330.62	$a\,^1P_1 - x\,^3D_1^\circ$	(0.32) 0.77nw_1 ?	(0.34) 0.80*b*
3293.146		50		30357.39	$b\,^1F_3 - x\,^1D_2^\circ$	(0) 0.97	(0) 0.97*b*
3291.04		5		30376.81	$a\,^3D_3 - y\,^3G_4^\circ$		
3290.240	2	50		30384.20	$c\,^3P_1 - y\,^3D_1^\circ$	(0.83) 0.51, **1.38**	(0.86) **0.49, 1.35**
3289.391	6	100		30392.04	$a\,^3F_3 - z\,^3G_3^\circ$	(0.87) 1.06nw_3 B	(0.20, 0.40, **0.60**) 0.44, 0.64, **0.84, 1.04**, 1.24, 1.44
3288.985		7		30395.79	$c\,^3P_2 - y\,^3P_1^\circ$	(0) 1.37	(0) 1.34*b*

See footnotes at end of table.

TABLE 1.—*Second spectrum of Vanadium*—Continued

1	2		3	4	5	6	
λ_{air}A	Intensity		Temp. class	Wave No. vac	Term combination	Zeeman effect	
	Arc	Spark				Observed	Computed
3288.324	1	20		30401.90	$a\ ^1I_6-z\ ^1H_5^0$	(0) 1.00	(0) 1.01*s*
3287.08		6*Hl*		30413.41		(0) 0.59	
3285.672		3		30426.44	$a\ ^1P_1-x\ ^1D_2^0$	(0) 1.16	(0) 1.16*b*
3285.022 b	2	50		30432.46	$c\ ^3P_2-y\ ^3D_3^0$	(0.45) 1.24	(0.45) 1.24*b*
3282.534	5	150		30455.53	$b\ ^1G_4-z\ ^1F_3^0$	(0) 0.93	(0) 1.00*b*
3281.755	1	10		30462.76	$b\ ^3D_3-y\ ^3D_3^0$	(0) 1.26	(0.03) 1.26*b*
3281.120	2	40		30468.65	$b\ ^3D_2-y\ ^3D_3^0$	(0) 1.32	(0) 1.31*s*
3279.844 b	8	300		30480.50	$b\ ^1G_4-z\ ^1H_5^0$	(0) 1.00	(0) 0.89*b*
3277.71	2	30		30500.35	$b\ ^3D_3-y\ ^3P_2^0$		
3277.448	1	15		30502.78	$a\ ^1F_3-y\ ^1D_2^0$	(0) 0.91	(0) 0.96*b*
3277.082	1	10		30506.19	$b\ ^3D_2-y\ ^3P_1^0$	(0.43) 1.43nw_1 ?	(0.47) 1.38*b*
3276.12	50	1500*R*		30515.15	$a\ ^3F_4-z\ ^3G_5^0$	(0?) 1.08pw_3 D?; nw_2 A?	(0) 1.07*s*
3274.50	1−	10		30530.24	$a\ ^1P_1-z\ ^1P_1^0$		
3271.124	40	1200*R*		30561.75	$a\ ^3F_3-z\ ^3G_4^0$	(0?) 1.00pw_3 D?; nw_3 A?	(0) 1.00*s*
3270.115		10		30571.18	$a\ ^1S_0-y\ ^3D_1^0$	(0) 0.53	(0) 0.49
3268.94		2		30582.17		(0) 1.21nw_1 ?	
3267.709	30	1000*R*		30593.69	$a\ ^3F_2-z\ ^3G_3^0$	(0?) 1.24pw_3 D?; nw_3 A?	(0) 1.22*s*
3266.91		1?		30601.17	$b\ ^3D_1-y\ ^3P_2^0$		
3265.893	5	100		30610.70	$b\ ^1G_4-z\ ^1G_4^0$	(0) 1.00	(0.07) 0.97*b*
3263.33	?	20		30634.74	$b\ ^3G_4-z\ ^3H_4^0$		
3261.80		5		30649.11	$c\ ^3P_1-y\ ^3P_1^0$		
3259.684		3		30669.01	$a\ ^1G_4-y\ ^3G_5^0$		
3257.893	2	100		30685.87	$c\ ^3P_1-y\ ^3D_2^0$	(0) 1.02	(0) 0.99*b*
3254.773 b	8	300		30715.28	$b\ ^3G_3-z\ ^3H_4^0$	(0) 0.90pw_3D;nw_3A	(0) 0. 84*s*
3251.869	4	200		30742.71	$c\ ^3P_2-y\ ^3D_3^0$	(0) 1.20	(0) 1.19*b*
3250.775	4	200		30753.06	$a\ ^1H_5-y\ ^1G_4^0$	(0) 1.00	(0) 1.12*b*
3249.617	?	40+I?		30764.01	$b^3G_3-z^3H_4^0$	(0.61) 1.11nw_2 C	(0.61) 1.08*b*
3249.464		4		30765.46	$b\ ^3P_2-z\ ^1D_2^0$		
3247.908		4		30780.20	$c\ ^3P_2-y^3P_2^0$		
3240.785		1		30847.85	$a^3D_3-y\ ^3F_3^0$		
3239.833		8		30856.91	$a^3D_2-y\ ^3F_2^0$	(0.76) 1.02nw nw_3 C	(0.80) 1.15*b*
3237.876 b	10	350	V *E*	30875.56	$b\ ^3G_4-z\ ^3H_5^0$	(0) 1.00	(0) 0.97*b*
3234.504		10		30907.74	$a\ ^3D_3-y\ ^3F_3^0$	(0.96) ?nw_3 B?	(0.90) 0.88*b*
3233.772	3	80	V *E*	30914.75	$a\ ^3D_3-y\ ^3F_4^0$	(0) 0.94pw_1; nw_1	(0) 0.82*s*
3233.546	1	40	V *E*	30916.91	$a^3D_3-y^3F_3^0$	(0) 0.83	(0) 0.85*b*
3231.952	2	80	V *E*	30932.15	$a\ ^3D_1-y\ ^3F_2^0$	(0) 0.81	(0) 0.77*s*
3230.919		4		30942.04	$a\ ^1G_4-y\ ^3G_5^0$	(?) 1.79pw_3 D;nw_3C	(0) 1.76*b*
3233.546	1	40	V *E*	30916.91	$a^3D_3-y^3F_3^0$	(0) 0.83	(0) 0.85*b*
3231.952	2	80	V *E*	30932.15	$a\ ^3D_1-y\ ^3F_2^0$	(0) 0.81	(0) 0.77*s*
3230.919		4		30942.04	$a\ ^1G_4-y\ ^3G_5^0$	(?) 1.79pw_3 D;nw_3C	(0) 1.76*b*
3226.924	1	40		30980.35	$b\ ^1D_2-y\ ^1P_1^0$	(0) 0.93	(0) 0.93*s*
3221.380		2		31033.66	$c\ ^3P_1-y\ ^3P_2^0$	(0) 1.50	(0) 1.59*b*
3217.121 b	15	400		31074.75	$b\ ^3G_5-z\ ^3H_6^0$	(0) 1.08	(0) 1.06*b*
3214.750	6	120	V *E*	31097.66	$a\ ^3F_4-z\ ^3F_3^0$	(0?) 1.46	(0) 1.52*b*
3208.345	6	100	V *E*	31159.74	$a\ ^3F_3-z\ ^3F_3^0$	(?)1.81pw_3 D;nw_3 B	(0) 1.82*s*
3206.16		15*Hl*		31180.98			
3202.711		2		31214.55	$a\ ^3D_3-z\ ^1F_3^0$		
3201.58		15*Hl*		21225.58		(0) 0.93	
3197.574		7		31264.70	$a\ ^1D_2-z\ ^3F_3^0$	(0.60) ?nw_1 C	(0.61) 0.85*b*
3196.574	1	20		31274.48	$a\ ^3D_3-z\ ^1F_3^0$	(0) 0.83	(0) 0.81*b*
3195.50		15*Hl*		31284.99		(0) 1.02	
3193.97	?	10?+I		31299.98	$a\ ^1G_4-y\ ^3F_3^0$		
3193.200	1	20		31307.53	$b\ ^3P_1-y\ ^3D_1^0$	(0.89) **0.47**, 1.42	(0.91) **0.49**, 1.40
3192.699	1	15		31312.44	$b\ ^3P_0-y\ ^3D_1^0$	(0) 0.54	(0) 0.49
3190.686 b	30	500*R*	V *E*	31332.19	$a\ ^3F_4-z\ ^3F_4^0$	(0) 1.22	(0.00) 1.22*b*
3189.76		3		31341.29	$b\ ^3P_2-y\ ^3D_1^0$	(0.98) 1.38, **2.39**	(**0**, 0.89) 0.49, 1.38, **2.27**
3188.522	20	300*R*	V *E*	31353.46	$a\ ^3F_3-z\ ^3F_4^0$	(0) 1.01	(0.05) 1.03*b*
3188.10	3	30		31357.61	$a\ ^1G_4-y\ ^3F_4^0$	(0.67) ?nw_3	(0.77) 1.06*b*

See footnotes at end of table.

TABLE 1.—*Second spectrum of Vanadium*—Continued

1	2		3	4	5	6	
λ_{air}A	Intensity		Temp. class	Wave No. vac	Term combination	Zeeman effect	
	Arc	Spark				Observed	Computed
3187.717	15	200*R*	V *E*	31361.38	$a\ ^3F_3-z\ ^3F^\circ_3$		
3186.86		10		31369.81	$a\ ^3D_3-z\ ^1G^\circ_4$		
3186.10		1		31377.29	$a\ ^3D_3-z\ ^3S^\circ_1$		
3182.674		20		31411.07	$a\ ^1D_2-x\ ^3F^\circ_3$		
3182.59		20		31411.89	$d\ ^3F_3-w\ ^3F^\circ_3$		
3179.416		8		31443.25	$d\ ^3F_3-w^3F^\circ_4$	(?)1.98pw$_3$ D	(0)1.99*s*
3177.696		6		31460.27	$d\ ^3F_3-w^3F^\circ_3$	(0?) 1.70pw$_2$ D; nw$_2$	(0) 1.66*s*
3174.531	1	60		31491.63	$d\ ^3F_3-w^3F^\circ_4$	(0) 1.00	(0.13) 1.02*b*
3174.077	2	30		31496.14	$b\ ^3P_1-y^3P^\circ_2$	(0) 1.41	(0) 1.40
3172.230		7		31514.48	$c\ ^3D_1-t^3D^\circ_1$	(0) 0.50	(0) 0.50:*b*
3171.739		9		31519.35	$d\ ^3F_4-w\ ^3F^\circ_4$	(0?) 1.51pw$_1$ D; nw$_1$B?	(0) 1.58*b*
3170.208		8		31534.58	$d\ ^3F_2-w\ ^3F^\circ_2$		
3169.21		2		31544.51	$a\ ^3D_3-z\ ^1D^\circ_2$?		
3168.127	4	40	V *E*	31555.29	$a\ ^3F_2-z\ ^3F^\circ_1$	(?) 1.83pw$_3$D; nw$_3$ B	(0) 1.76*s*
3167.49	1	30		31561.64	$b^1\ F_3-x\ ^1G^\circ_4$		
3167.420	1	40		31562.33	$d\ ^3F_4-w\ ^3F^\circ_4$	(0.42) 1.30	(0.43) 1.30*b*
3166.39		8		31572.60	$b\ ^3P_1-y\ ^3P^\circ_1$		
3165.89	1	30		31577.60	$b\ ^3P_0-y\ ^3P^\circ_1$	(0) 1.44	(0) 1.39
3164.82	4	40	V *E*	31588.26	$a\ ^3F_3-z\ ^3F^\circ_4$	(0?) 1.50pw$_2$D; nw$_1$B	(0) 1.49*b*
3163.76		10		31598.84	$c\ ^3D_2-t\ ^3D^\circ_3$	(0) 1.14	(0) 1.14:*b*
3163.024	2	30	V *E*	31606.20	$b\ ^3P_2-y\ ^3P^\circ_1$	(0) 1.41	(0) 1.38*b*
3162.714	2	30	V *E*	31609.29	$b\ ^3P_1-y\ ^3D^\circ_2$	(0.35) 0.77	(0, 0.29) **0.82**, 1.11, 1.40
3162.367		10		31612.76			
3161.313	1	30		31623.30	$a\ ^1D_2-x\ ^3D^\circ_1$	(0?) 1.29pw$_1$D; nw$_1$ B	(0) 1.22*b*
3160.781		15		31628.62	$b\ ^3D_2-x\ ^3F^\circ_2$ $a\ ^3D_1-z\ ^1D^\circ_2$	(**1.09** ...)?nw$_3$D	(0.57, **1.14**) 0.11, **0.68**, **1.25**, 1.82 (**0**, 0.44) 0.49, 0.93, **1.37**
3159.365	1	20		31642.80	$b\ ^3P_2-y\ ^3D^\circ_3$	(?) 1.25, 2p; nw$_2$C	(0.49) 1.25*b*
3157.900	2	40		31657.48	$a\ ^1G^1-z\ ^1F^\circ_3$	(0) 0.91	(0) 0.92*b*
3157.70		3 *H*		31659.48			
3155.409	2	60	V *E*	31682.47	$a\ ^1G_4-z\ ^1H^\circ_5$	(0) 0.98	(0) 0.95*s*
3154.80		1		31688.58	$c\ ^3D_1-t^3D^\circ_2$		
3151.319	2	100	V *E*	31723.59	$b\ ^3D_1-x\ ^3F^\circ_2$	(0) 0.72	(0) 0.73*b*
3148.738		15		31749.59	$c\ ^3D_3-t\ ^3D^\circ_3$	(0) 1.27	(0) 1.27:*b*
3146.818		10		31768.96	$b\ ^3D_3-z\ ^3F^\circ_4$	(0.56) 1.17*nw*$_3$	(0.49) 1.16*b*
3146.226	2	40 *l*		31774.94	$b\ ^3D_2-z\ ^3F^\circ_3$	(0) 0.95	(0) 0.89*b*
3145.971	3	20	V *E*	31777.51	$a\ ^3F_4-z\ ^5G^\circ_5$		
3145.337	6	30	IV *E*	31783.92	$a\ ^5F_5-z\ ^5G^\circ_6$ $a\ ^5F_3-z\ ^5G^\circ_4$	(**0**, 0.91, 1.79) 0.35, 1.17, 2.03, **2.94**	(**0**, 0.14, 0.28, 0.42, 0.56) 0.72, 0.86, 1.00, 1.14, 1.28, 1.42, 1.56, 1.70, **1.84** (**0.** 0.89, 1.78)—0.58, 0.31, 1.20, 2.09 **2.98**
3144.700		20		31790.36	$b\ ^3H_6-y\ ^3H^\circ_5$	(?) 1.55pw$_2$D; nw$_2$C	(0) 1.54*b*
3143.477		15		31802.72	$b\ ^3H_5-y\ ^3H^\circ_5$	(?) 1.66*pw*$_3$ D?; *nw*$_2$ B	(0) 1.63*b*
3142.484	6	150	V *E*	31812.78	$a\ ^1G_4-z\ ^1G^\circ_4$	(0) 0.96	(0.03) 0.96*b*
3142.183	1	20		31815.82	$a\ ^1H_5-x\ ^3G^\circ_5$	(0.68) 1.25*nw*$_3$ C	(0.11, 0.22, 0.33, 0.44, **0.55**) 0.60, 0.71, 0.82, 0.93, **1.04**, **1.15**, 1.26, 1.37, 1.48, 1.59
3141.486	1	40	V *E*	31822.88	$a\ ^1D_2-z\ ^1P^\circ_1$	(0) 1.05	(0) 1.07*b*
3141.07		2		31827.09	$c\ ^3F_3-w\ ^3F^\circ_3$	(0) 1.02	(0.15) 1.03*b*
3139.733	4	160	V *E*	31840.65	$b\ ^3H_4-y\ ^3H^\circ_4$	(0) 0.77	(0.40) 0.76*b*
3138.05		20		31857.72	$c\ ^3F_4-w\ ^3F^\circ_4$		
3136.503	4	160		31873.43	$b\ ^3H_5-y\ ^3H^\circ_6$	(0) 0.99	(0.12) 1.00*b*

See footnotes at end of table.

TABLE 1.—*Second spectrum of Vanadium*—Continued

1	2		3	4	5	6	
λ_{air}A	Intensity		Temp. class	Wave No. vac	Term combination	Zeeman effect	
	Arc	Spark				Observed	Computed
3134.928	5	200		31889.45	$b\ ^3H_6 - y\ ^3H_5^0$	(0) 1.09	(0.48) 1.09*b*
3133.329	15	150*r*	III *E*	31905.72	$a\ ^5F_3 - z\ ^5G_3^0$	(0.52, **1.39**) 0.32, 0.94, **1.62**	(0.66, **1.32**) −0.35, **0.31, 0.97,** 1.63
3132.793		3		31911.18	$b\ ^3H_4 - y\ ^3H_3^0$		
3130.262	10	100*R*	III *Er*	31936.98	$a\ ^5F_2 - z\ ^5G_3^0$	(?) 1.08pw_3 D?; nw_3 A?	(0.69) 1.07*b*
3128.686	1	20		31953.07	$b\ ^3P_2 - y\ ^3D_3^0$	(0) 1.14	(0) 1.16*b*
3128.288	1	10		31957.13	$b\ ^3P_1 - y\ ^3P_2^0$	(0) 1.53	(0) 1.56*b*
3126.79		2		31972.44	$b\ ^3H_5 - y\ ^3H_4^0$		
3126.215	15	150*R*	III *Er*	31978.32	$a\ ^5F_4 - z\ ^5G_4^0$	(0.69) 1.19pw_3 D?; nw_3 A?	(0.16, 0.32, 0.43, **0.64,**) 0.66, 0.82, 0.98, **1.14, 1.30,** 1.46, 1.62, 1.78
3125.282	30	600*R*	III *Er*	31987.87	$a\ ^5F_1 - z\ ^5G_2^0$	pw 3D?; nw_3 A?	
3125.01	2	20		31990.65	$b\ ^3P_2 - y\ ^3P_2^0$	(0?) 1.45	(0.23) 1.44*b*
3122.887	3	100	V *E*	32012.40	$a\ ^1H_5 - z\ ^1I_6^0$	(0) 0.93	(0) 0.93*b*
3121.138	10	80	IV *E*	32030.34	$a\ ^5F_5 - z\ ^5G_6^0$	(0.62) 1.21nw_3 C?	(0.60*s*) 1.22*b*
3120.726	3	50		32034.57	$b\ ^3D_3 - x\ ^3F_3^0$	(0) 1.05	(0) 1.06*b*
3119.32		4		32049.00	$c\ ^3P_2 - z\ ^3F_3^0$	(?) 0.75pw_1 D; nw_1 A	(0) 0.78*b*
3118.376	40	1000*R*	III *Er*	32058.71	$a\ ^5F_3 - z\ ^5G_4^0$	(0?) 0.86	(0) 0.85*s*
3116.78		40		32075.12	$b\ ^1F_3 - x\ ^1F_3^0$	(0) 0.97	(0.13) 0.97*b*
3116.11		2		32082.00	$b\ ^3D_1 - x\ ^3D_1^0$		
3116.02		3		32082.95	$b\ ^3D_2 - x\ ^3D_2^0$		
3115.16		2		32091.80	$c\ ^3P_1 - z\ ^3S_1^0$		
3113.560	4	100	V *E*	32108.29	$a\ ^1H_5 - y\ ^1H_5^0$	(0) 0.97	(0.04) 1.04*b*
3110.708	60	1500*R*	III *Er*	32137.73	$a\ ^5F_2 - z\ ^5G_3^0$	(0.36) 0.83, **1.28**	(**0,** 0.06, 0.12, 0.18) **0.96,** 1.02, 1.08, 1.14, 1.20, 1.26, 1.32
3110.07		3?		32144.3	$b\ ^3D_3 - x\ ^3D_3^0$		
3109.375	1	20		32151.51	$b\ ^1D_2 - y\ ^1D_2^0$	{(0) 1.29 (0) 0.96}	(0.02) 0.98*b*
3108.704	2	30	V *E*	32158.45	$b\ ^3G_4 - y\ ^3G_5^0$	(?) 1.70pw_2 D; nw_2 B	(**0,** 0.36, 0.72, 1.08) −0.05, 0.31, 0.67, 1.03, 1.39, 1.75, **2.11**
3106.829		3		32177.85	$b\ ^3D_1 - x\ ^3D_2^0$	(?) 1.60pw_2	(0) 1.62*s*
3105.973		5		32186.72	$b\ ^3D_2 - z\ ^1P_1^0$	(0?) 1.45pw_2 D; nw_1 B	(0) 1.42*b*
3105.39		5*H*		32192.76		(0) 1.21	
3104.906	2	25	V *E*	32197.78	$b\ ^3G_3 - y\ ^3G_3^0$	(0) 1.34nw	(0) 1.44*b*
3102.295	80	2000*R*	III *Er*	32224.88	$a\ ^5F_4 - z\ ^5G_5^0$	(?)0.65, 1.43	(**0,** 0.14, 0.28, 0.42, 0.56) **0.60,** 0.74, 0.88, 1.02, 1.16, 1.30, 1.44, 1.58, 1.72
3100.938	8	100	V *E*	32238.98	$b\ ^3G_3 - y\ ^3G_4^0$	(0) 0.71	(0.23) 0.72*b*
3094.196	8	100	V *E*	32309.22	$b\ ^3G_4 - y\ ^3G_5^0$	(0) 0.99	(0.03) 1.02*b*
3093.108[k]	100	2500*R*	III *Er*	32320.59	$a\ ^5F_3 - z\ ^5G_4^0$	(0.50) **0.62,** 1.54, 2.44	
3089.633		4		32356.94	$c\ ^3P_2 - x\ ^3D_3^0$	(0.45) 1.31 nw_1	(0.47) 1.23*b*
3086.507	2	30	V *E*	32389.71	$b\ ^3G_3 - y\ ^3G_4^0$	(?) 1.77pw_2 D; nw_2 B	(0) 1.80*s*
3086.210	1−	10		32392.82	$a\ ^3D_1 - y\ ^3P_2^0$	(0) 0.54	(0) 0.49
3085.47		1		32400.59	$a\ ^3G_5 - z\ ^3H_6^0$		
3083.208	1	40	V *E*	32424.36	$c\ ^3P_2 - x\ ^3D_2^0$	(0) 1.15	(0) 1.16*b*
3082.524	2	40	V *E*	32431.56	$b\ ^3G_4 - y\ ^3G_4^0$	(0?) 1.55pw_1 D; nw_1 B	(0) 1.60*b*
3081.30	1−	10		32444.44	$a\ ^1P_1 - x\ ^1P_1^0$		
3081.254	1	25	V *E*	32444.92	$a\ ^3D_3 - y\ ^3P_2^0$	(0?) 1.02pw_1 ?	(0) 1.00*b*
3081.01	1	20		32447.49	$c\ ^3P_0 - x\ ^3D_1^0$	(0) 0.71	(0) 0.63
3079.75		1		32460.77	$c\ ^3P_2 - z\ ^1P_1^0$		
3078.948		5		32469.23	$a\ ^3D_1 - y\ ^3P_1^0$	(0.90) **0.46,1.37**	(0.90) **0.49,1.39**
3076.016[d]		25		32500.17	$a\ ^5G_4 - z\ ^3H_5^0$	(0.85) 1.02nw_2	(0.22, 0.44, 0.66, **0.88**) 0.12, 0.34, 0.56, **0.78,1.00** 1.22, 1.44, 1.66
3075.58		5		32504.78	$d\ ^3P_1 - v\ ^3D_2^0$	(0) 0.79	(0) 0.79*b*

See footnotes at end of table.

TABLE 1.—*Second spectrum of Vanadium*—Continued

1	2		3	4	5	6	
λ_{air}A	Intensity		Temp. class	Wave No. vac	Term combination	Zeeman effect	
	Arc	Spark				Observed	Computed
3075.474		2		32505.90	$a\ ^3D_1 - y\ ^3D^\circ_2$		
3075.043		3		32510.45	$d\ ^3P_0 - v\ ^3D^\circ_1$	(0) 0.46	(0) 0.46:
3074.66		12		32514.50	$c\ ^3P_1 - x\ ^3D^\circ_1$	(0.71) **0.59, 1.36**	(0.72) **0.63, 1.35**
3071.77		2*h*		32545.09	$c\ ^3D_3 - u\ ^3F^\circ_4$		
3070.12		25*l*		32562.58	$d\ ^3P_2 - v\ ^3D^\circ_2$	(0) 1.07nw_1	(0) 1.06*b*
3067.104	10	200	IV *E*	32594.60	$a\ ^3G_3 - z\ ^3H^\circ_4$	(0) 0.83	(0) 0.84*b*
3066.80		4		32597.83	$b\ ^3H_5 - z\ ^3I^\circ_5$		
3065.61	1	50		32610.49	$c\ ^3P_1 - x\ ^3D^\circ_2$	(0) 0.96	(0) 0.98*b*
3063.247	8	200	V *E*	32635.64	$b\ ^3H_4 - z\ ^3I^\circ_5$	(0) 0.87	(0) 0.88*b*
3062.702	2	20	V *E*	32641.45	$a\ ^3G_5 - z\ ^3H^\circ_5$	(0.67) 0.99nw_2 C	(0.65) 1.09*b*
3062.178		3		32647.03	$c\ ^3P_0 - z\ ^1P^\circ_1$	(0) 0.86	(0) 0.92
3057.08		2		32701.47	$a\ ^1S_0 - x\ ^3D^\circ_1$	(0) 0.61	(0) 0.63
3055.942		7		32713.65	$b\ ^3H_6 - z\ ^3I^\circ_6$	(0.76) 1.05nw_3 C	(0.78) 1.06*b*
3054.24		7*h*		32731.88	$a\ ^3D_3 - y\ ^3D^\circ_3$	(0) 1.22nw_1 A	(0.08) 1.28*b*
3053.894	3	80	V *E*	32735.59	$b\ ^3G_3 - y\ ^3F^\circ_4$	(0) 1.12	(0) 1.12*b*
3053.39	6	200	V *E*	32740.99	$a\ ^3G_4 - z\ ^3H^\circ_5$	(0) 0.93	(0) 1.01*b*
3051.308		3		32763.33	$d\ ^3P_2 - v\ ^3D^\circ_3$		
3050.735		15		32769.48	$a\ ^3D_3 - y\ ^3P^\circ_2$	(0) 1.13	(0) 1.09*b*
3048.891	3	70	V *E*	32789.30	$b\ ^3G_4 - y\ ^3F^\circ_3$	(0) 1.02	(0) 1.09*b*
3048.65		4		32791.89	$a\ ^3D_2 - y\ ^3D^\circ_2$		
3048.214	6	200	V *E*	32796.59	$b\ ^3H_5 - z\ ^3I^\circ_6$	(0) 0.96	(0) 0.90*b*
3043.54	?	40+I		32846.95	$b\ ^3G_4 - y\ ^3F^\circ_4$	(0.54) 1.14 pw_3 B; nw_3 C	(0.50) 1.11*b*
3042.27	3	80	IV *E*	32860.66	$b\ ^3G_3 - y\ ^3F^\circ_2$	(0) 0.77	(0) 0.89*b*
3041.42	2	60	V *E*	32869.84	$b\ ^3G_3 - y\ ^3F^\circ_3$	(?) 0.93, 2*p*; nw_2 C	(0.59) 0.88*b*
3039.767		2		32887.72	$a\ ^1D_2 - w\ ^3D^\circ_2$	(0) 1.13	(0.14) 1.06*b*
3038.520	1	30		32901.21	$a\ ^1S_0 - z\ ^1P^\circ_1$	(0) 0.87	(0) 0.92
3038.00		2*H*?		32906.84	$z\ ^3F^\circ_4 - e\ ^5P_3$		
3036.07		2		32927.76	$b\ ^3G_3 - y\ ^3F^\circ_2$		
3035.14		3*H*		32937.85	$z\ ^3G^\circ_5 - e\ ^5H_4$		
3034.41		4*H*		32945.78			
3033.821	8	300	V *E*	32952.17	$a\ ^3G_5 - z\ ^3H^\circ_6$	(0) 0.98	(0) 1.03*b*
3033.445	6	200	V *E*	32956.25	$b\ ^3H_6 - z\ ^3I^\circ_7$	(0) 1.02	(0) 1.02*b*
3032.187		3		32969.93	$b\ ^1G_4 - y\ ^3H^\circ_4$		
3029.56		7		32998.52	$a\ ^3P_2 - z\ ^3P^\circ_2$	(0) 1.72	(0) 1.76*b*
3028.042	1	50		33015.05	$b\ ^3P_1 - z\ ^3S^\circ_1$	(0.49) **1.35, 2.10**	(0.45) **1.40, 1.85**
3027.600	1−	15		33019.88	$b\ ^3P_0 - z\ ^3S^\circ_1$	(0) 1.85	(0) 1.85
3025.68		1		33040.83	$b\ ^1G_4 - y\ ^3H^\circ_5$		
3024.981	1	50		33048.46	$b\ ^3P_2 - z\ ^3S^\circ_1$	(?) **0.94,** 1.39, 1.89	(0, 0.47) **0.91,** 1.38 1.85
3023.882	1	20		33060.47	$b\ ^3G_3 - z\ ^1H^\circ_4$	(0.82) 1.00nw_2	(0.86) 1.06*b*
3022.57	2	40		33074.82	$a\ ^3P_1 - z\ ^3P^\circ_2$	(0) 2.35	(0) 2.39
3022.146		4		33079.46	$b\ ^3P_1 - x\ ^3F^\circ_2$		
3020.65		6		33095.85	$a\ ^5P_2 - z\ ^5P^\circ_1$		
3020.25		7*Hl*		33100.23			
3019.09		3		33112.95	$b\ ^3P_2 - x\ ^3F^\circ_2$		
3018.96		3*h*		33114.37			
3016.775	6	120	V *E*	33138.35	$a\ ^5P_3 - z\ ^5P^\circ_2$	(?) 1.41	(0) 1.50*s*
3016.14		15		33145.33	$a\ ^5P_2 - z\ ^5P^\circ_2$		
3015.98		10		33147.09	$b\ ^3G_4 - z\ ^1F^\circ_3$		
3014.822	5	100	V *E*	33159.82	$a\ ^5P_2 - z\ ^5P^\circ_1$	(?) **1.03,** 1.71, 2.32	(0, 0.50) **1.28,** 1.78 2.28
3013.102	3	80	V *E*	33178.75	$a\ ^5P_1 - z\ ^5P^\circ_1$	(?) 1.43, 2.35	(0.95) **1.44, 2.39**
3012.020	1	30		33190.67	$b\ ^3G_3 - z\ ^1G^\circ_4$	(?) 1.57nw_2 B	(0) 1.56*b*
3011.258		1		33199.07			
3008.610	2	70	V *E*	33228.28	$a\ ^5P_1 - z\ ^5P^\circ_2$	(?) **0.49,** 1.39, 2.31	(0, 0.91) **0.57,** 1.48, 2.39
3008.508		15		33229.41	$b\ ^3D_1 - w\ ^3D^\circ_1$		
3007.296	1	15		33242.80	$a\ ^5P_1 - z\ ^5P^\circ_1$	(?) 2.30	(0.11) 2.34*b*
3007.035		1		33245.69	$b\ ^3D_2 - w\ ^3D^\circ_2$		
3006.502		20		33251.58	$b\ ^3D_2 - w\ ^3D^\circ_3$	(?) 1.13	(0.27) 1.18*b*
3005.813		30		33259.20	$b\ ^5P_3 - x\ ^5F^\circ_4$	(?) 0.45nw_3 A	(0) 0.45*s*
3003.461	3	80	V *E*	33285.25	$a\ ^5P_3 - z\ ^5P^\circ_2$	(?) 1.69	(0.18) 1.73*b*
1001.93		2		33302.22	$b\ ^3G_4 - z\ ^1G^\circ_4$	(?) 0.96	(0.23) 1.00*b*

See footnotes at end of table.

TABLE 1.—*Second spectrum of Vanadium*—Continued

1	2		3	4	5	6	
λ_{air}A	Intensity		Temp. class	Wave No. vac	Term combination	Zeeman effect	
	Arc	Spark				Observed	Computed
3001.754	1	30		33304.17	$b\ ^3D-w\ ^3D_3^1$	(?) 1.09	(0.28) 1.32*b*
3001.203	8	200	V *E*	33310.29	$a\ ^5P_3-z\ ^5P_2^1$	(?) 1.56	(0.18) 1.68*b*
2997.945		6		33346.49	$b\ ^3D_1-w\ ^3D_2^1$		
2996.70		3		33360.34	$a\ ^5P_3-u\ ^5D_4^1$		
2995.999	3	60	IV *E*	33368.15	$a\ ^5P_1-z\ ^5P_2^1$	(?) **0.96**, 1.69, 2.33	(**0**, 0.71) **0.97**, 1.68, 2.39
2994.540		60		33384.40	$d\ ^3F_3-w\ ^3G_3^1$	(?) 0.77	(0) 0.77*b*
2994.05		1		33389.86	$a\ ^1P_1-y\ ^3S_1^1$		
2992.99		4		33401.69			
2992.378		2		33408.52	$c\ ^3P_2-w\ ^3D_3^1$		
2991.737		3		33415.68	$d\ ^3F_2-w\ ^3G_3^1$		
2989.74		10		33438.00	$b\ ^3P_1-x\ ^3D_1^1$		
2989.594	2	40	V *E*	33439.63	$a\ ^5P_3-y\ ^5D_3^1$	(?) 1.55*nw*; B?	(0.36) 1.55*b*
2989.306	1	15		33442.85	$b\ ^3P_0-x\ ^3D_1^1$		
2988.027	3	80	V *E*	33457.17	$a\ ^5P_2-z\ ^5P_3^1$	(?) 1.38*nw*;	(0) 1.32*b*
2985.93		1		33480.66			
2985.184		60*h*		33489.03	$d\ ^3F_2-w\ ^3G_3^1$	(?) 0.96	(0) 0.98*b*
2983.558		80*h*		33507.28	$a\ ^5P_3-y\ ^5D_3^1$		
2983.009		10		33513.45	$b\ ^3F_3-z\ ^3H_4^1$ $a\ ^5P_2-y\ ^5D_1^1$		
2982.75	2	40		33516.36	$a\ ^5P_1-y\ ^5D_0^1$	(?) 2.35	(0) 2.39
2981.924		15		33525.64	$c\ ^3P_2-w\ ^3D_2^1$	(?) 1.18*nw*;	(0.47) 1.23*b*
2981.200	2	70	V *E*	33533.78	$b\ ^3P_1-x\ ^3D_2^1$	(?) 0.72, 1.40*nw*; A	(**0**, 0.30) **0.80**, 1.10, 1.40
2979.47		4*hl*		33553.25			
2979.102		5		33557.40	$b\ ^3G_3-z\ ^1D_2^1$		
2978.226	1	20		33567.27	$b\ ^3P_2-x\ ^3D_3^1$	(?) 1.22*nw*;	(0.50) 1.24*b*
2976.517	10	100	IV *E*	33586.54	$a\ ^5P_2-y\ ^5D_2^1$		
2976.197	4	60	V *E*	33590.15	$a\ ^5P_1-y\ ^5D_2^1$		
2975.650	3	50	V *E*	33596.32	$a\ ^5P_1-y\ ^5D_1^1$		
2973.975		40		33615.24	$d\ ^3F_4-w\ ^3G_4^1$		
2972.263	3	80	V *E*	33634.61	$b\ ^3P_2-x\ ^3D_2^1$		
2971.998		4		33637.61	$b\ ^3P_1-z\ ^1P_1^1$		
2971.571		8		33642.44	$b\ ^3P_0-z\ ^1P_1^1$		
2970.427		6		33655.40			
2969.846		5		33661.98	$c\ ^3P_1-w\ ^3D_1^1$		
2968.373	20	200	V *E*	33678.68	$a\ ^5P_3-y\ ^5D_4^1$	(0, 0.67, 1.27, 2.00)—?	(**0**, 0.66, 1.32, 1.98) 0.30, 0.96, 1.62, 2.28, 2.94, 3.60, **4.26**
2968.02		7*H*		33682.69			
2967.545		5		33688.08	$b\ ^3F_4-z\ ^3H_5^1$		
2963.86		4*Hl*		33729.96			
2963.249		9		33736.91	$a\ ^1D_2-x\ ^3P_1^1$		
2962.014		5		33750.98	$c\ ^3F_3-w\ ^3G_3^1$		
2960.777		6		33765.08	$b\ ^1G_4-z\ ^3I_5^1$		
2959.55		1		33779.08	$c\ ^3P_1-w\ ^3D_2^1$		
2958.61		20		33789.81	$c\ ^3F_2-w\ ^3G_3^1$		
2957.520	8	100		33802.27	$a\ ^5F_5-z\ ^5F_4^1$		
2956.645		2		33812.27	$c\ ^3F_4-w\ ^3G_4^1$		
2955.584		30		33824.39	$c\ ^3F_3-w\ ^3G_4^1$		
2953.45		1		33848.84	$a\ ^1S_0-w\ ^3D_1^1$		
2952.07	15	150	IV *Er*	33864.67	$a\ ^5F_3-z\ ^5F_3^1$		
2951.56		8*h*		33870.52			
2950.344	8	80	V *E*	33884.48	$a\ ^5F_1-z\ ^5F_1^1$		
2949.172	1	40	V *E*	33897.94	$a\ ^1P_1-y\ ^1P_1^1$		
2948.83		2		33901.87	$b\ ^3H_4-y\ ^1G_4^1$		
2948.076	1	60		33910.54	$c\ ^3F_4-w\ ^3G_5^1$		
2944.568	15	250	IV *Er*	33950.94	$a\ ^5F_4-z\ ^5F_5^1$		
2943.631		3		33961.75	$d\ ^3F_3-v\ ^3D_3^1$		
2942.37	3	15		33976.30	$a\ ^3D_1-x\ ^3F_2^1$		
2941.485	6	100	IV *E*	33986.52	$a\ ^5F_2-z\ ^5F_2^1$		
2941.372	10	200	IV *E*	33987.83	$a\ ^5F_5-z\ ^5F_5^1$		
2938.259	1	20		34023.84	$a\ ^3G_4-y\ ^3G_4^1$		
2937.030	1	15		34038.07	$a\ ^3D_3-x\ ^3F_3^1$		
2934.394	6	60	V *E*	34068.65	$a\ ^5F_1-z\ ^5F_2^1$		

See footnotes at end of table.

TABLE 1.—*Second spectrum of Vanadium*—Continued

1	2		3	4	5	6	
λ_{air}A	Intensity		Temp. class	Wave No. vac	Term combination	Zeeman effect	
	Arc	Spark				Observed	Computed
2933.833	1	15	V *E*	34075.16	$a\ ^3G_4 - y\ ^3G^\circ_4$		
2932.323	3	60	V *E*	34092.71	$b\ ^3D_3 - x\ ^3P^\circ_2$		
2931.859	1	10		34098.10	$a\ ^3D_2 - x\ ^3F^\circ_3$		
2931.624	1	20		34100.84	$b\ ^3D_3 - x\ ^3P^\circ_1$		
2930.798	10	150	IV *Er*	34110.45	$a\ ^3F_3 - z\ ^3F^\circ_3$		
2930.132	1	25	V *E*	34118.20	$a\ ^3G_3 - y\ ^3G^\circ_3$		
2929.017		4		34131.19	$d\ ^3F_2 - v\ ^3D^\circ_2$		
2926.442	2	40		34161.23	$a\ ^1D_2 - y\ ^1F^\circ_3$		
2926.35		10h		34162.29	$d\ ^3F_2 - v\ ^3D^\circ_3$		
2925.51		3h		34172.10	$a\ ^1G_4 - y\ ^3H^\circ_4$		
2925.288	1	15	V *E*	34174.69	$a\ ^3G_4 - y\ ^3G^\circ_5$		
2924.633	30	250*R*	IV *Er*	34182.35	$a\ ^5F_4 - z\ ^5F^\circ_5$		
2924.017	40	300*R*	IV *Er*	34189.55	$a\ ^5F_5 - z\ ^5F^\circ_5$		
2923.340	1	20		34197.46	$a\ ^3G_5 - y\ ^3G^\circ_5$		
2920.377	10	100	IV *E*	34232.16	$a\ ^3F_2 - z\ ^5F^\circ_1$ $a\ ^5F_3 - z\ ^5D^\circ_2$		
2919.989	6	50		34236.71	$a\ ^5F_4 - z\ ^5D^\circ_3$		
2919.681		6h		34240.32			
2918.21		15h		34257.58	$d\ ^3F_2 - v\ ^3D^\circ_1$		
2917.365	4	50	V *E*	34267.50	$a\ ^5F_3 - z\ ^3D^\circ_1$		
2917.230	1	7		34269.09	$a\ ^3G_3 - y\ ^3G_4$		
2915.875		40		34285.01	$c\ ^3F_4 - v\ ^3D^\circ_3$		
2915.330	5	30		34291.42	$b\ ^3D_1 - x\ ^3P^\circ_0$		
2914.87	?	10+I		34296.83	$a\ ^3G_4 - y\ ^3G^\circ_4$		
2914.208	2	40		34303.56	$a\ ^3D_3 - x\ ^3F^\circ_4$		
2913.716		2		34310.41	$a\ ^3D_3 - x\ ^3D^\circ_3$		
2913.04		3		34318.38			
2912.50		10*Hl*		34324.74			
2911.654		7		34334.71	$a\ ^3D_1 - x\ ^3D^\circ_1$		
2911.050	15	160*r*		34341.83	$a\ ^5F_3 - z\ ^5F^\circ_4$		
2910.380	15	150*r*		34349.74	$a\ ^5F_1 - z\ ^3D^\circ_1$		
2910.007	15	140*r*	IV *Er*	34354.14	$a\ ^5F_2 - z\ ^5D^\circ_2$		
2908.810	30	300*R*	IV *Er*	34368.28	$a\ ^5F_5 - z\ ^5D^\circ_4$	(1.00)0.68	(0)0.64*s*
2908.44	2	20		34372.65	$c\ ^3P_2 - x\ ^3P^\circ_2$		
2907.457*l*	10	120	IV *E*	34384.27	$a\ ^5F_4 - z\ ^5F^\circ_4$	(?)2.53 pw_3D; nw_2	(0)1.60*b*
2906.448	15	150*r*	IV *Er*	34396.21	$a\ ^5F_3 - z\ ^3D^\circ_3$		
2905.609	1	15	V *E*	34406.14	$a\ ^3D_2 - x\ ^3D^\circ_3$		
2905.307		1		24409.72			
2904.985		15		34413.53	$a\ ^3D_3 - x\ ^3D^\circ_3$		
2903.548		3		34430.56	$a\ ^3D_1 - x\ ^3D^\circ_2$		
2903.068	10	100	V *E*	34436.25	$a\ ^3F_1 - z\ ^3D^\circ_1$		
2902.54		1		34442.52			
2899.936		4		34473.44	$a\ ^3D_2 - x\ ^3D^\circ_2$		
2897.899		20		34497.67	$c\ ^3F_3 - v\ ^3D^\circ_2$		
2896.870		2		34509.93	$a\ ^3D_2 - z\ ^1P^\circ_1$		
2896.198[1]	10	100	V *E*	34517.93	$a\ ^5F_2 - z\ ^3D^\circ_1$	(0?)?pw_3D;nw_1	(0)1.67*b*
2895.609		4		34524.96	$b\ ^3D_2 - y\ ^1F^\circ_3$		
2894.833		3		34534.21	$a\ ^3D_1 - v\ ^1P^\circ_1$		
2893.314	20	250	IV *Er*	34552.34	$a\ ^5F_4 - z\ ^5D^\circ_4$		
2892.650	15	200*r*	IV *Er*	34560.27	$a\ ^5F_3 - z\ ^5D^\circ_3$		
2892.434	10	150*r*	V *Er*	34562.85	$a\ ^5F_4 - z\ ^5D^\circ_1$		
2891.636	10	150*r*	IV *Er*	34572.39	$a\ ^5F_3 - z\ ^5D^\circ_1$	(0,0.69)?	(0,0.42)0.55,0.97, 1.39
2890.553		5		34585.34	$b\ ^3P_1 - w\ ^3D^\circ_1$		
2890.144	1	7		34590.24	$b\ ^3P_0 - w\ ^3D^\circ_1$		
2889.614	15	100	V *E*	34596.58	$a\ ^5F_1 - z\ ^5D^\circ_0$		
2888.244	5	80	V *E*	34612.99	$a\ ^3G_5 - y\ ^3F^\circ_4$		
2887.75		1		34618.91	$b\ ^3P_2 - w\ ^3D^\circ_1$		
2887.158		8		34626.01	$c\ ^3P_1 - x\ ^3P^\circ_2$		
2886.967	1	10		34628.30	$c\ ^3P_1 - x\ ^3P^\circ_1$		
2884.776	20	150	V *E*	34654.60	$a^5F_1 - z\ ^5D^\circ_1$ $a\ ^3G_4 - y\ ^3F^\circ_3$	(0) 0.64	— (0) 1.02*b*
2884.064		6		34663.15	$c\ ^3F_3 - v\ ^3D^\circ_2$		

See footnotes at end of table.

TABLE 1.—*Second spectrum of Vanadium*—Continued

1	2		3	4	5	6	
λ_{air}A	Intensity		Temp. class	Wave No. vac	Term combination	Zeeman effect	
	Arc	Spark				Observed	Computed
2882.493	15	120	V *E*	34682.04	$a\ ^5F_3-z\ ^5D^0_4$		
2880.802	1	15		34702.40	$b\ ^3P_1-w\ ^3D^0_2$	(0) 1.53	(0) 0.95*b*
2880.026	10	150	V *E*	34711.75	$a\ ^5F_3-z\ ^5D^0_3$		
2879.158	6	40	V *E*	34722.22	$a\ ^5F_3-z\ ^5D^0_2$		
2879.013		2		34723.96	$c\ ^3P_1-x\ ^3P^0_0$	(0) 0.68	(0) 1.35
2878.299		3		34732.58	$b\ ^3D_3-x\ ^3G^0_4$		
2878.028	1	7		34735.84	$b\ ^3P_2-w\ ^3D^0_3$		
2877.689	4	60		34739.94	$a\ ^3G_3-y\ ^3F^0_3$		
2876.939	1	9		34749.00	$a\ ^3G_3-y\ ^3F^0_2$		
2875.687	3	30	V *E*	34764.12	$a\ ^3F_4-z\ ^5D^0_4$		
2874.205		5		34782.04	$a\ ^3P_2-z\ ^3P^0_1$		
2873.180	1	30		34794.45	$b\ ^3P_2-w\ ^3D^0_3$		
2872.806		1		34798.99	$c\ ^3P_2-y\ ^1F^0_3$		
2871.543		3		34814.29	$b\ ^1G_4-w\ ^3D^0_3$		
2871.463		4		34815.26	$a\ ^1S_0-x\ ^3P^0_1$		
2870.111	1	9		34831.66	$a\ ^3P_2-z\ ^3P^0_2$		
2869.957	1	10		34833.52	$a\ ^5F_2-z\ ^5D^0_2$		
2869.131	4	150		34843.56	$b\ ^3H_6-x\ ^3G^0_5$		
2864.517	1	30		34899.68	$b\ ^3H_4-y\ ^1F^0_3$		
2863.79		2*H*		34908.54			
2862.91		1*h*		34919.27			
2862.310		20		34926.58	$b\ ^3H_5-x\ ^3G^0_4$		
2861.401		5		34937.68	$a\ ^3G_5-z\ ^1H^0_5$		
2857.44		1		34986.11	$a\ ^3H_5-z\ ^3H^0_4$		
2855.298	1	40		35012.35	$a\ ^3G_4-z\ ^1F^0_3$		
2854.335	4	120	V *E*	35024.16	$b\ ^3H_5-x\ ^3G^0_4$	(0) 1.06	(0) 0.99*b*
2853.761		4		35031.21	$b\ ^1G_4-y\ ^1G^0_4$		
2852.540	1	30		35046.20	$b\ ^3D_3-y\ ^3S^0_1$		
2851.260		15		35061.94	$b\ ^3H_4-x\ ^3G^0_4$		
2850.765	1	20	V	35068.02	$a\ ^3G_5-z\ ^1G^0_4$		
2850.685	1	25		35069.01	$a\ ^1P_1-y\ ^1D^0_2$		
2850.477		1		35071.57	$a\ ^3P_1-z\ ^3P^0_0$		
2849.055	2	40		35089.07	$b\ ^3F_3-y\ ^3G^0_3$		
2847.573	3	100	V	35107.33	$b\ ^3H_4-x\ ^3G^0_3$		
2846.29		1		35123.16	$b\ ^3H_5-z\ ^1I^0_6$		
2845.241	2	50	V	35136.10	$b\ ^3H_6-y\ ^1H^0_5$		
2844.833		3		35141.14	$b\ ^3D_1-y\ ^3S^0_1$		
2844.22		4*Hl*		35148.72	$z\ ^5D^0_4-e\ ^5P_1$ $d\ ^3F_3-z\ ^1G^0_4$		
2843.82		9*Hl*		35153.66	$z\ ^5D^0_3-e\ ^5P_2$		
2842.699	1	4		35167.52	$a\ ^3G_4-z\ ^1G^0_4$		
2842.287		6*Hl*		35172.62			
2842.043		2		35175.64	$a\ ^3P_1-z\ ^3P^0_1$		
2841.039	3	50	V *E*	35188.07	$b\ ^3F_3-y\ ^3G^0_4$		
2840.825		3		35190.72	$a\ ^1D_2-y\ ^1P^0_1$		
2840.593		6		35193.59	$a\ ^3P_2-y\ ^5D^0_3$		
2840.10		10		35199.70	$a\ ^3P_2-y\ ^5D^0_4$		
2838.531		4		35219.16	$b\ ^5H_3-y\ ^1H^0_4$		
2838.053	4	10		35225.09	$a\ ^3P_1-z\ ^3P^0_2$		
2836.527	4	80	V *E*	35244.03	$b\ ^3F_4-y\ ^3G^0_4$		
2835.47		4		35257.18	$b\ ^3H_4-y\ ^1H^0_4$		
2835.35		6*H*		35258.67	$z\ ^5D^0_4-e\ ^5P_1$ $z\ ^5D^0_4-e\ ^5D_3$?		
2834.55		30*Hl*		35268.62	$z\ ^5D^0_4-e\ ^5D_4$?		
2831.60		10*H*		35305.36	$z\ ^5D^0_3-e\ ^5P_3$		
2830.97		3*Hl*		35313.22	$z\ ^5D^0_3-e\ ^5D_3$?		
2830.70		3*Hl*		35316.58	$z\ ^5D^0_2-e\ ^5P_1$		
2830.402	1	40		35320.30	$c\ ^3P^0_1-y\ ^3S^0_1$		
2826.89		5*Hl*		35364.18			
2825.86		50*Hl*		35377.07	$z\ ^5D^0_4-e\ ^5P_2$		
2825.02		5*Hl*		35387.59	$z\ ^5D^0_3-e\ ^5P_2$		
2824.444		4		35394.81	$a\ ^3P^0-z\ ^3P^0_1$		

See footnotes at end of table.

TABLE 1.—*Second spectrum of Vanadium*—Continued

1	2		3	4	5	6	
λ_{air}A	Intensity		Temp. class	Wave No. vac	Term combination	Zeeman effect	
	Arc	Spark				Observed	Computed
2822.44		80*Hl*		35419.93	$z\,^5D_4^1-e\,^5D_4$?		
2822.15		20*Hl*		35423.58			
2821.124	1	15		35436.46	$a\,^3G_3-z\,^1D_2^1$		
2819.444	1	20		35457.57	$a\,^3D_3-w\,^3D_2^1$		
2818.52		5*Hl*		35469.19	$z\,^3D_2^1-e\,^3P_2$		
2817.506	2	60	V *E*	35481.96	$a\,^3D_1-w\,^3D_1^1$		
2815.547		3		35506.64	$c\,^3P_0-y\,^3S_1^1$		
2815.032		5		35513.14	$a\,^3P_1-y\,^3D_0^1$		
2814.903	1	15		35514.77	$a\,^3D_2-w\,^3D_2^1$		
2812.71		3*H*		35542.46			
2812.164		6		35549.36	$b\,^3P_1-x\,^3P_2^1$		
2811.982		5		35551.66	$b\,^3P_1-x\,^3P_1^1$		
2811.597		7		35556.52	$b\,^3P_0-x\,^3P_1^1$		
2810.272	5	100	V *E*	35573.29	$a\,^3D_3-w\,^3D_3^1$		
2810.158	3	60		35574.73	$a\,^3D_3-w\,^3D_2^1$		
2809.513	1	15		35582.90	$b\,^3P_2-x\,^3P_2^1$		
2809.184		1		35587.06	$a\,^3P_1-y\,^3D_2^1$ $d\,^3F_3-y\,^3G_3^1$?		
2808.701		4		35593.18	$a\,^3P_1-y\,^3D_1^1$		
2808.237		25		35599.06	$a\,^3D_1-w\,^3D_2^1$		
2808.023		4		35601.78	$b\,^3F_4-y\,^3F_3^1$		
2806.79		3*H*		35617.42	$c\,^3F_3-x\,^3D_3^1$		
2806.544		4		35620.54	$b\,^3G_4-y\,^3H_4^1$		
2805.544	1	30		35633.24	$a\,^3D_1-w\,^3D_2^1$		
2804.443		4		35647.23	$b\,^3P_1-x\,^3P_2^1$		
2803.469	5	150	V *E*	35659.61	$b\,^3F_4-y\,^3F_4^1$		
2802.796	3	100	V *E*	35668.17	$b\,^3F_3-y\,^3F_3^1$		
2800.95		20*Hl*		35691.68	$z\,^5D_1^1-e\,^5F_2$		
2800.05		4*Hl*		35703.15	$z\,^3D_1^1-e\,^3P_2$		
2799.451	5	100	V *E*	35710.79	$b\,^3F_2-y\,^3F_2^1$		
2798.755	4	80	V *E*	35719.67	$b\,^3G_5-y\,^3H_4^1$		
2797.795	3	70		35731.92	$b\,^3G_4-y\,^3H_3^1$		
2797.017	3	60	V *E*	35741.86	$b\,^3G_3-y\,^3H_3^1$		
2795.72		4*H*		35758.44	$z\,^5D_1^1-e\,^5G_2$		
2795.39		3*H*		35762.66	$z\,^5F_1^1-e\,^5D_1$? $z\,^5D_1^1-e\,^5F_1$?		
2794.83		15*H*		35769.83			
2794.29		5*H*		35776.74	$z\,^5D_2^1-e\,^5G_3$		
2792.45		6*Hl*		35800.31	$z\,^5D_1^1-e\,^5F_1$?		
2791.63		10*H*		35810.83			
2791.50	1	7		35812.50	$a\,^3P_0-y\,^5D_1^1$		
2788.66		3*H*		35848.96			
2787.95		20*h*		35858.09			
2787.32		2*h*		35866.20			
2787.00		10*H*		35870.32	$z\,^5F_1^1-e\,^5F_4$ $z\,^5F_1^1-e\,^5D_3$?		
2785.83		5*H*		35885.38	$z\,^5D_1^1-e\,^5G_2$		
2784.25		60*H*		35905.74			
2783.94		30*H*		35909.74			
2782.95		6*H*		35922.52	$c\,^3F_3-y\,^5G_3^1$? $a\,^1F_3-1_3^1$		
2782.56		5*H*		35927.55			
2781.48		100*H*		35941.50	$z\,^5F_1^1-e\,^5F_3$?		
2780.09		5+*H*		35959.47	$b\,^3F_4-z\,^1F_3^1$		
2778.60		80*H*		35978.75			
2778.16		2		35984.45	$b\,^3F_4-z\,^1H_5^1$		
2777.748	8	80		35989.78	$a\,^3P_2-z\,^3S_1^1$		
2776.24*		6*H*		36009.33	$b\,^3P_2-y\,^1F_3^1$		
2775.770	2	70	V	36015.43	$a\,^1I_6-x\,^3G_5^1$		
2774.976	2	30		36025.74	$b\,^3F_3-z\,^1F_3^1$		
2774.718	2	60		36029.08	$b\,^1G_4-y\,^1F_3^1$		
2774.28	5	100	V *E*	36034.77	$a\,^3H_4-y\,^3G_3^1$		
2772.01		60*Hl*		36064.28	$z\,^5F_1^1-e\,^5G_2$		
2771.41		40*Hl*		36072.09	$z\,^5F_1^1-e\,^5F_4$		

See footnotes at end of table.

TABLE 1.—*Second spectrum of Vanadium*—Continued

1	2		3	4	5	6	
λ_{air}A	Intensity		Temp. class	Wave No. vac	Term combination	Zeeman effect	
	Arc	Spark				Observed	Computed
2770.99		4		36077.55	$t\ {}^3F_3 - z\ {}^1F^0_3$		
2769.731		20		36093.95	$b\ {}^1G_4 - x\ {}^3G^0_3$		
2768.566	5	100	V *E*	36109.14	$a\ {}^3H_5 - y\ {}^3G^0_3$		
2768.150	2	15		36114.57	$b\ {}^3F_4 - z\ {}^1G^0_4$		
2767.10		30 *Hl*		36128.27	$z\ {}^3F^0_4 - e\ {}^5G_4$		
2766.460	4	60		36136.62	$a\ {}^5P_2 - z\ {}^5S^0_2$		
2765.576	6	150+*Hl*	V *E*	36146.87	$a\ {}^3H_6 - y\ {}^3G^0_5$ $z\ {}^5F^0_5 - e\ {}^5G_6$		
2764.28		4*Hl*		36165.12			
2762.714		3		36185.62	$a\ {}^3H_4 - y\ {}^3G^0_3$		
2762.52		3*H*		36188.16			
2761.34		3*H*		36203.63			
2760.710	3	60	V *E*	36211.89	$a\ {}^1I_6 - z\ {}^1I^0_6$		
2760.122	3	40	V *E*	36219.60	$a\ {}^3P_1 - z\ {}^3S^0_1$		
2759.60		15*Hl*		36226.45	$z\ {}^5F^0_5 - e\ {}^5G_5$		
2759.22		1		36231.44	$a\ {}^3H_5 - y\ {}^3G^0_5$		
2759.08		2		36233.28	$a\ {}^1G_4 - y\ {}^1G^0_4$		
2758.810		15		36236.83	$b\ {}^1G_4 - x\ {}^3G^0_3$		
2758.53		9*Hl*		36240.50	$b\ {}^3F_2 - z\ {}^3S^0_1$ $a\ {}^5F_3 - z\ {}^3G^0_4$		
2756.58		20*Hl*		36266.14	$z\ {}^5F^0_4 - e\ {}^5G_5$		
2756.38		4*h*		36268.77	$a\ {}^1S_0 - y\ {}^1P^0_1$		
2755.05		10*Hl*		36286.28			
2753.407	7	150	V *E*	36307.93	$a\ {}^1I_6 - y\ {}^1H^0_5$		
2752.11		15*Hl*		36325.04			
2751.79		10*Hl*		36329.26			
2750.20		8*Hl*		36349.08	$c\ {}^3F_4 - y\ {}^5G^0_5$? $d\ {}^3F_4 - y\ {}^5G^0_4$?		
2749.97		7*H*		36353.30	$z\ {}^5F^0_5 - e\ {}^5G_5$		
2749.48		8*H*		36359.78	$z\ {}^5F^0_4 - e\ {}^5G_4$		
2747.462	2	80		36386.49	$b\ {}^1G_4 - y\ {}^1H^0_5$		
2745.893	1	6		36407.28	$b\ {}^3F_3 - z\ {}^1D^0_2$		
2744.80		1*h*		36421.77	$a\ {}^3D_2 - x\ {}^3P^0_2$		
2744.54	1	4		36425.22	$a\ {}^3F_3 - z\ {}^3G^0_3$		
2743.768	3	20	V	36435.47	$a\ {}^3F_4 - z\ {}^3G^0_4$		
2742.670	6	30	V *E*	36450.06	$a\ {}^3F_3 - z\ {}^3G^0_3$		
2742.43	4	25	V *E*	36453.25	$a\ {}^5D_1 - z\ {}^5F^0_1$		
2741.563	1	4		36464.78	$a\ {}^5D_2 - z\ {}^5F^0_1$		
2740.98		7*Hl*		36472.53	$z\ {}^5F^0_5 - e\ {}^5G_5$		
2739.715	10	100	V *E*	36489.37	$a\ {}^5D_0 - z\ {}^5F^0_1$		
2739.18		8*Hl*		36496.50			
2736.69	1	10		36529.70	$a\ {}^3G_4 - y\ {}^3D^0_3$		
2736.12		4*H*		36537.31	$z\ {}^5F^0_4 - e\ {}^5G_3$		
2734.27		15*Hl*		36562.03			
2733.906	5	25	V *E*	36566.90	$a\ {}^5D_2 - z\ {}^5F^0_2$		
2733.00		5*Hl*		36579.02			
2732.92	1	5		36580.09	$a\ {}^5D_4 - z\ {}^5F^0_5$		
27232.17		10*Hl*		36590.13			
2731.12		4*H*		36604.20			
2730.60		2*h*		36611.17			
2729.64		1		36624.04	$a\ {}^3G_3 - y\ {}^3D^0_3$		
2728.644	20	150	V *E*	36637.41	$a\ {}^5D_1 - z\ {}^5F^0_2$		
2727.929	1	6		36647.02	$a\ {}^3H_5 - y\ {}^3F^0_4$		
2726.544*	1	40		36665.63	$a\ {}^3H_4 - y\ {}^3F^0_3$		
2724.61		5*H*		36691.65			
2724.40		2		36694.48			
2723.455		10		36707.22			
2723.218	5	20	V *E*	36710.41	$a\ {}^5D_1 - z\ {}^5F^0_1$		
2722.258		3		36723.35	$a\ {}^3H_4 - y\ {}^3F^0_4$		
2722.095		1		36725.55	$b\ {}^3D_2 - y\ {}^1D^0_2$		
2720.77		2		36743.44	$a\ {}^3P_1 - z\ {}^1S^0_0$		
2717.464		5		36788.13	$a\ {}^5D_3 - y\ {}^1F^0_3$		
2715.676	30*r*	180*rs*	V *E*	36812.35	$a\ {}^5D_2 - z\ {}^5F^0_3$ $a\ {}^5D_4 - z\ {}^5F^0_4$		

See footnotes at end of table.

TABLE 1.—*Second spectrum of Vanadium*—Continued

1	2		3	4	5	6	
λ_{air}A	Intensity		Temp. class	Wave No. vac	Term combination	Zeeman effect	
	Arc	Spark				Observed	Computed
2714.42		10*H*		36829.39			
2714.205	10	50	V *E*	36832.30	$a\ ^5D_3-z\ ^5D^\circ_4$		
2713.050	8	40	V *E*	36847.98	$a\ ^5D_2-z\ ^5D^\circ_1$		
2712.81		7*Hl*		36851.24			
2712.21		30*Hl*		36859.39			
2711.740	15	100	V *E*	36865.78	$a\ ^5D_4-z\ ^5D^\circ_3$		
2710.17	2	15		36887.14	$a\ ^3H_6-z\ ^1H^\circ_5$		
2709.10		6*H*		36901.70			
2708.91		1?		36904.29	$d\ ^3P_2-u\ ^3D^\circ_3$		
2707.86	10	100	V *E*	36918.60	$a\ ^5D_1-z\ ^5D^\circ_0$		
2706.70	20	150*r*	V *E*	36934.42	$a\ ^5D_2-z\ ^5D^\circ_2$		
2706.17	30	200*r*	V *Ers*	36941.66	$a\ ^5D_3-z\ ^5F^\circ_4$		
2705.220	7	40	V *E*	36954.63	$a\ ^5D_0-z\ ^5D^\circ_1$		
2703.15		3		36982.93	$b\ ^3F_2-y\ ^3D^\circ_3$		
2702.185	30	200*r*	V *E*	36996.13	$a\ ^5D_2-z\ ^5D^\circ_3$		
2701.535	4	10	V	37005.03	$a\ ^5D_1-z\ ^5D^\circ_2$		
2700.944	40	300*r*	V *Ers*	37013.13	$a\ ^5D_4-z\ ^5F^\circ_5$		
2700.20		1?		37023.33	$a\ ^3H_4-z\ ^1F^\circ_3$		
2699.63		4*Hl*		37031.14			
2697.201		10		37064.49	$d\ ^3F_3-v\ ^3F^\circ_4$		
2696.51		20*H*		37073.99			
2694.74*	2	20*H*		37098.34	$a\ ^5D_3-z\ ^3D^\circ_3$		
2694.65		10*H*		37099.58			
2694.47	1	5		37102.06	$a\ ^3H_5-z\ ^1G^\circ_4$		
2693.00	2	5*H*+I		37122.31			
2690.792	20	200	V *Ea*	37152.77	$a\ ^5D_3-z\ ^5D^\circ_4$		
2690.252	15	150	V *Ea*	37160.22	$a\ ^5D_3-z\ ^5D^\circ_3$		
2689.883	10	100	V *Ea*	37165.32	$a\ ^5D_1-z\ ^5D^\circ_0$		
2688.717	10	100	V *Ea*	37181.44	$a\ ^5D_4-z\ ^5D^\circ_4$		
2687.960	60*r*	300*r*	V *Ea*	37191.91	$a\ ^5D_4-z\ ^5D^\circ_3$		
2685.689	4	30		37223.36	$a\ ^5D_1-z\ ^5D^\circ_1$		
2685.41		1?		37227.22	$a\ ^5P_1-y\ ^5P^\circ_1$ $a\ ^5F_4-z\ ^5F^\circ_5$		
2685.138	10	20+*I*	V *E*	37230.99	$a\ ^1G_4-y\ ^1F^\circ_3$		
2684.78		15*H*		37235.96			
2683.09	15	100	V *Ea*	37259.41	$a\ ^5D_0-z\ ^5D^\circ_1$		
2682.875	15	100	V *Ea*	37262.40	$a\ ^5D_2-z\ ^5D^\circ_2$		
2682.535	1	6		37267.12	$a\ ^5F_5-z\ ^5F^\circ_4$		
2681.29		1		37284.42	$b\ ^3F_3-y\ ^3D^\circ_3$?		
2680.822		1		37290.93	$a\ ^1F_3-w\ ^3G^\circ_4$ $d\ ^3F_4-v\ ^3F^\circ_4$		
2680.470	1	8		37295.83	$a\ ^1G_4-x\ ^3G^\circ_4$	(0)1.64	(0)1.55*b*
2679.327	30	200*r*	V *Ea*	37311.74	$a\ ^5D_3-z\ ^5D^\circ_3$		
2678.572	10	100*r*		37322.25	$a\ ^5D_3-z\ ^5D^\circ_2$		
2677.804	25	150*r*	V *Ea*	37332.95	$a\ ^5D_1-z\ ^5D^\circ_2$		
2677.00		1		37344.17	$a\ ^5P_3-y\ ^5D^\circ_3$		
2676.33		7*H*		37353.52	$z\ ^5G^\circ_4-e\ ^5H_4$		
2676.05		9*H*		37357.42	$z\ ^5G^\circ_3-e\ ^5H_4$		
2675.17		2*h*		37369.71			
2674.28		3*h*		37382.15			
2673.955	1	4		37386.69	$a\ ^5F_3-z\ ^5F^\circ_3$		
2673.25	1	50*H*		37396.55			
2672.005	20	150*r*	V *Ea*	37413.97	$a\ ^5D_3-z\ ^5D^\circ_2$		
2670.237	2	40		37438.74	$a\ ^1G_4-x\ ^3G^\circ_3$		
2668.595		4		37461.78	$a\ ^5F_4-z\ ^5F^\circ_4$		
2668.01		10*H*		37469.99	$c\ ^3F_2-v\ ^3F^\circ_2$		
2667.532		4		37476.71	$b\ ^3F_4-y\ ^3D^\circ_3$		
2666.79		10*H*		37487.13	$z\ ^5G^\circ_5-e\ ^5H_5$		
2666.50		1		37491.21	$a\ ^5P_2-y\ ^5D^\circ_3$		
2665.490		2		37505.42	$d\ ^3F_3-v\ ^3F^\circ_3$		
2665.277		3		37508.41	$a\ ^5F_2-z\ ^5F^\circ_3$		
2663.837		2*h*		37528.69	$a\ ^5P_3-y\ ^5P^\circ_3$		

See footnotes at end of table.

TABLE 1.—*Second spectrum of Vanadium*—Continued

1	2		3	4	5	6	
λ_{air}A	Intensity		Temp. class	Wave No. vac	Term combination	Zeeman effect	
	Arc	Spark				Observed	Computed
2663.526		4*h*		37533.07	$d\ ^3F_4-y\ ^3F^0_4$		
2663.25	2*e*	250*H*		37536.96	$z\ ^5G^0_6-e\ ^5H_7$		
2661.47		30*H*		37562.06			
2661.243		3		37565.27			
2659.60	2	25		37588.47	$a\ ^1G_4-y\ ^1H^0_5$		
2658.97	3*d*	30		37597.37	$a\ ^3G_4-y\ ^3H^0_5$ $a\ ^3G_5-y\ ^3H^0_6$		
2658.49		7*HI*		37604.16	$z\ ^5G^0_4-e\ ^5H_4$		
2657.97		1		37611.52	$a\ ^1P_1-y\ ^3P^0_2$		
2657.295	1	10		37621.07	$a\ ^3G_3-y\ ^3H^0_4$		
2655.68	2*e*	200*H*		37643.95	$z\ ^5G^0_5-e\ ^5H_6$		
2654.89		2		37655.15			
2654.39		3*H*		37662.24			
2652.76		20*H*		37685.38			
2651.57		5*H*		37702.30	$z\ ^5G^0_3-e\ ^5H_3$		
2650.41		3*h*		37718.80			
2650.136		1		37722.70	$b\ ^3G_4-y\ ^1G^0_4$		
2649.37	1*e*	150*H*		37733.60	$z\ ^5G^0_4-e\ ^5H_5$		
2648.475	1	30		37746.35	$a\ ^1F_3-x\ ^1D^0_2$		
2646.225		2		37778.44			
2645.840	6	80		37783.94	$a\ ^3G_3-x\ ^3F^0_2$		
2644.363	1	100*HI*		37805.04	$z\ ^5G^0_3-e\ ^5H_4$		
2643.69		4*H*		37814.67		(0)0.48	
2643.11		2		37822.96	$a\ ^3P_2-z\ ^5S^0_2$		
2642.72		6		37828.55	$c\ ^3F_4-v\ ^3F^0_4$		
2642.212[1]	5	80		37835.82	$a\ ^3G_4-x\ ^3F^0_3$	$2p;nw_3$ A	
2640.86		80*H*		37855.19	$z\ ^5G^0_2-e\ ^5H_3$		
2639.29		2		37877.70	$a\ ^3D_3-y\ ^1P^0_1$		
2638.74		2		37885.60			
2638.52		7*H*		37888.76			
2637.886		2		37897.86	$a\ ^3F_3-z\ ^3P^0_2$		
2637.623		2*h*		37901.64			
2637.25		6*H*		37907.00			
2636.40		2*H*		37919.22			
2636.00		5*H*		37924.98	$z\ ^5G^0_2-e\ ^5P_1$		
2635.640	1	10		37930.16	$a\ ^3G_3-x\ ^3F^0_3$		
2635.43		7*H*		37933.18	$^5G^0_6-e\ ^5G_5$		
2634.37		3*H*		37948.44			
2633.91		3*H*		37955.07			
2633.28		2*H*?		37964.15	$a\ ^1F_3-v\ ^3D^0_2$		
2632.96		3*H*		37968.76			
2631.484		3		37990.06	$a\ ^3P_2-z\ ^1D^0_2$		
2630.665	10	150		38001.88	$a\ ^3G_3-x\ ^3F^0_4$	(?) 3?p; nw_2 B	(0) 1.15*b*
2629.72[i]		60*H*		38015.54	$z\ ^5G^0_3-e\ ^5G_4$	(0) nw_1	
2628.75[m]		30*H*		38029.56		(1.06) 1.83	
2628.09		4*H*		38039.11			
2627.32		1		38050.26	$a\ ^3F_2-z\ ^3P^0_1$		
2626.42		2*H*?		38063.30	$b\ ^1F_3-w\ ^1G^0_4$		
2625.01		4*H*?		38083.74			
2624.860		15*H*		38085.92	$z\ ^5G^0_2-e\ ^5G_4$		
2623.792	1	15+*H*		38101.42	$a\ ^3G_4-x\ ^3F^0_4$		
2622.74		50*H*		38116.71			
2621.80		40*H*		38130.37		(?) $0.92nw_1$ A	
2620.06[1]	2?	3		38155.69		(0) 2.29	
2619.48		5*H*		38164.14			
2618.63		1*h*?		38176.52	$b\ ^3P_1-y\ ^1D^0_2$		
2618.40		3*H*		38179.88			
2617.10		9*H*		38198.84	$z\ ^5G^0_4-e\ ^5G_3$		
2616.66		10*H*		38205.27	$z\ ^5G^0_3-e\ ^5D_4$?		
2616.24	3	40		38211.40	$a\ ^3G_4-x\ ^3D^0_3$		
2615.89		2		38216.51	$a\ ^3P_1-z\ ^3S^0_1$		

See footnotes at end of table.

TABLE 1.—*Second spectrum of Vanadium*—Continued

1	2		3	4	5	6	
λ_{air} A	Intensity		Temp. class	Wave No. vac	Term combination	Zeeman effect	
	Arc	Spark				Observed	Computed
2615.40[1]		40*H*		38223.67	$z\ ^5G^0_3 - e\ ^5G_3$	(0) 2.33	
2614.395	1	10		38238.36	$a\ ^3G_3 - x\ ^3D^0_3$		
2612.26		15*H*		38269.61			
2611.51		7*H*		38280.60	$z\ ^5G^0_2 - e\ ^5G_2$		
2611.24		10*H*		38284.56			
2610.61		30*H*		38293.80			
2609.80		5		38305.68	$a\ ^3G_3 - x\ ^3D^0_3$ $z\ ^5G^0_3 - e\ ^5G_3$		
2609.60		3		38308.62			
2608.66		1		38322.42	$a\ ^3F_4 - y\ ^3D^0_3$		
2608.00		20*H*		38332.12	$z\ ^5G^0_4 - e\ ^5G_4$		
2607.41		3*H*		38340.79			
2605.70		7*H*		38365.95			
2604.51		1		38383.48	$a\ ^3P_1 - z\ ^1D^0_2$		
2603.40		15*H*		38399.84	$z\ ^5G^0_3 - e\ ^5G_3$		
2602.94		15*H*		38406.63			
2602.32		6*H*		38415.78			
2601.08		25*H*		38434.09	$z\ ^5G^0_2 - e\ ^5G_2$		
2600.60		4*H*		38441.19			
2600.03		2*H*?		38449.61			
2598.65		2*H*		38470.03	$z\ ^5G^0_4 - e\ ^5G_5$		
2597.21[1,n]		6*h*		38491.36	$c\ ^3F_3 - u\ ^3D^0_2$ $c\ ^3F_3 - u\ ^3D^0_3$	(0)2.36	
2594.43		3*h*		38532.60	$z\ ^5G^0_3 - e\ ^5G_4$		
2593.91		2*H*		38540.32	$b\ ^3F_3 - y\ ^3H^0_4$		
2593.64		1?		38544.33	$b\ ^3F_4 - y\ ^3H^0_5$?		
2592.215		4		38565.52	$a\ ^3P_2 - y\ ^3D^0_1$		
2591.10		3*H*		38582.12			
2590.55		5*H*		38590.31			
2590.17		4*H*		38595.97			
2588.789		3*h*		38616.56			
2588.48		3*H*		38621.17			
2588.128		3		38626.42	$c\ ^3F_4 - u\ ^3D^0_2$		
2587.37		5*H*		38637.73			
2585.87	2	10+Fe		38660.15			
2584.951	3	80		38673.89	$b\ ^3G_3 - x\ ^3G^0_3$		
2583.58		2*H*		38694.41			
2583.007	2	20		38702.99	$b\ ^3F_3 - x\ ^3F^0_2$		
2581.839		4		38720.50	$b\ ^3G_4 - y\ ^1F^0_3$		
2578.451		8		38771.37	$b\ ^3G_5 - x\ ^3G^0_4$		
2577.682	3	40		38782.94	$b\ ^3F_4 - x\ ^3F^0_3$		
2577.528		3		38785.26	$a\ ^1H_5 - w\ ^3F^0_4$ $b\ ^3G_4 - x\ ^3G^0_5$		
2576.478[o]	1	20		38801.06	$b\ ^3G_3 - y\ ^1F^0_3$	(0.41)?	(0.46)0.85
2574.520	4	60		38830.57	$a\ ^3P_2 - y\ ^3P^0_1$		
2573.20		4*H*		38850.49			
2572.71		4*H*		38857.89			
2572.096		2		38867.16	$a\ ^3P_2 - y\ ^3D^0_2$		
2571.059	2	50		38882.84	$b\ ^3G_4 - x\ ^3G^0_4$		
2568.31		3		38924.45			
2568.065		3		38928.17	$b\ ^3G_4 - x\ ^3G^0_5$		
2567.45		15*H*		38937.49			
2566.602		15		38950.36	$a\ ^1F_3 - x\ ^1G^0_4$		
2566.033	1	7		38958.99	$a\ ^3P_1 - y\ ^3D^0_1$		
2565.743		2		38963.39	$b\ ^3G_3 - x\ ^3G^0_4$		
2565.543	1	15		38966.43	$b\ ^3G_5 - y\ ^1H^0_5$		
2565.24		3		38971.03	$d\ ^3F_2 - v\ ^3G^0_3$		
2562.760	1	30		39008.74	$b\ ^3G_3 - x\ ^3G^0_3$		
2561.65		2*h*		39025.65	$a\ ^5D_3 - z\ ^5G^0_3$ $a\ ^5P_3 - x\ ^5D^0_3$		
2560.149		4		39048.53	$b\ ^3F_4 - x\ ^3F^0_4$ $a\ ^3D_3 - y\ ^1D^0_2$		
2559.088		2		39064.71	$a\ ^5D_4 - z\ ^5G^0_4$		
2556.43		1		39105.33	$a\ ^5P_3 - x\ ^5D^0_3$		
2555.905	2	40		39113.36	$b\ ^3F_3 - x\ ^3D^0_3$		

See footnotes at end of table.

TABLE 1.—*Second spectrum of Vanadium*—Continued

1	2		3	4	5	6	
λ_{air}A	Intensity		Temp. class	Wave No. vac	Term combination	Zeeman effect	
	Arc	Spark				Observed	Computed
2554.22		15*H*		39139.16			
2554.06		10*H*		39141.61			
2553.668	4	40		39147.62	$a\ ^3P_1-y\ ^3P^0_0$		
2553.028	3	40		39157.43	$b\ ^3F_3-x\ ^3D^0_3$		
2552.960	4	60		39158.48	$b\ ^3F_4-x\ ^3D^0_3$		
2552.264		2h		39169.15			
2551.724	1	15		39177.44	$a\ ^3P_2-y\ ^3D^0_3$		
2550.580		3		39195.01	$a\ ^5D_3-z\ ^3G^0_4$		
2549.653		10		39209.26	$b\ ^3F_2-x\ ^3D^0_2$		
2549.272	8	120		39215.12	$a\ ^3P_2-y\ ^3P^0_2$		
2548.685	3	60		39224.15	$a\ ^3P_1-y\ ^3P^0_1$		
2546.311		5		39260.72	$a\ ^3P_1-y\ ^3D^0_2$		
2545.696		2		39270.20	$d\ ^3F_3-v\ ^3G^0_4$		
2545.460	2	15		39273.85	$a\ ^5D_4-z\ ^3G^0_5$		
2544.29		10*H*		39291.90	$a\ ^5P_1-z\ ^1P^0_1$		
2542.935	2	15		39312.84	$b\ ^3F_2-z\ ^1P^0_1$		
2542.46		20*H*		39320.18			
2539.20		20*H*		39370.66	$a\ ^1H_5-1^0_4$		
2537.619		20		39395.19	$b\ ^1D_2-x\ ^1D^0_2$		
2536.854		2		39407.07	$a\ ^3G_3-w\ ^3D^0_2$		
2536.65		2h		39410.24			
2534.519	5	80		39443.37	$a\ ^3P_0-y\ ^3P^0_1$		
2534.263		9		39447.35	$a\ ^3H_6-y\ ^3H^0_5$		
2533.969	1−	9		39451.93			
2533.365	1	15		39461.34	$a\ ^3H_5-y\ ^3H^0_4$		
2531.902		4+*H*?		39484.14			
2531.616		3		39488.60	$a\ ^3G_5-y\ ^1G^0_4$		
2528.833	10	220		39532.05	$a\ ^3H_5-y\ ^3H^0_5$		
2528.466	10	200		39537.79	$a\ ^3H_4-y\ ^3H^0_4$		
2527.903	15	250		39546.59	$a\ ^3H_6-y\ ^3H^0_6$		
2523.953	5	100		39608.48	$a\ ^3H_4-y\ ^3H^0_3$ $a\ ^3P_1-y\ ^3P^0_2$		
2523.61		1		39613.86	$d\ ^3F_4-v\ ^3G^0_5$		
2522.513	2	20		39631.09	$a\ ^3H_5-y\ ^3H^0_6$		
2522.392		6		39632.99	$a\ ^3F_4-y\ ^3G^0_4$		
2521.370		4h		39649.05			
2520.408		2		39664.19			
2517.97		2h		39702.59			
2515.722	1	9		39738.06	$a\ ^3F_3-y\ ^3G^0_3$		
2514.633	7	200		39755.27	$a\ ^3F_4-y\ ^3G^0_5$		
2513.322		1		39776.00			
2512.812		2h		39784.08			
2508.854		4		39846.84	$a\ ^3H_4-x\ ^3F^0_4$		
2508.26		2h		39856.27	$a\ ^1D_4-z\ ^3F^0_4$		
2506.215	10	200		39888.79	$a\ ^3F_3-y\ ^3G^0_4$		
2505.236		2h		39904.38			
2504.94		2h		39909.09	$c\ ^3F_4-v\ ^3G^0_5$		
2504.290		7h		39919.45			
2503.018	9	180		39939.74	$a\ ^3F_2-y\ ^3G^0_3$	(0)0.76	(0)0.71s
2500.076		4		39986.73	$a\ ^5D_2-z\ ^3F^0_3$		
2497.002		4		40035.96	$a\ ^3H_5-x\ ^3F^0_4$		
2494.721	2h	4h		40072.56			
2494.562	2h	3h		40075.11			
2493.576	3	15		40090.96	$a\ ^5D_4-z\ ^3F^0_4$		
2488.616	1−	6		40170.86	$a\ ^3F_4-y\ ^3F^0_4$		
2485.490		3		40221.37	$a\ ^5D_3-z\ ^3F^0_4$		
2483.064	4	120		40260.67	$b\ ^3F_2-w\ ^3D^0_1$		
2482.307	5	150		40272.94	$a\ ^3P_2-z\ ^3S^0_1$		
2479.518[4]	7	180		40318.24	$b\ ^3F_4-w\ ^3D^0_3$	(0)0.93	(0)0.92b
2479.043	8	200		40325.96	$b\ ^3F_3-w\ ^3D^0_2$		
2478.621	2	20		40332.83	$a\ ^3H_4-z\ ^3I^0_5$		

See footnotes at end of table.

TABLE 1.—*Second spectrum of Vanadium*—Continued

1	2		3	4	5	6	
λ_{air}A	Intensity		Temp. class	Wave No. vac	Term combination	Zeeman effect	
	Arc	Spark				Observed	Computed
2478.340		1		40337.40	$a\ ^3P_2-x\ ^3F^0_3$		
2476.963		1		40359.82	$a\ ^3F_3-y\ ^3F^0_3$		
2476.295		5h		40370.71	$a\ ^3H_6-z\ ^3I^0_6$		
2475.865	2	30		40377.72	$b\ ^3F_2-w\ ^3D^0_2$		
2475.451	2	20		40384.48	$b\ ^3F_3-w\ ^3D^0_3$		
2472.870		5		40426.62	$a\ ^3F_3-y\ ^3F^0_4$		
2471.119	2	25		40455.27	$a\ ^3H_5-z\ ^3I^0_6$		
2469.388		5		40483.62	$a\ ^3P_2-x\ ^3F^0_3$		
2468.654	1	8		40495.66	$a\ ^3F_4-z\ ^1H^0_5$		
2465.270	5	150		40551.24	$a\ ^3G_5-x\ ^3G^0_5$		
2464.65		1		40561.44	$a\ ^3F_3-y\ ^3F^0_2$		
2464.094	1	15		40570.59	$a\ ^3F_2-y\ ^3F^0_3$		
2463.157		3		40586.03	$a\ ^3G_4-y\ ^1F^0_3$		
2461.495	3	40		40613.43	$a\ ^3H_6-z\ ^3I^0_7$		
2460.73		1		40626.05	$a\ ^3F_4-z\ ^1G^0_4$		
2459.358	1	15		40648.71	$a\ ^3G_5-x\ ^3G^0_4$		
2459.233		5		40650.77	$a\ ^3G_4-x\ ^3G^0_5$		
2458.288	3	50		40666.40	$a\ ^3P_1-z\ ^3S^0_1$		
2457.803		5		40674.43			
2457.446	1	30		40680.34	$a\ ^3G_3-y\ ^1F^0_3$		
2456.508		3		40695.87	$a\ ^3P_2-x\ ^3D^0_1$		
2454.654		2		40726.60	$a\ ^3F_3-z\ ^1F^0_3$		
2453.857		3		40739.83	$a\ ^1H_5-w\ ^3G^0_4$		
2453.346	4	80		40748.32	$a\ ^3G_4-x\ ^3G^0_4$		
2452.773		4		40757.84			
2450.734	1	20		40791.74	$a\ ^3P_2-x\ ^3D^0_2$		
2450.619	1—	9		40793.65	$a\ ^3G_4-x\ ^3G^0_3$		
2450.236		10h		40800.03			
2448.46		5H		40829.63			
2447.608	1	20		40843.84	$a\ ^3G_5-y\ ^1H^0_5$		
2446.697	2	30		40859.04	$a\ ^3P_2-x\ ^3D^0_3$		
2445.336		4		40881.78	$a\ ^3F_3-z\ ^1G^0_4$		
2445.107		6		40885.61	$a\ ^3P_0-z\ ^3S^0_1$		
2444.967	2	60		40887.95	$a\ ^3G_3-x\ ^3G^0_3$		
2441.664		4h		40943.26	$a\ ^3G_4-y\ ^1H^0_5$		
2439.774		4h		40974.97			
2438.039		10h		41004.13			
2436.570		5H		41028.85			
2434.94		5?		41056.31	$a\ ^3F_3-z\ ^1D^0_2$		
2432.976	2	20		41089.46	$a\ ^3P_1-x\ ^3D^0_1$		
2431.59		4		41112.87	$b\ ^1D_2-x\ ^1F^0_3$		
2427.316	1	20		41185.26	$a\ ^3P_1-x\ ^3D^0_2$		
2423.030		6		41258.10	$a\ ^3F_2-z\ ^1D^0_2$		
2408.430	2	15		41508.19	$a\ ^3P_0-z\ ^1P^0_1$		
2407.592		5		41522.64	$a\ ^3H_5-y\ ^1G^0_4$		
2406.989		5		41533.04	$b\ ^3F_4-y\ ^1F^0_3$		
2405.817		2		41553.27	$b\ ^3D_3-w\ ^3F^0_4$		
2403.240	1	9		41597.82	$b\ ^3F_4-x\ ^3G^0_5$		
2400.892	1	40h		41638.50			
2400.166		4		41651.09	$b\ ^3F_2-y\ ^1F^0_3$		
2397.622		6		41695.28	$b\ ^3F_4-x\ ^3G^0_4$		
2396.927		4H		41707.37			
2394.92		2h?		41742.32	$c\ ^3P_2-w\ ^3F^0_3$		
2393.814	1	8		41761.61	$b\ ^3F_3-x\ ^3G^0_4$		
2392.698		8h		41781.08			
2392.17		2h		41790.30	$c\ ^3P_2-w\ ^3F^0_3$		
2391.226*		10h		41806.80	$b\ ^3F_3-x\ ^3G^0_3$		
2390.470		15h		41820.02			
2389.696	10	100		41833.56	$a\ ^3F_2-y\ ^3D^0_1$		
2389.144		2		41843.23	$a\ ^3P_2-w\ ^3D^0_1$		
2388.260		5		41858.72	$b\ ^3F_2-x\ ^3G^0_3$	(0)1.32	(0)1.28s
2387.93		3h		41864.50			
2386.45		2		41890.46	$b\ ^3F_4-y\ ^1H^0_5$		
2384.996		6h		41916.00			
2383.995	10	80		41933.60	$a\ ^3F_3-y\ ^3D^0_3$	(0)0.96	(0)0.97b

See footnotes at end of table.

TABLE 1.—*Second spectrum of Vanadium*—Continued

1	2		3	4	5	6	
λ_{air}A	Intensity		Temp. class	Wave No. vac	Term combination	Zeeman effect	
	Arc	Spark				Observed	Computed
2383.432		6*H*		41943.50			
2382.032	8	60+Fe?		41968.15			
2380.910	12	120		41987.92	$a\ ^3F_4-y\ ^3D_3^\circ$		
2379.149	10	100		42019.00	$a\ ^3P_2-w\ ^3D_3^\circ$		
2376.33		1		42068.84	$a\ ^3P_2-y\ ^3S_1^\circ$		
2374.649	1	6		42098.62	$a\ ^3F_2-y\ ^3P_1^\circ$		
2374.31		2*H*?		42104.63	$a\ ^1F_3-u\ ^3D_2^\circ$		
2372.584	4	20		42135.26	$a\ ^3F_2-y\ ^3D_2^\circ$		
2372.168		15*H*		42142.65			
2366.883	3	20		42236.73	$a\ ^3P_1-w\ ^3D_1^\circ$		
2366.490	4	25		42243.75	$a\ ^3F_3-y\ ^3D_3^\circ$		
2364.390		2		42281.27	$a\ ^5F_3-y\ ^3P_2^\circ$		
2362.632	2	20		42312.73	$a\ ^1P_1-x\ ^1D_2^\circ$		
2360.334	5	50		42353.92	$a\ ^3P_1-w\ ^3D_2^\circ$		
2357.810	6	60		42399.25	$a\ ^1H_5-x\ ^1G_4^\circ$	(0)1.30nw$_2$	(0)1.24b
2357.532		3*H*		42404.25			
2356.209		3*H*		42428.06			
2355.232		4		42445.66	$a\ ^3F_2-y\ ^3D_3^\circ$		
2354.656	2	20		42456.04	$a\ ^3P_0-w\ ^3D_1^\circ$		
2353.16		1?		42483.03	$a\ ^3F_2-y\ ^3P_2^\circ$		
2352.177	10	100		42500.78	$a\ ^3H_6-x\ ^3G_5^\circ$		
2351.24		6*H*		42517.72			
2347.507	1	8		42585.31	$a\ ^3H_5-x\ ^3G_5^\circ$		
2346.868	5	25		42596.92	$a\ ^3H_4-y\ ^1F_3^\circ$		
2342.142	10	60+*h*		42682.86	$a\ ^3H_5-x\ ^3G_4^\circ$	(0) 1.03	(0) 1.02b
2341.358		4		42697.15	$a\ ^3H_6-z\ ^1I_6^\circ$		
2337.956		4		42759.27	$a\ ^3H_4-x\ ^3G_4^\circ$		
2336.098	4	30		42793.28	$a\ ^3H_6-y\ ^1H_5^\circ$		
2335.480	6	40		42804.60	$a\ ^3H_4-x\ ^3G_3^\circ$		
2335.326	2	10		42807.42	$a\ ^3P_2-x\ ^3P_2^\circ$		
2335.204		2		42809.66	$a\ ^3P_2-x\ ^3P_1^\circ$		
2330.144	1	12		42902.62			
2321.855		1		43055.76	$a\ ^3F_4-y\ ^3H_5^\circ$		
2314.99		2*h*?		43183.44			
2314.055		3		43200.88	$a\ ^3P_1-x\ ^3P_2^\circ$		
2313.939	1	9		43203.04	$a\ ^3P_1-x\ ^3P_1^\circ$		
2312.299		2		43233.68	$a\ ^3P_2-y\ ^1F_3^\circ$		
2311.91		1?		43240.96	$a\ ^3F_2-y\ ^3H_4^\circ$		
2309.072		10		43294.10	$a\ ^3F_4-x\ ^3F_4^\circ$		
2308.831		5		43298.62	$a\ ^3P_1-x\ ^3P_0^\circ$		
2304.785		7*h*		43374.62			
2303.238	2	10		43403.75	$a\ ^3F_3-x\ ^3F_3^\circ$		
2302.256		5		43422.26	$a\ ^3P_0-x\ ^3P_1^\circ$		
2295.504	4	20		43549.97	$a\ ^3F_3-x\ ^3F_2^\circ$		
2294.992	7	40		43559.68	$a\ ^3F_4-x\ ^3F_4^\circ$		
2292.588	5	30		43605.36	$a\ ^3F_2-x\ ^3F_2^\circ$ $a\ ^1D_2-x\ ^1D_2^\circ$		
2291.381		3*h*		43628.32			
2289.219	4	70		43669.53	$a\ ^3F_4-x\ ^3D_3^\circ$		
2284.920	1	15		43751.68	$a\ ^3F_2-x\ ^3F_3^\circ$		
2284.748		10		43754.97	$a\ ^3P_2-y\ ^3S_1^\circ$		
2283.766		40		43773.79			
2283.469		7		43779.48	$a\ ^3D_3-w\ ^3F_3^\circ$		
2282.863		6		43791.10	$a\ ^3D_2-w\ ^3F_2^\circ$		
2281.601	2	60		43815.32	$a\ ^3F_3-x\ ^3F_4^\circ$ $a\ ^3D_1-w\ ^3F_2^\circ$ $b\ ^3H_4-w\ ^3G_3^\circ$		
2281.235	2	60		43822.35	$a\ ^3D_3-w\ ^3F_4^\circ$		
2280.581		4		43834.91			
2280.338		60		43839.58	$a\ ^3D_2-w\ ^3F_3^\circ$		
2279.762		20		43850.66	$b\ ^3H_5-w\ ^3G_4^\circ$		
2279.376	1	15		43858.08	$a\ ^3F_3-x\ ^3D_3^\circ$		
2278.972	1	40		43865.86	$b\ ^3H_6-w\ ^3G_5^\circ$		

See footnotes at end of table.

TABLE 1.—*Second spectrum of Vanadium*—Continued

1	2		3	4	5	6	
λ_{air}A	Intensity		Temp. class	Wave No. vac	Term combination	Zeeman effect	
	Arc	Spark				Observed	Computed
2278.098		4h		43882.69			
2277.792		1		43888.58	$b\ ^3H_4 - w\ ^3G^0_4$		
2275.883		7		43925.39	$a\ ^5F_3 - x\ ^3D^0_3$		
2275.586		7		43931.12	$a\ ^5F_3 - z\ ^3P^0_2$		
2274.658		1		43949.04	$b\ ^3H_3 - w\ ^3G^0_3$		
2273.89		2		43963.88	$a\ ^3F_3 - x\ ^3D^0_1$		
2273.616		9		43969.18	$b\ ^3D_3 - x\ ^1D^0_2$		
2273.024		40h		43980.63	$a\ ^5F_1 - z\ ^3P^0_0$ $b\ ^3D_3 - v\ ^3D^0_3$		
2272.437		1		43991.99	$d\ ^3F_2 - w\ ^1F^0_3$		
2271.848	1	10		44003.40	$a\ ^5F_4 - z\ ^3P^0_4$		
2271.185		8		44016.24			
2269.293		3		44052.94	$a\ ^5F_3 - z\ ^3P^0_2$		
2268.55		1		44067.36	$a\ ^5F_2 - z\ ^5P^0_1$		
2268.361		4		44071.03	$a\ ^5F_3 - z\ ^5P^0_2$		
2267.712		3		44083.65	$a\ ^5F_4 - z\ ^5P^0_3$		
2267.612		5		44085.59	$a\ ^5F_1 - z\ ^3P^0_1$		
2263.612		3		44163.48	$a\ ^5F_2 - z\ ^1P^0_1$		
2262.70		2		44181.28	$b\ ^3D_3 - v\ ^3D^0_2$		
2262.404		9h		44187.06	$b\ ^3D_2 - v\ ^3D^0_2$		
2261.850		10h		44197.89			
2261.084	5	30		44212.85	$a\ ^5F_4 - y\ ^5D^0_3$		
2258.814	?	50+I		44257.28	$a\ ^5F_3 - y\ ^5D^0_4$		
2258.64		2		44260.69	$c\ ^3P_2 - v\ ^3D^0_3$		
2256.984		20+I?		44293.17	$a\ ^5F_3 - y\ ^5D^0_2$		
2255.95		1?		44313.46	$b\ ^3D_2 - v\ ^3D^0_1$		
2252.953	1−	7		44372.41	$a\ ^5F_2 - y\ ^5D^0_3$		
2251.550		7		44400.05			
2251.114		6		44408.65	$b\ ^3D_1 - v\ ^3D^0_1$		
2250.800		5		44414.85	$a\ ^5F_2 - y\ ^5D^0_2$		
2250.490		5		44420.96	$a\ ^5F_2 - y\ ^5D^0_1$		
2250.382		3		44423.10	$a\ ^5F_1 - y\ ^5D^0_0$		
2248.913		4		44452.11	$a\ ^5F_4 - y\ ^5D^0_4$		
2248.45		1		44461.26	$c\ ^3P_2 - v\ ^3D^0_2$		
2246.65		1?		44496.88	$a\ ^5F_1 - y\ ^5D^0_2$ $c\ ^3P_1 - x\ ^1D^0_2$?		
2246.332		3		44503.18	$a\ ^5F_1 - y\ ^5D^0_1$		
2243.468		4h		44559.98			
2229.985	3	80		44829.37	$a\ ^3F_4 - w\ ^3D^0_3$		
2224.845		1		44932.93			
2220.214	3	100		45026.65	$a\ ^3F_3 - w\ ^3D^0_2$		
2219.408		3		45043.00	$d\ ^3F_3 - t\ ^3D^0_1$?		
2217.32		8		45085.41	$a\ ^3F_3 - w\ ^3D^0_3$ $d\ ^3F_2 - t\ ^3D^0_2$		
2215.786		9h		45116.62	$d\ ^3F_3 - t\ ^3D^0_2$		
2211.38		2h?		45206.50	$d\ ^3F_3 - t\ ^3D^0_3$		
2211.16		2		45211.00			
2210.305	1−	8		45228.48	$a\ ^3F_2 - w\ ^3D^0_3$		
2210.029	1	10		45234.13	$d\ ^3F_4 - t\ ^3D^0_3$		
2205.70		2		45322.90	$a\ ^1D_2 - x\ ^1F^0_3$		
2199.660		7		45447.34	$c\ ^3F_3 - t\ ^3D^0_1$?		
2199.443		10		45451.82	$c\ ^3F_3 - t\ ^3D^0_3$		
2198.524	2	20		45470.82	$b\ ^3P_2 - v\ ^3D^0_3$		
2195.69		15		45529.50	$c\ ^3F_4 - t\ ^3D^0_4$		
2195.10		2		45541.74	$c\ ^3F_3 - t\ ^3D^0_3$		
2194.84		8		45547.13	$d\ ^3F_3 - u\ ^3F^0_3$		
2193.34		2		45578.27	$d\ ^3F_3 - u\ ^3F^0_2$		
2192.91		2h		45587.21			
2190.48		8		45637.78	$b\ ^3P_1 - v\ ^3D^0_2$		
2190.22	2	30		45643.20	$b\ ^3G_3 - w\ ^3F^0_4$		
2188.86		2		45671.56	$b\ ^3P_2 - v\ ^3D^0_2$		
2186.94	2	20		45711.65	$b\ ^3G_4 - w\ ^3F^0_3$		
2185.96	3	40		45732.14	$d\ ^3F_3 - 2^0_3$		

See footnotes at end of table.

TABLE 1.—*Second spectrum of Vanadium*—Continued

1	2		3	4	5	6	
λ_{air}A	Intensity		Temp. class	Wave No. vac	Term combination	Zeeman effect	
	Arc	Spark				Observed	Computed
2185.39	4	50		45744.06	$\begin{cases} b\ ^3G_3-w\ ^3F_2^? \\ d\ ^3F_3-u\ ^3F_3^? \end{cases}$		
2184.89		2		45754.53	$b\ ^3G_4-w\ ^3F_3^?$		
2184.41		2		45764.58	$b\ ^3P_1-v\ ^3D_1^?$		
2184.17		5		45769.61	$b\ ^3P_0-v\ ^3D_1^?$		
2183.08		2		45792.46	$b\ ^3G_3-w\ ^3F_3^?$		
2175.833		5		45944.96			
2171.840		25		46029.42	$d\ ^3F_4-u\ ^3F_3^?$		
2171.12		2		46044.4	$\begin{cases} a\ ^3F_4-y\ ^1F_3^? \\ b\ ^3D_3-y\ ^1G_4^? \end{cases}$		
2170.38		15		46060.4			
2170.05		10*H*		46067.4	$c\ ^3F_4-u\ ^3F_3^?$		
2168.56		0*h*		46099.0	$c\ ^3F_3-2_3^?$		
2168.08		10		46109.2	$a\ ^3F_4-x\ ^3G_3^?$		
2167.69		8		46117.5	$c\ ^3F_2-u\ ^3F_2^?$		
2166.15		20*h*		46150.3			
2164.38		15		46188.1			
2163.68		20*h*		46203.0			
2161.48		20		46250.0	$a\ ^3D_3-v\ ^3D_3^?$		
2160.55		5		46269.9			
2159.53		0*h*		46291.8	$a\ ^3D_3-x\ ^1D_2^?$		
2159.13		0*h* Fe II?		46300.4	$\begin{cases} a\ ^5F_4-y\ ^3F_4^? \\ a\ ^5F_3-y\ ^1F_3^? \end{cases}$		
2158.36		0*H*		46316.9	$a\ ^3D_1-x\ ^1D_2^?$?		
2157.05		8		46345.0			
2155.61		15		46375.9	$a\ ^1G_4-y\ ^3F_3^?$		
2154.42		0		46401.6	$a\ ^3F_4-y\ ^1H_5^?$		
2151.812	5	50		46457.79			
2151.032	5	50		46474.64			
2150.835	6	60		46478.89			
2149.386		8		46510.22	$a\ ^3D_2-v\ ^3D_2^?$		
2148.42	15	40		46531.1	$a\ ^5D_3-z\ ^3P_2^?$		
2148.00		8		46540.3			
2147.52		20		46550.6	$a\ ^5D_1-z\ ^3P_0^?$		
2145.990	10	40		46583.8	$a\ ^5D_2-z\ ^3P_1^?$		
2145.37*		0*h*		46597.3	$a\ ^5F_1-y\ ^3F_2^?$		
2144.10		5 V I?		46624.9	$a\ ^5F_4-z\ ^1H_5^?$		
2143.706		5		46633.44	$a\ ^5D_3-z\ ^3P_2^?$		
2143.038	30	60		46647.98	$a\ ^5D_2-z\ ^5P_1^?$		
2142.74	1	4		46654.5	$a\ ^5D_1-z\ ^3P_1^?$		
2142.40		3		46661.9	$a\ ^3D_1-v\ ^3D_1^?$		
2141.973	40	100		46671.17	$a\ ^5D_3-z\ ^5P_2^?$		
2141.70	0	4*h*?		46677.1	$b\ ^1G_4-x\ ^1G_4^?$		
2140.064	60	150		46712.79	$a\ ^5D_4-z\ ^5P_3^?$		
2139.798	40	100		46718.60	$a\ ^5D_1-z\ ^5P_1^?$		
2138.17	30	60		46754.2	$a\ ^5D_0-z\ ^5P_1^?$		
2137.31	50	100		46773.0	$a\ ^5D_2-z\ ^5P_2^?$		
2134.12	100	200		46842.9	$a\ ^5D_3-z\ ^5P_3^?$		
2133.04		60		46866.6			
2131.85	30	80		46892.8	$a\ ^5D_3-y\ ^5D_3^?$		
2130.85		0		46914.8	$a\ ^5F_3-z\ ^1G_4^?$		
2130.42		5		46924.2	$a\ ^1D_2-v\ ^3F_2^?$		
2129.477	10	40		46945.01	$a\ ^5D_3-z\ ^5P_3^?$		
2128.241	1	7		46972.26	$a\ ^5D_3-y\ ^5D_3^?$		
2127.34	1	5		46992.2	$a\ ^5D_1-y\ ^5D_0^?$		
2126.932	6	20		47001.17	$a\ ^5D_3-y\ ^5D_1^?$		
2126.585		25*h*		47008.84			
2124.00		5*d*?		47066.0	$a\ ^5D_1-y\ ^5D_2^?$		
2123.62	3	10		47074.5	$a\ ^5D_2-y\ ^5D_3^?$		
2123.340	20	60		47080.67	$a\ ^5D_4-y\ ^5D_4^?$		
2122.11	1?	1		47108.0	$a\ ^5D_0-y\ ^5D_1^?$		
2121.54		10		47120.6	$b\ ^3D_3-v\ ^3F_3^?$		
2119.562		15		47164.58			

See footnotes at end of table.

TABLE 1.—*Second spectrum of Vanadium*—Continued

1	2		3	4	5	6	
	Intensity					Zeeman effect	
λ_{air}A	Arc	Spark	Temp. class	Wave No. vac	Term combination	Observed	Computed
2119.15		40*h*		47173.7			
2118.84	1	25		47180.6			
2118.43*		30*h*		47189.8	$b\ ^1G_4 - x\ ^1F_3^\circ$		
2117.482	4	12		47210.90	$a\ ^3D_3 - y\ ^3D_3^\circ$		
2117.293		25		47215.12	$b\ ^3D_1 - v\ ^3F_2^\circ$		
2114.30		15		47281.9	$b\ ^3D_3 - v\ ^3F_4^\circ$		
2114.03		30		47288.0	$b\ ^3D_2 - v\ ^3F_3^\circ$		
2111.04		15		47354.9			
2110.48		5		47367.5			
2109.27		8		47394.7	$c\ ^3P_2 - v\ ^3F_3^\circ$		
2107.40		10*h*		47436.7	$a\ ^3D_3 - x\ ^1G_4^\circ$		
2103.70	8	80		47520.2	$a\ ^3G_5 - w\ ^3F_4^\circ$		
2103.53	10	30		47524.0	$b\ ^3D_3 - v\ ^3F_4^\circ$		
2101.86	*tr*	20		47561.8	$c\ ^3P_2 - v\ ^3F_3^\circ$		
2101.17	5	50		47577.4	$a\ ^3G_4 - w\ ^3F_3^\circ$		
2100.25		0		47598.2	$b\ ^3G_5 - w\ ^3G_4^\circ$		
2099.47		0		47615.9	$a\ ^3D_1 - x\ ^3D_2^\circ$		
2099.16	3	30		47622.9	$a\ ^3G_3 - w\ ^3F_2^\circ$		
2098.60		0		47635.6	$b\ ^3G_4 - w\ ^3G_3^\circ$		
2098.00		5*d*?		47649.2	$c\ ^3P_1 - v\ ^3F_2^\circ$?		
2097.03		?		47671.3	$a\ ^3G_3 - w\ ^3F_3^\circ$		
2095.94	0	25		47696.1	$b\ ^3G_5 - w\ ^3G_5^\circ$		
2095.37	5	15		47709.0	$b\ ^3G_4 - w\ ^3G_4^\circ$		
2095.05		15		47716.3	$b\ ^3G_3 - w\ ^3G_3^\circ$		
2091.81		2*h*		47790.2	$b\ ^3G_3 - w\ ^3G_4^\circ$		
2090.33	*tr*	25		47824.1	$a\ ^1F_3 - w\ ^1F_3^\circ$		
2087.92		20		47879.3	$a\ ^1G_4 - x\ ^1G_4^\circ$		
2087.54		15		47888.0			
2079.29		10*H*		48077.9			
2077.79	*tr*?	40*H*		48112.7			
2077.58	*tr*?	15*H*		48117.5	$d\ ^3F_2 - w\ ^1D_2^\circ$		
2076.87	30	60*h*		48134.0			
2076.52	0?	0??		48142.1	$b\ ^3D_2 - u\ ^3D_1^\circ$		
2075.13		15		48174.3	$b\ ^3D_3 - u\ ^3D_2^\circ$		
2074.87	0*h*	25		48180.4	$b\ ^3D_2 - u\ ^3D_2^\circ$		
2072.43	*tr*	30		48237.1	$b\ ^3D_1 - u\ ^3D_1^\circ$		
2070.79		15		48275.3	$b\ ^3D_1 - u\ ^3D_2^\circ$		
2068.80	10	60		48321.7	$b\ ^3D_2 - u\ ^3D_2^\circ$		
2068.54	0	15		48327.8	$b\ ^3D_2 - u\ ^3D_3^\circ$		
2066.83		8*h*		48367.8	$d\ ^3F_2 - 3_3^\circ$		
2065.76	10	40		48392.8	$a\ ^1G_4 - x\ ^1F_3^\circ$		
2064.78		2		48415.8	$c\ ^3P_2 - u\ ^3D_1^\circ$		
2063.12		20		48454.7	$c\ ^3P_2 - u\ ^3D_2^\circ$		
2062.00		10		48481.0			
2061.56	*tr*	15		48491.4			
2058.34	10	40		48567.2	$b\ ^3F_4 - w\ ^3F_4^\circ$		
2057.36	8	25		48590.4	$b\ ^3F_3 - w\ ^3F_3^\circ$		
2057.20	5	15		48594.1	$b\ ^3F_2 - w\ ^3F_2^\circ$		
2056.89		15		48601.5	$c\ ^3P_2 - u\ ^3D_3^\circ$ $c\ ^3P_0 - u\ ^3D_1^\circ$		
2055.55		8		48633.1	$b\ ^3F_3 - w\ ^3F_2^\circ$		
2055.15		5		48642.6	$b\ ^3F_3 - w\ ^3F_3^\circ$		
2054.85	10	70		48649.7			
2054.27		0*h*		48663.4	$a\ ^1D_2 - v\ ^3G_3^\circ$		
2054.01		0		48669.6	$c\ ^3P_1 - u\ ^3D_1^\circ$		
2052.38		10		48708.2	$c\ ^3P_1 - u\ ^3D_2^\circ$		
2051.79		30*h*		48722.2	$c\ ^3F_4 - 3_4^\circ$		
2051.27		5*h*		48734.6	$c\ ^3F_3 - 3_3^\circ$		
2049.67		5*h*		48772.6	$b\ ^3P_2 - v\ ^3F_3^\circ$? $c\ ^3F_2 - 3_3^\circ$		
2048.75	*tr*	15		48794.5			
2046.12		0		48857.2	$a\ ^1S_0 - u\ ^3D_1^\circ$		

See footnotes at end of table.

TABLE 1.—*Second spectrum of Vanadium*—Continued

1	2		3	4	5	6	
λ_{air}A	Intensity		Temp. class	Wave No. vac	Term combination	Zeeman effect	
	Arc	Spark				Observed	Computed
2044.28	2h	5		48901.2	$a\ ^1H_5-w\ ^1G_4^0$		
2039.29		60		49020.9	$a\ ^5P_3-1_4^0$		
2037.83		50		49056.0			
2037.50		25		49063.9			
2035.78		15		49105.4			
2035.06		60		49122.7			
2033.50		10		49160.4			
2031.40		30h		49211.2			
2028.88		15		49272.3			
2025.47		15		49355.3	$a\ ^3G_3-y\ ^3F_3^0$		
2024.84		0??		49370.6	$a\ ^3G_4-p\ ^3F_4^0$?		
2023.56	10	50		49401.9	$b\ ^3H_4-p\ ^3G_3^0$		
2022.66		15h		49423.9			
2021.83		5		49444.1	$a\ ^3D_2-p\ ^3F_2^0$		
2021.38		10h		49455.1			
2020.83	0	15		49468.6	$a\ ^3D_1-p\ ^3F_2^0$		
2020.54	0h	10		49475.7	$a\ ^3G_3-w\ ^3G_4^0$		
2019.47	*tr*	10		49501.9	$a\ ^3G_4-w\ ^3G_3^0$		
2017.46		2		49551.2	$a\ ^3D_3-p\ ^3F_3^0$		
2017.32		2		49554.6	$a\ ^3H_5-w\ ^3F_4^0$		
2016.53	15	60		49574.1	$a\ ^3G_5-w\ ^3G_5^0$ $a\ ^3G_4-w\ ^3G_4^0$ $a\ ^3G_3-w\ ^3G_3^0$ $b\ ^3P_1-u\ ^3D_1^0$		
2015.74	*tr*	20		49593.5			
2015.56	*tr*	20		49597.9	$b\ ^3P_0-u\ ^3D_1^0$		
2015.02	0h	15		49611.2	$a\ ^3D_2-p\ ^3F_3^0$		
2014.18	20	90		49631.9	$b\ ^3P_1-u\ ^3D_2^0$ $a\ ^3G_3-y\ ^3F_3^0$ $b\ ^3H_5-p\ ^3G_4^0$		
2012.84	*tr*	20		49664.9	$b\ ^3P_2-u\ ^3D_3^0$		
2012.64	0h	10		49669.9	$b\ ^3H_4-p\ ^3G_4^0$ $a\ ^3G_3-w\ ^3G_4^0$		
2010.15	3	5h		49731.4	$a\ ^3G_4-y\ ^3F_3^0$		
2007.66	*tr*	25		49793.0	$a\ ^3D_3-p\ ^3F_4^0$		
2006.88	10	80		49812.4	$b\ ^3P_2-u\ ^3D_2^0$		
2006.08		0??		49832.3	$b\ ^1G_4-u\ ^3D_3^0$		
2005.88		15		49837.2			
2004.77	15	80		49864.8	$b\ ^3H_6-p\ ^3G_5^0$		
2004.03		0		49883.2	$b\ ^3G_4-x\ ^1F_3^0$?		
2002.82		0		49913.4	$a\ ^5F_5-z\ ^3I_6^0$		
2001.65	*tr*	40		49942.5			
2001.43		10		49948.0	$b\ ^3H_5-p\ ^3G_5^0$		
2001.14	*tr*	30		49955.3			
2000.78		5		49964.2	$b\ ^3G_3-x\ ^1F_3^0$?		
2000.14		10h		49980.2			
λVac							
1995.02		0		50124.8	$a\ ^3G_3-x\ ^1D_2^0$		
1992.80		30		50180.7			
1987.82		3		50306.4			
1984.05	10	90		50402.0			
1982.41		8		50443.7	$a\ ^3D_3-u\ ^3D_3^0$		
1982-21		0		50448.7	$b\ ^3F_4-w\ ^3G_4^0$		
1981.53		8		50466.1	$a\ ^3D_2-u\ ^3D_1^0$		
1980.59	0	25		50490.0	$a\ ^3D_1-u\ ^3D_1^0$		
1980.04	0	40		50504.0	$a\ ^3D_2-u\ ^3D_2^0$		
1978.96	0	20		50531.6	$b\ ^1G_4-p\ ^3G_4^0$		
1977.60	1	0??I?		50566.3	$b\ ^3F_3-w\ ^3G_3^0$		
1976.62	0	60		50591.4	$a\ ^3D_3-u\ ^3D_2^0$		
1972.62		20		50694.0	$b\ ^3H_4-x\ ^1H_5^0$		
1960.98		2		50994.9	$b\ ^3F_4-p\ ^3D_3^0$		
1950.77		0		51261.8	$b\ ^3F_3-p\ ^3D_2^0$ $b\ ^3G_5-y\ ^3G_5^0$?		

See footnotes at end of table.

TABLE 1.—*Second spectrum of Vanadium*—Continued

1	2		3	4	5	6	
λ_{air}Å	Intensity		Temp. class	Wave No. vac	Term combination	Zeeman effect	
	Arc	Spark				Observed	Computed
1945.64	3	30		51397.0	$b\,^3G_3-v\,^3F_2^3$		
1945.35		30*Bl* Fe III?		51404.6	$a\,^3H_5-y\,^3F_4^4$		
1943.99		*tr*		51440.6	$a\,^3G_4-x\,^5D_3^3$ $b\,^3F_3-v\,^3D_1^1$		
1942.35	8	40		51484.0	$b\,^3G_4-v\,^3F_3^3$		
1941.40	10	30		51509.2	$a\,^3H_5-w\,^3G_4^4$		
1941.27	10	30		51512.7	$a\,^3H_4-w\,^3G_3^3$		
1940.86	10	40		51523.6	$a\,^3H_6-w\,^3G_5^4$		
1939.32		8		51564.5	$b\,^3G_3-v\,^3F_2^2$		
1938.70		8		51581.0	$a\,^3H_6-y\,^5F_5^5$		
1938.50		10		51586.3	$a\,^3H_4-w\,^3G_4^4$		
1937.68		7		51608.1	$a\,^3H_5-w\,^3G_5^5$		
1937.44	10	60		51614.5	$b\,^3G_5-v\,^3F_4^4$		
1933.97		30		51707.1			
1933.28		10		51725.6	$b\,^3G_4-v\,^3F_4^4$		
1932.99		3		51733.3	$a\,^1G_4-v\,^3G_3^3$		
1932.55		0*h*		51745.1	$a\,^1I_6-x\,^1I_5^5$		
1929.61	10	60		51823.9	$b\,^1G_4-x\,^1H_5^5$		
1924.87		30		51951.6	$a\,^1F_3-w\,^1D_2^2$		
1921.24		15*he*?		52049.7	$b\,^3H_4-w\,^1G_4^4$		
1920.36		12		52073.6	$a\,^5D_2-z\,^3S_1^2$?		
1919.35		20		52101.0			
1917.79		15		52143.4	$a\,^5P_3-x\,^5D_2^2$		
1915.71		*tr*		52200.0	$a\,^1F_3-3_2^3$		
1914.91	0	15		52221.8	$a\,^5P_2-x\,^5D_1^1$		
1913.70	8	50		52254.8	$a\,^5P_3-x\,^5D_3^3$		
1913.10	2	20		52271.2	$a\,^5P_1-x\,^5D_0^0$		
1912.39	8	40		52290.6	$a\,^5P_2-x\,^5D_2^2$		
1911.88	6	40		52304.5	$a\,^5P_1-x\,^5D_1^1$		
1909.36	8	40		52373.6	$a\,^5P_1-x\,^5D_2^2$		
1908.32	10	40*h*		52402.1	$a\,^5P_2-x\,^5D_3^3$		
1907.79	15	50		52416.7	$a\,^5P_3-x\,^5D_4^4$		
1904.54		*tr*		52506.1	$b\,^3F_2-x\,^5D_3^3$		
1903.86		5?		52524.9	$b\,^3G_4-u\,^3D_3^3$?		
1897.70		1		52695.4	$a\,^3P_2-v\,^3D_3^3$ $b\,^3F_4-x\,^1F_3^3$		
1885.90		10		53025.1	$a\,^1G_4-x\,^1H_5^5$		
1883.98	6	20		53079.1	$a\,^3F_4-w\,^3F_4^4$		
1880.43		40*e*?		53179.3	$b\,^1G_4-w\,^1G_4^4$		
1878.90		10		53222.6	$b\,^3G_4-v\,^3G_3^3$		
1878.19		0		53242.7	$a\,^3F_3-w\,^3F_2^2$		
1877.85		*tr*		53252.4	$a\,^1H_5-u\,^3F_4^4$		
1877.00		10		53276.5	$a\,^3G_3-v\,^3F_2^2$		
1876.47	3	10		53291.6	$a\,^3F_3-w\,^3F_3^3$		
1876.06	3	20		53303.2	$b\,^3G_3-v\,^3G_2^2$		
1874.97		1		53334.2	$a\,^3F_3-w\,^3F_4^4$		
1874.45		12		53349.0	$a\,^3G_4-v\,^3F_3^3$		
1873.39		10		53379.2	$b\,^3G_5-v\,^3G_4^4$		
1871.08	3	12		53445.1	$a\,^3F_2-w\,^3F_2^2$		
1869.47	10	50		53491.1	$a\,^3G_5-v\,^3F_4^4$ $b\,^3H_4-v\,^3G_4^4$		
1867.47		20		53548.4			
1866.68		5		53571.0	$b\,^3G_3-v\,^3G_3^3$		
1865.99		3		53590.9	$a\,^3G_4-v\,^3F_4^4$		
1865.68		2*hd*?		53599.8	$b\,^1D_2-w\,^1D_2^2$		
1862.76		25		53683.8	$a\,^1D_2-w\,^1F_3^3$		
1862.37	8	30		53695.0	$b\,^3G_5-v\,^3G_5^5$		
1858.50		2		53806.8	$b\,^3G_4-v\,^3G_4^4$		
1848.80		0*Bl* Fe II?		54089.1	$a\,^3P_2-x\,^5D_3^3$		
1843.43		5		54246.7	$b\,^3F_2-v\,^3F_3^3$		
1842.68		0*h*		54268.8	$a\,^3P_1-x\,^5D_0^0$		
1839.54		20		54361.4	$b\,^3F_3-v\,^3F_2^2$		
1838.86		25		54381.5	$a\,^1G_4-w\,^1G_4^4$		

See footnotes at end of table.

TABLE 1.—*Second spectrum of Vanadium*—Continued

1	2		3	4	5	6	
λ_{air}A	Intensity		Temp. class	Wave No. vac	Term combination	Zeeman effect	
	Arc	Spark				Observed	Computed
1837.76		*tr*		54414.1	$b\ ^3F_2-v\ ^3F_3^4$		
1833.58		10		54538.1	$b\ ^3F_4-v\ ^3F_4^4$		
1828.84		50		54679.5			
1823.61		25		54836.3			
1817.09		*tr*		55033.0	$a\ ^3F_4-w\ ^3G_4^4$		
1816.30		20*h*		55057.0			
1815.32		2*hd*?		55086.7	$a\ ^3D_4-v\ ^3G_4^4$?		
1814.93		5		55098.5	$b\ ^3G_3-t\ ^3D_3^4$		
1813.87		8		55130.7	$a\ ^3F_4-w\ ^3G_3^4$		
1811.51		*tr*		55202.6	$a\ ^5P_3-u\ ^3D_3^4$ $a\ ^5P_2-u\ ^3D_2^4$		
1810.57		3*e*		55231.2	$b\ ^3D_3-t\ ^3D_2^4$?		
1810.31		*tr*		55239.2	$a\ ^1D_2-u\ ^3F_2^4$		
1809.81		8*d*?		55254.4	$b\ ^3F_3-u\ ^3D_2^4$ $a\ ^3G_5-v\ ^3G_4^4$?		
1809.36		10*e*		55268.2	$b\ ^3F_2-u\ ^3D_1^4$		
1808.66		0		55289.6	$a\ ^3F_3-w\ ^3G_3^4$		
1807.15		1		55335.7	$b\ ^3F_4-u\ ^3D_3^4$		
1806.49		8*h*		55356.0	$a\ ^3G_4-v\ ^3G_4^4$		
1804.53		0*h*		55416.1	$a\ ^3F_3-w\ ^3G_3^4$ $c\ ^3P_3-t\ ^3D_3^4$		
1801.61		0		55505.9	$a\ ^3F_4-v\ ^3D_3^4$ $c\ ^3P_2-t\ ^3D_2^4$		
1800.13		0*h*		55551.5	$b\ ^1G_4-w\ ^1F_3^4$		
1799.97		3		55556.5	$a\ ^5D_2-y\ ^3S_1^4$		
1799.47		12		55571.9	$a\ ^3G_3-v\ ^3G_3^4$		
1796.80		20		55654.5			
1796.52		3*h*		55663.2	$a\ ^3D_0-y\ ^3S_1^4$		
1796.26		0		55671.2	$a\ ^3G_4-v\ ^3G_3^4$		
1795.38		0		55698.5	$b\ ^3D_1-u\ ^3F_2^4$		
1794.62		50		55722.1			
1793.13		3		55768.4	$b\ ^3D_2-u\ ^3F_3^4$		
1792.49		5		55788.3	$b\ ^3D_3-2_3^4$		
1789.61		5*h*		55878.1	$c\ ^3P_2-u\ ^3F_2^4$?		
1788.30		25		55919.0			
1786.91		0		55962.5	$a\ ^3F_2-v\ ^3D_2^4$		
1785.07		5		56020.2	$b\ ^3D_3-u\ ^3F_3^4$		
1780.52		5*h*		56163.4	$a\ ^3F_2-v\ ^3D_3^4$ $b\ ^3H_4-2_5^4$		
1776.48		*tr*?		56291.1	$a\ ^3F_2-v\ ^3D_1^4$		
1773.00		*tr*		56401.6	$b\ ^3H_4-u\ ^3F_4^4$		
1767.02		0		56592.5	$b\ ^3P_1-t\ ^3D_2^4$		
1766.21		0		56618.4	$b\ ^3F_4-v\ ^3G_3^4$		
1763.20		0		56715.1	$b\ ^3P_2-t\ ^3D_3^4$		
1760.11		25		56814.6			
1759.00		*tr*		56850.5	$a\ ^3P_2-u\ ^3D_1^4$		
1757.76		20		56890.6			
1748.99		5		57175.9	$a\ ^3F_2-x\ ^3D_1^4$		
1739.33		10*l*		57493.4	$a\ ^3D_3-t\ ^3D_2^4$?		
1737.02		0*H*		57569.9	$a\ ^3F_4-y\ ^3G_4^4$?		
1729.78		10*e*		57810.8	$a\ ^1D_2-w\ ^1D_2^4$		
1722.62		10*e*		58051.1	$a\ ^3D_3-2_3^4$		
1716.50		0		58258.1	$a\ ^3F_4-y\ ^3G_3^4$?		
1715.57		2		58289.7	$a\ ^3D_3-u\ ^3F_4^4$		
1711.66		0		58422.8	$b\ ^3D_3-3_3^4$		
1700.47		3		58807.3	$a\ ^3F_4-v\ ^3F_4^4$		
1697.90		2		58896.3	$a\ ^3F_3-v\ ^3F_3^4$		
1693.49		12		59049.7	$a\ ^3F_4-v\ ^3F_3^4$		
1693.09		10		59063.6	$a\ ^3F_3-v\ ^3F_2^4$		
1692.11		10		59097.8	$a\ ^3F_3-v\ ^3F_3^4$		
1687.36		1*h*		59264.2	$a\ ^3F_2-v\ ^3F_2^4$		
1686.19		1		59305.3	$a\ ^3F_3-v\ ^3F_4^4$		
1682.17		0		59447.0	$a\ ^3F_2-w\ ^3F_3^4$		
1681.22		5		59480.6	$a\ ^3F_4-w\ ^3F_4^4$		
1677.88		3		59599.0	$a\ ^5F_5-1_4^4$		

See footnotes at end of table.

TABLE 1.—*Second spectrum of Vanadium*—Continued

1	2		3	4	5	6	
λ_{air}A	Intensity		Temp. class	Wave No. vac	Term combination	Zeeman effect	
	Arc	Spark				Observed	Computed
1674.09		8		59733.9			
1672.44		15		59792.9	$a\ ^5F_4-1^0_4$		
1670.90		5		59848.0	$a\ ^3F_4-u\ ^3D^0_3$		
1670.01		10		59879.9	$b\ ^3G_3-u\ ^3F^0_3$		
1667.88		5		59956.4	$a\ ^3F_3-u\ ^3D^0_3$		
1667.66		10		59964.3	$b\ ^3G_4-u\ ^3F^0_3$		
1665.42		8e		60044.9	$b\ ^3G_3-u\ ^3F^0_4$		
1664.87		0		60064.7	$b\ ^3G_3-2^0_3$		
1663.80		0		60103.4	$a\ ^3F_3-u\ ^3D^0_2$		
1663.60		15		60110.6	$b\ ^3G_3-u\ ^3F^0_4$		
1663.34		3		60120.0	$a\ ^3F_2-u\ ^3D^0_1$		
1662.28		0		60158.3	$a\ ^3F_2-u\ ^3D^0_2$		
1661.27		60		60194.9			
1660.53		8		60221.7	$b\ ^3G_4-u\ ^3F^0_4$		
1643.43		30		60848.3	$a\ ^5F_4-y\ ^5F^0_5$ $a\ ^5F_3-y\ ^5F^0_4$		
1643.02		30		60863.5	$a\ ^5F_5-y\ ^5F^0_5$ $a\ ^5F_2-y\ ^5F^0_1$		
1640.86		30		60943.7	$a\ ^5F_1-y\ ^5F^0_1$		
1640.15		35		60970.0	$a\ ^5F_3-y\ ^5F^0_3$		
1639.13		40		61008.0	$a\ ^5F_3-y\ ^5F^0_4$		
1637.93		10		61052.7	$a\ ^5F_1-y\ ^5F^0_2$		
1637.77		50		61058.6	$a\ ^5F_4-y\ ^5F^0_4$		
1637.55		5		61066.8	$a\ ^5F_5-w\ ^3G^0_5$		
1636.02		40		61123.9	$a\ ^5F_5-y\ ^5F^0_5$		
1635.86		20		61129.9	$a\ ^5F_2-y\ ^5F^0_3$		
1634.98		*tr*		61162.8	$a\ ^5F_4-w\ ^3G^0_4$		
1633.51		25		61217.9	$a\ ^5F_3-y\ ^5F^0_3$		
1630.82		20		61318.8	$a\ ^5F_4-y\ ^5F^0_3$		
1619.18		10		61759.7	$a\ ^3G_3-u\ ^3F^0_2$		
1617.35		10		61829.5	$a\ ^3G_4-u\ ^3F^0_3$		
1613.40		0		61980.9	$a\ ^5F_1-x\ ^1D^0_2$		
1613.20		15		61988.6	$a\ ^3G_3-u\ ^3F^0_4$		
1587.40		50		62996.1	$a\ ^5F_5-x\ ^5D^0_4$		
1586.58		40		63028.7	$a\ ^5F_4-x\ ^5D^0_3$		
1585.361		30		63077.1	$a\ ^5F_3-x\ ^5D^0_2$		
1584.06		15		63128.9	$a\ ^5F_2-x\ ^5D^0_1$		
1582.80		8		63179.2	$a\ ^5F_1-x\ ^5D^0_0$		
1582.57		15		63188.4	$a\ ^5F_4-x\ ^5D^0_4$ $a\ ^5F_3-x\ ^5D^0_3$		
1582.32		8		63198.3	$a\ ^5F_3-x\ ^5D^0_3$		
1581.99		8		63211.5	$a\ ^5F_1-x\ ^5D^0_1$		
1573.78		0		63541.3	$a\ ^5F_2-y\ ^5G^0_2$?		
1571.74		2		63623.8	$a\ ^5F_1-y\ ^5G^0_2$?		
1565.98		8		63857.8	$a\ ^5F_3-y\ ^5G^0_3$?		
1562.98		10		63980.3	$a\ ^5F_2-y\ ^5G^0_3$?		
1558.76		15		64153.6	$a\ ^5F_3-y\ ^5G^0_4$?		
1556.05		0		64265.3	$a\ ^5D_4-v\ ^3D^0_3$		
1553.09		15		64387.8	$a\ ^5F_4-y\ ^5G^0_5$?		
1550.47		0		64496.6	$a\ ^5D_3-v\ ^3D^0_3$ $a\ ^3P_2-2^0_3$		
1547.20		15		64632.9	$a\ ^5F_5-y\ ^5G^0_6$?		
1358.40		3		73616.0	$a\ ^5F_1-u\ ^5F^0_2$		
1313.82		0		76113.9	$a\ ^5D_3-u\ ^3F^0_3$		

[a] Blend with V I.
[b] Zeeman pattern diffuse.
[c] Violet member of observed Zeeman pattern double line.
[d] Observed Zeeman pattern possible blend with V I.
[e] Observed Zeeman pattern affected by superposed line.
[f] Red member of observed Zeeman pattern double line.
[g] Observed Zeeman pattern affected by reversal.
[h] Observed Zeeman pattern unsymmetrical; doubtful.
[i] Observed Zeeman pattern blended.
[j] Intensities in observed Zeeman pattern unsymmetrical.
[k] Multiplet designation discordant with observed Zeeman pattern.
[l] Violet π-component of observed Zeeman pattern blended.
[m] Red π-component of observed Zeeman pattern weaker and blended.
[n] Red π-component of observed Zeeman pattern weaker.
[o] π-component of observed Zeeman pattern blended.
[p] Line probably a blend.

The total number of V II lines listed in table 1 is 1,700. Of these, 1,456, or 86 percent, have been classified as combinations of singlet, triplet, and quintet terms, as follows: 81 singlet, 780 triplet, 215 quintet, 210 singlet-triplet, 202 triplet-quintet, 8 singlet-quintet, and 18 miscellaneous levels, 53 doing double and 2 triple duty because of blends. In such a complex spectrum it is inevitable that some predictable lines are unobserved because of masking by coincident or adjacent lines of greater intensity. A list of 24 such lines is displayed in table 2, where successive columns show (1) the masking spectrum line, (2) its observed wavelength, (3) the difference in wavelength between observed masking and calculated masked line, (4) estimated intensities of observed lines and expected intensities of masked lines, (5) wave number of observed line, and (6) term combination of the masked line. Considering their closeness to strong lines, their relatively low intensity, and the general characteristics of spark lines at atmospheric pressure, the number of masked lines is not unduly large.

The average difference in wavelength between these masking and masked lines is 0.04 A, so that resolving power of the order of 100,000 would separate them if they were of equal intensity and reasonably sharp. But when the lines are somewhat diffuse and the intensity ratios average 10 or more, it appears to be impracticable to distinguish them if their separations are less than about 0.2 A.

TABLE 2.—*Masking and masked* V II *lines*

Spectrum	Observed λ	Δλ o–c	Intensity		Observed wave number	Term combination
			Observed	Expected		
V I	4875.462	−0.03	40	5	20505.17	$c\,^3D_3 - v\,^3D_3^0$
V I	4577.173	+.04	40	15	21841.44	$a\,^3D_2 - z\,^3F_3^0$
V II	4205.080	+.03	250	15	23774.09	$a\,^5P_2 - z\,^5D_3^0$
V I	3844.442	−.04	20	10	26004.23	$b\,^3F_4 - z\,^3G_5^0$
V II	3337.845	+.08	200	20	29950.87	$b\,^3D_1 - y\,^3D_2^0$
V II	3093.108	−.05	2500*R*	150	32320.59	$b\,^3G_5 - y\,^3G_5^0$
V II	2982.75	+.05	40	3	33516.36	$d\,^3F_4 - w\,^3G_5^0$
V II	2944.568	+.08	250	15	33950.94	$a\,^3D_2 - x\,^3F_3^0$
V II	2941.372	+.15	200	20	33987.83	$d\,^3F_4 - v\,^3D_3^0$
V II	2892.650	+.08	200*r*	8	34560.27	$c\,^3P_0 - x\,^3P_1^0$
V II	2880.026	+.06	150	9	34711.75	$a\,^3G_4 - y\,^3F_4^0$
V II	2810.272	+.03	100	20	35573.29	$c\,^3P_1 - y\,^3S_1^0$
V II	2803.469	−.05	150	4	35659.61	$b\,^3F_3 - y\,^3F_3^0$
V II	2798.755	+.02	80	4	35719.67	$b\,^3F_2 - y\,^3F_2^0$
V II	2756.58	−.02	20*Hl*	3	36266.14	$a\,^3F_4 - z\,^3G_4^0$
V II	2682.875	+.07	100	6	37262.39	$d\,^3F_3 - v\,^3F_3^0$
V II	2657.295	+.04	10	3	37621.07	$a\,^3F_3 - z\,^3F_3^0$
V II	2628.75	.00	30*H*	?	38029.56	$z\,^5G_3^0 - e\,^5F_4$
V III	2593.052	.00	50*He*	2	38553.08	$z\,^5G_2^0 - e\,^5G_3$
V II	2548.686	+.04	60	10	39224.14	$b\,^3F_3 - x\,^3D_3^0$
V I	2420.115	+.05	100*R*	10	41307.79	$a\,^3P_0 - x\,^3D_1^0$
V III	2382.468	−.01	80*He*	20	41960.47	$a\,^3P_1 - w\,^3D_2^0$
V III	2216.033	−.02	100*e*	50	45111.59	$a\,^3F_3 - w\,^3D_3^0$
V II	2134.12	−.04 +.05	200	100 50	46842.9	$a\,^5D_4 - y\,^5D_4^0$ $a\,^5D_1 - z\,^5P_2^0$
V II	1797.64	−.04	15*N*	3	55628.5	$a\,^5D_1 - y\,^3S_1^0$

2. TERMS OF THE V II SPECTRUM

The established terms of the V II spectrum are described in table 3, where singlet, triplet, and quintet terms are presented in groups. Successive columns show (1) the electron configuration responsible for the term, (2) term symbols, (3) level values, (4) level separations or intervals, (5) *g*-values derived from observed Zeeman effects, and

(6) observed combinations. All level values are relative to $(3d^4)$ $a\ ^5D_0=0.00$. The total number of levels is 223, including 89 terms which are divided among multiplicities as follows: 31 singlet, 41 triplet, 17 quintet terms, and 3 miscellaneous levels. A large majority of the terms are regular, only 10 being wholly or partially inverted, as shown by negative signs in column 4. Landé's interval rules are reasonably well obeyed, as is shown by some examples in table 4; but $b\ ^3P$, $c\ ^3P$, $b\ ^3D$, $c\ ^3F$, $d\ ^3F$, $z\ ^3P^\circ$, $y\ ^3P^\circ$, $x\ ^3P^\circ$, $x\ ^3D^\circ$, $w\ ^3D^\circ$, and $y\ ^3F^\circ$ are exceptions, many of which exhibit partial inversion. Of special interest is $z\ ^5D^\circ$, whose first three intervals are law-abiding but the fourth is abnormally small, only $\frac{1}{20}$ of its expected value. These irregular intervals cannot be accounted for in any simple manner.

TABLE 3.—*Terms of the* V II *spectrum* *

Electron configuration	Term symbol	Level	Difference	Observed g	Combinations
$3d^4$	$a\ ^1S_0$	19902.60			$z\ ^1P^\circ, y\ ^1P^\circ, z\ ^3P^\circ, x\ ^3P^\circ, z\ ^3D^\circ, y\ ^3D^\circ, z^3D^\circ, w\ ^3D^\circ, u\ ^3D^\circ, y\ ^3D^\circ, z\ ^3F^\circ.$
$3d^3\ 4s$	$a\ ^1P_1$	22273.54		0.97	$z\ ^1S^\circ, z\ ^1P^\circ, y\ ^1P^\circ, z\ ^1D^\circ, y\ ^1D^\circ, x\ ^1D^\circ, y\ ^3S^\circ, y^3P^\circ, x\ ^3P^\circ, y\ ^3D^\circ, x\ ^3D^\circ, y\ ^3F^\circ, x\ ^3F^\circ, y\ ^3D^\circ.$
$3d^4$	$a\ ^1D_2$	20980.92		1.02	$z\ ^1P^\circ, y\ ^1P^\circ, z\ ^1D^\circ, x\ ^1D^\circ, w\ ^1D^\circ, z\ ^1F^\circ, y\ ^1F^\circ, x\ ^1F^\circ, w\ ^1F^\circ, z\ ^3P^\circ, y\ ^3P^\circ, x\ ^3P^\circ, y\ ^3D^\circ, z\ ^3D^\circ, w\ ^3D^\circ, z\ ^3F^\circ, y\ ^3F^\circ, x\ ^3F^\circ, v\ ^3F^\circ, u\ ^3F^\circ, y\ ^3G^\circ, v\ ^3G^\circ.$
$3d^3\ 4s$	$b\ ^1D_2$	25191.08		0.99	$z\ ^1P^\circ, y\ ^1P^\circ, z\ ^1D^\circ, y\ ^1D^\circ, x\ ^1D^\circ, w\ ^1D^\circ, z\ ^1F^\circ, y\ ^1F^\circ, x\ ^1F^\circ, x\ ^3P^\circ, y\ ^3D^\circ, x\ ^3D^\circ, w\ ^3D^\circ, y\ ^3F^\circ, x\ ^3F^\circ.$
$3d^4$	$c\ ^1D_2$	44657.99			$x\ ^1D^\circ, x\ ^1F^\circ.$
$3d^4$	$a\ ^1F_3$	26839.82		.97	$y\ ^1D^\circ, x\ ^1D^\circ, w\ ^1D^\circ, z\ ^1F^\circ, y\ ^1F^\circ, w\ ^1F^\circ, y\ ^1G^\circ, x\ ^1G^\circ, w\ ^3D^\circ, ?\ ^3D^\circ, u\ ^3D^\circ, x\ ^3G^\circ, w\ ^3G^\circ, y^3H^\circ, 1^\circ, 3^\circ.$
$3d^3\ 4s$	$b\ ^1F_3$	34228.79		1.00	$z\ ^1D^\circ, y\ ^1D^\circ, x\ ^1D^\circ, z\ ^1F^\circ, x\ ^1F^\circ, y\ ^1G^\circ, x\ ^1G^\circ, w\ ^1G^\circ, y\ ^3F^\circ, w\ ^3G^\circ.$
$3d^4$	$a\ ^1G_4$	17910.98		0.95	$z\ ^1F^\circ, y\ ^1F^\circ, x\ ^1F^\circ, z\ ^1G^\circ, y\ ^1G^\circ, x\ ^1G^\circ, w\ ^1G^\circ, z\ ^1H^\circ, y\ ^1H^\circ, x\ ^1H^\circ, z\ ^3F^\circ, y\ ^3F^\circ, y\ ^3G^\circ, x\ ^3G^\circ, v\ ^3G^\circ, z\ ^3H^\circ, y\ ^3H^\circ, y\ ^3I^\circ.$
$3d^3\ 4s$	$b\ ^1G_4$	19112.93		.98	$z\ ^1F^\circ, y\ ^1F^\circ, x\ ^1F^\circ, w\ ^1F^\circ, z\ ^1G^\circ, y\ ^1G^\circ, x\ ^1G^\circ, w\ ^1G^\circ, z\ ^1H^\circ, y\ ^1H^\circ, x\ ^1H^\circ, w\ ^3D^\circ, u\ ^3D^\circ, y\ ^3F^\circ, z\ ^3G^\circ, y\ ^3G^\circ, x\ ^3G^\circ, v\ ^3G^\circ, z\ ^3H^\circ, y\ ^3H^\circ, z\ ^3I^\circ.$
$3d^4$	$c\ ^1G_4$	36425.07		.96	$y\ ^1F^\circ, x\ ^1F^\circ, y\ ^1G^\circ, x\ ^1G^\circ, y\ ^1H^\circ, x\ ^3G^\circ, w\ ^3G^\circ.$
$3d^3\ 4s$	$a\ ^1H_5$	23391.09		1.04	$z\ ^1G^\circ, y\ ^1G^\circ, x\ ^1G^\circ, w\ ^1G^\circ, z\ ^1H^\circ, y\ ^1H^\circ, x\ ^1H^\circ, x\ ^3F^\circ, w\ ^3F^\circ, u\ ^3F^\circ, y\ ^3G^\circ, x\ ^3G^\circ, w\ ^3G^\circ, y\ ^3H^\circ, z\ ^3I^\circ, 1^\circ.$
$3d^4$	$a\ ^1I_6$	19191.50		0.96:	$z\ ^1H^\circ, y\ ^1H^\circ, x\ ^1H^\circ, z\ ^1I^\circ, y\ ^3G^\circ, x\ ^3G^\circ.$
$3d^4$	$a\ ^3P_2$	11908.27	393.51	1.49	$z\ ^3S^\circ, y\ ^3S^\circ, z\ ^3P^\circ, y\ ^3P^\circ, x\ ^3P^\circ, z\ ^3D^\circ, y\ ^3D^\circ, x\ ^3D^\circ, w\ ^3D^\circ, v\ ^3D^\circ, u\ ^3D^\circ, z\ ^3F^\circ, x\ ^3F^\circ, z\ ^1S^\circ, z\ ^1P^\circ, z\ ^1D^\circ, y\ ^1F^\circ, z\ ^3S^\circ, z\ ^3D^\circ, y\ ^3D^\circ, x\ ^3D^\circ, z\ ^3F^\circ, 2^\circ.$
	$a\ ^3P_1$	11514.76	219.25	1.48	
	$a\ ^3P_0$	11295.51			
$3d^3\ 4s$	$b\ ^3P_2$	19132.69	−33.50	1.38	$z\ ^3S^\circ, z\ ^3P^\circ, y\ ^3P^\circ, x\ ^3P^\circ, y\ ^3D^\circ, x\ ^3D^\circ, w\ ^3D^\circ, v\ ^3D^\circ, u\ ^3D^\circ, t\ ^3D^\circ, y\ ^3F^\circ, x\ ^3F^\circ, v\ ^3F^\circ?, y\ ^3G^\circ, z\ ^1S^\circ, z\ ^1P^\circ, z\ ^1D^\circ, y\ ^1D^\circ, y\ ^1F^\circ, z\ ^3P^\circ, y\ ^3D^\circ.$
	$b\ ^3P_1$	19166.19	4.92	1.40	
	$b\ ^3P_0$	19161.27			
$3d^3\ 4s$	$c\ ^3P_2$	20343.00	253.44	1.36	$z\ ^3S^\circ, y\ ^3S^\circ, z\ ^3P^\circ, y\ ^3P^\circ, x\ ^3P^\circ, z\ ^3D^\circ, y\ ^3D^\circ, x\ ^3D^\circ, w\ ^3D^\circ, v\ ^3D^\circ, u\ ^3D^\circ, t\ ^3D^\circ, y\ ^3F^\circ, x\ ^3F^\circ, w\ ^3F^\circ, v\ ^3F^\circ, u\ ^3F^\circ?, z\ ^1S^\circ, z\ ^1P^\circ, z\ ^1D^\circ, x\ ^1D^\circ, z\ ^1F^\circ, y\ ^1F^\circ, z\ ^3S^\circ, z\ ^3P^\circ, z\ ^3D^\circ, y\ ^3D^\circ, z\ ^3F^\circ.$
	$c\ ^3P_1$	20089.56	−67.08	1.35	
	$c\ ^3P_0$	20156.64			
$3d^4$	$d\ ^3P_2$	32040.76	−258.48	1.38	$z\ ^3S^\circ, y\ ^3S^\circ, z\ ^3P^\circ, x\ ^3P^\circ, y\ ^3D^\circ, x\ ^3D^\circ, v\ ^3D^\circ, u\ ^3D^\circ, x\ ^3F^\circ, y\ ^1P^\circ, y\ ^1D^\circ.$
	$d\ ^3P_1$	32299.24	−120.80	1.48	
	$d\ ^3P_0$	32420.04			

* Colon denotes values are poorly determined.

TABLE 3.—*Terms of the* V II *spectrum*—Continued

Electron configuration	Term symbol	Level	Difference	Observed g	Combinations
$3d^4$	$a\ ^3D_3$	18353.89	60.02	1.30	$z\ ^3P^\circ$, $y\ ^3P^\circ$, $x\ ^3P^\circ$, $z\ ^3D^\circ$, $y\ ^3D^\circ$, $x\ ^3D^\circ$, $w\ ^3D^\circ$, $v\ ^3D^\circ$, $u\ ^3D^\circ$, $t\ ^3D^\circ$?, $z\ ^3F^\circ$, $y\ ^3F^\circ$, $x\ ^3F^\circ$, $w\ ^3F^\circ$, $v\ ^3F^\circ$, $u\ ^3F^\circ$, y^1G°, $z\ ^1S^\circ$, $z\ ^1P^\circ$, $y\ ^1P^\circ$, $z\ ^1D^\circ$, $y\ ^1D^\circ$, $x\ ^1D^\circ$, $z\ ^1F^\circ$, $y\ ^1F^b$, $z\ ^1G^\circ$, $x\ ^1G^\circ$, $z\ ^1S^\circ$, $z\ ^1D^\circ$, $y\ ^1D^\circ$, $x\ ^1D^\circ$, $z\ ^1F^\circ$, 2°.
	$a\ ^3D_2$	18293.87	24.38	1.13	
	$a\ ^3D_1$	18269.49		0.49	
$3d^3\ 4s$	$b\ ^3D_3$	20622.99	5.94	1.26	$y\ ^3S^\circ$, $z\ ^3P^\circ$, $y\ ^3P^\circ$, $x\ ^3P^\circ$, $z\ ^3D^\circ$, $y\ ^3D^\circ$, $x\ ^3D^\circ$, $w\ ^3D^\circ$, $v\ ^3D^\circ$, $u\ ^3D^\circ$, $t\ ^3D^\circ$, $z\ ^3F^\circ$, $y\ ^3F^\circ$, $x\ ^3F^\circ$, $w\ ^3F^\circ$, $v\ ^3F^\circ$, $u\ ^3F^\circ$, $x\ ^3G^\circ$, $z\ ^1S^\circ$, $z\ ^1P^\circ$, $z\ ^1D^\circ$, $y\ ^1D^\circ$, $x\ ^1D^\circ$, $z\ ^1F^\circ$, $y\ ^1F^\circ$, $z\ ^1G^\circ$, $z\ ^1S^\circ$, $z\ ^1D^\circ$, $y\ ^1D^\circ$, $z\ ^1F^\circ$, $y\ ^3G^\circ$?, 2°, 3°.
	$b\ ^3D_2$	20617.05	−5.09	1.25	
	$b\ ^3D_1$	20522.14		0.58	
$3d^3\ 4s$	$c\ ^3D_3$	44098.46	−60.97	(1.27:)	$v\ ^3D^\circ$, $t\ ^1D^\circ$, $w\ ^3F^\circ$, $u\ ^3F^\circ$.
	$c\ ^3D_2$	44159.43	−41.54	(1.14:)	
	$c\ ^3D_1$	44200.97:?		(0.50:)	
$3d^3\ 4s$	$a\ ^3F_4$	9097.81	255.84	1.22	$z\ ^3P^\circ$, $y\ ^3P^\circ$, $z\ ^3D^\circ$, $y\ ^3D^\circ$, $x\ ^3D^\circ$, $w\ ^3D^\circ$, $v\ ^3D^\circ$, $u\ ^3D^\circ$, $z\ ^3F^\circ$, $y\ ^3F^\circ$, $x\ ^3F^\circ$, $w\ ^3F^\circ$, $v\ ^3F^\circ$, $z\ ^3G^\circ$, $y\ ^3G^\circ$, $x\ ^3G^\circ$, $w\ ^3G^\circ$, $y\ ^3H^\circ$, $z\ ^1P^\circ$, $z\ ^1D^\circ$, $z\ ^1F^\circ$, $y\ ^1F^\circ$, $z\ ^1G^\circ$, $z\ ^1H^\circ$, $y\ ^1H^\circ$, $z\ ^3D^\circ$, $y\ ^3D^\circ$, $z\ ^1D^\circ$, $z\ ^3F^\circ$, $z\ ^3G^\circ$, $y\ ^3G^\circ$?
	$a\ ^3F_3$	8841.97	201.76	1.04	
	$a\ ^3F_2$	8640.21		0.65	
$3d^4$	$b\ ^3F_4$	13609.00	66.32	1.19	$z\ ^3D^\circ$, $y\ ^3D^\circ$, $x\ ^3D^\circ$, $w\ ^3D^\circ$, $v\ ^3D^\circ$, $u\ ^3D^\circ$, $z\ ^3F^\circ$, $y\ ^3F^\circ$, $x\ ^3F^\circ$, $w\ ^3F^\circ$, $v\ ^3F^\circ$, $z\ ^3G^\circ$, $y\ ^3G^\circ$, $z\ ^1G^\circ$, $w\ ^3G^\circ$, $v\ ^3G^\circ$, $z\ ^3H^\circ$, $y\ ^3H^\circ$, $z\ ^1P^\circ$, $z\ ^1D^\circ$, $z\ ^1F^\circ$, $y\ ^1F^\circ$, $z\ ^1F^\circ$, $z\ ^1G^\circ$, $z\ ^1H^\circ$, $y\ ^1H^\circ$, $z\ ^1S^\circ$, $z\ ^1D^\circ$, $x\ ^1D^\circ$, $z\ ^3F^\circ$, $z\ ^3G^\circ$.
	$b\ ^3F_3$	13542.68	51.84	1.06	
	$b\ ^3F_2$	13490.84		0.59	
$3d^4$	$c\ ^3F_4$	30318.63	12.23	1.25	$y\ ^3D^\circ$, $x\ ^3D^\circ$, $w\ ^3D^\circ$, $v\ ^3D^\circ$, $u\ ^3D^\circ$, $t\ ^3D^\circ$, $y\ ^1F^\circ$, $x\ ^3F^\circ$, $w\ ^3F^\circ$, $v\ ^3F^\circ$, $u\ ^3F^\circ$, $x\ ^3G^\circ$, $w\ ^3G^\circ$, $v\ ^3G^\circ$, $y\ ^1D^\circ$, $y\ ^1F^\circ$, $z\ ^1G^\circ$, $y\ ^1H^\circ$, $x\ ^3D^\circ$, $y\ ^3G^\circ$? 2°, 3°.
	$c\ ^3F_3$	30306.40	38.94	1.06	
	$c\ ^3F_2$	30267.46		0.67	
$3d^3\ 4s$	$d\ ^3F_4$	30613.97	−27.74	1.23	$y\ ^3D^\circ$, $x\ ^3D^\circ$, $w\ ^3D^\circ$, $v\ ^3D^\circ$, $t\ ^3D^\circ$, $x\ ^3F^\circ$, $w\ ^1F^\circ$, $v\ ^3F^\circ$, $u\ ^3F^\circ$, $x\ ^3G^\circ$, $w\ ^3G^\circ$, $v\ ^3G^\circ$, $z\ ^1H^\circ$, $z\ ^1D^\circ$, $w\ ^1D^b$, $z\ ^1F^\circ$, $y\ ^1F^\circ$, $w\ ^1F^\circ$, $x\ ^1G^\circ$, y^1H°, $y\ ^3G^\circ$? 2°, 3°.
	$d\ ^3F_3$	30641.71	−31.43	1.05	
	$d\ ^3F_2$	30673.14		0.67	
$3d^4$	$a\ ^3G_5$	14655.63	99.54	1.17	$y\ ^3D^\circ$, $x\ ^3D^\circ$, $w\ ^3D^\circ$, $z\ ^3F^\circ$, $y\ ^3F^\circ$, $x\ ^3F^\circ$, $w\ ^3F^\circ$, $v\ ^3F^\circ$, $u\ ^3F^\circ$, $z\ ^3G^\circ$, $y\ ^3G^\circ$, $x\ ^3G^\circ$, $w\ ^3G^\circ$, $v\ ^3G^\circ$, $z\ ^3H^\circ$, $y\ ^3H^\circ$, $z\ ^1D^\circ$, $x\ ^1D^\circ$, $z\ ^1F^\circ$, $y\ ^1F^\circ$, $z\ ^1G^\circ$, $y\ ^1G^\circ$, $z\ ^1H^\circ$, $y\ ^1H^\circ$, $z\ ^3D^\circ$, $x\ ^3D^\circ$, $z\ ^3F^\circ$, $y\ ^3F^\circ$.
	$a\ ^3G_4$	14556.09	94.36	1.00	
	$a\ ^3G_3$	14461.73		0.74	
$3d^3\ 4s$	$b\ ^3G_5$	16533.00	111.49	1.16	$z\ ^3D^\circ$, $u\ ^3D^\circ$?, $z\ ^3F^\circ$, $y\ ^3F^\circ$, $w\ ^3F^\circ$, $v\ ^3F^\circ$, $u\ ^3F^\circ$, $z\ ^3G^\circ$, $y\ ^3G^\circ$, $x\ ^3G^\circ$, $w\ ^3G^\circ$, $v\ ^3G^\circ$, $z\ ^3H^\circ$, $y\ ^3H^\circ$, $z\ ^1D^\circ$, $z\ ^1F^\circ$, $y\ ^1F^\circ$, $x\ ^1F^\circ$, $z\ ^1G^\circ$, $y\ ^1G^\circ$, $z\ ^1H^\circ$, $y\ ^1H^\circ$, $y\ ^3G^\circ$?, 2°.
	$b\ ^3G_4$	16421.51	80.54	1.03	
	$b\ ^3G_3$	16340.97		0.76	
$3d^4$	$a\ ^3H_6$	12706.15	84.58	1.27:	$y\ ^3F^\circ$, $x\ ^3F^\circ$, $w\ ^3F^\circ$, $z\ ^3G^\circ$, $y\ ^3G^\circ$, $x\ ^3G^\circ$, $w\ ^3G^\circ$, $z\ ^3H^\circ$, $y\ ^3H^\circ$, $z\ ^1F^\circ$, $y\ ^1F^\circ$, $z\ ^1G^\circ$, $y\ ^1G^\circ$, $z\ ^1H^\circ$, $y\ ^1H^\circ$, $z\ ^1I^\circ$, $z\ ^3F^\circ$, $y\ ^3F^\circ$.
	$a\ ^3H_5$	12621.57	76.42	1.02	
	$a\ ^3H_4$	12545.15		0.83:	
$3d^3\ 4s$	$b\ ^3H_6$	20363.22	83.03	1.14	$y\ ^3F^\circ$, $u\ ^3F^\circ$, $z\ ^3G^\circ$, $y\ ^3G^\circ$, $x\ ^3G^\circ$, $w\ ^3G^\circ$, $v\ ^3G^\circ$, $z\ ^3H^\circ$, $y\ ^3H^\circ$, $z\ ^3I^\circ$, $z\ ^1F^\circ$, $y\ ^1F^\circ$, $z\ ^1G^\circ$, $y\ ^1G^\circ$, $w\ ^1G^\circ$, $z\ ^1H^\circ$, $y\ ^1H^\circ$, $x\ ^1H^\circ$, $z\ ^1I^\circ$, 2°.
	$b\ ^3H_5$	20280.19	37.87	1.01	
	$b\ ^3H_4$	20242.32		0.82	
$3d^3\ 4s$	$a\ ^3P_2$	13741.61	146.88	1.62	$z\ ^5S^\circ$, $z\ ^3P^\circ$, $z\ ^5D^\circ$, $y\ ^5D^\circ$, $x\ ^5D^\circ$, $z\ ^3F^\circ$, $z\ ^1P^\circ$, $y\ ^3S^\circ$, $z\ ^3P^\circ$, $y\ ^3P^\circ$, $z\ ^3D^\circ$, $y\ ^3D^\circ$, $x\ ^3D^\circ$, $u\ ^3D^\circ$, 1°.
	$a\ ^3P_1$	13594.73	83.02	1.78	
	$a\ ^3P_0$	13511.71		2.39	
$3d^4$	$a\ ^5D_4$	339.21	130.32		$z\ ^5P^\circ$, $z\ ^5D^\circ$, $y\ ^5D^\circ$, $z\ ^5F^\circ$, $z\ ^3S^\circ$?, $y\ ^3S^\circ$, $z\ ^1P^\circ$, $z\ ^3D^\circ$, $v\ ^3D^\circ$, $z\ ^3F^\circ$, $u\ ^3F^\circ$, $z\ ^3G^\circ$.
	$a\ ^5D_3$	208.89	102.26		
	$a\ ^5D_2$	106.63	70.58		
	$a\ ^5D_1$	36.05	36.05		
	$a\ ^5D_0$	0.00			
$3d^3\ 4s$	$a\ ^5F_5$	3162.80	194.58	1.28:	$z\ ^5P^\circ$, $z\ ^5D^\circ$, $y\ ^5D^\circ$, $x\ ^5D^\circ$, $z\ ^5F^\circ$, $y\ ^5F^\circ$, $z\ ^5G^\circ$, $y\ ^5G^\circ$?, $x\ ^1D^\circ$, $z\ ^1G^\circ$, $z\ ^1H^\circ$, $z\ ^3P^\circ$, $z\ ^3D^\circ$, z^3F°, $y\ ^3F^\circ$, $w\ ^3F^\circ$, $u\ ^3F^\circ$, $z\ ^3G^\circ$, $w\ ^3G^\circ$, $z\ ^1I^\circ$, 1°.
	$a\ ^5F_4$	2968.22	159.46	1.30:	
	$a\ ^5F_3$	2808.76	121.75	1.20	
	$a\ ^5F_2$	2687.01	82.19	0.97	
	$a\ ^5F_1$	2604.82			
$3d^3\ 4d$ (^4F)	$e\ ^5P_3$	72908.17	233.89		$z\ ^5D^\circ$, $z\ ^5G^\circ$, $z\ ^3D^\circ$, $z\ ^3F^\circ$.
	$e\ ^5P_2$	72674.28	156.44		
	$e\ ^5P_1$	72517.84:			
$3d^3\ 4d$ (^4F)	$e\ ^5D_4$	72951.00:	161.77		$z\ ^5D^\circ$, $z\ ^5F^\circ$, $z\ ^5G^\circ$.
	$e\ ^5D_3$	72789.23:?	107.17		
	$e\ ^5D_2$	72682.06:?			
	$e\ ^5D_1$				
	$e\ ^5D_0$				

TABLE 3.—*Terms of the* V II *spectrum*—Continued

Electron configuration	Term symbol	Level	Difference	Observed g	Combinations
$3d^3\,4d(^4F)$	$e\ ^5F_5$	73293.82:?	71.10		$z\ ^5D^\circ$, $z\ ^5F^\circ$, $z\ ^5G^\circ$.
	$e\ ^5F_4$	73222.72:			
	$e\ ^5F_3$				
	$e\ ^5F_2$				
	$e\ ^5F_1$				
$3d^3\,4d(^4F)$	$e\ ^3G_4$	73498.93:	82.30		z^3D°, $z\ ^3F^\circ$, $z\ ^3G^\circ$.
	$e\ ^3G_5$	73416.63	137.71		
	$e\ ^3G_4$	73278.92	133.24		
	$e\ ^3G_3$	73145.68	118.92		
	$e\ ^3G_3$	73026.76			
$3d^3\,4d(^4F)$	$e\ ^3H_7$	73020.35:	183.35		$z\ ^3G^\circ$, $z\ ^3G^\circ$.
	$e\ ^3H_6$	72837.00:	156.80		
	$e\ ^3H_5$	72680.20:	129.49		
	$e\ ^3H_4$	72550.71	102.75		
	$e\ ^3H_3$	72447.96:			
$3d^3\,4p(^3P)$	$z\ ^1S_0^\circ$	*48258.28*			$a\ ^1P$, $a\ ^3P$, $b\ ^3P$, $c\ ^3P$, $a\ ^3D$, $b\ ^3D$.
$3d^3\,4p(^3P)$	$z\ ^1P_1^\circ$	*52803.75*		0.92	$a\ ^1S$, $a\ ^1P$, $a^1\ D$, $b\ ^1D$, $a\ ^3P$, $b\ ^3P$, $c\ ^3P$, $a\ ^3D$, $b\ ^3D$, $a\ ^3F$, $b\ ^3F$, $d\ ^3F$, $a\ ^5P$.
$3d^3\,4p(^3D)$	$y\ ^1P_1^\circ$	*56171.49*		1.05:	$a\ ^1S$, $a\ ^1P$, $a\ ^1D$, $b\ ^1D$, $d\ ^3P$, $a\ ^3D$.
$3d^3\,4p(^3P)$	$z\ ^1D_2^\circ$	*49898.22*		0.93	$a\ ^1P$, $a\ ^1D$, $b\ ^1D$, $b\ ^1F$, $a\ ^3P$, $b\ ^3P$, $c\ ^3P$, $a\ ^3D$, b^3D, $a\ ^3F$, $b\ ^3F$, $d\ ^3F$, $a\ ^3G$, $b\ ^3G$.
$3d^3\,4p(^3D)$	$y\ ^1D_2^\circ$	*57342.59*		.98	$a\ ^1P$, $b\ ^1D$, $a\ ^1F$, $b\ ^1F$, $b\ ^3P$, $d\ ^3P$, $a\ ^3D$, $b\ ^3D$, $c\ ^3F$.
$3d^3\,4p(^3F)$	$x\ ^1D_2^\circ$	*64586.23*		1.03:	$a\ ^1P$, $a\ ^1D$, $b\ ^1D$, $c\ ^1D$, $a\ ^1F$, $b\ ^1F$, $c\ ^3P$, $a\ ^3D$, $b\ ^3D$, $a\ ^3G$, $a\ ^3F$.
	$w\ ^1D_2^\circ$	*78791.3*:			$a\ ^1D$, $b\ ^1D$, $a\ ^1F$, $d\ ^3F$.
$3d^3\,4p(^3G)$	$z\ ^1F_3^\circ$	*49568.45*		0.97	$a\ ^1D$, $b\ ^1D$, $a\ ^1F$, $b\ ^1F$, $a\ ^1G$, $b\ ^1G$, $c\ ^3P$, $a\ ^3D$, $b\ ^3D$, $a\ ^3F$, $b\ ^3F$, $d\ ^3F$, $a\ ^3G$, $b\ ^3G$, $a\ ^3H$, $b\ ^3H$.
$3d^3\,4p(^3D)$	$y\ ^1F_3^\circ$	*56142.01*		.94	$a\ ^1D$, $b\ ^1D$, $a\ ^1F$, $a\ ^1G$, $b\ ^1G$, $c\ ^1G$, $a\ ^3P$, $b\ ^3P$, $c\ ^3P$, $a\ ^3D$, $b\ ^3D$, $a\ ^3F$, $b\ ^3F$, $c\ ^3F$, $d\ ^3F$, $a\ ^3G$, $b\ ^3G$, $a\ ^3H$, $b\ ^3H$.
$3d^3\,4p(^3F)$	$x\ ^1F_3^\circ$	*66303.88*		.95	$a\ ^1D$, $b\ ^1D$, $c\ ^1D$, $b\ ^1F$, $a\ ^1G$, $b\ ^1G$, $c\ ^1G$, $b\ ^3F$, $b\ ^3G$.
$3d^3\,4s4p(^3G)$	$w\ ^1F_3^\circ$	*74664.5*			$a\ ^1D$, $a\ ^1F$, $b\ ^1G$, $d\ ^3F$.
$3d^3\,4p(^3G)$	$z\ ^1G_4^\circ$	*49723.68*		.96	$a\ ^1G$, $b\ ^1G$, $a\ ^1H$, $a\ ^3D$, $b\ ^3D$, $a\ ^3F$, $b\ ^3F$, $c\ ^3F$, $a\ ^3G$, $b\ ^3G$, $a\ ^3H$, $b\ ^3H$, $a\ ^5F$.
$3d^3\,4p(^3H)$	$y\ ^1G_4^\circ$	*54144.20*		1.00	$a\ ^1F$, $b\ ^1F$, $a\ ^1G$, $b\ ^1G$, $c\ ^1G$, $a\ ^1H$, $a\ ^3G$, $b\ ^3G$, $a\ ^3H$, $b\ ^3H$.
$3d^3\,4p(^3F)$	$x\ ^1G_4^\circ$	*65790.28*		0.94	$a\ ^1F$, $b\ ^1F$, $a\ ^1G$, $b\ ^1G$, $c\ ^1G$, $a\ ^1H$, $a\ ^3D$, $d\ ^3F$.
$3d^3\,4s4p(^3G)$	$w\ ^1G_4^\circ$	*72292.2*:			$b\ ^1F$, $a\ ^1G$, $b\ ^1G$, $a\ ^1H$, $b\ ^3H$.
$3d^3\,4p(^3G)$	$z\ ^1H_5^\circ$	*49593.41*		.95	$a\ ^1G$, $b\ ^1G$, $a\ ^1H$, $a\ ^1I$, $a\ ^3F$, $b\ ^3F$, $a\ ^3G$, $b\ ^3G$, $a\ ^3H$, $b\ ^3H$, $a\ ^5F$.
$3d^3\,4p(^3H)$	$y\ ^1H_5^\circ$	*55499.38*		1.03:	$a\ ^1G$, $b\ ^1G$, $c\ ^1G$, $a\ ^1H$, $a\ ^1I$, $a\ ^3F$, $b\ ^3F$, $c\ ^3F$, $d\ ^3F$, $a\ ^3G$, $b\ ^3G$, $a\ ^3H$, $b\ ^3H$.
$3d^3\,4s4p(^3G)$	$x\ ^1H_5^\circ$	*70936.4*			$a\ ^1G$, $b\ ^1G$, $a\ ^1I$, $b\ ^3H$.
$3d^3\,4p(^3H)$	$z\ ^1I_6^\circ$	*55403.38*		1.01:	$a\ ^1H$, $a\ ^1I$, $a\ ^3H$, $b\ ^3H$.
$3d^3\,4p(^3P)$	$z\ ^3S_1^\circ$	*52181.18*		1.85	$a\ ^3P$, $b\ ^3P$, $c\ ^3P$, $d\ ^3P$, $a\ ^5D$?
$3d^3\,4p(^3P)$	$y\ ^3S_1^\circ$	*55663.27*		1.92	$a\ ^3P$, $c\ ^3P$, $d\ ^3P$, $b\ ^3D$, $a\ ^1P$, $a\ ^3P$, $a\ ^5D$.
$3d^3\,4p(^4P)$	$z\ ^3P_2^\circ$	*46739.98*	49.55	1.48	$a\ ^3P$, $b\ ^3P$, $c\ ^3P$, $d\ ^3P$, $a\ ^3D$, $b\ ^3D$, $a\ ^3F$, $a\ ^1S$, $a\ ^1D$, $a\ ^5P$, $a\ ^5D$, $a\ ^5F$.
	$z\ ^3P_1^\circ$	*46690.43*	104.00	1.44	
	$z\ ^3P_0^\circ$	*46586.43*			
$3d^3\,4p(^2P)$	$y\ ^3P_2^\circ$	*51123.51*	384.49	1.51	$a\ ^3P$, $b\ ^3P$, $c\ ^3P$, $a\ ^3D$, $b\ ^3D$, $a\ ^3F$, $a\ ^1P$, $a\ ^1D$, $a\ ^5P$.
	$y\ ^3P_1^\circ$	*50738.82*	76.46	1.39	
	$y\ ^3P_0^\circ$	*50662.36*			
$3d^3\,4p(^2D)$	$x\ ^3P_2^\circ$	*54715.63*	−2.22		$a\ ^3P$, $b\ ^3P$, $c\ ^3P$, $d\ ^3P$, $a\ ^3D$, $b\ ^3D$, $a\ ^1S$, $a\ ^1P$. $a\ ^1D$, $b\ ^1D$.
	$x\ ^3P_1^\circ$	*54717.85*	−95.60		
	$x\ ^3P_0^\circ$	*54813.45*			

TABLE 3.—*Terms of the* V II *spectrum*—Continued

Electron configuration	Term symbol	Level	Difference	Observed g	Combinations
$3d^3\,4p(^4F)$	$z\,^3D_3^\circ$	37205.01	163.90	1.32	$a\,^3P$, $c\,^3P$, $a\,^3D$, $b\,^3D$, $a\,^3F$, $b\,^3F$, $b\,^1G$, $a\,^1S$,
	$z\,^3D_2^\circ$	37041.11	86.53	1.08	$a\,^5P$, $e\,^5P$, $a\,^5D$, $a\,^5F$.
	$z\,^3D_1^\circ$	36954.58		0.24	
$3d^3\,4p(^4P)$	$y\,^3D_3^\circ$	51085.77	310.30	1.27	$a\,^3P$, $b\,^3P$, $c\,^3P$, $d\,^3P$, $a\,^3D$, $b\,^3D$, $a\,^3F$, $b\,^3F$,
	$y\,^3D_2^\circ$	50775.47	301.71	1.11	$c\,^3F$, $d\,^3F$, $a\,^3G$, $a\,^1S$, $a\,^1P$, $a\,^1D$, $b\,^1D$, $a\,^3P$.
	$y\,^3D_1^\circ$	50473.76		0.49	
$3d^3\,4p(^2P)$	$x\,^3D_3^\circ$	52767.36	67.33	1.26	$a\,^3P$, $b\,^3P$, $c\,^3P$, $d\,^3P$, $a\,^3D$, $b\,^3D$, $a\,^3F$, $b\,^3F$,
	$x\,^3D_2^\circ$	52700.03	95.92	1.10	$c\,^3F$, $d\,^3F$, $a\,^3G$, $a\,^1S$, $a\,^1P$, $a\,^1D$, $b\,^1D$, $a\,^3P$.
	$x\,^3D_1^\circ$	52604.11		0.63	
$3d^3\,4p(^2D)$	$w\,^3D_3^\circ$	53927.19	58.56	1.37	$a\,^3P$, $b\,^3P$, $c\,^3P$, $a\,^3D$, $b\,^3D$, $a\,^3F$, $b\,^3F$, $c\,^3F$,
	$w\,^3D_2^\circ$	53868.63	117.17	1.10	$d\,^3F$, $a\,^3G$, $a\,^1S$, $a\,^1D$, $b\,^1D$, $a\,^1F$, $b\,^1G$.
	$w\,^3D_1^\circ$	53751.46		0.49:	
$3d^3\,4p(^2F)$	$v\,^3D_3^\circ$	64603.53	−200.60	1.22:	$a\,^3P$, $b\,^3P$, $c\,^3P$, $d\,^3P$, $a\,^3D$, $b\,^3D$, $c\,^3D$, $a\,^1F$,
	$v\,^3D_2^\circ$	64804.13	−126.63	1.02:	$b\,^3F$, $c\,^3F$, $d\,^3F$, $a\,^1F$, $a\,^3D$.
	$v\,^3D_1^\circ$	64930.76		0.46:	
$3d^24s4p(^4F)$	$u\,^3D_3^\circ$	68945.0	147.3		$a\,^3P$, $b\,^3P$, $c\,^3P$, $d\,^3P$, $a\,^3D$, $b\,^3D$, $a\,^3F$, $b\,^3F$,
	$u\,^3D_2^\circ$	68797.7	38.3		$c\,^3F$, $b\,^3G$?, $a\,^1S$, $a\,^1F$, $b\,^1G$, $a\,^3P$.
	$u\,^3D_1^\circ$	68759.4			
$3d^3\,4p(\text{high}^2D)$?	$t\,^3D_3^\circ$	75848.18	89.84	(1.27:)	$b\,^3P$, $c\,^3P$, $a\,^3D$?, $b\,^3D$, $c\,^3D$, $c\,^3F$, $d\,^3F$.
	$t\,^3D_2^\circ$	75758.29	42.84	(1.14:)	
	$t\,^3D_1^\circ$	75715.46:		(0.50:)	
$3d^3\,4p(^4F)$	$z\,^3F_4^\circ$	40430.10	234.58	1.22	$a\,^3P$, $a\,^3D$, $b\,^3D$, $a\,^3F$, $b\,^3F$, $a\,^3G$, $b\,^3G$, $a\,^1D$,
	$z\,^3F_3^\circ$	40195.52	193.86	1.02	$a\,^1G$, $e\,^5P$, $a\,^5D$, $a\,^5F$.
	$z\,^3F_2^\circ$	40001.66		0.65	
$3d^3\,4p(^2G)$	$y\,^3F_4^\circ$	49268.61	57.83	1.18	$b\,^3P$, $c\,^3P$, $a\,^3D$, $b\,^3D$, $a\,^3F$, $b\,^3F$, $c\,^3F$, $a\,^1G$,
	$y\,^3F_3^\circ$	49210.78	9.12	0.99	$b\,^3G$, $a\,^3H$, $b\,^3H$, $a\,^1P$, $a\,^1D$, $b\,^1D$, $b\,^1F$, $a\,^1G$,
	$y\,^3F_2^\circ$	49201.66		.63	$b\,^1G$, $a\,^5F$.
$3d^3\,4p(^2D)$	$x\,^3F_4^\circ$	52657.51	265.57	1.18:	$a\,^3P$, $b\,^3P$, $c\,^3P$, $d\,^3P$, $a\,^3D$, $b\,^3D$, $a\,^3F$, $b\,^3F$,
	$x\,^3F_3^\circ$	52391.94	146.26	1.07	$c\,^3F$, $d\,^3F$, $a\,^3G$, $a\,^3H$, $a\,^1P$, $a\,^1D$, $b\,^1D$, $a\,^1H$.
	$x\,^3F_2^\circ$	52245.68		0.68	
$3d^3\,4p(^2F)$	$w\,^3F_4^\circ$	62176.24	42.85	1.36:	$c\,^3P$, $a\,^3D$, $b\,^3D$, $c\,^3D$, $a\,^3F$, $b\,^3F$, $c\,^3F$, $d\,^1F$,
	$w\,^3F_3^\circ$	62133.39	48.37	1.00	$a\,^3G$, $b\,^3G$, $a\,^3H$, $a\,^1H$, $a\,^5F$.
	$w\,^3F_2^\circ$	62085.02		0.58:	
$3d^24s4p(^4F)$	$v\,^3F_4^\circ$	68147.2	242.1		$b\,^3P$?, $c\,^3P$, $a\,^3D$, $b\,^3D$, $a\,^3F$, $b\,^3F$, $c\,^3F$, $d\,^1F$,
	$v\,^3F_3^\circ$	67905.1	167.3		$a\,^3G$, $b\,^3G$, $a\,^1D$.
	$v\,^3F_2^\circ$	67737.8			
	$u\,^3F_4^\circ$	76643.5	257.7		$c\,^3P$?, $a\,^3D$, $b\,^3D$, $c\,^3D$, $c\,^3F$, $d\,^3F$, $a\,^3G$, $b\,^3G$,
	$u\,^3F_3^\circ$	76385.8	165.4		$b\,^3H$, $a\,^1D$, $a\,^1H$, $a\,^3D$, $a\,^5F$.
	$u\,^3F_2^\circ$	76220.4			
$3d^3\,4p(^4F)$	$z\,^3G_5^\circ$	39612.97	209.20	1.19	$a\,^3F$, $b\,^3F$, $a\,^3G$, $b\,^3G$, $a\,^3H$, $b\,^3H$, $b\,^1G$, $a\,^3D$, $a\,^1F$,
	$z\,^3G_4^\circ$	39403.77	169.72	1.03	$e\,^5H$.
	$z\,^3G_3^\circ$	39234.05		0.84	
$3d^3\,4p(^2G)$	$y\,^3G_5^\circ$	48853.04	122.28	1.22	$b\,^3P$, $a\,^3D$, $a\,^3F$, $b\,^3F$, $a\,^3G$, $b\,^3G$, $a\,^3H$, $b\,^3H$,
	$y\,^3G_4^\circ$	48730.76	150.80	1.02	$a\,^1D$, $a\,^1G$, $b\,^1G$, $a\,^1H$, $a\,^1I$.
	$y\,^3G_3^\circ$	48579.96		0.67	
$3d^24p(^2H)$	$x\,^3G_5^\circ$	55206.87	−97.47	1.15	$b\,^3D$, $a\,^3F$, $b\,^3F$, $c\,^3F$, $d\,^3F$, $a\,^3G$, $b\,^3G$, $a\,^1H$,
	$x\,^3G_4^\circ$	55304.34	−45.29	1.02	$b\,^3H$, $a\,^1F$, $a\,^1G$, $b\,^1G$, $c\,^1G$, $a\,^1H$, $a\,^1I$.
	$x\,^3G_3^\circ$	55349.63		0.82	
$3d^24p(^2F)$	$w\,^3G_5^\circ$	64229.10	98.26		$a\,^3F$, $b\,^3F$, $c\,^3F$, $d\,^3F$, $a\,^3G$, $b\,^3G$, $a\,^3H$, $b\,^3H$, $a\,^1F$,
	$w\,^3G_4^\circ$	64130.84	73.45	1.02	$b\,^1F$, $c\,^1G$, $a\,^1H$, $a\,^5F$.
	$w\,^3G_3^\circ$	64057.39		0.72:	
$3d^24s4p(^4F)$	$v\,^3G_5^\circ$	70227.8	315.7		$b\,^3F$, $c\,^3F$, $d\,^3F$, $a\,^3G$, $b\,^3G$, $b\,^3H$, $a\,^1D$, $a\,^1G$, $b\,^1G$.
	$v\,^3G_4^\circ$	69912.1	267.9		
	$v\,^3G_3^\circ$	69644.2			
$3d^24p(^2G)$	$z\,^3H_6^\circ$	47607.79	310.71	1.13	$b\,^3F$, $d\,^3F$, $a\,^3G$, $b\,^3G$, $a\,^3H$, $b\,^3H$, $a\,^1G$, $b\,^1G$.
	$z\,^3H_5^\circ$	47297.08	240.76	1.01	
	$z\,^3H_4^\circ$	47056.32		0.78	
$3d^24p(^2H)$	$y\,^3H_6^\circ$	52252.70	99.15	1.04:	$a\,^3F$, $b\,^3F$, $a\,^3G$, $b\,^3G$, $a\,^3H$, $b\,^3H$, $a\,^1F$, $a\,^1G$, $b\,^1G$,
	$y\,^3H_5^\circ$	52153.55	70.67	0.98	$a\,^1H$.
	$y\,^3H_4^\circ$	52082.88		.70	

TABLE 3.—*Terms of the* V II *spectrum*—Continued

Electron configuration	Term symbol	Level	Difference	Observed g	Combinations
$3d^3 4p(^2H)$	$z\,^3I^0_5$	*53819.52*	242.70	1.11:	$a\,^3H$, $b\,^3H$, $b\,^1G$, $a\,^1H$, $a\,^3F$.
	$z\,^3I^0_6$	*53076.82*	198.83	0.98	
	$z\,^3I^0_7$	*52877.99*		.84:	
$3d^3 4p\ (^4P)$	$z\,^5S^0_2$	*49731.32*			$a\,^5P$, $a\,^3P$, $c\,^5P$, $a\,^3D$, $b\,^3D$, $b\,^3F$.
$3d^3 4p\ (^4P)$	$z\,^5P^0_3$	*47051.89*	171.95	1.55	$a\,^5P$, $a\,^5D$, $a\,^5F$, $b\,^3P$, $c\,^3P$.
	$z\,^5P^0_2$	*46879.94*	125.35	1.68	
	$z\,^5P^0_1$	*46754.59*		2.28	
$3d^3 4p\ (^4F)$	$z\,^5D^0_4$	*37551.09*	10.48	1.44	$a\,^5P$, $e\,^5P$, $a\,^5D$, $e\,^5D$, $a\,^5F$, $e\,^5F$, $e\,^5G$, $a\,^3P$, $c\,^3P$, $a\,^3D$, $b\,^3D$, $a\,^3F$, $b\,^3F$, $a\,^3G$.
	$z\,^5D^0_3$	*37520.61*	151.60	1.47	
	$z\,^5D^0_2$	*37369.01*	109.59	1.39	
	$z\,^5D^0_1$	*37259.42*	58.01	1.39	
	$z\,^5D^0_0$	*37201.41*			
$3d^3 4p\ (^4P)$	$y\,^5D^0_4$	*47420.10*	238.93	2.28	$a\,^5P$, $a\,^5D$, $a\,^5F$, $a\,^1S$, $a\,^1P$, $a\,^3P$, $b\,^3P$, $c\,^3P$, $a\,^3D$, $b\,^3D$, $a\,^3F$.
	$y\,^5D^0_3$	*47181.17*	79.29	1.48:	
	$y\,^5D^0_2$	*47101.88*	−6.10	1.47	
	$y\,^5D^0_1$	*47107.98*	80.10	1.43	
	$y\,^5D^0_0$	*47027.88*			
$3d^3 4s\ 4p\ (^4F)$	$x\,^5D^0_4$	*66158.6*	161.9		$a\,^5P$, $a\,^5F$, $a\,^3P$, $a\,^3D$, $a\,^3F$, $b\,^3F$, $c\,^3F$, $a\,^3G$.
	$x\,^5D^0_3$	*65996.7*	111.4		
	$x\,^5D^0_2$	*65885.3*	69.1		
	$x\,^5D^0_1$	*65816.2*	32.8		
	$x\,^5D^0_0$	*65783.4*			
$3d^3 4p\ (^4F)$	$z\,^5F^0_5$	*37852.39*	201.82	1.40:	$a\,^5P$, $a\,^5D$, $e\,^5D$, $a\,^5F$, $e\,^5F$, $e\,^5G$, $a\,^1S$, $a\,^3P$, $c\,^3P$, $a\,^3D$, $b\,^3D$, $a\,^3F$, $b\,^3F$, $a\,^3G$, $a\,^3H$.
	$z\,^5F^0_4$	*37650.57*	231.34		
	$z\,^5F^0_3$	*36919.23*	245.72	1.24	
	$z\,^5F^0_2$	*36673.51*	184.17	1.08	
	$z\,^5F^0_1$	*36489.34*		0.35	
$3d^3 4s 4p(^4F)$	$y\,^5F^0_5$	*64287.1*	260.5		$a\,^5F$, $a\,^1G$, $a\,^3G$, $a\,^3H$.
	$y\,^5F^0_4$	*64026.6*	209.7		
	$y\,^5F^0_3$	*63816.9*	159.7		
	$y\,^5F^0_2$	*63657.2*	108.7		
	$y\,^5F^0_1$	*63548.5*:			
$3d^3 4p(^4F)$	$z\,^5G^0_6$	*35483.39*	290.26		$e\,^5P$, $e\,^5D$, $a\,^5F$, $e\,^5F$, $e\,^5G$, $e\,^5H$, $a\,^3F$, $b\,^3F$.
	$z\,^5G^0_5$	*35193.13*	246.58	1.16	
	$z\,^5G^0_4$	*34946.55*	200.83	1.14	
	$z\,^5G^0_3$	*34745.72*	153.00	0.93	
	$z\,^5G^0_2$	*34592.72*		0.31	
$3d^3 4s4p(^4F)$	$y\,^5G^0_6$	*67795.7*:?	439.7		$a\,^5F$?, $b\,^3D$?, $a\,^3F$?, $c\,^3F$?, $d\,^3F$?, $b\,^3G$?.
	$y\,^5G^0_5$	*67356.0*:	393.3		
	$y\,^5G^0_4$	*66962.7*:	295.4		
	$y\,^5G^0_3$	*66667.3*:	438.9		
	$y\,^5G^0_2$	*66228.4*:			
	1^0_4	*62761.9*			$a\,^1F$, $a\,^1H$, $a\,^5P$, $a\,^5F$.
	2^0_3	*76405.4*			$a\,^3P$, $a\,^3D$, $b\,^3D$, $c\,^3F$, $d\,^3F$, $b\,^3G$, $b\,^3H$.
	3^0_3	*79040.4*			$a\,^1F$, $b\,^3D$, $c\,^3F$, $d\,^3F$.

TABLE 4.—*Intervals of some* V II *terms*

Term	Level intervals	Interval ratios		Term	Level intervals	Interval ratios	
		Observed	Theoretical			Observed	Theoretical
$a\,^3P$	393.51	2.00	2		82.19	2.11	2
	219.25	1.11	1				
				$z\,^3F°$	234.58	4.00	4
$d\,^3P$	−258.48	2.00	2		193.86	3.30	3
	−120.80	0.94	1				
				$z\,^3G°$	209.20	5.00	5
$c\,^3D$	−60.97	3.00	3		169.72	4.05	4
	−41.54	2.06	2				
				$z\,^3H°$	310.71	6.00	6
$a\,^3F$	255.84	4.00	4		240.76	4.66	5
	201.76	3.15	3				
				$z\,^3I°$	242.70	7.00	7
$b\,^3F$	66.32	4.00	4		198.83	5.72	6
	51.84	3.12	3				
				$z\,^5P°$	171.95	3.00	3
$b\,^3G$	111.49	5.00	5		125.35	2.09	2
	80.54	3.61	4				
				$z\,^5D°$	10.48	0.20	4
$a\,^3H$	84.58	6.00	6		151.60	3.00	3
	76.42	5.42	5		109.59	2.08	2
					58.01	1.15	1
$a\,^5P$	146.88	3.00	3				
	83.02	1.70	2	$y\,^5F°$	260.5	5.00	5
					209.7	4.04	4
$a\,^5D$	130.32	4.00	4		159.7	3.07	3
	120.26	3.14	3		108.7	2.09	2
	70.58	2.16	2				
	36.05	1.10	1	$z\,^5G°$	290.26	6.00	6
					246.58	5.11	5
$a\,^5F$	194.58	5.00	5		200.83	4.15	4
	159.46	4.10	4		153.00	3.16	3
	121.75	3.12	3				

Observed magnetic splitting factors (g–values) for 146 levels entered in column 5 of table 3 may be compared with Landé values by referring to the tables already mentioned [21]. In calculating g–values from Babcock's observations of Zeeman patterns, the actual formulas used were those given by Russell [14], and double weight was assigned to results from resolved patterns, or from combinations with one $j=0$. Single or/and uncertain determinations are followed by colons.

In table 3 the g–values of $c\,^3D$ and $t\,^3D°$ are enclosed in parentheses. This combination was identified by the g–values, and therefore the entered g's are not rigorously "observed" g's. There are no other observations to check these three g–values.

Since both the term analysis and the Zeeman-effect data are most nearly complete for the $3d^3\,4s$ configuration, we have chosen these levels to illustrate the agreement of observed and theoretical g–values in table 5. Comparison of the observed and theoretical sums shows that the former are about 2 percent too small. The same difference was noted by Russell and Babcock [22] in their analysis of the Zeeman effect for V I lines, and was explained as a probable error in determining the magnetic field strength at the time the observations were made nearly 20 years ago. If the observed g–values for V I and V II levels are increased by 2 to 3 percent, the general agreement between observed and theoretical splitting factors becomes quite satisfactory

TABLE 5.—*Observed and theoretical g-values for $3d^3 4s$ levels*

Term	$J=6$	5	4	3	2	1	0	Sum
$a\ ^5F$		1.28	1.30:	1.20	0.98	-------		4.76
Landé		1.40	1.35	1.25	1.00	0.00		5.00
$a\ ^3P$				1.63	1.75	2.38		5.76
Landé				1.67	1.83	2.50		6.00
$b\ ^3P$					1.38	1.41	-------	2.79
$c\ ^3P$					1.38	1.38	-------	2.76
Landé					1.50	1.50	0.00	3.00
$b\ ^3D$				1.31	1.23	0.58		3.12
$c\ ^3D$				1.27:	1.14:	.50:		2.91:
Landé				1.33	1.17	.50		3.00
$a\ ^3F$			1.21	1.09	0.65			2.95
$d\ ^3F$			1.23	1.06	.68			2.97
Landé			1.25	1.08	.67			3.00
$b\ ^3G$		1.16	1.03	0.73				2.92
Landé		1.20	1.05	.75				3.00
$b\ ^3H$	1.14	1.01	0.81					2.96
Landé	1.17	1.03	.80					3.00
$a\ ^1P$						0.98		
$b\ ^1D$					1.01			
$b\ ^1F$				0.99				
$b\ ^1G$			0.96					
$a\ ^1H$		1.09						5.03
Landé		1.00	1.00	1.00	1.00	1.00		5.00
Sum observed	1.14	4.54	6.54:	9.28:	10.20:	7.23:	-------	38.93:
Sum Landé	1.17	4.63	6.65	9.49	10.51	7.50	0.00	40.00

The observed combinations of each term are indicated in the last column of table 3; they may serve to exhibit the combining properties of the terms in lieu of a diagram of transitions. All combinations obey the simple selection rules $\Delta L=0, \pm 1, \pm 2$, and $\Delta J=0$ (except 0 to 0), ± 1, but, as usual, not all permitted combinations have been observed. Failure to find a predicted line is occasionally explained by masking (table 2), but more generally be extremely low intensity. Relative intensities appear to be law-abiding for the most part, but in triplet-system multiples the satellite lines appear to be abnormally weak when the L-values are large.

The total number of observed multiplets is 572, of which 81 are singlet-singlet, 205 triplet-triplet, 29 quintet-quintet, 164 singlet-triplet, 70 triplet-quintet, 8 singlet-quintet, and 15 combinations with 3 miscellaneous odd levels.

3. ELECTRON CONFIGURATIONS AND SPECTRAL TERMS

Vanadium has atomic number 23, and the extra-nuclear structure of normal vanadium atoms is represented by $1s^2\ 2s^2\ 2p^6\ 3s^2\ 3p^6\ 3d^3\ 4s^2$ electrons. The last five electrons account for the V I spectrum [7]; and when one is removed by ionization, the remaining four will account

for the V II spectrum. It was first believed that $(3d^3\ 4s)\ ^5F$ represented the normal (unexcited) state of V^+ ions, but further analysis proved that $(3d^4)\ ^5D$ had this distinction [3]. Both configurations yield quintet, triplet, and singlet terms, the former 16 terms with 38 levels, and the latter 16 terms with 34 levels. These even terms combine with a multitude of odd terms resulting from configurations that include a *p*-electron, $3d^3\ 4p$, $3d^2\ 4s\ 4p$, thus accounting for a majority of the observed V II lines.

The low (even) terms theoretically associated with the above-mentioned configurations [6] are as follows:

$3d^3\ 4s$: ^{5}(PF), ^{3}(PF), ^{3}(PDFGH), ^{1}(PDFGH), ^{3}D, ^{1}D.
$3d^4$: ^{5}D, ^{3}(PDFGH), ^{1}(SDFGI), ^{3}(PF), ^{1}(SDG).

Terms resulting from this analysis of the V II spectrum have been paired off with each and every one of these theoretical terms, except two, the highest ^{1}D of the first configuration and the highest ^{1}S of the second. In no other spectrum are expected terms of these two configurations so completely established. Theoretical values of the two missing levels have been calculated by Ufford [23], as follows: $(3d^3\ 4s)\ ^1D = 50274$ and $(3d^4)\ ^1S = 61919\ cm^{-1}$. Owing to the great elevation of these metastable levels, their strongest expected combinations would be in the infrared region where no V II lines have been found.

Another configuration of electrons that might be expected to yield metastable terms in the V II spectrum is

$3d^2\ 4s^2$: ^{3}(PF), ^{1}(SDG),

but no evidence for this has been found among our data. In this respect the V II spectrum differs most strikingly from the Ti I spectrum, which it should resemble according to the displacement law. In fact, the relative importance of the three configurations (or even terms) above-mentioned is completely reversed in the two spectra; $3d^2\ 4s^2$ includes the ground state of Ti I but is not detected in V II, whereas $3d^4$ yields the ground state of V II but produces only very high and relatively inconspicuous terms in Ti I. However, in both spectra the strongest lines involve $3d^3\ 4s$, as might be expected.

All this is in accord with the general properties of spectra of elements of the first long period. The low even configurations in the first spectra are $d^{n-2}\ s^2$ and $d^{n-1}\ s$, and those in second spectra are $d^{n-1}\ s$ and d^n. As the *d* shell nears completion or half completion, the levels of d^n drop below those of $d^{n-1}\ s$, while the available data indicate a corresponding rise of $d^{n-2}\ s^2$ relative to $d^{n-1}\ s$. In V II $(3d^2\ 4s^2)\ ^3F$ might be expected at about 34000 cm^{-1} above $(3d^4)\ ^5D$, but almost all of the observed lines in the spectral region where its combinations should lie have been otherwise classified.

From the configurations $3d^3\ 4p$ and $3d^2\ 4s4p$, the following (odd) middle terms are expected to arise:

$3d^3\ 4p$: ^{5}(SPD), ^{5}(DFG), ^{3}(SPD), ^{3}(DFG), ^{3}(SPD), ^{3}(PDF), ^{3}(DFG), ^{3}(FGH), ^{3}(GHI), ^{1}(SPD), ^{1}(PDF), ^{1}(DFG), ^{1}(FGH), ^{1}(GHI), ^{3}(PDF), ^{1}(PDF).
$3d^2\ 4s4p$: ^{5}(SPD), ^{5}(DFG), ^{3}(SPD), ^{3}(DFG), ^{3}P, ^{1}P, ^{3}(SPD), ^{1}(SPD), ^{3}(PDF), ^{1}(PDF), ^{3}(DFG), ^{1}(DFG), ^{3}(FGH), ^{1}(FGH).

V II levels have been assigned to all the terms of $3d^3\,4p$, except the last five, which are theoretically very high, but only a few could be ascribed to $3d^2\,4s4p$.

All V II terms that, with increasing total quantum numbers, form spectral series approach as limits the normal or metastable state of V^{++} ions, described as follows:

$3d^3$: ^{4}(PF), ^{2}(PDFGH), ^{2}D

A partial analysis of the V III spectrum has been published by White [24], who gave values to all these terms except ^{2}F and the second (high) ^{2}D. The normal state of V^{++} ions is represented by $(3d^3)$ ^{4}F, and its absolute value is estimated to be 214 000 cm^{-1}.

The first high (even) terms to be expected in series with the low (even) terms of V II are as follows:

$3d^3 5s$: ^{5}(PF), ^{3}(PF), ^{3}(PDFGH), ^{1}(PDFGH), ^{3}D, ^{1}D.
$3d^3 4d$: ^{5}(PDFGH), etc.

The latter have been recognized in whole or in part, but no trace of the former could be established. This is very surprising, since the $4p$–$5s$ transitions should be prominent because $4s$–$4p$ produces the strongest lines in the V II spectrum. However, after repeated failure to find any $3d^3\,5s$ levels, it became apparent that the unclassified lines in table 1 are neither grouped nor located properly to disclose such levels. An explanation is not obvious, but the fact is regretted because it foils any attempt to derive a trustworthy spectoscopic ionization potential from our data. Investigation with some other type of source, like the Paschen hollow cathode, which favors spectral series, appears to be necessary in this case.

At the present time the only available information on the absolute value of V II terms is that given by Russell [25]. From comparisons of analogous spectra, he adopted 114 600 cm^{-1} as the probable distance between the ground states of V II and V III. This corresponds to an ionization potential of 14.1 volts for the V^+ ion.

Our assignment of observed V II terms to electron configurations and convergence limits is summarized in table 6. These assignments are based on considerations of combining properties, relative positions of terms, level separations, and in many cases on theoretical calculations made by Ufford. Unfortunately these guiding criteria are not always quantitative or decisive, and then there is a temptation to become more or less arbitrary about the interpretation.

Indeed, the mutual perturbations of neighboring terms may result in a partial "sharing of identity." The configuration which is mainly responsible for the term may, however, often be assigned with considerable probability.

To each low even term of the configuration, $(3d)^3 4s$ corresponds a proper triad of terms of $(3d)^3 4p$, which has the same limit term in V III. The terms of this triad are usually roughly at the same level, and their combinations with the related low terms are stronger than with other low terms (except when badly perturbed). The intensities have been given the most weight in the assignments; then the levels.

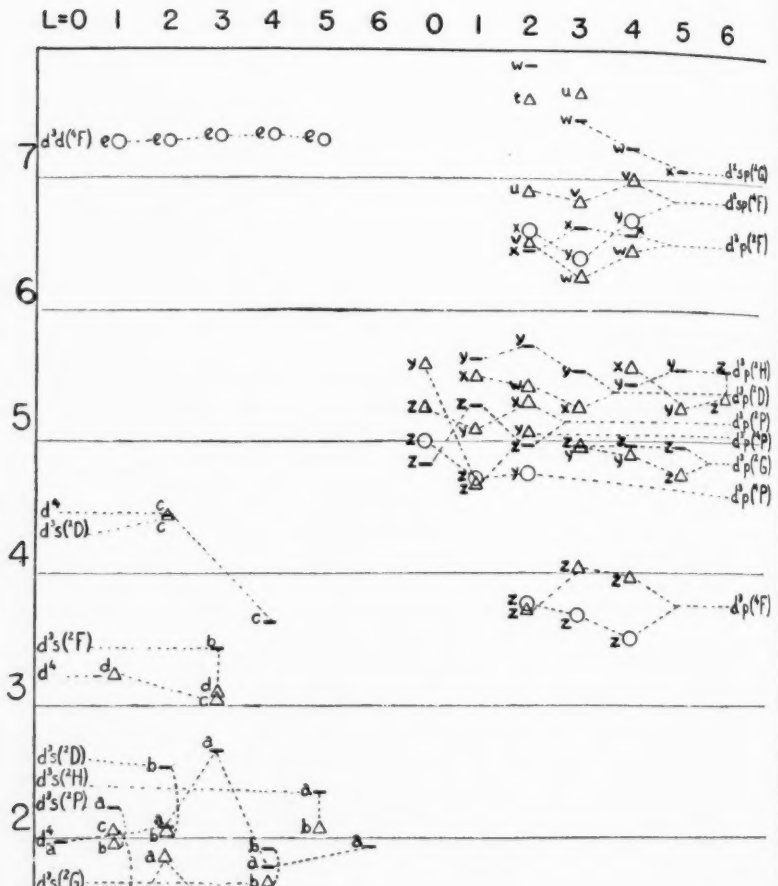

FIGURE 1.—*Diagram of* V II *terms, showing relative magnitudes and assignments to configurations and limits.*

— =singlet term, △=triplet term, ○=quintet term.

TABLE 6.—V II *predicted and observed terms*

Electron configuration	Limit V III	Predicted	Observed
$(3d)^4$		^{5}D; ^{3}(PF) ^{3}(PDFGH) ^{1}(SDG) ^{1}(SDFGI)	*a* ^{5}D; *d* ^{3}P *c* ^{3}F *a* ^{3}P *a*^{3}D *b*^{3}F *a*^{3}G *a*^{3}H ---- *c*^{1}D *c*^{1}G *a* ^{1}S *a*^{1}D *a*^{1}F *a*^{1}G *a*^{1}I
$(3d)^3\,4s$	^{4}F	^{5}F; ^{3}F	*a* ^{5}F; *a* ^{3}F
	^{4}P	^{5}P; ^{3}P	*a* ^{5}P; *c* ^{3}P
	^{2}P	^{3}P; ^{1}P	*b* ^{3}P; *a* ^{1}P
	^{2}D	^{3}D; ^{1}D	*b* ^{3}D; *b* ^{1}D
	^{2}F	^{3}F; ^{1}F	*d* ^{3}F; *b* ^{1}F
	^{2}G	^{3}G; ^{1}G	*b* ^{3}G; *b* ^{1}G
	^{2}H	^{3}H; ^{1}H	*b* ^{3}H; *a* ^{1}H
	(^{3}D)	^{3}D; ^{1}D	*c* ^{3}D; ----
$(3d)^3\,4p$	^{4}F	^{5}(DFG); ^{3}(DFG)	*z* ^{5}D° *z* ^{5}F° *z* ^{5}G°; *z* ^{3}D° *z*^{3}F° *z* ^{3}G°
	^{4}P	^{5}(SPD); ^{3}(SPD)	*z* ^{5}S° *z* ^{5}P° *y* ^{5}D°; *y* ^{3}S° *z* ^{3}P° *y* ^{3}D°
	^{4}P	^{3}(SPD); ^{1}(SPD)	*z* ^{3}S° *y* ^{3}P° *x* ^{3}D°; *z* ^{1}S° *z* ^{1}P° *z* ^{1}D°
	^{2}D	^{3}(PDF); ^{1}(PDF)	*x* ^{3}P° *w* ^{3}D° *x* ^{3}F°; *y* ^{1}P° *y* ^{1}D° *y* ^{1}F°
	^{2}F	^{3}(DFG); ^{1}(DFG)	*v* ^{3}D° *w* ^{3}F° *w* ^{3}G°; *x* ^{1}D° *x* ^{1}F° *x* ^{1}G°
	^{2}G	^{3}(FGH); ^{1}(FGH)	*y* ^{3}F° *y* ^{3}G° *x* ^{3}H°; *z* ^{1}F° *z* ^{1}G° *z* ^{1}H°
	^{2}H	^{3}(GHI); ^{1}(GHI)	*x* ^{3}G° *y* ^{3}H° *z* ^{3}I°; *y* ^{1}G° *y* ^{1}H° *z* ^{1}I°
	(^{3}D)	^{3}(PDF); ^{1}(PDF)	----- *t* ^{3}D°? ----; ----- ----- -----
$(3d)^3\,4s4p$	^{4}F	^{5}(DFG); ^{3}(DFG)	*x* ^{5}D° *y* ^{5}F° *y* ^{5}G°; *u* ^{3}D° *v* ^{3}F° *v* ^{3}G°
	^{4}P	^{5}(SPD); ^{3}(SPD)	----- ----- -----; ----- ----- -----
	^{4}S	^{5}P ; ^{1}P	----- ; ------
	^{2}P	^{3}(SPD); ^{1}(SPD)	----- ----- -----; ------ ----- -----
	^{2}D	^{3}(PDF); ^{1}(PDF)	----- ----- -----; ------ ----- -----
	^{2}F	^{3}(DFG); ^{1}(DFG)	
	^{2}G	^{3}(FGH); ^{1}(FGH)	----- ----- -----; *w* ^{1}F° *w* ^{1}G° *x* ^{1}H°
$(3d)^3\,4d$	^{4}F	^{5}(PDFGH)	*e* ^{5}P *e* ^{5}D *e* ^{5}F *e* ^{5}G *e* ^{5}H
$(3d)^3\,5s$	^{4}F	^{5}F; ^{3}F	--; --
	^{4}P	^{5}P; ^{3}P	--; --
	^{2}P	^{3}P; ^{1}P	--; --
	^{2}D	^{3}D; ^{1}D	--; --
	^{2}F	^{3}F; ^{1}F	--; --
	^{2}G	^{3}G; ^{1}G	--; --
	^{2}H	^{3}H; ^{1}H	--; --

The terms *d* ^{3}P and *c* ^{3}F have been assigned to $(3d)^4$ rather than to $(3d)^2\,(4s)^2$ because of their narrow or inverted intervals. Terms from $(3d)^2\,(4s)^2$ would have wide intervals, in normal order.

The term *x*^{1}H° can come only from $(3d)^2 4s\ (^2\text{G})4p$; and *w*^{1}G° and *w*^{1}F°, being nearly at the same level, have been tentatively assigned to the same configuration.

Two very high terms (*w* ^{1}D=78,791, *u* ^{3}F=76,643) have not been definitely assigned to electron configurations; they probably belong to $3d^2\ 4s\ 4p$.

The relative positions of identified V II terms, and correlations with configurations are shown in figure 1.

There can be no doubt about the identifications and correlations of the low terms, but in the present state of our knowledge the assignment of highly excited states to definite configurations and limits cannot be guaranteed to be correct in all cases. Our greatest disappointment is our failure to establish spectral series involving transitions of a single *s*-type electron and thus obtain absolute values for the V II terms.

The authors are grateful to Jerome K. Strauss for pure vanadium metal, to H. D. Babcock for permission to use and publish his Zeeman-effect data, to A. G. Shenstone for making a spectrogram in the extreme ultraviolet, to C. W. Ufford for theoretical calculations of relative terms, and especially to H. N. Russell for advice and stimulating discussion throughout this investigation.

IV. REFERENCES

[1] W. F. Meggers, J. Wash. Acad. Sci. **13,** 317 (1923).
[2] W. F. Meggers, C. C. Kiess, and F. M. Walters, Jr., J. Opt. Soc. Am. **9,** 355 (1924).
[3] W. F. Meggers, Z. Physik **33,** 509 (1925); **39,** 114 (1926).
[4] W. Kossel and A Sommerfeld, Verhandl. deut. Phys. Ges. **19,** 241 (1919).
[5] E. Back and A. Landé, Zeemaneffekt und Multipletstruktur der Spektrallinien (Julius Springer, Berlin, 1925).
[6] F. Hund, Linienspektren und periodisches System der Elemente (Julius Springer, Berlin, 1927).
[7] W. F. Meggers and H. N. Russell, J. Research NBS **17,** 126 (1936) RP906.
Charlotte E. Moore, Phys. Rev. **55,** 710 (1939).
[8] W. F. Meggers and C. E. Moore, J. Opt. Soc. Am. **28,** 176 (A), (1938); Pub. Am. Astron. Soc. **9,** 225 (1939).
[9] R. Thalén, Upsala Univ. Årsskr. (1866); Nova Acta Regiae Soc. Sci. Upsaliensis (3) **6** (1868).
[10] N. J. Lockyer, Proc. Roy. Soc. (London) **65,** 451 (1899).
[11] F. Exner and E. Haschek, Spektren der Elemente bei normalem Druck, **3,** 285 (F. Deuticke, Leipzig and Vienna, 1912).
[12] A. S. King, Astrophys. J. **41,** 86 (1915); **60,** 282 (1924).
[13] H. D. Babcock, Astrophys. J. **34,** 209 (1911).
[14] A. G. Shenstone and H. A. Blair, Phil. Mag. **8,** 764 (1929).
H. N. Russell, Phys. Rev. **36,** 1590 (1930).
[15] H. Gieseler and W. Grotrian, *Z.* Physik **25,** 342 (1924).
[16] A. S. King, Astrophys. J. **60,** 282 (1924).
[17] Revision of Rowland's Preliminary Table of Solar Spectrum Wave lengths (Carnegie Inst., Washington, 1928); C. E. Moore, A Multiplet Table of Astrophysical Interest (Princeton, 1933).
[18] H. Kayser, Tabelle der Schwingungszahlen (S. Hirzel, Leipzig, 1925); Phys. Rev. **48,** 99 (1935).
[19] H. N. Russell, A. G. Shenstone and L. Turner, Phys. Rev. **33,** 900 (1929).
[20] Trans. Int. Astron. Union. **6,** 100 (1938).
[21] C. C. Kiess and W. F. Meggers, BS J. Research **1,** 641 (1928), RP23.
[22] H. N. Russell and H. D. Babcock, Pieter Zeeman Verhandelingen, p. 286 (1935).
[23] C. W. Ufford, Private communication.
[24] H. E. White, Phys. Rev. **33,** 674 (1929).
[25] H. N. Russell, Astrophys. J. **46,** 434 (1927)

WASHINGTON, February 29, 1940.

○